Ring-Opening Polymerisation of Lactide and Other Related Monomers

Manton, Lois

Award date:
2014

Awarding institution:
University of Bath

Ring-Opening Polymerisation of Lactide and Other Related Monomers

Lois B. Manton

A thesis submitted for the degree of Doctor of Philosophy

Department of Chemistry

University of Bath

March 2014

This thesis is dedicated to Mama and Pops

Contents

Acknowledgements

Firstly, I would like to thank Professor Matthew Davidson for the opportunity to undertake a PhD within his research group. The University of Bath and Corbion Purac are also acknowledged for their sponsorship, and Dr Gerrit Gobius du Sart for his guidance over the last 3 years.

Dr Gabriele Kociok-Köhn and Dr John Lowe are thanked for their assistance with X-ray crystal structure determination and NMR problem solving respectively.

A sincere thank you to all members of the Davidson and Jones groups, past and present, especially Emma, Carlo, Tom, Daniel, Kirsty, Chris R, Chris H, Chris C, and Rhodri. Antoine, for all his knowledge and proof-reading, and those who made the department and lunchtime a fun place to be (Jeff, Dave and Heather). A big thank you to Ben for all his pearls of wisdom and support… I can't believe we did it!

I also wish to thank Abi for being the best friend a girl can have, and my sister Hannah for always looking out for me. Justin, I love you, and cannot put into words how much I appreciate all that you have done for me. Thank you for all your encouragement, and for everything, I could not have done it without you. I cannot wait to become Dr Manton-O'Byrne.

Finally, I would like to thank my lovely parents, you always had faith in me and told me I could achieve anything I put my mind to. Mum, I am the person I am today because of you. Dad, it was definitely worth it in the end.

Abstract

Polylactide (PLA) as a biodegradable and biocompatible polymer has had a lot of interest as an alternative to petrochemical-based polymers. PLA is synthesised from bio-renewable resources by the ring-opening polymerisation (ROP) of cyclic monomer lactide (LA). A variety of polymers can be synthesised with variations of microstructure and molecular weight. Initiators currently utilized in industry exhibit little stereocontrol, allowing a high demand for active stereoselective initiators. This thesis will discuss the synthesis of initiators, as well as investigations into co-polymerisations with other monomer.

Chapter 1 initially introduces the synthesis of PLA, with a detailed discussion of possible polymer architectures along with previously reported initiators will be discussed and their influences on the polymeric physical properties. To date, the formation of lactide co-polymers and investigations into the morphology and microstructures of the resulting co-polymers.

Chapter 2 describes a series of Group 4 isopropoxide complexes using inexpensive, commercially available ligands. Interesting coordination chemistry of such complexes will be discussed and their potential as initiators in the ROP of PLA will be investigated with kinetic studies to probe the control of architecture and molecular weights.

Chapter 3 concerns the formation of lactide co-polymers using inexpensive, commercially available co-monomers. The study of block co-polymers by either one-pot or sequential polymerisations will be assessed and subsequent thermal properties analysed.

Chapter 4 initially details the synthesis of cyclic monomers for lactide co-polymerisations. The ability to synthesise random or alternating lactide co-polymers in a one-pot synthesis will be probed with a variety of different cyclic monomers with varying stoichiometries and their properties examined.

Chapter 5 reports the overall conclusions of the thesis and what work should be carried forward.

Chapter 6 provides details analytical techniques, procedures and characterisations used throughout this thesis.

Glossary of Abbreviations

ε-CL	ε-caprolactone
δ-VL	δ-valerolactone
ω-PDL	ω-pentadecalactone
BDI	β-diiminate
BINAP	2,2'-bis(diphenylphosphino)-1,1'-binaphthyl
D-LA	D-Lactide
DMSO	Dimethyl sulfoxide
DRI	differential refractometer
DSC	differential scanning calorimetry
FT-IR	Fourier transform infrared
FDA	Food and drug administration
GPC	gel permeation chromatography
h	hours
HTMA	hexamethylenetetramine
Hz	hertz
i	isotactic
O^iPr	isopropoxide
IR	infrared spectroscopy
J	coupling constant
k_{app}	apparent rate of propagation
k_p	propagation rate constant
$\mathbf{L_1}$	lactic acid ligand
$\mathbf{L_2}$	2,2',2",2"'-(ethane-1,2-diylbis(azanetriyl))tetraethanol ligand
$\mathbf{L_3}$	amine tris(phenolate) $\mathbf{L_2}$ derivative ligand
L-LA	L-LA
LALLS	low angle light scattering detectors
MALLS	multi angle light scattering
Me	methyl
MHz	megahertz
Min	minutes
M_n	number average molecular weight
$M_{n,\,theo}$	theoretical number average molecular weight (calculated)
M_w	weight average molecular weight
NBS	*N*-bromosuccimide

NMR	nuclear magnetic resonance
PDI	polydispersity index
PDLA	poly(D-lactide)
Ph	phenyl
PLA	polylactide
PLLA	poly(L-lactide)
P_m	probability of *meso* enchainment
ppm	parts per million
P_r	probability of racemic enchainment
rac	racemic
RI	refractive index
ROP	ring-opening polymerisation
s	syndiotactic
T_c	polymer crystallisation temperature
T_g	glass transition temperature
THF	tetrahydrofuran
T_m	polymer melting temperature
TOEED	2,2',2",2"'-(ethane-1,2-diylbis(azanetriyl))tetraethanol
Toluene-d_8	deuterated toluene
w_i	weight fraction

Publications

Chuck, C. J., Davidson, M. G., Gobius du Sart, G., Ivanova-Mitseva, P. K., Kociok-Köhn, G. I., & **Manton, L. B**. Synthesis and Structural Characterization of Group 4 Metal Alkoxide Complexes of N,N,N',N'-Tetrakis(2-hydroxyethyl)ethylenediamine and Their Use As Initiators in the Ring-Opening Polymerization (ROP) of *rac*-Lactide under Industrially Relevant Conditions. *Inorganic chemistry*, **2013**, *52*(19), 10804–11. doi:10.1021/ic400667z

Conferences

American Chemical Society (ACS) international conference, Indianapolis *2013*. Poster presented.

SuBiCat Conference, St Andrews *2013*. Poster presented.

Chapter 1

Introduction

1 Introduction

This thesis concerns the synthesis of industrially relevant sustainable polymers. The introduction will cover product and reactant sustainability, polymerisations, co-polymerisations and initiators used to date.

1.1 Sustainable plastics

Sustainability is a seemingly easy concept to grasp, but when asked for a definition, it becomes more difficult to distil to a single concept. Depending on who you ask, the answer will be different. This means that a multi-faceted answer must be described, which means a multi-faceted approach will be needed to tackle issues related to sustainability. Figure 1.1.1 shows a Venn diagram where the Social, Economic, and Environmental issues are addressed to find a *Sustainable* solution.

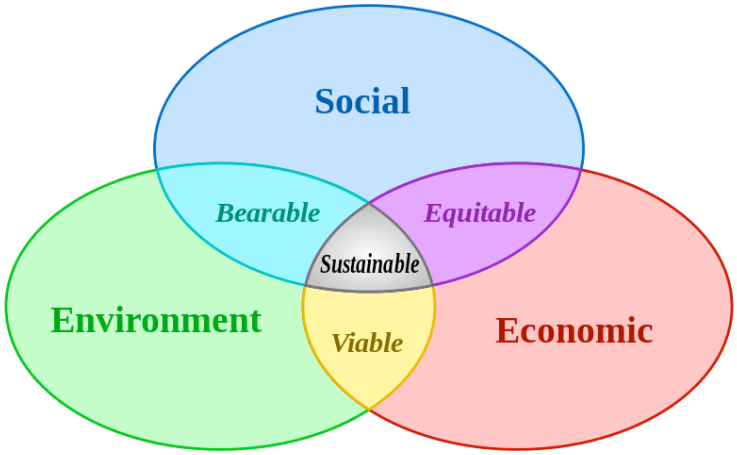

Figure 1.1.1: Venn diagram showing Sustainability as a combination of Economic, Social, and Environmental approaches.[1]

Plastics are ubiquitous in modern life, generating 140 million tons in the global marketplace.[2,3] Our increasingly disposable lifestyles mean that more and more waste plastics are making their way into the environment. Many Western governments are making concerted efforts to recycle waste plastics but large volumes still make their way to landfill and to the environment at large. Many of these generated plastics are unable to degrade in the environment within acceptable lifetimes, and pose a threat to natural ecosystems. The Great Pacific garbage patch is a prime example of an area of the natural environment which has been damaged by, among other things,

plastics that have not been degraded fully. Figure 1.1.2 shows how natural currents cause plastic in the ocean to form large "islands" of un-degraded waste.

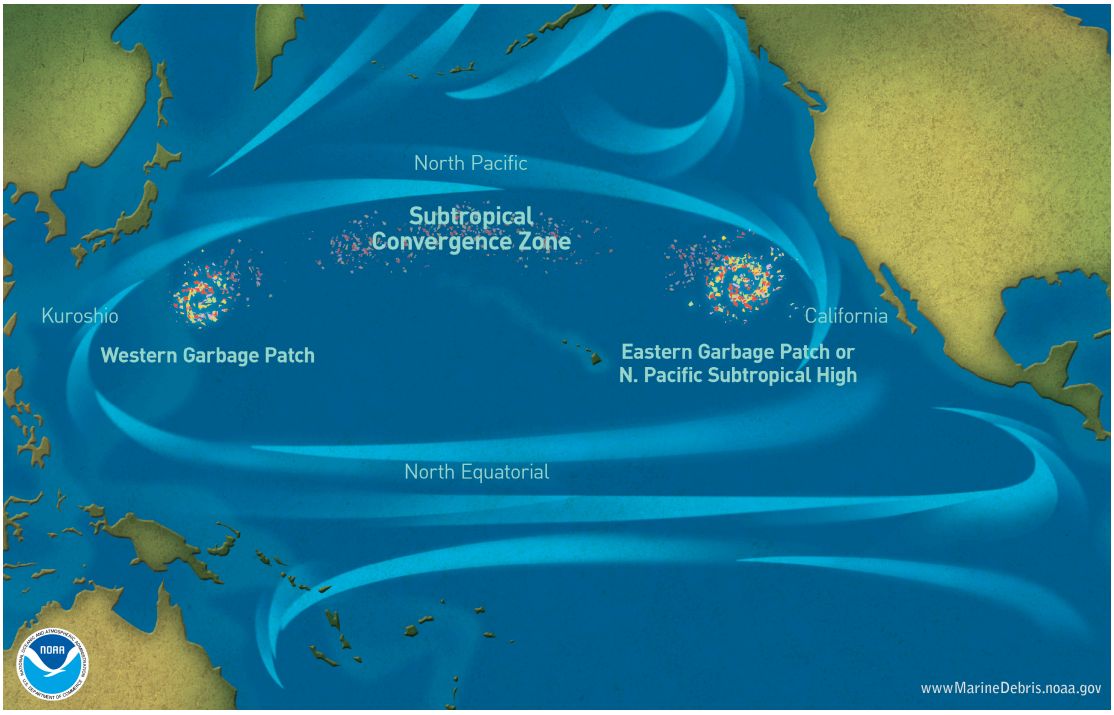

Figure 1.1.2: Map of garbage patches and convergence zones in the Pacific Ocean.[4]

These garbage patches are a major example of how waste can interfere with the environment, but there are many other examples of plastic waste interfering with the natural world. One major source of waste plastic comes in the form of shopping bags. Shopping bags, if not disposed correctly can block drains, cause animals and fish to choke, and can contaminate soils and waterways. In order the combat this, either the usage of plastic should be reduced, or recycled where possible. There are many initiatives in place to combat plastic usage, recently there has been a push to charge a fee per plastic bag in supermarkets. This has proven very successful in Ireland which has seen a reduction in usage of plastic bags by 90 %. In the cases where substantial plastic use reduction is inappropriate or difficult, a replacement plastic that can degrade more easily and be synthesised from sustainable sources should be found.

Traditionally, large-volume plastics are generally produced from oil based sources. Reserves of oil globally are not infinite, and some have predicted that we have nearly consumed more oil than is left in reserves. In any case, we will inevitably run out of fossil precursors for plastic so an alternative source of starting materials will need to be found. Bioplastics is a term coined often with different definitions. Sometimes it is meant to refer to bio-based polymers, sometimes it represents a class of biodegradable polymers. It is also used to define the

combination, a polymer which are biobased and biodegradable. A claim for biodegradability in turn should only be used if the product complies with well-established testing protocols and norms, such as EN13432 or ASTM D6400.[5] Globally, the market for bioplastics is growing exponentially whereby approximately 1 million metric tons were produced in 2011 and a forecast of over 6 million metric tons is predicted for 2017.[6,7]

Polylactide is a biodegradable and biocompatible aliphatic polyester produced by the polymerisation of lactide, the cyclic monomer of two lactate units. Lactic acid, ultimately being the starting material for PLA can be produced by fermentative processes, from for example starch. Currently, sugar beet and corn-starch are the most widely used feedstocks due to their economic feasibility. In the future, however, cellulose based materials such as agricultural waste and residual biomass will be used in place of food plants. In the interim, as demand increases for PLA the biomass feedstock could be supplemented by purpose grown crops.[8] Due to increased pressure on the world's oil supplies as well as rising prices and a move toward "green" industry, degradable and biocompatible plastics are increasingly sort. PLA is seen as a "green" alternative to oil based plastics not only due to its eco-friendly nature but also for its physical properties such as tensile strength and stiffness of subsequent polymeric materials.[9–12]

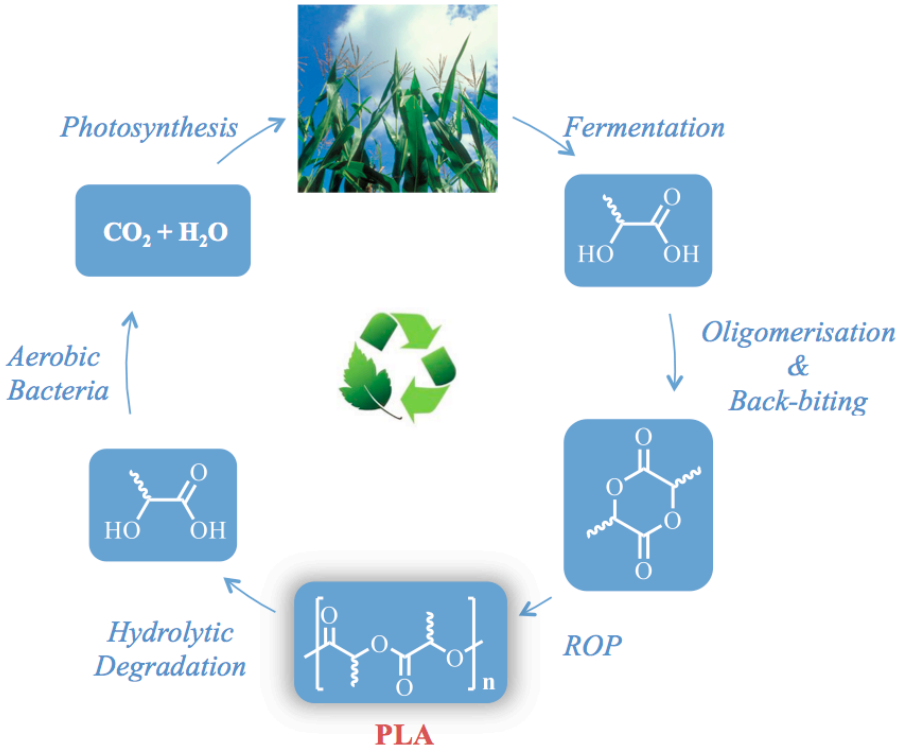

Figure 1.1.3: PLA cycle showing the formation of lactide, ring-opening polymerisation, and degradation steps.[13]

There are two possible routes to PLA, polycondensation of lactic acid or ring-opening polymerisation of lactide. Lactic acid is synthesised by the fermentation of sugars in plants as shown in Figure 1.1.3. The oligomerisation of lactic acid gives off H_2O and affords a low molecular weight LA oligomer, which in turn is depolymerized to the cyclic dimer of lactic acid, lactide. By using lactide, high molecular weight PLA can be produced *via* ring-opening polymerisation. The mechanical and thermal properties of the resultant PLA can vary greatly and are determined by the varying chirality of the methyl substituents.

Due to the biologically recyclable nature of PLA it can be composted when the product is no longer required. Breakdown of the PLA takes place through hydrolytic degradation where enzymes break down PLA to form lactic acid. PLA can be hydrolysed in the body (*in vivo*) or in the environment, which in turn is broken down into CO_2 and H_2O closing the PLA cycle. The tacticity of the polymer chains determine the kinetics and products of the degradation.

There are many uses for renewable biodegradable plastics synthesised from lactic acids as shown below (Figure 1.1.4).

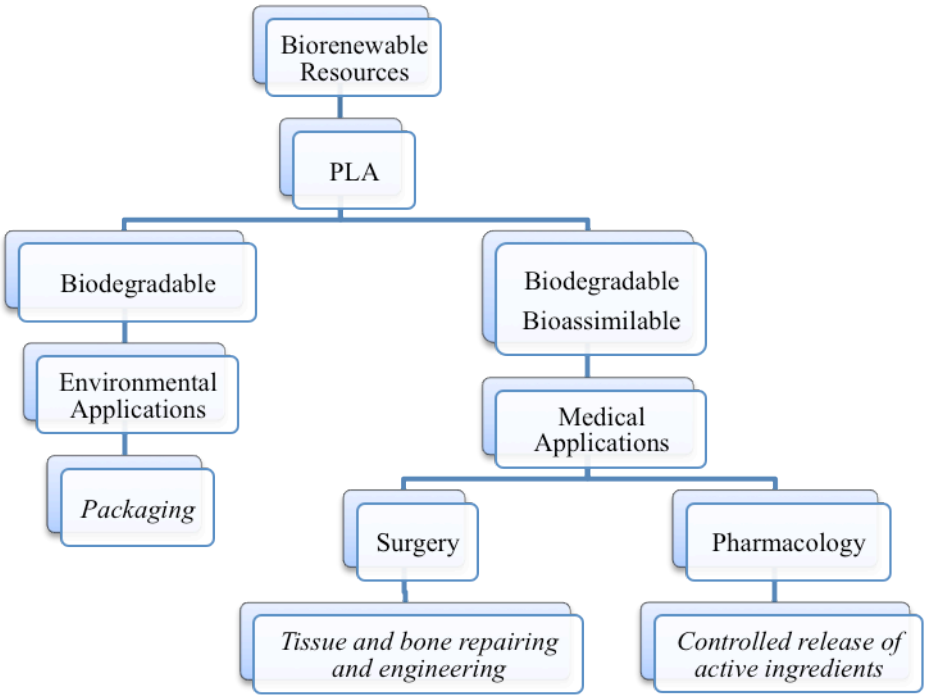

Figure 1.1.4: Applications of the biodegradable polymers based on lactic acids.[10]

PLA is a versatile bioplastic that has many applications such as food packaging that can be readily composted, cutting down on problematic waste. The degradability of PLA to

biocompatible molecules is utilized in medical applications such as in surgery. For bone fixation, PLA screws can be used that will degrade *in vivo* and eliminate the need for follow-up surgery to remove the screw. PLA can also be used as an erodible vehicle for controlled drug delivery enabling the controlled release of active ingredients at the required site in the body.[14]

1.2 Polymerisation

Many initiators have been investigated for the ring-opening polymerisation (ROP) of lactide such as enzymes, organo-catalysts and organometallic catalysts.[10,11] The most widely studied ROP utilises organometallic complexes due to the high levels of stereo-control achieved. Three mechanisms will be discussed in this section including anionic, cationic and coordination-insertion.

1.2.1 Anionic Polymerisation

To date, lithium complexes are reported to have the highest stereocontrol in ROP of *rac*-lactide *via* anionic ROP mechanism. Kasperczyk *et al*. reported PLA using lithium *tert*-butoxide as the initiator at 25°C, with increased stereocontrol at reduced temperature (-20 °C).[15] The anionic mechanism is initiated by either the deprotonation of the methine proton of the monomer (**Scheme 1.2.1**i) or nucleophilic attack on the carbonyl carbon of the monomer (**Scheme 1.2.1**ii), breaking the acyl bond forming a metal alkoxide. Propagation occurs with the addition of another monomer forming a growing polymer chain.

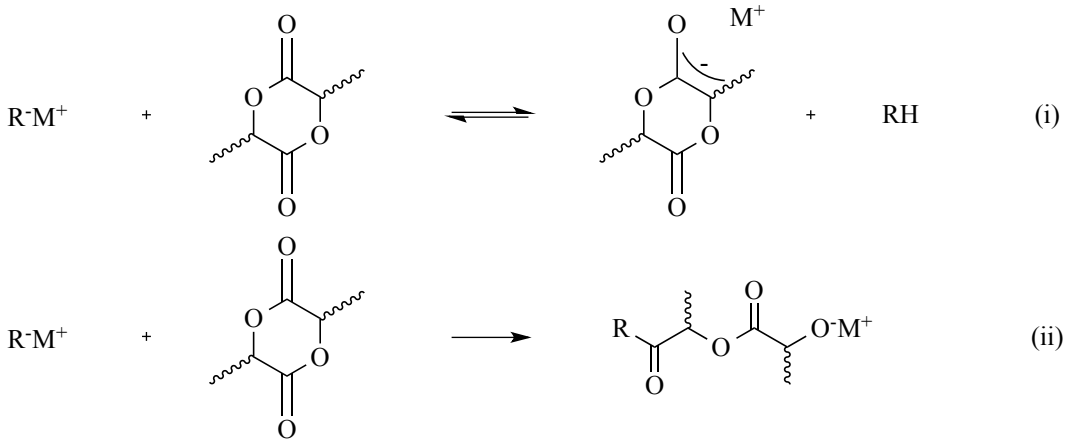

R = alkyl, alkoxy and M = Li, K, Mg

Scheme 1.2.1: Anionic mechanism in the ROP of lactide *via* i) deprotonation and ii) direct nucleophilic attack.[10]

Anionic ROP tends to give uncontrolled molecular weights and PDI due to side reactions such as epimerisation, chain termination and inter/intra molecular transesterification.[16]

1.2.2 Cationic Polymerisation

Cationic polymerisation is a type of chain growth polymerisation where a cationic initiator transfers charge to a monomer which becomes reactive. Cationic ROP of lactide is the least favoured of the polymerisation routes, due to poor control. In 1980's, Dittrich and co-workers followed by Kricheldorf *et al.* illustrated that only a few initiators such as trifluoromethanesulfonate (MeOTf) and trifluoromethanesulfonic acid (HOTf) were active in the cationic polymerisation of lactide.[17,18] Studies by ^{1}H NMR spectroscopy using trifluoromethanesulfonate as an initiator, showed the end group to be a methyl ester, which suggests the mechanism was initiated by the protonation of the carbonyl-oxygen leading to cleavage of the alkyl-oxygen bond by nucleophilic attack (S_N2) rather than an acyl-oxygen cleavage (Scheme 1.2.2).[19]

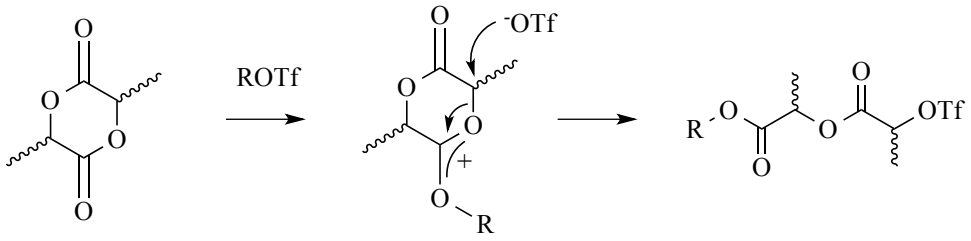

R = H, Me, or growing polymer chain, Tf = CF_3SO_2.

Scheme 1.2.2: Proposed cationic mechanism in the ROP of lactide *via* cleavage of alkyl-oxygen bond.[10]

Conversely, Bourissou *et al.* later investigated trifluoromethanesulfonic acid as a catalyst in the presence of a protic solvent.[20] It was reported that the mechanism in this case underwent cleavage of acyl-oxygen bond as shown below (Scheme 1.2.3).

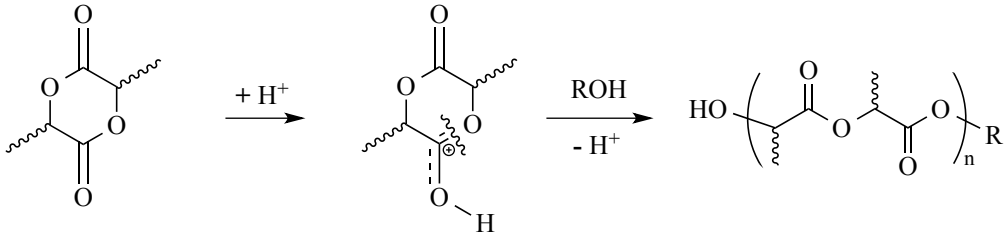

Scheme 1.2.3: Proposed cationic mechanism in the ROP of lactide *via* cleavage of acyl-oxygen bond.[20,21]

The disadvantage of this method is the optimum reaction temperature is 50 °C resulting in a slow conversion with varying low molecular weights. At higher temperatures the reaction rate increased, however an undesired dark-coloured product was recovered. Lower temperatures give slow conversion and low yields.

1.2.3 Coordination-Insertion Ring-Opening Polymerisation

Ring-opening polymerisation *via* a coordination-insertion mechanism can achieve PLA with high stereocontrol and high molecular weights using metal alkoxides as initiators. The lactide monomer coordinates to the Lewis acidic metal centre. The coordination of the monomer to the metal centre of the catalyst through the carbonyl group is thought to control the stereochemistry. Insertion proceeds *via* nucleophillic addition of the alkoxide to the activated carbonyl carbon leading to the ring-opening of the monomer and the breaking of the acyl-oxygen bond. Insertion of a new lactide monomer propagates the growing polymer chain. Termination of the polymerisation occurs by protonation (Scheme 1.2.4).[10]

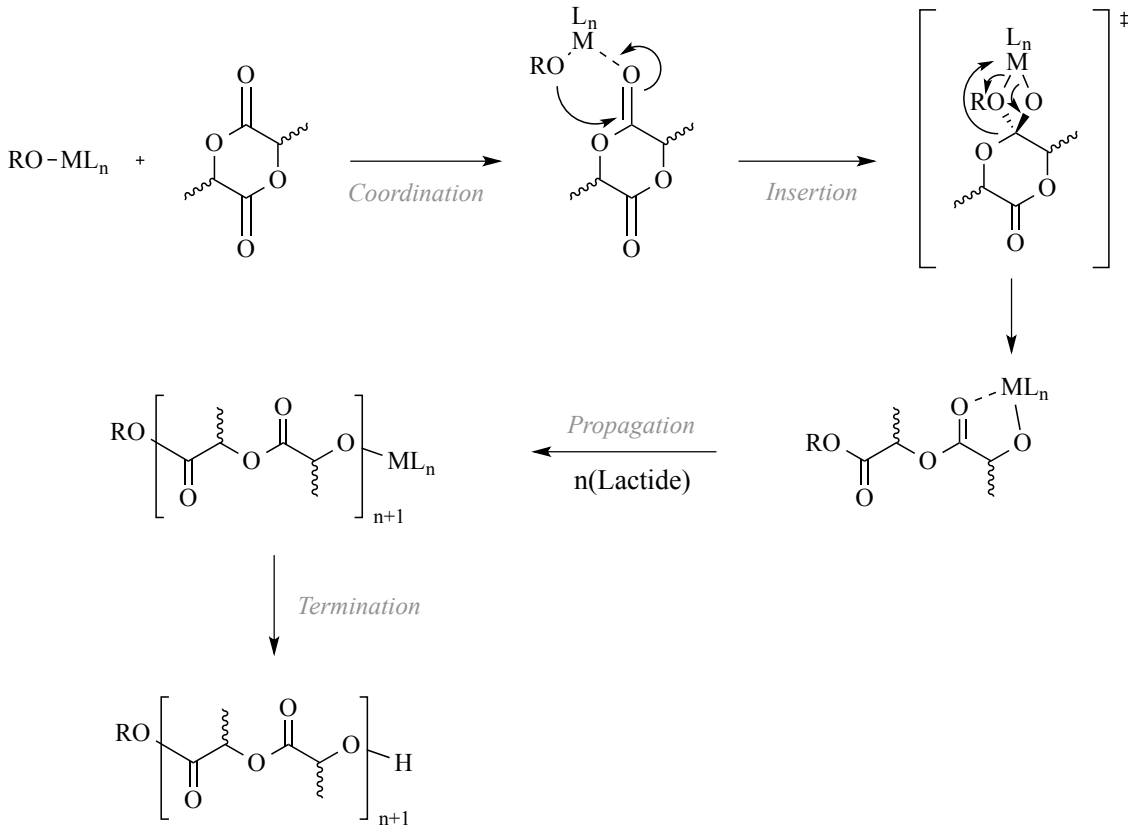

M = Metal.
L_n = Ligand
RO = refers to either the initiating alkoxide or the growing polymer chain.

Scheme 1.2.4: Proposed mechanism for the coordination-insertion ROP of lactide.[10]

There are many variants on designing the metal based catalysts which affect this mechanism. The steric bulk of the ligand, the identity of the metal, the ratio of metal centres to ligands and the nature of the metal centre in the system all influence the rate and stereocontrol of the polymerisation reaction. The lability of the ligand also contributes to the activity of the initiator.

The main disadvantage with ring-opening polymerisation is transesterification. This is the breaking of the polymer chain due to initiator groups competitively reacting with the polymer chains breaking the bonds and increasing the polydispersity of the polymer. Transesterification can occur *via* intra- or inter-molecular reactions (Scheme 1.2.5).

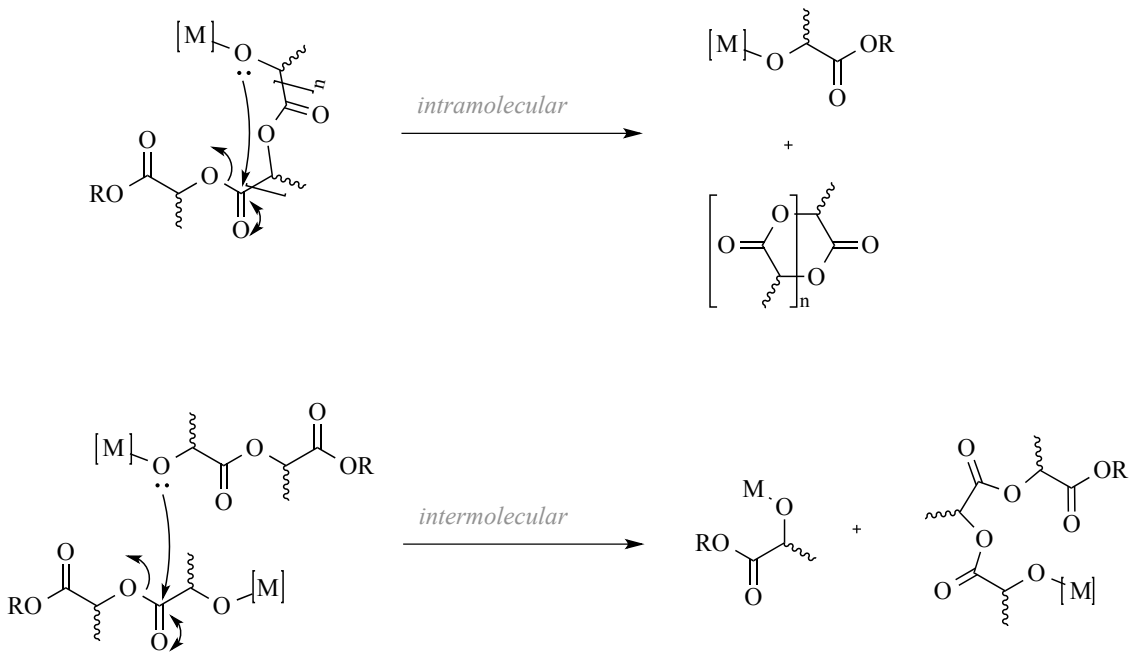

Scheme 1.2.5: Schematic representation of intra- and inter-molecular transesterification side reactions in the ROP of lactide.[10]

Intramolecular transesterification occurs when the chain end reacts with the propagating end of the same polymer resulting in a large cyclic oligomer. Intermolecular transesterification can be observed as the propagating chain end reacts with another polymer chain limiting propagation.[22,23] An increased reaction temperature is thought to increase the rate of transesterification. Intermolecular transesterification between random ester bonds in the chains will result in a broadening of PDI.

The stereocontrol of the growing polymer chain can be developed by two different routes; chain end control and enantiomorphic site control. Chain-end control is when the chirality of the last inserted monomer of the growing polymer chain determines the chirality of the next monomer to be inserted. Enantiomorphic site control is when the chirality of the inserted monomer on the growing polymer chain is determined by the catalyst.

1.3 Polylactide Architecture

Lactide contains two chiral centres with the three possible configurations; L-lactide (*RR*), D-lactide (*SS*) and *meso*-lactide (*RS*) (**Figure 1.3.1**). *Rac*-lactide (DL-LA) refers to a 50:50 mixture of L-LA and D-LA.

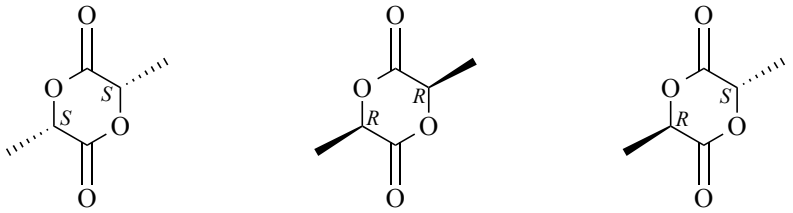

Figure 1.3.1: The three stereoisomer structures of lactide (3,6-dimethyl-1,4-dioxane-2,5-dione).[24]

The distribution of stereocontrol within the polymer determines the physical properties of the material. There are four possible microstructures of PLA; isotactic, heterotactic, syndiotactic and atactic (Figure 1.3.2). Isotactic PLA can be produced from either L-LA or D-LA or a mixture of both in combination with a stereoselective catalyst. Heterotactic and atactic PLA can be synthesised from *rac*-lactide. Heterotactic, syndiotactic and atactic PLA can be synthesised from *meso*-LA.

The relative probability of the next stereocentre being racemic is represented as P_r and the relative probability of the next stereocentre being the same (*meso*) is represented as P_m. Heterotactic PLA has a P_r value of 1 ($P_m = 0$). This shows that the next consecutive pair of stereocentres must be different (-*RR*-*SS*-), giving a double alternating stereogenic polymer. Isotactic PLA has a P_r value of 0 ($P_m = 1$), where the neighbouring stereo-centres must have the same orientation. Atactic PLA, $P_r = 0.5$ ($P_m = 0.5$), thus a random enchainment of stereocentres occurs.

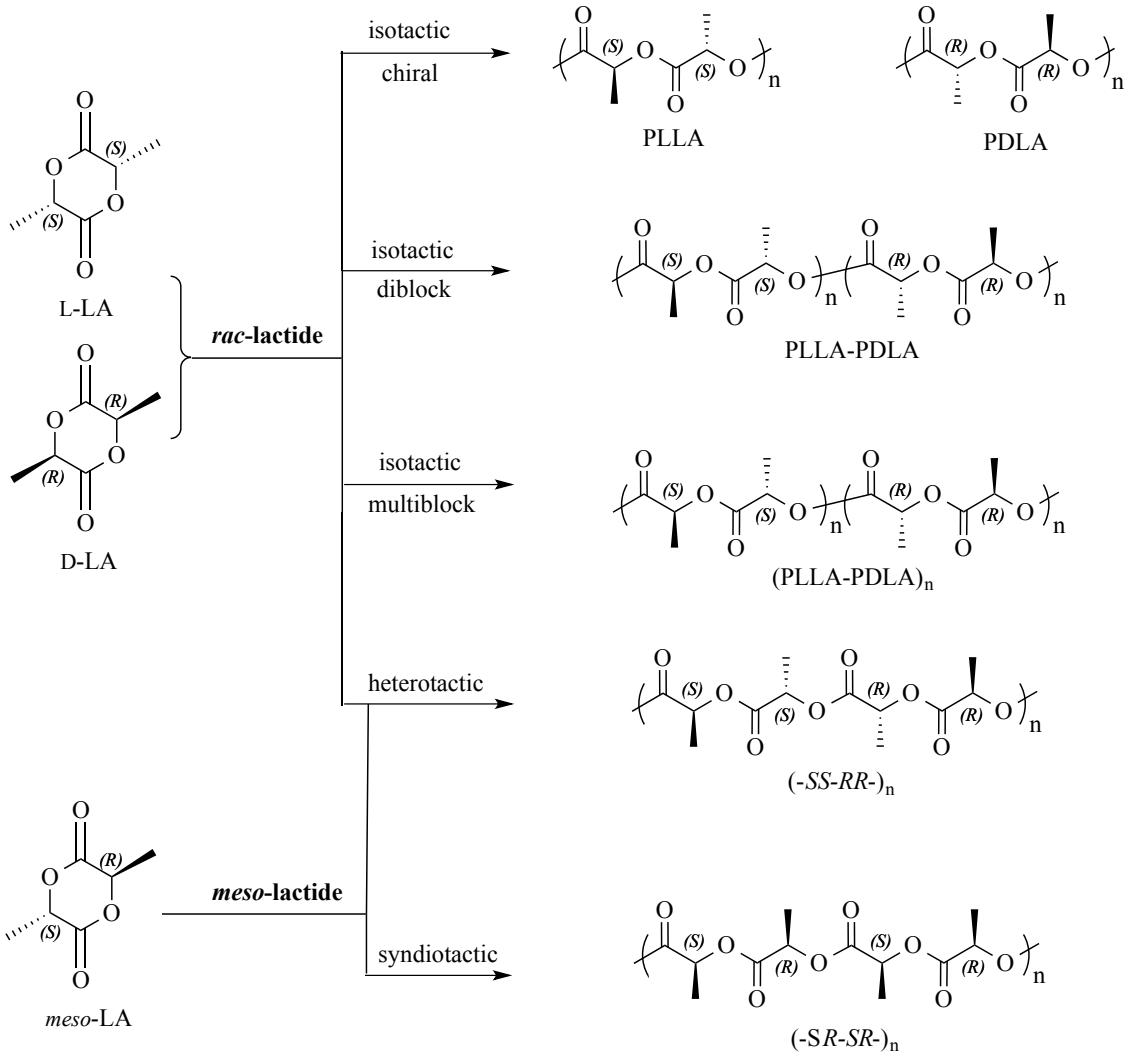

Figure 1.3.2: PLA microstructures from the stereocontrolled ROP of lactide from *rac*-lactide (*rac*-LA) and *meso*-lactide (*meso*-LA).[11]

A polymer with high regularity of methyl substituents in the same orientation along the polymer chain (isotactic) will have a semi-crystalline morphology such that poly L-lactide (PLLA) displays a melting temperature (T_m) up to 180 °C with a glass transition temperature (T_g) around 50 °C. Whereas, a polymer with random orientation of stereocontrol (atactic), will exhibit an amorphous structure with a phase transition at the T_g only. An eqimolar mixture of PLLA and poly D-lactide (PDLA) can result in an unusually stable type of crystal, called stereocomplex PLA. These crystals are of particular interest, since they exhibit a significantly higher melting point around 220-260°.[11,25] Stereocomplexation occurs when opposite chains (PLLA and PDLA) come into close proximity and form significantly more stable and crystalline stereocomplexed PLA than their isolated counterparts. Stereoblock copolymers also show stereocomplexation with an increase in T_m. Syndiotactic PLA is prepared from *meso*-LA giving

a polymer with singly alternating stereocentres.[26] Due to the high stereo-regularity of the polymer, syndiotactic PLA is also typically crystalline.

The combination of stereocentre pairs is used to describe the relationship of the neighbouring stereocentres. If the next subsequent stereocentre in the polymer chain is the same as the previous such as *–RR-RR-* and *–SS-SS-* it is described as isotactic (*i*). If the next subsequent stereocentre in the polymer chain is different to the previous such as *–RS-RS-* and *–SR-SR-* it is described as syndiotactic (*s*). It is possible to think of polylactide at a tetrad level (four stereocentres in a row, Figure 1.3.3).[27]

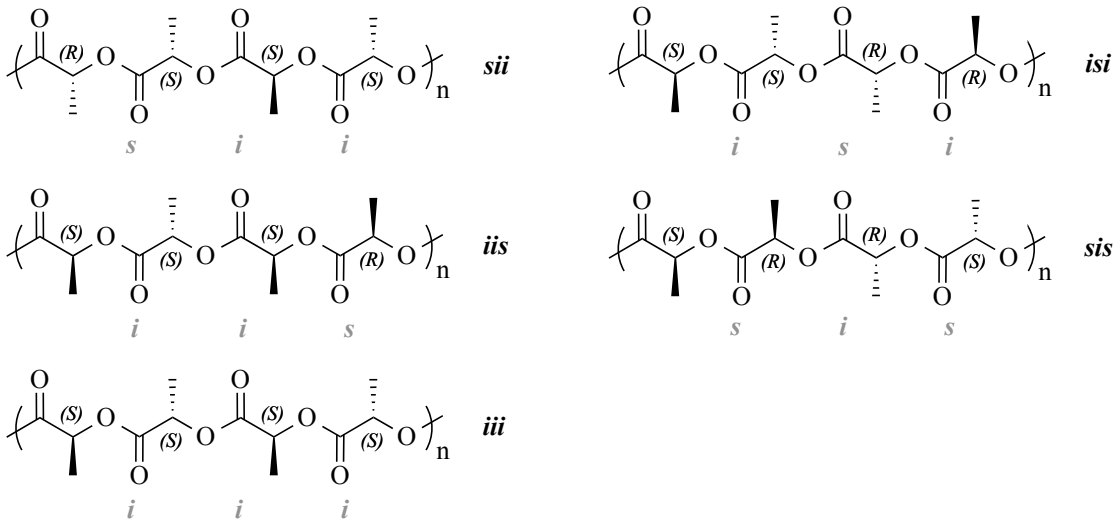

Figure 1.3.3: Tetrads of poly(*rac*)-lactide.[27]

Poly(L-LA) and poly(D-LA) have isotactic relationship between stereocentres and can be denoted as ***iii***. The polymerisation of *rac*-lactide or *meso*-LA will have additional stereocentre relationships such as ***sii,*** and ***iis***, ***sis*** and ***isi*** (Figure 1.3.3).[27] Di(syndiotactic) tetrads cannot be formed in the synthesis of poly(*rac*)lactide (i.e. ***sss***, ***iss*** or ***ssi***).

1.3.1 Homonuclear decoupled NMR spectroscopy

The schematic representation of poly(*rac*-)lactide below shows the ^{1}H homonuclear decoupled NMR and $^{13}C\{^{1}H\}$ NMR proton decoupled NMR for atactic PLA. For poly(*rac*-)lactide it is assumed that ***iis*** and ***sii*** are equivalent due to Bernoullian statistics. The integrals of the proton NMR are 1:1:1:3:2 as shown in Figure 1.3.4.

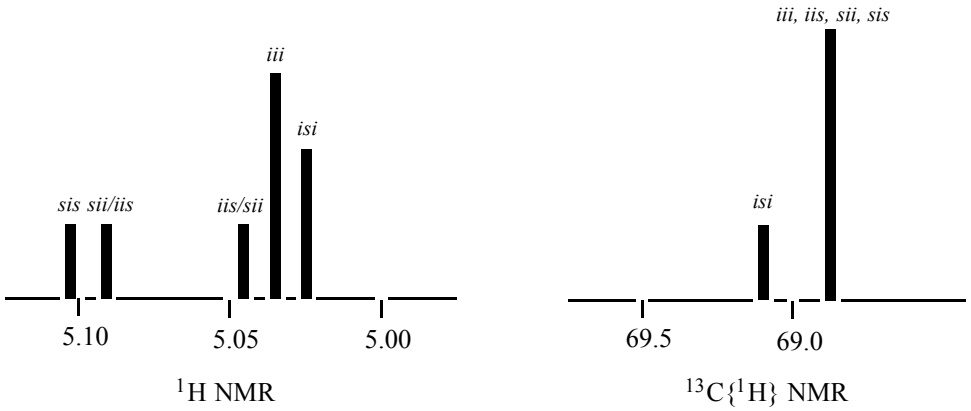

Figure 1.3.4: Schematic representation of poly(*rac*)-lactide at tetra level.[27]

Atactic PLA will exhibit five resonances in the homonuclear decoupled ^{1}H NMR, heterotactic PLA will display two resonances (***sis*** and ***isi***) and isotactic PLA will show one resonance (***iii***). The polymerisation of *meso*-LA will have stereocentre relationships such as ***sss***, ***ssi***, ***iss***, ***sis***, ***isi***. No di(isotactic) tetrads can be present for poly(*meso*-)lactide.

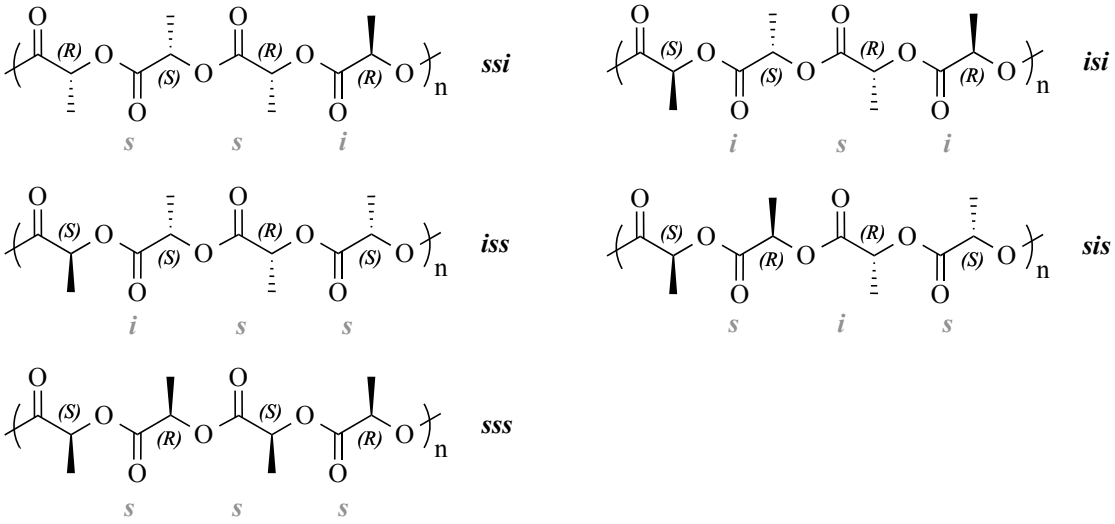

Figure 1.3.5: Tetrads of poly(*meso*)-lactide.[27]

For poly(*meso*-)lactide it is assumed that ***ssi*** and ***iss*** are equivalent due to Bernoullian statistics (Figure 1.3.6).

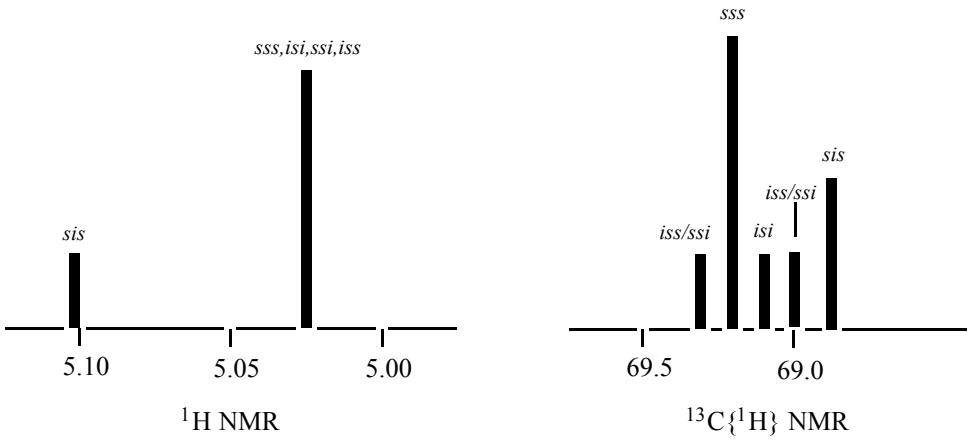

Figure 1.3.6: Schematic representation of poly(*meso*)-lactide at tetrad level.[27]

Previously, Munson *et al.* illustrated optical activity as a way of determining the tacticity of a polymer with poly(L-LA) PLLA as the standard (M_w > 6000, $\alpha^{22}{}_D$ = 142°).[24,26,28] More recently ^{13}C{^{1}H} NMR and ^{1}H NMR homonuclear decoupled spectroscopy are used to determine the tacticity of the polymer. Decoupling the methine proton from the methyl group allows the integrals of the peaks to be compared accurately.[24] Homonuclear decoupled NMR can be used to determine the tacticity of the polymer using the tetrad probabilities with current NMR fields. Reports by Thakur *et al.* even showed that hexad probabilities are possible to measure with a field of 500MHz.[29] There are five possible tetrads for PLA derived from both *rac*- and *meso*-lactide (Table 1.3.1).

Table 1.3.1: Tetrad probabilities based on Bernoullian statistics.[30]

	Probability	
Tetrad	*rac*-lactide	*meso*-lactide
[iii]	$P_m^2 + P_rP_m/2$	0
[iis]	$P_rP_m/2$	0
[sii]	$P_rP_m/2$	0
[sis]	$P_r^2/2$	$(P_m^2 + P_rP_m)/2$
[sss]	0	$P_r^2 + P_rP_m/2$
[ssi]	0	$P_rP_m/2$
[iss]	0	$P_rP_m/2$
[isi]	$(P_r^2 + P_rP_m)/2$	$P_m^2/2$

equations must be used to deduce the P_r value. Polymers derived from *meso*-LA use the equation [isi] = $P_m^2/2$.

1.3.2 Co-polymers

A co-polymer is a polymer that contains two or more different repeat units. Interestingly, the properties of polylactide can be adjusted, not only by adjusting the tacticity as discussed in the preceeding paragraph, but also by incorporation of chemically different co-monomers into the chain. The physical properties of the resulting co-polymer are determined by the sequence and stoichiometric proportions of monomers in the copolymer. The ability to exploit the change in thermal and mechanical properties of the polymer with the introduction of another monomer by copolymerization is of great interest both academically and industrially.[31] There are a variety of polymer architectures from linear to branched co-polymers, of which just a few are shown below (Figure 1.3.7).

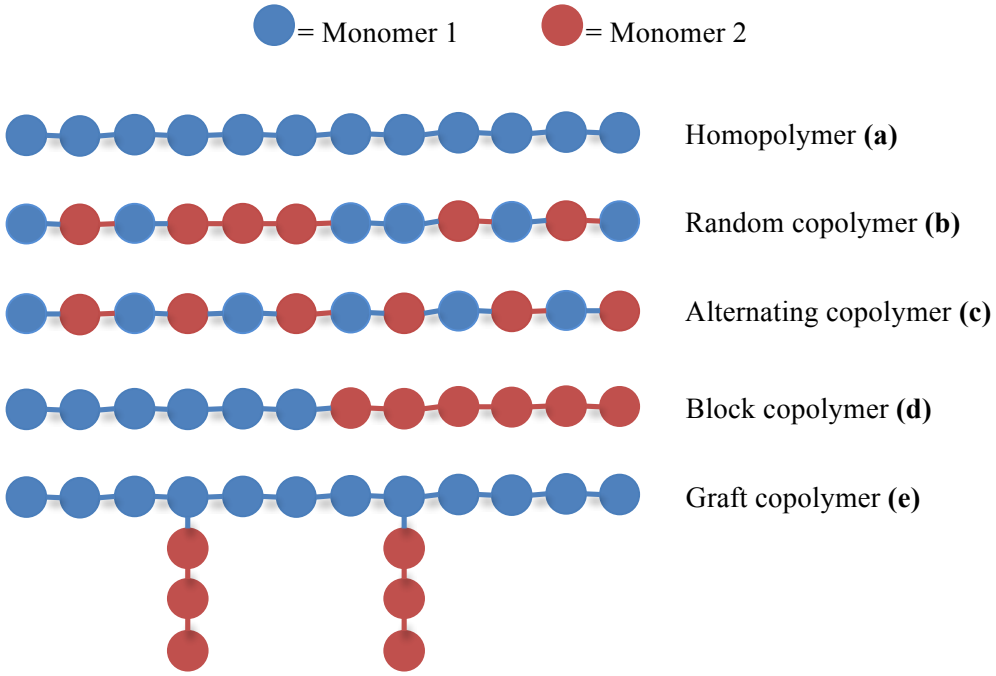

Figure 1.3.7: Co-polymer architectures.

A homo-polymer describes a polymer where the next monomer inserted is always the same as the previous (P_r = 0) and repeat units in the chain are all the same (Figure 1.3.7a). In a one-pot co-polymerisation of two different monomers (monomer 1 = M_1 and monomer 2 = M_2), the co-

polymer composition is dependent on the rate of propagation reactions as shown below (where k is the rate coefficient).

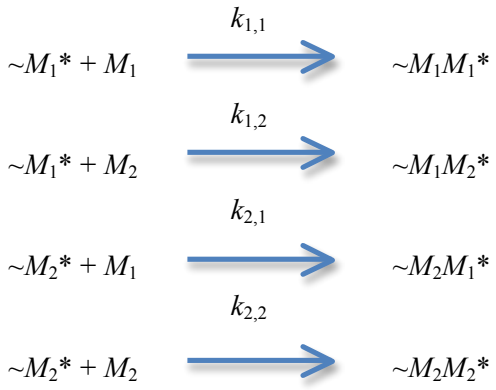

Figure 1.3.8: Four possible propagation reactions of co-polymerisation.

A random co-polymer (Figure 1.3.7b) is a type of statistical co-polymer and the repeat units are randomly distributed along the polymer chain. Alternating co-polymers (Figure 1.3.7c) consist of equal amounts of each monomer sequenced in a strictly alternating fashion (only $k_{1,2}$ and $k_{2,1}$, Figure 1.3.8). The distribution of repeat units alternates along the polymer chain and the probability of the next monomer in the chain being different is 1 ($P_r = 1$) and is relatively rare. The ability to fully disperse two different monomers with different properties in the chain is of great interest. Block co-polymers (Figure 1.3.7d) exhibit long blocks of one type of repeat unit followed by a long block of another type of repeat unit. There are different methods to synthesising block co-polymers; two of them being a one-pot synthesis or a sequential polymerisation. For a one-pot polymerisation, both monomers are put into a reaction flask in the presence of an active initiator. If the reaction rates of the monomers are different under these conditions, one monomer will preferentially polymerise, initially forming a homo-polymer. Thus, monomer 1 will preferentially polymerise after the polymerisation of a monomer 1 unit ($k_{1,1}$), and monomer 2 will preferentially polymerise after the polymerisation of a monomer 2 unit ($k_{2,2}$). As the monomer reaches near depletion, the other monomer will start to polymerise forming a di-block co-polymer. In order to determine the co-polymer composition, Mayo and Lewis devised an equation (Equation 1.3.1) using the kinetic data of co-polymerisations at low conversions (below 15 %).

Equation 1.3.1: Mayo-Lewis equation for the co-polymerisation of *rac*-LA with Ph-LA.

$$F_1 = 1 - F_2 = \frac{r_1 f_1^{\,2} + f_1 f_2}{r_1 f_1^{\,2} + 2 f_1 f_2 + r_2 f_2^{\,2}}$$

The Mayo-Lewis equation can be used to determine the reactivity ratios of the co-polymerisation of M_1 with M_2 where f_1 and f_2 are the mole fraction of LA and Ph-LA in the feed. F_1 and F_2 are the mole fraction of M_1 and M_2 in co-polymer. r_1 and r_2 are the reactivity ratios of M_1 and M_2 respectively in the co-polymer and are defined below:

$$r_1 = \frac{k_{1,1}}{k_{1,2}} \qquad r_2 = \frac{k_{2,2}}{k_{2,1}}$$

Alternatively, sequential polymerisation is achieved when monomer feed is controlled throughout the reaction. The polymerisation of one monomer (reaches near completion), followed by the introduction of another monomer to the reaction vessel allowing the formation the desired di-block co-polymer. Enantiopure lactide segments as the blocks in block co-polymers can be utilized for the formation of stereocomplexed PLA crystals. Graft polymers are a type of branched polymers, where generally a core homo-polymer backbone is observed with branches of a different homo-polymer consisting of a different repeat unit, as shown in Figure 1.3.7e. As previously mentioned, stereocomplex PLA (**sc**-PLA) is the mixing of enantiomerically pure poly L-lactide (PLLA) with pure poly D-lactide (PDLA) either as two homo-polymers or as components of the copolymer itself (Figure 1.3.9).[32–34]

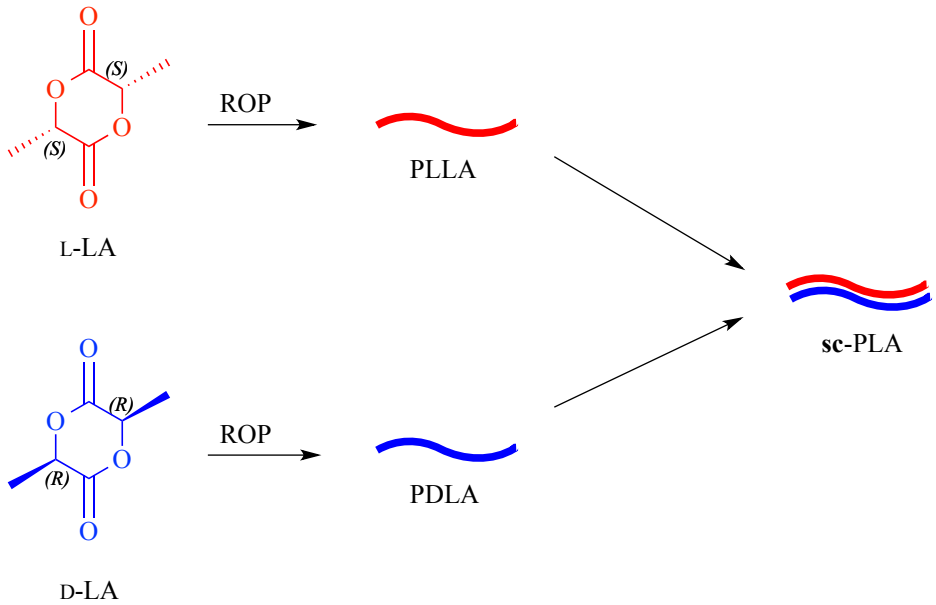

Figure 1.3.9: Synthesis of stereocomplexed PLA.

These hydrogen bond interactions between two pure forms of polylactide enhance the mechanical properties, as well as the thermal resistance and the hydrolysis-resistance of the PLA based material. The result is a significant increase in both melting temperature (T_m) and glass transition temperature (T_g) which can be monitored using differential scanning calorimetry (DSC).[14]

1.4 Initiators

1.4.1 Tin Initiators

PLA is predominantly synthesised using tin (II) bis(2-ethylhexanoate), otherwise known as tin(II) octanoate or $Sn(Oct)_2$.[35] It is commercially available, inexpensive, easy to handle and soluble in common organic solvents and lactide. Many mechanisms were reported for the reaction of $Sn(Oct)_2$ with lactide including activated monomer, cationic and ROP. During the reaction of $Sn(Oct)_2$ with lactide, a non-linear relationship on catalyst amount was observed; the reaction was dependent on the quantity of impurities such as water and octanoic acid present in the initiator. Interestingly, these impurities allow the *in situ* formation of tin (II) alkoxides which act as the active species in the polymerisation of lactide. Thus, it is accepted that the mechanism in question is in fact coordination insertion[13] In the presence of a protic reagent, such as an alcohol, additional formation of tin (II) alkoxides occurs from $Sn(Oct)_2$ (Figure 1.4.1).[12,36]

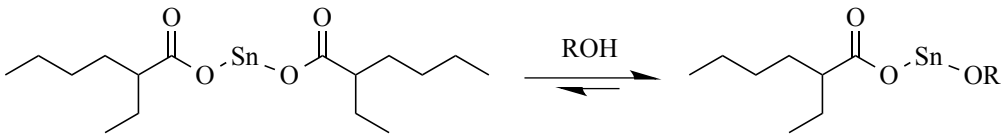

Figure 1.4.1: Formation of active tin(II) alkoxide in the presence of a protic reagent.[36]

Addition of benzyl alcohol which acts as a co-initiator allows a much faster reaction rate. In the ROP of lactide, $Sn(Oct)_2$ in the presence of benzyl alcohol forms high molecular weight polymers using low catalytic loadings under solvent free conditions (at 110°C for 24 h affords 98% conversion). Benzyl alcohol is generally used as it is inexpensive, commercially available, easy to handle and is also a valuable end group due to possible cleavage by H_2/Pd in order to re-activate the carboxylic end group. This cleavage enables the possibility of functionalising the final polymer, which is of great interest.[37] Although $Sn(Oct)_2$ is accepted as a non-toxic initiator

and is approved by the American Food and Drug Administration (FDA), the toxicity associated with harmful tin hydroxide species contribute to considerable limitations for use in the biomedical industry.[38]

In 2001, Gibson and co-workers reported the first single-site tin(II) initiator for the ROP of lactide. A tin(II) isopropoxide coordinated to a BDI ligand was synthesised as shown below (Scheme 1.4.1).

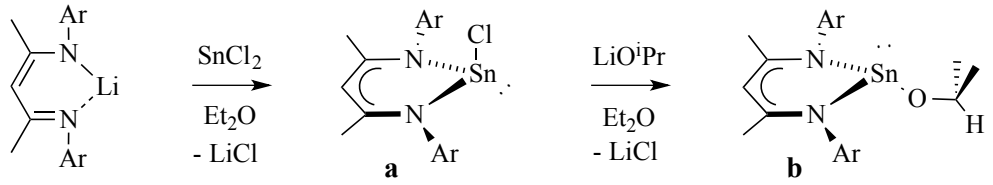

Ar = 2,6-Pr^i_2-C_6H_3

Scheme 1.4.1: Synthesis of tin initiator developed by Gibson *et al*.[39]

Initially, [HC{C(Me)NAr}$_2$]Li was reacted with $SnCl_2$ to afford **a**, followed by treatment with lithium isopropoxide to yield the desired initiator **b**. Investigations into the ROP of *rac*-lactide using initiator **b** were undertaken in CH_2Cl_2 at 25°C with a monomer to initiator loading of 100:1. Under these conditions, complete conversion (>99%) of monomer occurred after 96 h to yield a resulting polymer that coincided with the theoretical molecular weight (M_n = 17100 and 14400 g.mol^{-1}, are the observed and calculated molecular weights respectively), with a narrow PDI (PDI = 1.11). The reaction was repeated at the elevated temperature of 60°C in toluene, increasing the activity of the initiator (85% conversion in 4 h) whilst maintaining a narrow molecular weight distribution (PDI = 1.05). Various tin BDI-type derivatives including some aromatic and alkyl substituents were synthesised and trialled for the ROP of *rac*-lactide. All initiators demonstrated a moderate heterotactic bias and polymerised *via* chain end control due to the $5s^2$ lone pair of electrons present on the central tin(II) moiety.

Later, in 2002, Tolman *et al.* reported monomeric initiators of tin(II) alkoxide complexed to bulky amidinate ligands.[40] Various complexes with modified alkyl silyl moieties were active for the polymerisation of lactide at 80°C in toluene with a monomer: initiator loading of 450:1. Further control of polymerisations was achieved with addition of an exogenous alcohol co-initiator such as benzyl alcohol.

In 2003, Chisholm and co-workers reported the synthesis of tin(IV) initiators including Ph_2SnX_2 (where X = NMe_2 or OPr^i) complexes.[41] These initiators demonstrated activity for the ROP of

L-lactide, although at a slow rate. For $Ph_2Sn(NMe)_2$, GPC analyses of the final polymer displayed bi-modal traces indicative of cyclic and long chains (24 kDa) polymers *via* both intra- and inter-chain transesterification. $Ph_2Sn[OCHMeC(O)OPr^i]_2$ was generated due to the vast amount of transesterification taking place. Conversely, polymers obtained using $Ph_2Sn(O^iPr)_2$ displayed mono-modal GPC traces along with the formation of $Ph_2Sn[OCHMeC(O)OPr^i]_2$ suggesting only inter-chain transesterification occurred. Further investigations with Ph_3SnX complexes were trialled and showed similar results.[41]

1.4.2 Group 4 Initiators

Group 4 metal initiators are recognized to give high activity and selectivity due to their strong Lewis acidic nature.[42–49] Kricheldorf *et al.* first reported active Group IV metal alkoxides for the ROP of various cyclic esters. It was reported that zirconium *n*-propoxide was active in the polymerisation of L-lactide under solvent free conditions (95°C), converting 92 % of monomer in 24 h.[50] Later, Kol and co-workers reported titanium and zirconium complexes incorporating bulky dianionic and trianionic amine-phenolate ligands which were active in the ROP of L-lactide.[51,52] Zirconium initiators were found to have a much higher activity than the titanium complexes.

Group 4 metal complexes coordinated to tetradentate bis(phenolate) (ONNO)-type ligands such as salan, salen and salalen and their activity in the ROP of lactide will be discussed in this section. Davidson and co-workers investigated symmetrically substituted salan-type ligands which when complexed to Group 4 metals exhibit a C_2 *pseudo*-octahedral orientation as shown below (Scheme 1.4.2).[44]

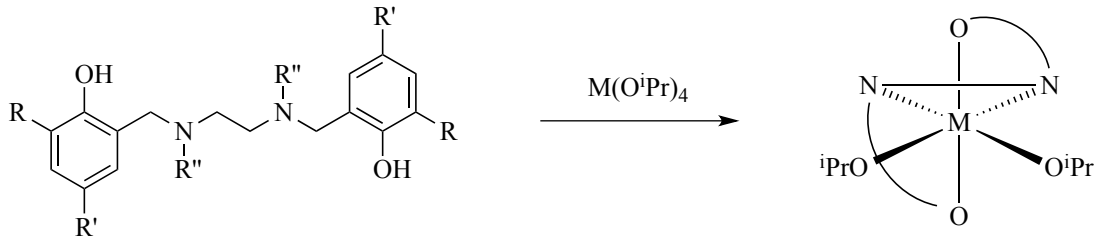

1aH$_2$ R = R' = R" = Me
1bH$_2$ R = R' = ^{t}Bu, R" = Me
1cH$_2$ R = H, R' = NO_2, R" = Me

C_2 symmetry

M = Ti, Zr, Hf

Scheme 1.4.2: Synthesis of Group 4 amine bis(phenolate) complexes.[44]

The Group 4 amine bis(phenolate) complexes (Scheme 1.4.2) were trialled in the ROP of L-lactide and *rac*-lactide. Kol and co-workers synthesised chloro- substituted and *tert*-butyl substituted Ti**1b**(O^iPr)$_2$ complexes which demonstrated moderate activity for the ROP of L-lactide under solvent-free conditions.[45] In solution, Davidson and co-workers reported only Zr**1a**(O^iPr)$_2$ was active in the ROP of *rac*-lactide in toluene converting >99 % monomer with a monomer to initiator loading of 100:1 at 110°C. Under solvent-free conditions, analogous titanium initiators afforded atactic PLA (62 % - 74 % conversion, 2 h, 130°C, 300:1 monomer:initiator loading). Promisingly, under solvent free conditions, where M = Zr, M**1a**(O^iPr)$_2$, afforded isotactic PLA in the ROP of *rac*-lactide.[44] The C_2-orientation of the Zr and Hf complexes attributes to the tacticity of the resulting polymer. The lack of stereocontrol for titanium species was attributed to the inability of the titanium-lactate species to back-chelate due to its small coordination sphere.

More recently, Davidson *et al*. investigated zirconium and hafnium amine tris(phenolate) analogues in the ROP of *rac*-lactide under solvent-free conditions at 130°C (Figure 1.4.2).[53]

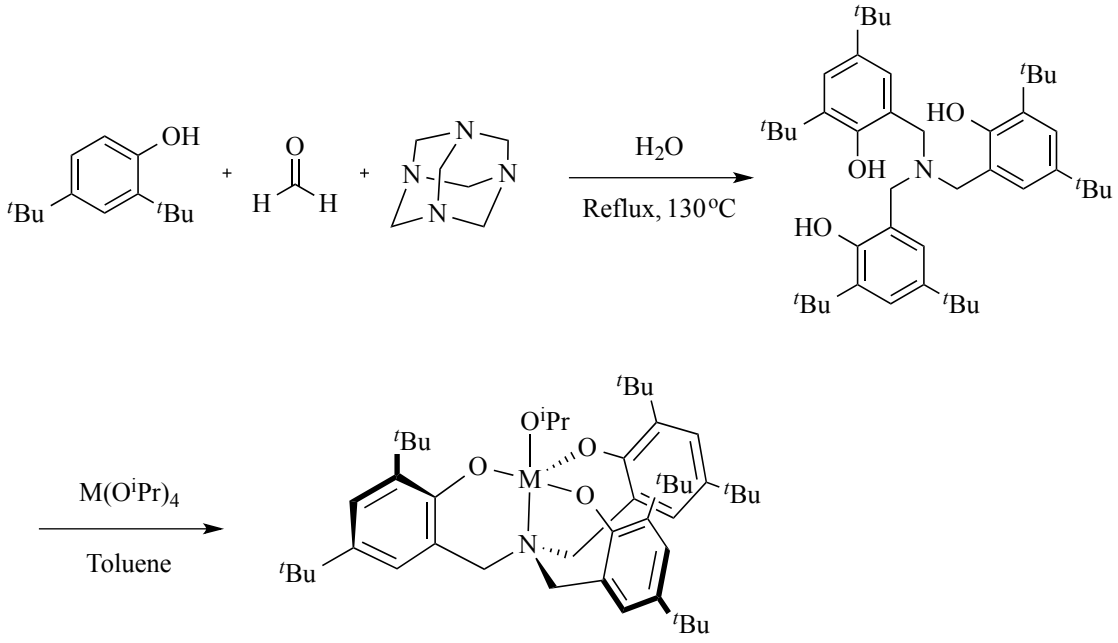

Figure 1.4.2: Amine tris(phenolate) initiators reported by Davidson *et al.*[53]

Interestingly, zirconium and hafnium complexes demonstrate an unprecedented combination of high activity (95 % conversion in 30 min) whilst retaining high stereoselectivity (P_r > 0.90.[53] Conversely, titanium amine tris(phenolate) afforded atactic PLA (P_r = 0.5). It is suggested that small differences in the coordination mode of the metal centre to the growing chain account for

the differences in tacticity between metal centres.[54] Furthermore, the ligand exhibits C_3 – symmetry and appears propeller-like. In the case of zirconium and hafnium amine tris(phenolate) complexes, it is proposed that axial inversion of the ligand occurs after addition of a monomer to the propagating chain, which is responsible for the desired heterotactic bias (alternating stereochemistry) at the active metal centre of the initiator. It is still unknown which mechanism is predominant during polymerisation, either ligand dependent sterical chain-end control or dynamic enantiomorphic site control.[53]

Verkade and co-workers synthesised a variety of 5-coordinate titanium complexes (titanatranes) with varying steric bulk and ring sizes as shown below (Scheme 1.4.3). Titanatranes where an alkoxyl moiety lies *trans*-axial to Ti-N in orientation was utilized in order to further labilize the OR group and forming OR as the end group, thus controlling molecular weight. The complexes were trialled for the ROP of L- and *rac*-lactide under solvent free conditions (300:1 monomer:initiator, 130°C).[55]

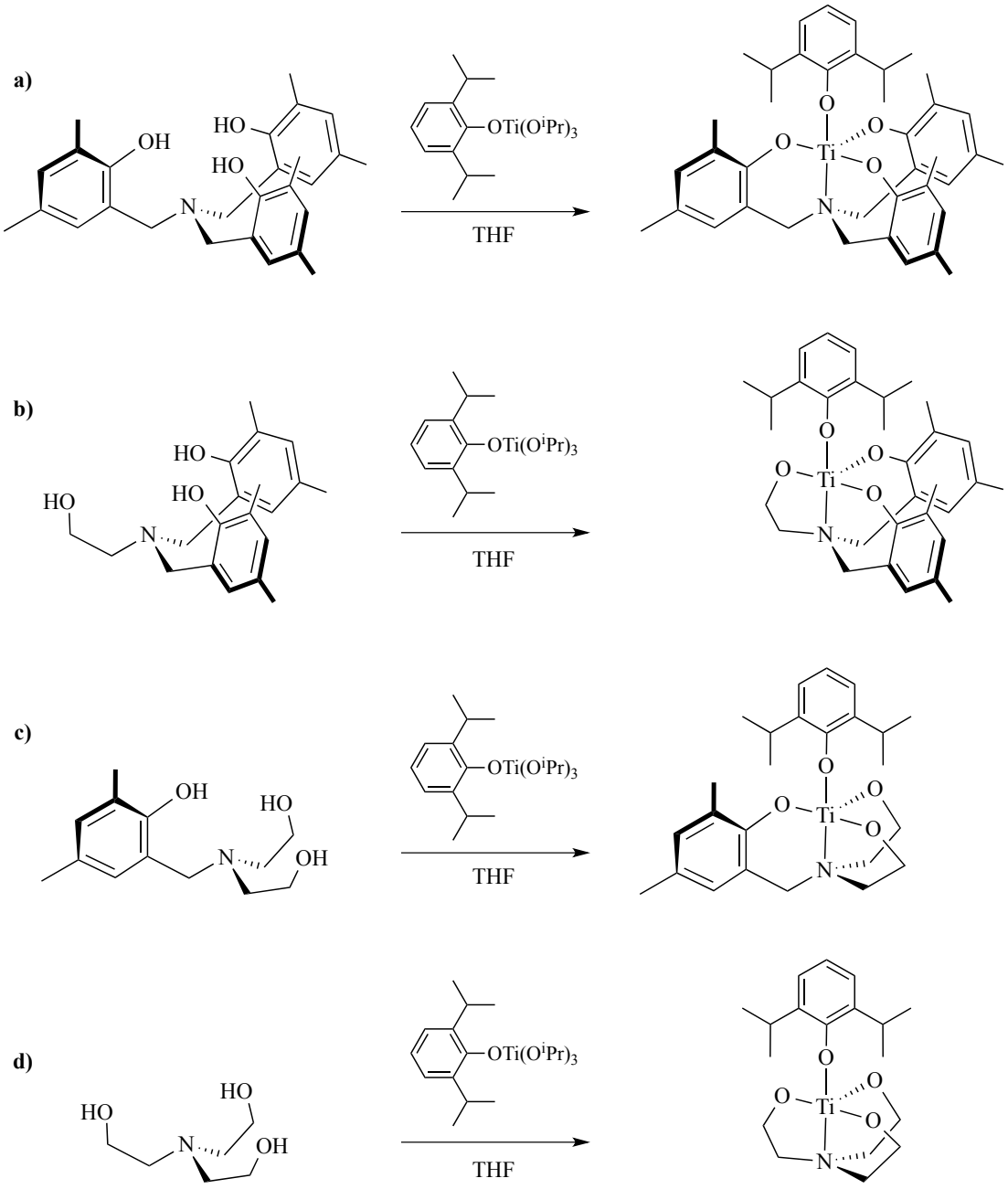

Scheme 1.4.3: Synthesis of titanatranes as reported by Verkade *et al.*[55]

Verkade *et al.* reported as the number of 5-membered rings in the tetradentate ligand increases, the activity of the initiator increases along with increased PDI.[56] Unfortunately, the initiators generally yielded polymers with high PDI values and low molecular weights. This could be attributed to $k_{initiation} < k_{propagation}$. Furthermore, bimodal traces were observed by GPC for some of the polymers, which is indicative of transesterification or slow initiation. All polymers synthesised from *rac*-lactide yielded atactic polymers, whereas for L-lactide only isotactic PLA was afforded, as expected.

Verkade and co-workers also studied dimeric titanium alkoxides in the ROP of lactide under solvent free conditions.[56,57] (Ti(**L**)O^{i}Pr)$_2$ was synthesised using commercially available triethanolamine ligands with titanium *tetra*-isopropoxide as shown in Scheme 1.4.4.

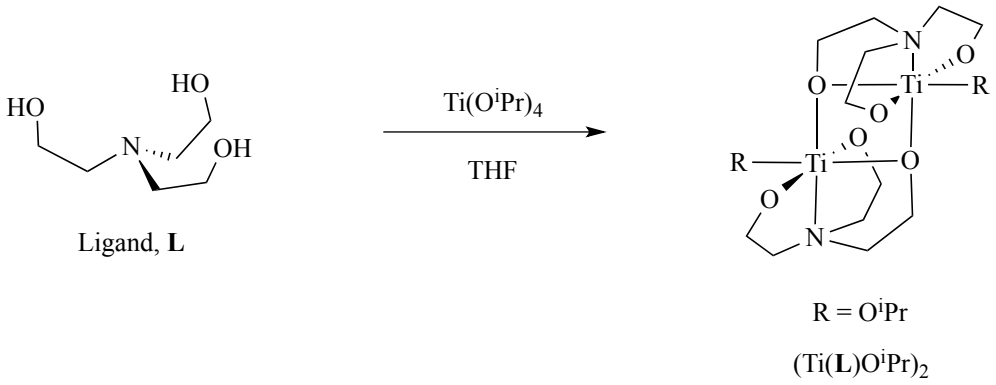

Scheme 1.4.4: Synthesis of bi-meric (Ti(**L**)O^{i}Pr)$_2$.[56]

(Ti(**L**)O^{i}Pr)$_2$ was screened for the ROP of L-lactide and *rac*-lactide and proved an active initiator in both solution and bulk conditions. The solvent free polymerisation of *rac*-lactide was trialled ([monomer]:[Ti] 300:1 at 130°C) and converted 66 % in 2 h with molecular weight of 135.0 kg.mol^{-1} (PDI = 1.70) . The reaction was repeated and allowed to reach near completion (90%), here, a much higher molecular weight and PDI were observed (M_w = 303.6 kg.mol^{-1}, PDI = 2.55). A linear relationship was observed for Mw and conversion suggesting a well-controlled polymerisation.[56] A mono-modal trace was observed by GPC for the first reaction however, with the second polymerisation exceeding 80% conversion a bi-modal trace was reported suggesting higher degrees of transesterification are present at elevated conversion.[56]

Verkade *et al.* also reported a tetrameric titanium alkoxide initiator (Scheme 1.4.5) for the ROP of lactide both in solution and under solvent free conditions (130°C).[58]

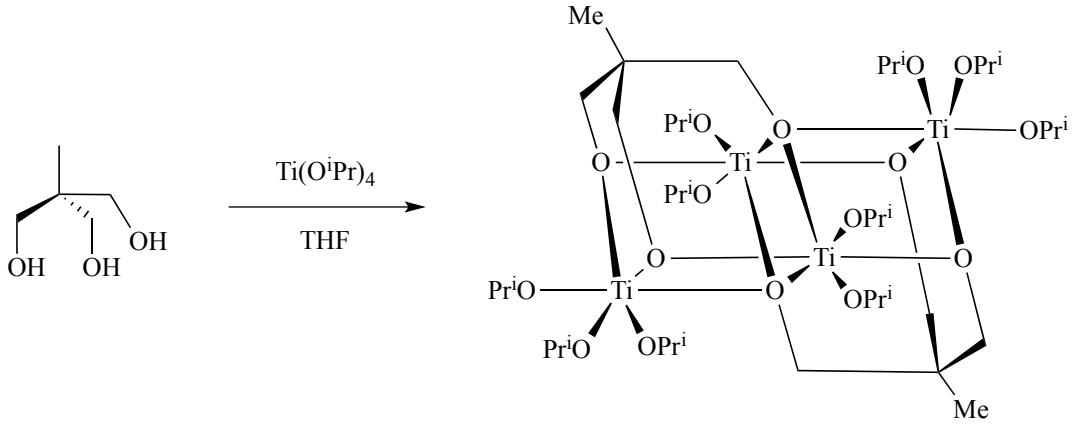

Scheme 1.4.5: Synthesis of tetrameric titanium alkoxide initiator.[58]

It was thought that the increased number of possible labile initiator groups would increase possible activity of the complex.[59] Moderate activity was achieved converting L-lactide under solvent free conditions converting to near completion after 12 h. Broad molecular weight distributions were observed for bulk polymerisation whereas solution polymerisation afforded polymers with a narrower molecular weight distribution and thus a more controlled polymerisation.[58]

1.4.3 Other Initiators

There are many ligand systems that have been studied in the synthesis of stereocontrolled PLA as shown below (Figure 1.4.3).

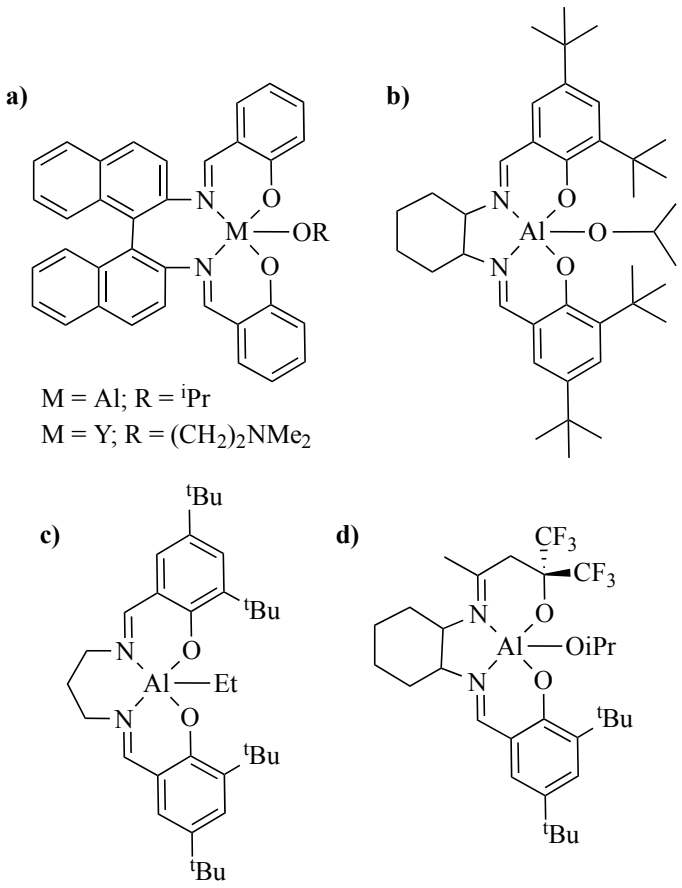

Figure 1.4.3: Reported salen-type initiators for the ROP of lactide.[11]

Spassky *et al*. first reported the stereoselective ROP of *rac*-lactide with an aluminium initiator containing a chiral BINAP derived salen Schiff base-type ligand (Figure 1.4.3a).[60] Initial conversion was slow but relatively enantiomerically enriched with poly-(D-LA). This suggests that most of the D-LA was used up first, then L-LA is incorporated into the polymer. An increase in melting point was reported suggesting stereocomplexation. Coates *et al.* used this chiral initiator and formed highly syndiotactic PLA from *meso*-LA. By replacing aluminium for yttrium, atactic PLA from *meso*-LA was afforded.[26] Majerska and Duda devised an experiment using one enantiomer of the chiral aluminium initiator until 50 % of the *rac*-lactide is converted. Then addition of the other enantiomer of the chiral aluminium initiator, this afforded a PLLA-PDLA stereoblock co-polymer which is thought to occur *via* a ligand exchange mechanism. Stereocomplexation is observed as the thermal stability significantly increased (T_m = 210 °C).[61]

Feijen *et al*. complexed aluminium to commercially available cyclohexylsalen ligand, otherwise known as Jacobsen's ligand (Figure 1.4.3b). ROP of lactide in toluene at 70°C generated PLA with controlled M_w and low PDI. Kinetic analysis of the reaction suggests *pseudo*-first order

reaction. (R,R)-CyclohexylsalenAlO^{i}Pr polymerises L-LA preferentially over D-LA (k_L/k_D of ~14). The polymerisation of *rac*-lactide under melt conditions (solvent free, 135 °C) affords crystalline PLA. The polymerisation of L-LA: D-LA 80:20 yields isotactic-atactic block co-polymer with highly crystalline properties (T_m = 155 °C) due to domains of stereocomplexation.[62]

A number of achiral salen-type ligands have been reported with promising results. Nomura *et al.* and Gibson and co-workers reported that by increasing the steric bulk around the metal centre of the initiator PLA with increased stereocontrol was produced, resulting in heterotactic PLA (Pr = 0.81) (Figure 1.4.3c). Whilst the polymerisation rates are slow with increased steric bulk at the *ortho*-position of the phenoxy-moiety, the increase in resulting stereocontrol more than compensates (T_m = 170-192 °C). This suggests a chain end control mechanism is taking place. Nomura reported that by increasing the imine linker moiety and thus making the linker more flexible, an increase in stereocontrol was observed.[63,64]

Carpentier *et al*. introduced electron withdrawing trifluoromethyl substituents to the salen Schiff base type ligand asymmetrically (Figure 1.4.3d). In solution (70 °C, toluene), the polymerisation afforded isotactic PLA (P_m = 0.81).[65]

β-Diketiminato (BDI) complexes have also illustrated stereocontrol in the ROP of *rac*-lactide (Figure 1.4.4).

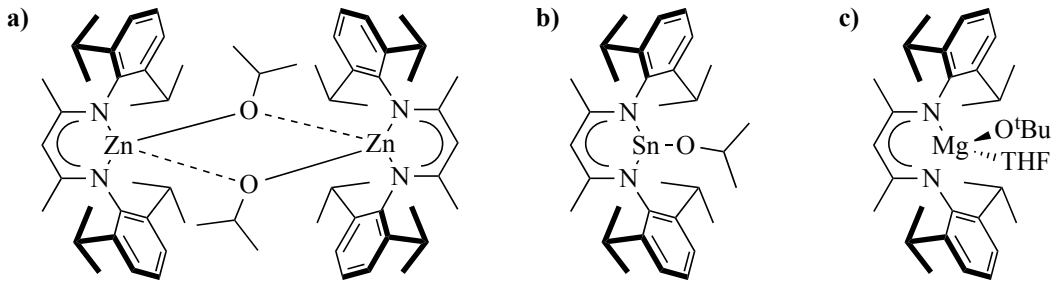

Figure 1.4.4: Reported BDI-type initiators for the ROP of lactide.[11]

Coates *et al*. studied zinc isopropoxide BDI systems (Figure 1.4.4a) which afforded heterotactic PLA (P_r = 0.94) with low PDI. Decreasing the steric hindrance of the *ortho*-substituents on the aromatic rings around the metal centre results in decreased rate and stereocontrol of polymerisation.[66] Tin (II) and magnesium BDI complexes were also active in the ROP of lactide and demonstrate a degree of stereocontrol. Tin (II) isopropoxide BDI complex (Figure 1.4.4b)

produces PLA with a slight heterotactic bias ($P_r = 0.70$). It is thought this value is low due to the lone pair on the metal centre.[9,11] Interestingly, magnesium BDI complexes (Figure 1.4.4c) are only stereoselective in THF solvent ($P_r = 0.90$).[67] Under the same conditions changing the solvent to dichloromethane or benzene resulted in atactic PLA. Chisholm and co-workers investigated the effect of THF studying low temperature ^{1}H NMR of ROP using zinc and magnesium BDI systems. Chisholm and co-workers concluded that for the zinc complex the THF moiety rapidly dissociates with toluene-*d8* or CD_2Cl_2. Conversely, both THF coordinated to the metal centre, and free THF were observed in the low temperature ^{1}H NMR spectrum for the analogous magnesium complex.[67] It is proposed that THF coordinated to the magnesium BDI complex, yielding a more sterically hindered metal centre. Computational studies determined both electrostatic and stereocelectronic interactions control the insertion of monomer and a chain end control mechanism occurs.[54]

The reader is directed to the following recent publications for further details regarding numerous other known initiators in the ring-opening polymerisation of lactide.[68–73]

1.5 Co-polymers

Industrially, the use of inexpensive commercially available monomers is of great interest in synthesising functional copolymers that are industrially viable. The ability to incorporate copolymers blocks with a significantly different glass transition with blocks of lactide will be probed, with the further intention of stereo-complexing the copolymers either with themselves or with the addition of another copolymer. Fusing the two principles of copolymerisation and stereocomplexation to obtain a polymer with fine-tuned properties is a useful tool for the design of functional materials.

1.5.1 Lactide co-polymers with ε-caprolactone and δ-valerolactone

The co-polymerisation of lactide with ε-caprolactone (ε-CL) and δ-valerolactone (δ-VL) have been well documented as they are both biodegradable and biocompatible.[74,75] Thus, there have been various investigations in their potential in both medical and pharmaceutical applications. PCL is flexible, tough and has great potential in drug delivery as it hydrolyses into 6-hydroxy caproic acid *in vivo* which can be fully metabolised by the citric cycle.[14] PVL (T_m 62°C) exhibits similar properties to PCL, however as it is less reactive in ROP than PCL, it is less explored.[75,76] The ability of combining the physical properties of each polymer with lactide in the resulting co-polymer through co-polymerisation is of great interest (Scheme 1.5.1). For

example, PCL (T_m 61°C, T_g -60°C) exhibits good elasticity at room temperature but with a low modulus. Conversely, PLA displays a high Young's modulus but poor elasticity, hence co-polymers of PCL-PLA could show both good elasticity and mechanical properties. The combination of rapid degradation (PLA) and permeability at body temperature (PCL) allow co-polymers to be utilised in drug delivery systems.[44]

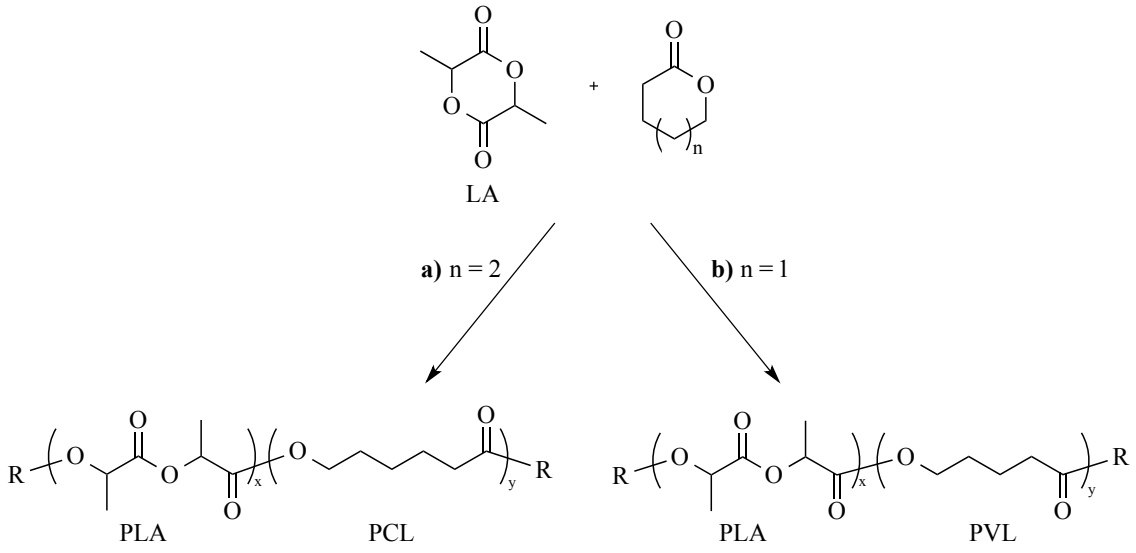

Scheme 1.5.1: Synthesis of lactide co-polymers with **a)** ε-caprolactone and **b)** δ-valerolactone.

Davidson *et al.* reported the synthesis of PCL-PLA block co-polymers using Group 4 amine bis(phenolates).[44] In order to generate block co-polymers, the importance of monomer addition was highlighted. By sequential polymerisation, only PCL-PLA co-polymers were synthesised. Conversely, attempts to synthesise PLA-PCL co-polymer were unsuccessful, only generating PLA homo-polymers.[44] In 2008, Florczak and Duda reported the one-pot synthesis of PLA-PCL co-polymers in solution (THF, 80°C) using a chiral Schiff base-type ligand coordinated to aluminium alkoxide.[74] Interestingly, the co-polymer architecture differed depending on the chirality of the diphenolate Schiff base. (S)-ligand complexed to aluminium alkoxide yielded block co-polymers whereas the (*R*)-ligand analogue afforded random copolymers.[74] More recently (2012), Pellecchia *et al.* studied the synthesis of random co-polymerisation of *rac*-lactide and ε-caprolactone. It was found that depending on the relative proportional content of PCL and PLA within the resulting co-polymer, the thermal properties could be modified in a linear fashion (T_g ranging from -60°C to 45°C).[77]

Similar to PCL, in the co-polymerisation of lactide with PVL, the amount of PVL present in the resulting co-polymer can alter its polymeric physical properties.[78] Darensbourg and co-workers probed the activity of Schiff base aluminium complexes for the ROP of δ-valerolactone and lactide. The results showed lactide was preferentially polymerised over δ-valerolactone. Thus, yielding a PLA-PVL co-polymer from a one-pot synthesis.[76]

1.5.2 Lactide co-polymers with PDL

ω-Pentadecalactone (PDL) is a commercially available 16-membered cyclic ester. Due to abundance of methylene moieties within the structure, a low ring strain is observed compared to lactide and therefore a reduction in reactivity. The ROP of PDL to PPDL is little explored and the ability to incorporate long aliphatic chains into a lactide co-polymer is of great interest (Scheme 1.5.2).

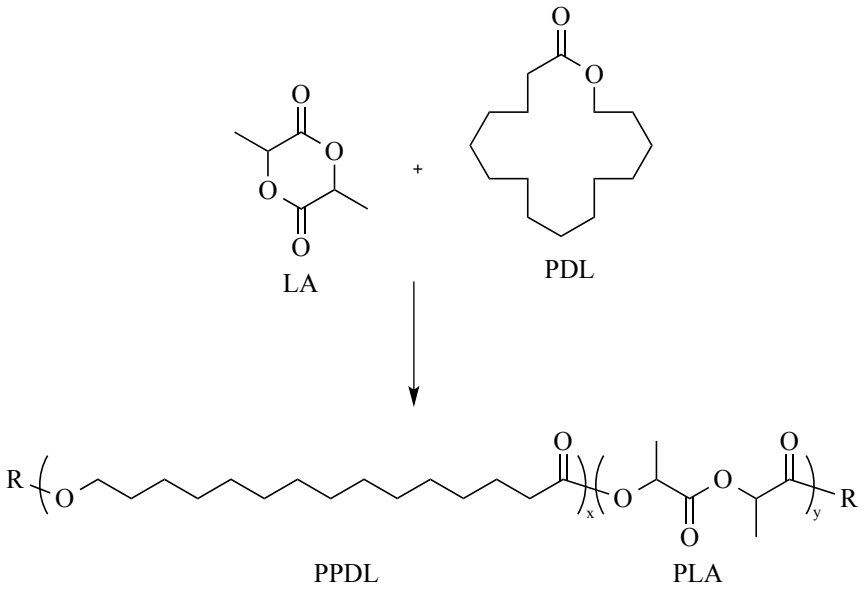

Scheme 1.5.2: Co-polymerisation of lactide and ω-pentadecalactone.

Initially, Kobayashi and co-workers investigated the polymerisation of PDL enzymatically using lipase. Gross *et al.* then successfully achieved high molecular weight PPDL (M_w 86.00 kg.mol^{-1}) using Novozyme 435 (lipase B from *Candida Antarctica*) converting 90 % of monomer in 2 hours. Later, investigations into organometallic initiators were of interest. Feijen and co-workers utilised commercially available yttrium isopropoxide under solvent free conditions (400:1 monomer: initiator, 100°C) converting 70 % to PPDL in 5 minutes.[79] In 2011, Tsutsumi *et al.* demonstrated rare earth tetrahydroborates were highly active in the ROP of PDL converting 83 % in 1 minute in solution (THF, 60°C 150:1 monomer: initiator).[80] More recently,

Duchateau and co-workers have probed the co-polymerisation of PDL with other small-ring lactones such as ε-caprolactone.[81,82] PCL-PDL co-polymers exhibit a good combination for biodegradable shape-memory materials.[83,84] Co-polymerisation of PDL with ε-caprolactone was investigated using an inexpensive commercially available *N*-heterocyclic organo-catalyst (1,5,7-triazabicyclo[4.4.0]dec-5-ene (TBD)) in the presence of benzyl alcohol under solvent free conditions.[81] Various PCL-PDL random co-polymers were afforded by careful control of monomer feed. The ability to modify thermal properties was observed by varying the co-monomer content. For example, the melting temperature (T_m) of the co-polymer decreases with increasing amounts of PCL (T_m from 95°C to 54°C).[81] In 2013, Duchateau *et al.* reported the co-polymerisation of PDL with small-ring lactones using aluminium salen initiators.[85] The influence of initiator, kinetics and co-polymerisation were investigated. Initially, the synthesis of PCL-PPDL block co-polymers was unsuccessful due to rapid transesterification yielding random co-polymers. However, it was found that block-co-polymers were achieved by careful monitoring of monomer feed during sequential polymerisation.[85]

1.5.3 Synthesised Monomers

In order to enhance and improve the properties of lactide, a range of related monomers have been reported with the intention to polymerise and co-polymerise with lactide. A variety of methods are reported in the literature.

Baker *et al.* reported the synthesis of various functionalised lactides. Commercially available α-hydroxy acids were selected and reacted *via* three different methods:[86] Method a) formation of cyclic ester occurs by acid catalysed oligomerisation of the α-hydroxy acid followed by cracking at 180°C. Method b) involves the addition of bromoacyl bromide in the presence of triethylamine. Method c) utilises the dimerization of α-hydroxy acid in the presence of *p*-toluenesulfonic acid.[87]

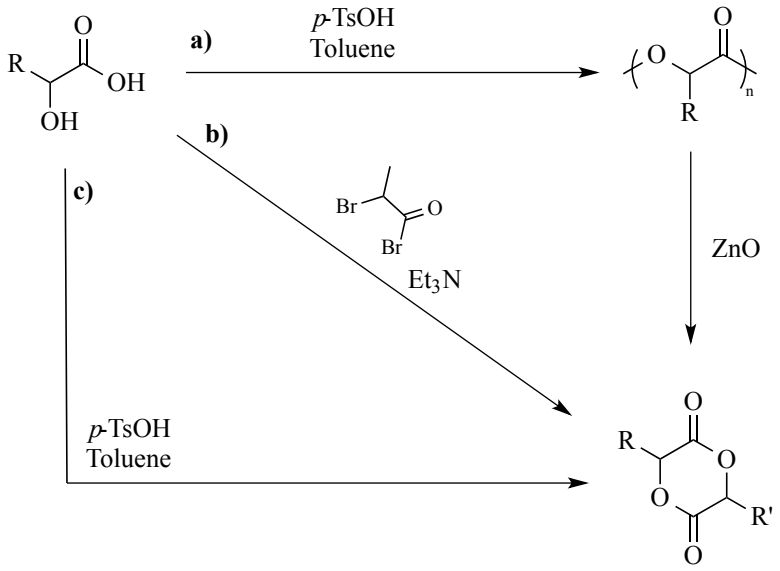

Scheme 1.5.3: Synthesis of functionalised cyclic monomer. [86,87]

The synthesised cyclic monomers were trialled for the ROP with $Sn(Oct)_2$ in the presence benzyl alcohol under solvent free conditions (130°C, 100:1:1 monomer: initiator: ROH). It was reported that with increased steric bulk of the monomer, a decrease in reactivity rate was observed.[87]

Alternatively, by utilizing the commercial abundance of L-lactide, Hillmyer and co-workers devised an approach to synthesise novel monomers using L-lactide as a starting material. Initially, L-lactide underwent bromination, followed by elimination to yield an alkene substituent (vinyl-LA). This could then be utilised and exploited as a potential dienophile and reacted with various cyclic dienes *via* a Diels-Alder reaction to afford a new tricyclic monomer on a multi-gram scale as shown below in Scheme 1.5.4.[88]

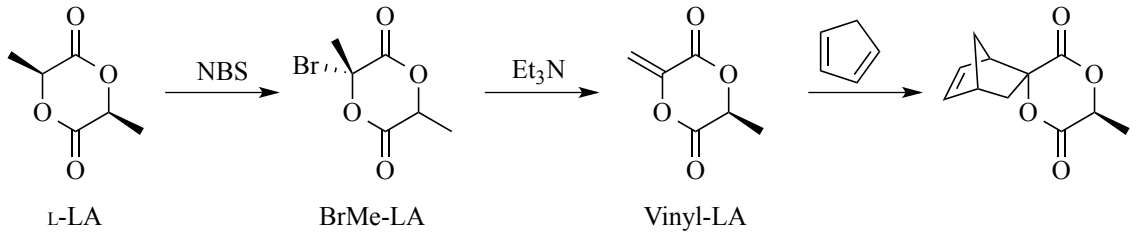

Scheme 1.5.4: Synthesis of novel monomers from L-lactide.[88]

Various monomers were synthesised *via* this method (Scheme 1.5.4) enabling polymers with varying properties to be investigated. ROP of monomers was attempted using organo-catalyst TBD in the presence of benzyl alcohol with subsequent polymer properties investigated.

Trimaille and co-workers developed the synthesis of hexyl-LA as shown below from heptaldehyde (Scheme 1.5.5).[37,89]

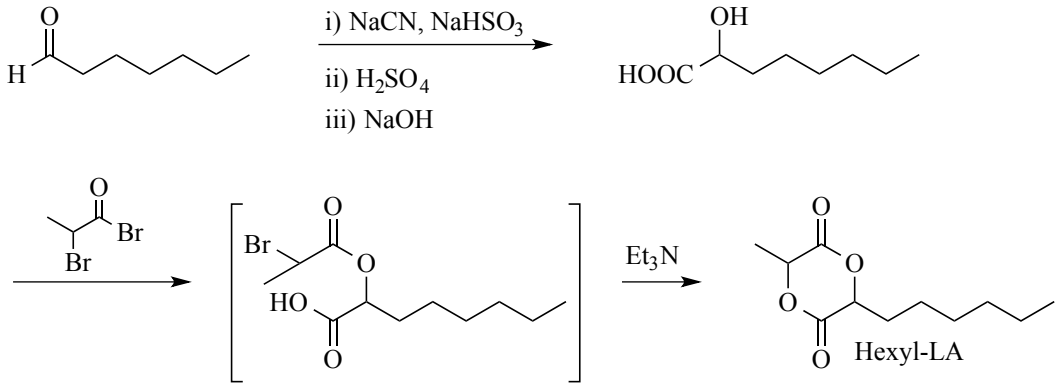

Scheme 1.5.5: Synthesis of Hexyl-LA.[37]

Initially, commercially available heptaldehyde was treated with sodium cyanide to afford 2-hydroxy octanoic acid. A 'one pot, two step' reaction was performed with the addition of 2-bromopropionyl bromide to afford a brominated intermediate. [37] A cyclic monomer is afforded with the addition of a base (Et_3N).

Baker and co-workers investigated the thermal properties of the AB- type polymers as shown below (Scheme 1.5.6).[90]

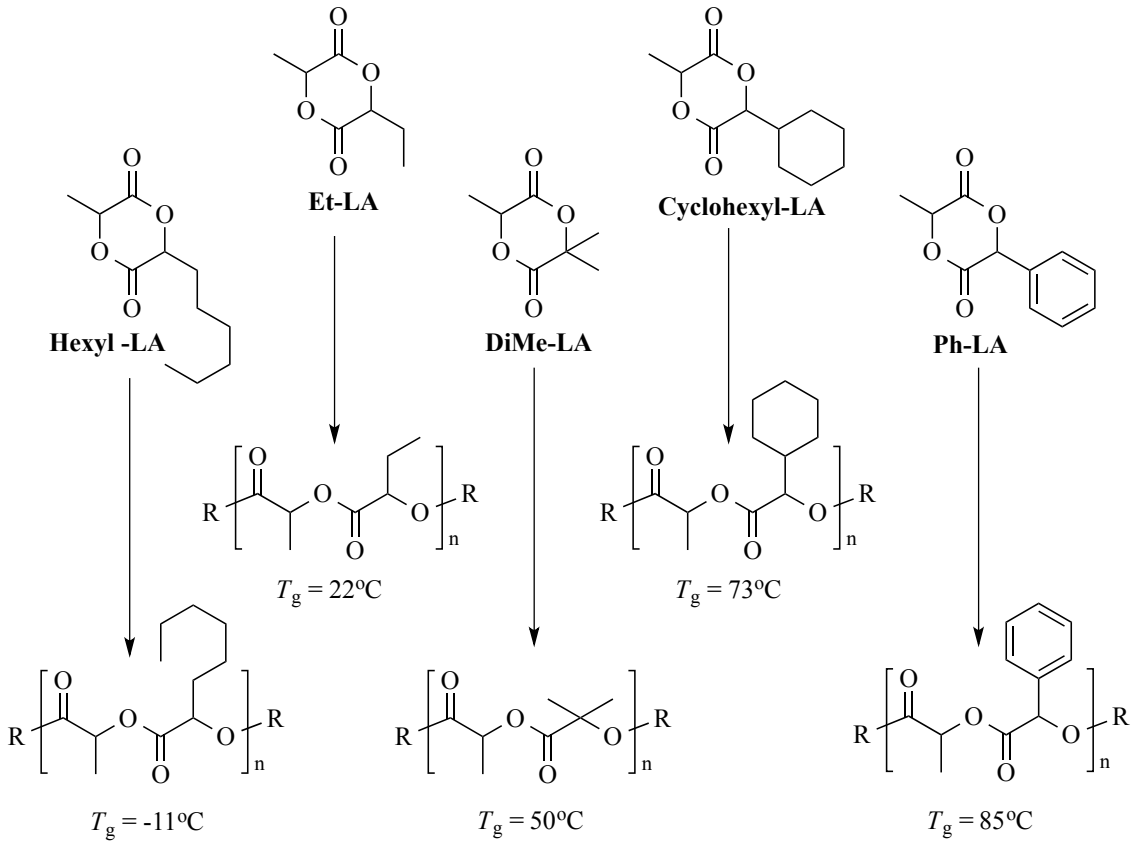

Scheme 1.5.6: Polymerisation of unsymmetrical (AB-type) lactide derivatives and their thermal properties.[90]

A trend in thermal properties was observed, as steric bulk of the substituent on the lactide derivative increase, the T_g increases. Furthermore, in the case of poly(Ph-LA) π-π stacking is thought to occur hence increasing the T_g further.[90] Conversely, this trend does not suffice for alkyl chain substituents, whereby the longer the chain (increased steric bulk) the lower the glass transition temperatures.[37] The ability to incorporate these properties into lactide co-polymers is extremely interesting, allowing polymers with tuneable properties to be synthesised.

1.6 Outlook

Recent developments in coordination chemistry of Group 4 metal complexes in the ROP of lactide and other cyclic esters have been ample and well documented. However, the ability to couple inexpensive, commercially available ligands to Group 4 metals with ROP under industrially relevant solvent-free conditions is little explored. Additionally, the ability to co-polymerise lactide with other cyclic monomers to favourably combine the properties and afford a co-polymer for a tailored purpose is of great interest and requires deeper exploration.

1.7 Research aims

Polylactide as a biodegradable polymer, has had a lot of interest as it is synthesised from bio-renewable resources and also degrades into non-toxic products. The use of PLA in biomedical applications has enabled developments in production of large-volume lactide production, thus enabling the manufacture of traditional commodity PLA materials. In order to synthesise such polymers, developments in synthesis of initiators that form well defined, stereospecific polymers with controlled molecular weights are required. Furthermore, the capability of co-polymerising polylactide with other cyclic monomers to form statistical co-polymers or block co-polymers is of great interest from a morphology and materials science point of view. From block co-polymers, stereocomplexation can be exploited to further increase thermal and mechanical properties. Statistical co-polymerisation allows the incorporation of co-monomers with different properties to be combined to form a co-polymer with finely tuned properties. The main topics covered in this thesis are;

a) The synthesis of Group 4 initiators using inexpensive, commercially available ligands for the well-defined controlled synthesis of PLA. The effect of metal and ligand stoichiometry in the synthesis of such complexes will be investigated and the interesting coordination chemistry discussed. It is proposed that these initiators will synthesise PLA with controlled architecture and controlled molecular weights.
b) The synthesis of block co-polymers of lactide with other commercially available cyclic esters to yield polymers with desired altered properties. The exploitation of stereo-controlled initiators will be investigated along with both one-pot and sequential polymerisation. Further improvements by combining enantiomerically pure PLA segments of block co-polymers will be probed to afford stereocomplexed domains with improved thermal properties.
c) Synthesis of cyclic monomers using different techniques will be investigated and the ability to synthesise alternating or random co-polymers with lactide is rare. This will be probed with a variety of different cyclic monomers with varying stoichiometries and their properties examined.

1.8 References

(1) http://www.solihull.gov.uk/sustainability/default.htm (Accessed 18.01.2014).

(2) Nampoothiri, K. M.; Nair, N. R.; John, R. P. *Bioresour. Technol.* **2010**, *101*, 8493–8501.

(3) Nair, L. S.; Laurencin, C. T. *Prog. Polym. Sci. 32*, 762–798.

(4) www.marinedebris.noaa.gov (Accessed 15.01.2014).

(5) Kale, G.; Kijchavengkul, T.; Auras, R.; Rubino, M.; Selke, S. E.; Singh, S. P. *Macromol. Biosci.* **2007**, *7*, 255–277.

(6) Vilela, C.; Sousa, A. F.; Fonseca, A. C.; Serra, A. C.; Coelho, J. F. J.; Freire, C. S. R.; Silvestre, A. J. D. *Polym. Chem.* **2014**.

(7) http://en.european-bioplastics.org/bioplastics/. (Accessed 23.12.2013).

(8) Chen, P.-S.; Liu, Y.-C.; Lin, C.-H.; Ko, B.-T. *J. Polym. Sci. Part A Polym. Chem.* **2010**, *48*, 3564–3572.

(9) Dove, A. P. *Chem. Commun.* **2008**, 6446–6470.

(10) Dechy-Cabaret, O.; Martin-Vaca, B.; Bourissou, D. *Chem. Rev.* **2004**, *104*, 6147–76.

(11) Stanford, M. J.; Dove, A. P. *Chem. Soc. Rev.* **2010**, *39*, 486–494.

(12) Dechy-Cabaret, O.; Martin-Vaca, B.; Bourissou, D. *Chem. Rev.* **2004**, *104*, 6147–6176.

(13) Platel, R. H.; Hodgson, L. M.; Williams, C. K. *Polym. Rev.* **2008**, *48*, 11–63.

(14) Albertsson, A.-C.; Varma, I. K. *Biomacromolecules* **2003**, *4*, 1466–1486.

(15) Kasperczyk, J. E. *Macromolecules* **1995**, *28*, 3937–3939.

(16) Dobrzynski, P.; Li, S.; Kasperczyk, J.; Bero, M.; Gasc, F.; Vert, M. *Biomacromolecules* **2004**, *6*, 483–488.

(17) Dittrich, V. W.; Schulz, R. C. *Die Angew. Makromol. Chemie* **1971**, *15*, 109–126.

(18) Kricheldorf, H. R.; Dunsing, R. *Die Makromol. Chemie* **1986**, *187*, 1611–1625.

(19) Kricheldorf, H. R. *Chemosphere* **2001**, *43*, 49–54.

(20) Bourissou, D.; Martin-Vaca, B.; Dumitrescu, A.; Graullier, M.; Lacombe, F. *Macromolecules* **2005**, *38*, 9993–9998.

(21) Hancock, S. Thesis, 2013.

(22) Tsuji, H.; Hyon, S. H.; Ikada, Y. *Macromolecules* **1991**, *24*, 5651–5656.

(23) Albertsson, A. C.; Varma, I. K. *Degrad. Aliphatic Polyesters* **2002**, *157*, 1–40.

(24) Zell, M. T.; Padden, B. E.; Paterick, A. J.; Thakur, K. A. M.; Kean, R. T.; Hillmyer, M. A.; Munson, E. J. *Macromolecules* **2002**, *35*, 7700–7707.

(25) Fukushima, K.; Kimura, Y. *Polym. Int.* **2006**, *55*, 626–642.

(26) Ovitt, T. M.; Coates, G. W. *J. Am. Chem. Soc.* **1999**, *121*, 4072–4073.

(27) H. Chisholm, M.; S. Iyer, S.; E. Matison, M. *Chem. Commun.* **1997**, 1999–2000.

(28) Chisholm, M. H.; Eilerts, N. W.; Huffman, J. C.; Iyer, S. S.; Pacold, M.; Phomphrai, K. *J. Am. Chem. Soc.* **2000**, *122*, 11845–11854.

(29) Thakur, K. A. M.; Kean, R. T.; Hall, E. S.; Doscotch, M. A.; Munson, E. J. *Anal. Chem.* **1997**, *69*, 4303–4309.

(30) Chamberlain, B. M.; Cheng, M.; Moore, D. R.; Ovitt, T. M.; Lobkovsky, E. B.; Coates, G. W. *J. Am. Chem. Soc.* **2001**, *123*, 3229–3238.

(31) Hiljanen-Vainio, M.; Karjalainen, T.; Seppala, J. *J. Appl. Polym. Sci.* **1996**, *59*, 1281–1288.

(32) Ikada, Y.; Jamshidi, K.; Tsuji, H.; Hyon, S. H. *Macromolecules* **1987**, *20*, 904–906.

(33) Masutani, K.; Lee, C. W.; Kimura, Y. *Macromol. Chem. Phys.* **2012**, *213*, 695–704.

(34) Sarasua, J.-R.; Rodríguez, N. L.; Arraiza, A. L.; Meaurio, E. *Macromolecules* **2005**, *38*, 8362–8371.

(35) Nijenhuis, A. J.; Grijpma, D. W.; Pennings, A. J. *Macromolecules* **1992**, *25*, 6419–6424.

(36) Dijkstra, P. J.; Du, H.; Feijen, J. *Polym. Chem.* **2011**, *2*, 520.

(37) Trimaille, T.; Gurny, R.; Möller, M. *J. Biomed. Mater. Res. A* **2007**, *80*, 55–65.

(38) Ren, J. *Biodegradable Poly (Lactic Acid): Synthesis, Modification, Processing and Applications*; Springer, 2011.

(39) Dove, A. P.; Gibson, V. C.; Marshall, E. L.; White, A. J. P.; Williams, D. J. *Chem. Commun.* **2001**, 283–284.

(40) Aubrecht, K. B.; Hillmyer, M. A.; Tolman, W. B. *Macromolecules* **2002**, *35*, 644–650.

(41) Chisholm, M. H.; Delbridge, E. E. *New J. Chem.* **2003**, *27*, 1177–1183.

(42) Platel, R. H.; Hodgson, L. M.; Williams, C. K. *Polym. Rev.* **2008**, *48*, 11–63.

(43) Jeffery, B. J.; Whitelaw, E. L.; Garcia-Vivo, D.; Stewart, J. A.; Mahon, M. F.; Davidson, M. G.; Jones, M. D. *Chem. Commun.* **2011**, *47*, 12328–12330.

(44) Chmura, A. J.; Davidson, M. G.; Jones, M. D.; Lunn, M. D.; Mahon, M. F.; Johnson, A. F.; Khunkamchoo, P.; Roberts, S. L.; Wong, S. S. F. *Macromolecules* **2006**, *39*, 7250–7257.

(45) Gendler, S.; Segal, S.; Goldberg, I.; Goldschmidt, Z.; Kol, M. *Inorg. Chem.* **2006**, *45*, 4783–4790.

(46) Sarazin, Y.; Howard, R. H.; Hughes, D. L.; Humphrey, S. M.; Bochmann, M. *Dalt. Trans.* **2006**, 340–350.

(47) Whitelaw, E. L.; Jones, M. D.; Mahon, M. F. *Inorg. Chem.* **2010**, *49*, 7176–7181.

(48) Hancock, S. L.; Mahon, M. F.; Kociok-Kőhn, G.; Jones, M. D. *Eur. J. Inorg. Chem.* **2011**, *2011*, 4596–4602.

(49) Hancock, S. L.; Mahon, M. F.; Jones, M. D. *Dalton Trans.* **2011**, *40*, 2033–2037.

(50) Kricheldorf, H. R.; Berl, M.; Scharnagl, N. *Macromolecules* **1988**, *21*, 286–293.

(51) Gendler, S.; Segal, S.; Goldberg, I.; Goldschmidt, Z.; Kol, M. *Inorg. Chem.* **2006**, *45*, 4783–4790.

(52) Yeori, A.; Groysman, S.; Goldberg, I.; Kol, M. *Inorg. Chem.* **2005**, *44*, 4466–4468.

(53) Chmura, A. J.; Davidson, M. G.; Frankis, C. J.; Jones, M. D.; Lunn, M. D. *Chem. Commun.* **2008**, 1293–1295.

(54) Marshall, E. L.; Gibson, V. C.; Rzepa, H. S. *J. Am. Chem. Soc.* **2005**, *127*, 6048–6051.

(55) Kim, Y.; Verkade, J. G. *Organometallics* **2002**, *21*, 2395–2399.

(56) Kim, Y.; Jnaneshwara, G. K.; Verkade, J. G. *Inorg. Chem.* **2003**, *42*, 1437–1447.

(57) Menge, W. M. P. B.; Verkade, J. G. *Inorg. Chem.* **1991**, *30*, 4628–4631.

(58) Kim, Y.; Verkade, J. G. *Macromol. Rapid Commun.* **2002**, *23*, 917–921.

(59) Kim, Y.; Verkade, J. G. *Macromol. Symp.* **2005**, *224*, 105–118.

(60) Spassky, N.; Wisniewski, M.; Pluta, C.; Le Borgne, A. *Macromol. Chem. Phys.* **1996**, *197*, 2627–2637.

(61) Majerska, K.; Duda, A. *J. Am. Chem. Soc.* **2004**, *126*, 1026–1027.

(62) Zhong, Z.; Dijkstra, P. J.; Feijen, J. *J. Am. Chem. Soc.* **2003**, *125*, 11291–11298.

(63) Nomura, N.; Ishii, R.; Yamamoto, Y.; Kondo, T. *Chem. – A Eur. J.* **2007**, *13*, 4433–4451.

(64) Nomura, N.; Ishii, R.; Akakura, M.; Aoi, K. *J. Am. Chem. Soc.* **2002**, *124*, 5938–5939.

(65) Alaaeddine, A.; Thomas, C. M.; Roisnel, T.; Carpentier, J.-F. *Organometallics* **2009**, *28*, 1469–1475.

(66) Cheng, M.; Attygalle, A. B.; Lobkovsky, E. B.; Coates, G. W. *J. Am. Chem. Soc.* **1999**, *121*, 11583–11584.

(67) Chisholm, M. H.; Gallucci, J.; Phomphrai, K. *Inorg. Chem.* **2002**, *41*, 2785–2794.

(68) Della Monica, F.; Luciano, E.; Roviello, G.; Grassi, A.; Milione, S.; Capacchione, C. *Macromolecules* **2014**, *47*, 2830–2841.

(69) Chuang, H.; Wu, B.; Li, C.; Ko, B. *Eur. J. Inorg. Chem.* **2014**.

(70) Jayaramudu, J.; Das, K.; Sonakshi, M.; Siva Mohan Reddy, G.; Aderibigbe, B.; Sadiku, R.; Sinha Ray, S. *Int. J. Biol. Macromol.* **2014**, *64*, 428–34.

(71) Guo, B.; Ma, P. *Sci. China Chem.* **2014**, *57*, 490–500.

(72) Thomas, C.; Gladysz, J. A. *ACS Catal.* **2014**, *4*, 1134–1138.

(73) Pilone, A.; Press, K.; Goldberg, I.; Kol, M.; Mazzeo, M.; Lamberti, M. *J. Am. Chem. Soc.* **2014**, *136*, 2940–2943.

(74) Florczak, M.; Duda, A. *Angew. Chemie Int. Ed.* **2008**, *47*, 9088–9091.

(75) Cao, H.; Han, H.; Li, G.; Yang, J.; Zhang, L.; Yang, Y.; Fang, X.; Li, Q. *Int. J. Mol. Sci.* **2012**, *13*, 12232–41.

(76) Darensbourg, D. J.; Karroonnirun, O.; Wilson, S. J. *Inorg. Chem.* **2011**, *50*, 6775–87.

(77) Li, G.; Lamberti, M.; Pappalardo, D.; Pellecchia, C. *Macromolecules* **2012**, *45*, 8614–8620.

(78) Nakayama, A.; Kawasaki, N.; Maeda, Y.; Arvanitoyannis, I.; Aiba, S.; Yamamoto, N. *J. Appl. Polym. Sci.* **1997**, *66*, 741–748.

(79) Zhong, Z.; Dijkstra, P. J.; Feijen, J. *Macromol. Chem. Phys.* **2000**, *201*, 1329–1333.

(80) Nakayama, Y.; Watanabe, N.; Kusaba, K.; Sasaki, K.; Cai, Z.; Shiono, T.; Tsutsumi, C. *J. Appl. Polym. Sci.* **2011**, *121*, 2098–2103.

(81) Bouyahyi, M.; Pepels, M. P. F.; Heise, A.; Duchateau, R. **2012**.

(82) Pepels, M. P. F.; Bouyahyi, M.; Heise, A.; Duchateau, R. *Macromolecules* **2013**, *46*, 4324–4334.

(83) Langer, R. S.; Lendlein, A.; Schmidt, A.; Grablowitz, H. Biodegradable shape memory polymers., August 26, 1999.

(84) Lendlein, A.; Schmidt, A.; Kratz, K.; Schultz, J. Polyesterurethane containing pentadecalactone polymer as a hard segment., November 19, 2003.

(85) Pepels, M. P. F.; Bouyahyi, M.; Heise, a.; Duchateau, R. *Macromolecules* **2013**, *46*, 4324–4334.

(86) Jing, F.; Smith, M. R.; Baker, G. L. *Macromolecules* **2007**, *40*, 9304–9312.

(87) Becker, J. M.; Pounder, R. J.; Dove, A. P. *Macromol. Rapid Commun.* **2010**, *31*, 1923–1937.

(88) Jing, F.; Hillmyer, M. A. *J. Am. Chem. Soc.* **2008**, *130*, 13826–13827.

(89) Trimaille, T.; Moller, M.; Gurny, R. *J. Polym. Sci. Part A Polym. Chem.* **2004**, *42*, 4379–4391.

(90) Baker, G.; Vogel, E.; Smith, M. *Polym. Rev.* **2008**, *48*, 64–84.

Chapter 2

Group 4 Complexes as Initiators

2 Preamble

As mentioned in Chapter 1, the quest for more stereoselective and robust initiators is of great interest. Currently, commercially available $Sn(Oct)_2$ is widely used for the ROP of lactide, due to its air stability, low cost and solubility. [1] However, polymerisation using $Sn(Oct)_2$ requires addition of a co-initiator and while the molecular weight can be controlled, stereocontrol of the resulting polymer cannot, thus yielding atactic PLA. Group 4 metal initiators are recognized to give high activity and selectivity due to their strong Lewis acid nature.[2–10] Kricheldorf *et al.* first reported active Group 4 metal alkoxides for the ROP of various cyclic esters.[6,11,12] In this chapter, the use of inexpensive ligands complexed to Group 4 metals will be investigated. Lactic acid (**L_1**) is an inexpensive, commercially available bidentate ligand that has the ability to form Group 4 metal complexes.[13] Interestingly, by forming a complex, this will give an insight into the binding mode of lactide moieties to Group 4 metal initiators during the coordination insertion ring-opening polymerisation of lactide. Tulloch and co-workers reported Group 4 metals complexed to *N,N,N',N'*-tetrakis(2-hydroxyethyl)ethylenediamine (**L_2**) in a 1:1 stoichiometric ratio. $Ti_2(\mathbf{L_2})_2$ was synthesized by reacting **L_2** with $Ti(O^iPr)_4$ in the presence of water at 25°C, while $Zr(\mathbf{L_2})_2$ was reportedly synthesised by reacting tetra-*n*-propyl zirconate in *n*-propyl alcohol with **L_2** at 25°C in the presence of air. These complexes displayed a unique air and water stability whilst retaining catalytic activity and show great promise for the ring-opening polymerisation of lactide.[14] By incorporating labile isopropoxide groups into the complex, its activity as an initiator should increase, and this will be investigated in this chapter. Ligand **L_3**, a synthesised analogue of **L_2** with increased steric bulk, will be complexed to Group 4 metals and trialled in the ring-opening polymerisation of *rac*-lactide. By varying the nature of the coordinating group, the effect on the activity and stereocontrol of the polymerisation can be assessed.

A range of Group 4 complexes with such ligands were synthesised and structurally characterised (Table 2.0). The potential of the resulting complexes was initially probed for the ROP of sublimed *rac*-LA at both 135°C and 165°C with investigations into activity, stereocontrol and molecular weight control. The most promising initiators were trialled on a larger scale with recrystallized (non-sublimed) *rac*-LA and monitored in real time by FT-IR spectroscopy using a diamond composite insertion probe and compared to commercially available initiators: $Ti(O^iPr)_4$, $Zr(O^iPr)_4HO^iPr$ and $Sn(Oct)_2$.

Table 2.0: List of complexes synthesised in this chapter.

	Complexes		
Ligand	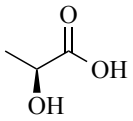 **(L_1)**	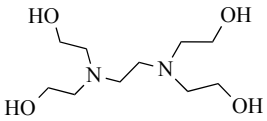 **(L_2)**	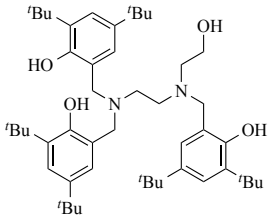 **(L_3)**
	$Ti_8[dimer]_2(\mathbf{L_1})_4(O^iPr)_{20}$ **1**	$Ti_4(\mathbf{L_2})_3(O^iPr)_4$ **3**	$Ti_2(\mathbf{L_3})_2$ **9**
	$Zr(\mathbf{L_1})_2$ **2**	$Ti_4(\mathbf{L_2})(O^iPr)_{12}$ **4**	
		$Zr_2(\mathbf{L_2})_2$ **5**	
		$Hf_2(\mathbf{L_2})_2$ **6**	
		$Zr_3(\mathbf{L_2})(O^iPr)_8$ **7**	
		$Hf_3(\mathbf{L_2})(O^iPr)_8$ **8**	

Synthesis of complexes

2.1 Synthesis of L_1 Complexes

L-lactic acid, $\mathbf{L_1}$, an inexpensive commercially available ligand, was used to study and mimic the binding mode of a growing polylactide chain from the active titanium metal centre in the ROP of lactide. The incorporation of isopropoxide groups into the complex should increase the activity of the complex for the ROP of *rac*-LA, whilst obviating the addition of a co-initiator. A stoichiometric reaction of $\mathbf{L_1}$ with $Ti(O^iPr)_4$ afforded $Ti_8[dimer]_2(\mathbf{L_1})_4(O^iPr)_{20}$, **1** (Scheme 2.1.1).

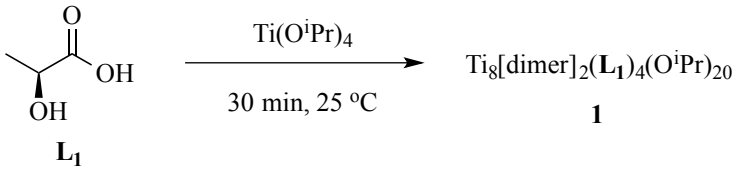

Scheme 2.1.1: Synthesis of $Ti_8[dimer]_2(\mathbf{L_1})_2(O^iPr)_{20}$, **1**.

The compound obtained was characterised by ^1H NMR spectroscopy and single crystal X-ray crystallography. In the solid state, $Ti_8[dimer]_2(\mathbf{L_1})_4(O^iPr)_{20}$, **1**, displays eight metal centres in four different environments, all of which are in a six coordinate *pseudo*-octahedral geometry (**Figure 2.1.1**).

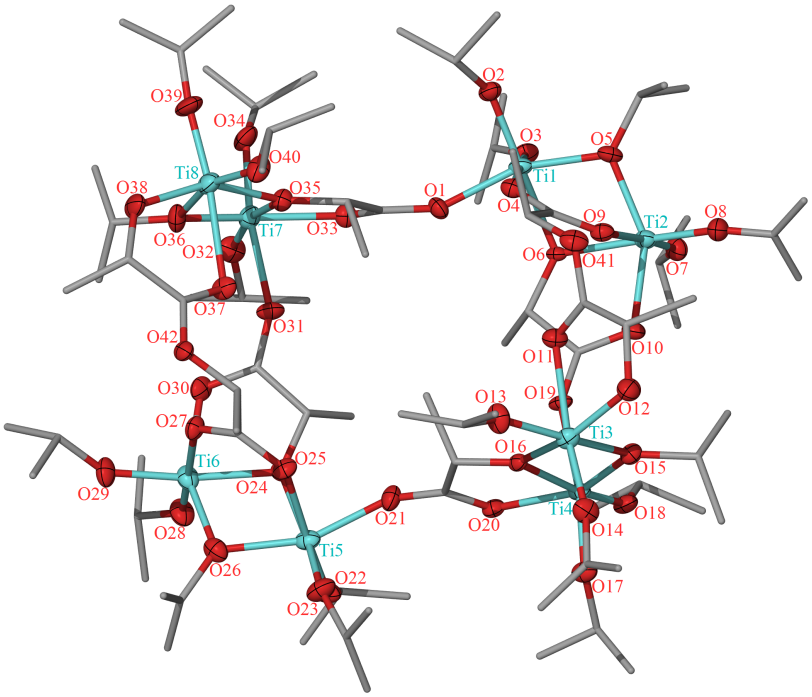

Figure 2.1.1: Crystal structure of Ti_8[dimer]$_2$($\mathbf{L_1}$)$_4$(O^iPr)$_{20}$, **1**, (Thermal ellipsoids for Ti and O are drawn at 30% probability level. H atoms were omitted for clarity).

The unit cell is arranged monoclinically with a primitive-type lattice. Each titanium centre formed a dimer with one bridging lactic acid and one bridging isopropoxide group. Each of these dimers are linked to two other dimers by various lactate bridges to afford a 'tetramer of dimers'. The bond angles do not fit the true octahedral orientation of 90° and 180°, instead, four lactic acid bridging groups exhibit a bond angle distortion of < 90° due to chelation (O31-Ti7-O33 = 81°). Equally, terminal isopropoxide groups showed a bond angle distortion of > 90° due to electronic repulsion and the chelating effect of the opposing lactic acid bridge (O28-Ti6-O29 = 96°). The M-O bond lengths of the titanium metal centres to the bridging isopropoxide groups are elongated (> 1.8 Å) due to their bridging properties and also due to steric hindrance around the metal centre (Ti4-O15 = 1.96 Å). The titanium-isopropoxide bond lengths also differ throughout the structure due to the differing steric environments afforded by the lactic acid ligands around the metal centre.

Interestingly the ligand, $\mathbf{L_1}$, has been esterified *in situ* forming a dimer that is incorporated into the complex (Scheme 2.1.2). The structure can be thought of as a partial representation of the coordination displayed by propagating lactide with the active Ti metal centre. A simplified drawing of **1** is shown below (Figure 2.1.2).

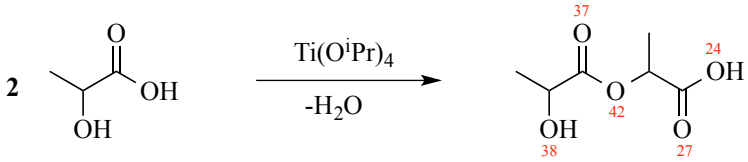

Scheme 2.1.2: Formation of lactic acid dimer by *in situ* esterification (O atoms labelled in accordance with **Figure** 2.1.1).

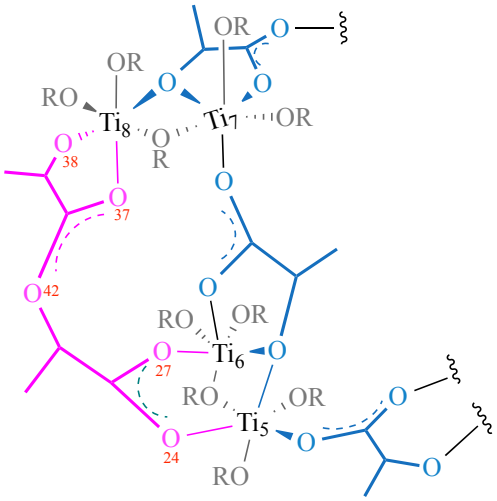

Figure 2.1.2: Simplified drawing of **1** (Lactic acid dimer (purple), lactic acid (**L**$_1$, blue)).

A simplified drawing of **1** (Figure 2.1.2) illustrates the connectivity of the differing titanium metal centres. In the solid state, Ti8 is connected to Ti5 and Ti6 by a lactic acid dimer bridge (Figure 2.1.2 (purple)). The dimer is linked to Ti8 through a bidentate chelate of O38, an α-hydroxyl group (C76-O38 = 1.413 Å), and a carboxylic group (O37) forming a stable 5-membered ring. Formation of such ring conformation stability has been observed by Nakamura *et al*. for the synthesis of water soluble diammonium tris(2-hydroxyproionato)titanate with a Ti:**L**$_1$ ratio of 1:3.[13] An observed shortening of bond lengths C76-O37 and C78-O42 of 1.215 Å and 1.336 Å respectively is due to delocalised electrons of the carbonyl moiety. Interestingly, the dimer is linked to Ti5 and Ti6 by a carboxylate bridge, here, similar shortened C-O bond lengths (C61-O27 = 1.245 Å and C61-O24 = 1.265 Å) are observed in accordance with delocalised electrons across the carboxylate bridge. Meyer *et al*. demonstrated comparable characteristics of delocalised electrons over a carboxylate bridging in dizinc complexes.[15] Ti5 and Ti6 are μ^2-bridged by both an isopropoxide group and an **L**$_1$ ligand which also μ^2-bridges Ti6 and Ti7. Again, a shortening of interatomic distances, C51-O30 (1.296 Å) and C51-O31 (1.264 Å), is indicative of a delocalised carboxylate. Ti5 is linked by the delocalised carbonyl (C36-O21 = 1.238 Å) of **L**$_1$ to Ti3 and Ti4 by O16 and O20. Ti7 and Ti8 are μ^2-bridged by an isopropoxide group and a **L**$_1$ (O33 and O34) which is connected to Ti1 by O1 of **L**$_1$.

The proton NMR spectrum shown below (Figure 2.1.3), was consistent with the single crystal X-ray crystallographic structure obtained of **1** (Figure 2.1.3).

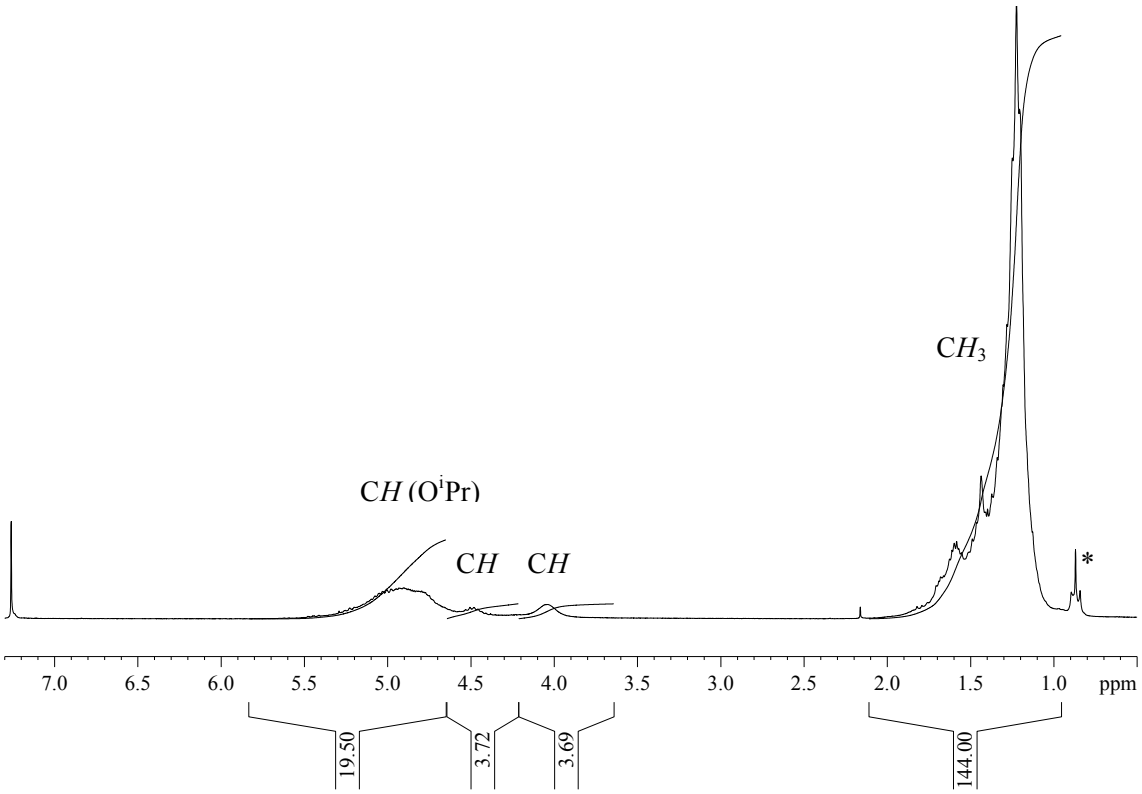

Figure 2.1.3: ^{1}H NMR spectrum of $Ti_8[dimer]_2(\mathbf{L_1})_4(O^iPr)_{20}$, **1**, in $CDCl_3$ at 298K (* denotes residual solvent peak of hexane).

In Figure 2.1.3, broad peaks are observed for **1** indicating protons may be fluctuating in solution. The integrals are consistent with the crystal structure of **1**, with the broad peak at 5.27-4.70 ppm attributing to methine protons of the isopropoxide moiety. Peaks at 4.51 and 4.21-3.90 ppm correspond to methine protons of $\mathbf{L_1}$ and dimer. All methyl protons are accounted for in the broad multiplet of 1.41-1.10 ppm. A residual solvent peak (hexane) was observed at 0.88 ppm.

The reaction was repeated using $Zr(O^iPr)_4.HO^iPr$ and $Hf(O^iPr)_4.HO^iPr$ instead of $Ti(O^iPr)_4$. However, both reactions yielded products that were insoluble in all common solvents (hexane, Tol, AcOEt, EtOH, CH_2Cl_2, THF, AcN, $CHCl_3$). Elemental analysis was inconclusive as the results were not consistent with a valid ligand:metal ratio. An alternative method using tetrakis(dimethylamido)zirconium yielded **2** that again, was insoluble in all common solvents (Scheme 2.1.3).

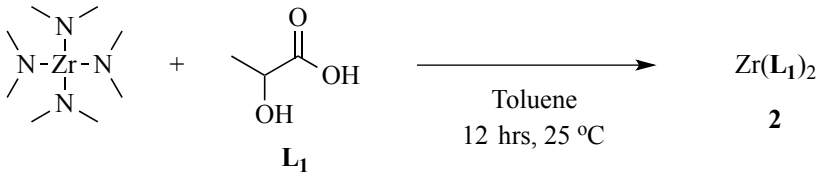

Scheme 2.1.3: Synthesis of $Zr(\mathbf{L_1})_2$, **2**.

Commercially available zirconium lactate displays a Zr:$\mathbf{L_1}$ ratio of 1:4.[16] In our case however, the elemental analysis of the insoluble product **2** using tetrakis(dimethylamido)zirconium was consistent with the calculated results of $Zr(\mathbf{L_1})_2$ complex (Anal: Calc C: 26.96 %, H: 3.02 %. Found C: 26.87 %; H: 3.15 %). This is consistent with the empirical formula of $C_6H_8O_6Zr$ whereby a ratio of 1:2 zirconium metal centre to $\mathbf{L_1}$ ligand was observed (Scheme 2.1.3).

2.2 Synthesis of L_2 Complexes

N,N,N',N'-tetrakis(2-hydroxyethyl)ethylenediamine, $\mathbf{L_2}$, is an inexpensive, benign and commercially available ligand similar to EDTA exhibiting hexadentate chelating properties. Verkade and co-workers first reported monomeric and dimeric titanatranes as initiators in the ROP of lactide.[17,18] As discussed previously, Tulloch and co-workers complexed Group 4 metals to $\mathbf{L_2}$ in a 1:1 stoichiometric ratio. Tulloch *et al.* reported $Ti(O^iPr)_4$ was complexed to $\mathbf{L_2}$ in the presence of water at 25°C to afford $Ti_2(\mathbf{L_2})_2$, whilst $Zr(\mathbf{L_2})_2$ was reportedly synthesised by reacting tetra-*n*-propyl zirconate in *n*-propyl alcohol with $\mathbf{L_2}$ at 25°C in the presence of air. These complexes displayed a unique air and water stability whilst retaining catalytic activity.[14] A series of novel complexes were synthesised by the reaction of ligand $\mathbf{L_2}$ with $Ti(O^iPr)_4$, $Zr(O^iPr)_4HO^iPr$ and $Hf(O^iPr)_4HO^iPr$ to give a collection of well-defined complexes with varying amount of labile isopropoxide groups as summarised Scheme 2.2.1. All were characterized by NMR spectroscopy, elemental analysis and single X-ray diffraction.[19]

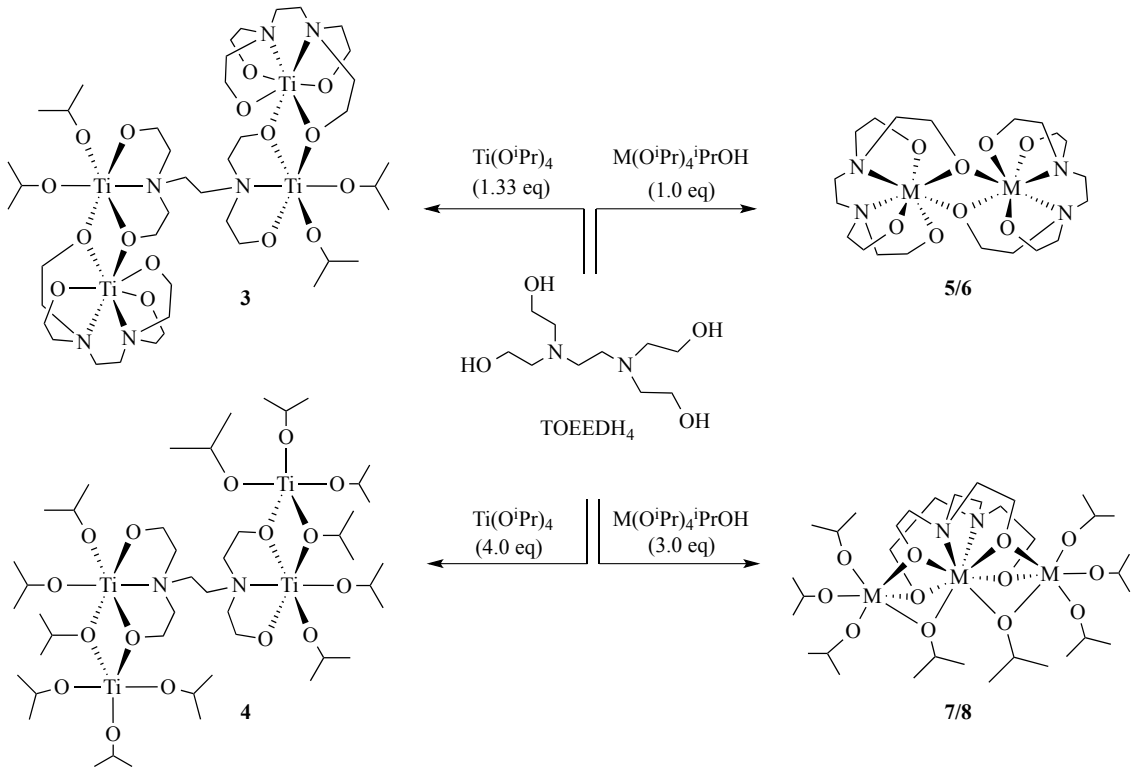

Scheme 2.2.1 Synthesis of Group 4 $\mathbf{L_2}$ complexes (M = Zr / Hf, structures **5**/**6** and **7**/**8** respectively) under inert conditions, in toluene at 25°C.

Initially, under inert conditions, the reaction of $\mathbf{L_2}$ and $Ti(O^iPr)_4$ in 1:1 stoichiometric amounts in toluene at 25°C was expected to yield dimeric complex $Ti_2(\mathbf{L_2})_2$ as reported by Tulloch and co-workers. However, $Ti_4(\mathbf{L_2})_3(O^iPr)_4$, **3**, was isolated as the only product due to differing synthetic procedures. The reaction was repeated under the correct 4:3 stoichiometry and the product was fully characterized (Figure 2.2.1).

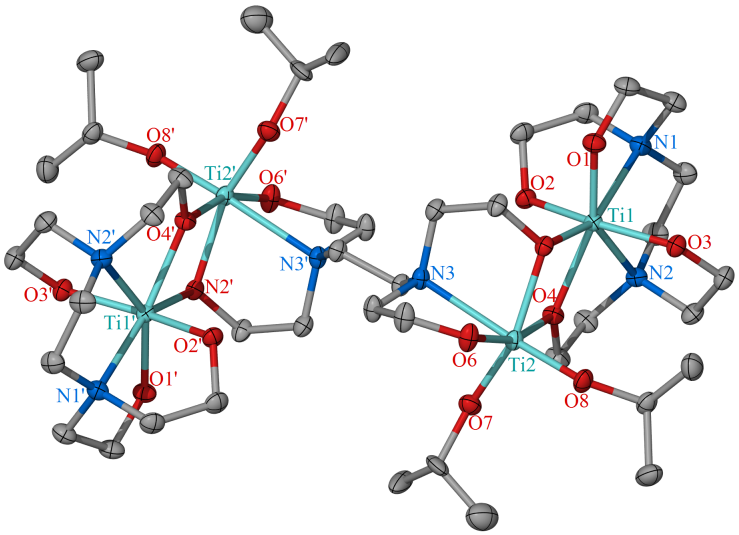

Figure 2.2.1: X-ray molecular structure of $Ti_4(\mathbf{L_2})_3(O^iPr)_4$, **3** (Thermal ellipsoids are drawn at 50% probability level. H atoms were omitted for clarity).

In the solid state, $Ti_4(\mathbf{L_2})_3(O^iPr)_4$, **3**, exhibits a triclinic crystal system with space group consisting of a primitive-type lattice. Complex **3** consists of four Ti metal centres interestingly, in two different environments; two metal centres lie in a 6 coordinate environment bridged by a ligand (Ti(1)), and two terminal metal centres (Ti(2)) in a 7 coordinate environment (Figure 2.2.1). Ti(2) possesses a distorted octahedral geometry with two mutually *cis* N atoms and isopropoxide groups.

In order to increase the number of isopropoxide groups within the complex a similar reaction of $Ti(O^iPr)_4$ and $\mathbf{L_2}$ with 4:1 stoichiometry yielded $Ti_4(\mathbf{L_2})(O^iPr)_{12}$, **4**. The proton NMR spectrum was consistent with the presence of twelve isopropoxide groups per $\mathbf{L_2}$ ligand.

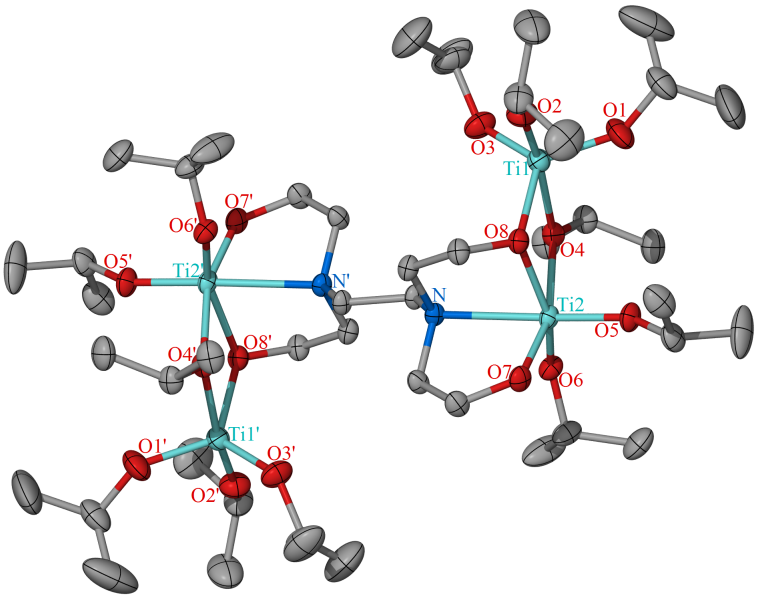

Figure 2.2.2: X-ray molecular structure of $Ti_4(\mathbf{L_2})(O^iPr)_{12}$, **4** (Thermal ellipsoids are drawn at 50% probability level. H atoms were omitted for clarity).

Inspection of the structural parameters revealed similar to **3**, the unit cell displayed triclinic motif with space group consisting of primitive-type lattice. Complex **4** exhibits two metal centres (Ti(2)) which lie in a 6 coordinate environment bridged by a ligand ($\mathbf{L_2}$). The bond angles at Ti(2) suggest pseudo-octahedral geometry, which was consistent with that of Ti(2) in $Ti_4(\mathbf{L_2})_3(O^iPr)_4$. Two terminal metal centres (Ti(1)) lie in a 5 coordinate orientation, both surrounded by labile isopropoxide groups. The bond angles of Ti(1) imply a distorted trigonal bipyramidal geometry.

In contrast, initial reactions of $Zr(OiPr)_4HO^iPr$ and $Hf(O^iPr)_4HO^iPr$ (instead of $Ti(O^iPr)_4$) with $\mathbf{L_2}$ in 1:1 stoichiometric amounts yielded $Zr_2(\mathbf{L_2})_2$, **5**, and $Hf_2(\mathbf{L_2})_2$, **6**, respectively as reported by Tulloch *et al* via a modified synthesis.[14]

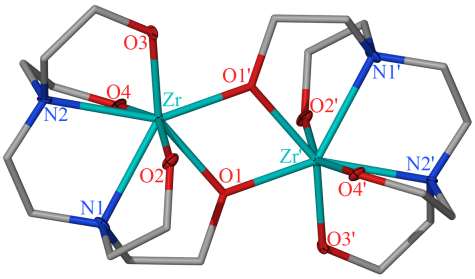

Figure 2.2.3: X-ray molecular structure of $Zr_2(\mathbf{L_2})_2$, **5** (Thermal ellipsoids of Zr, O and N are drawn at 30% probability level and C is represented as sticks. H atoms were omitted for clarity).

Although the structure can still be elucidated by single crystal X-ray crystallography, the crystals diffracted weakly resulting in a disordered poor quality structure. In the solid state, the acquired structure of **5** suggests that both metal centres lie in 7 coordinate environment encapsulated by the chelating ligand. Both complexes exhibit a monoclinic system with base centring Bravais lattice. The ligand geometry around the metal centres favours mutually *cis* N atoms. Due to the chelating nature of the ligand the ^{1}H NMR spectrum was consistent with the replacement of all isopropoxide groups (Figure 2.2.4).

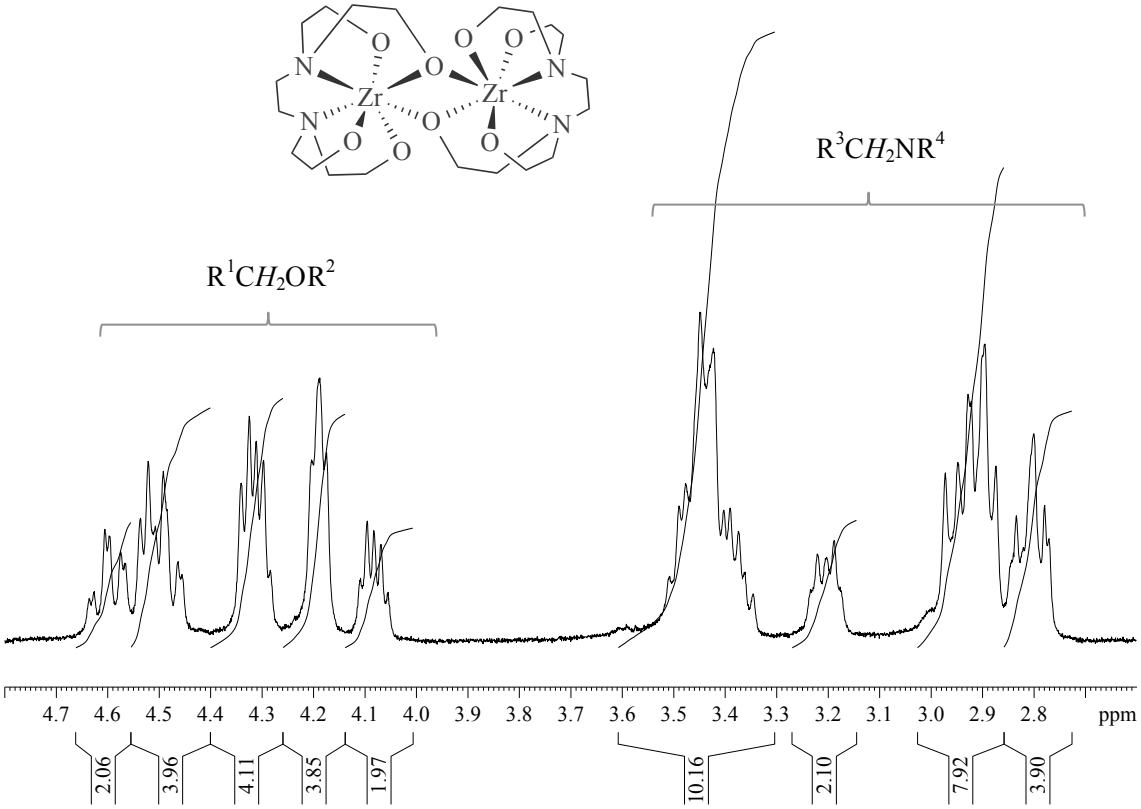

Figure 2.2.4: Detail of ^{1}H NMR spectrum of $Zr_2(\mathbf{L_2})_2$ **5**, at 223K.

Variable temperature NMR (VT-NMR) spectroscopy was undertaken of $Zr_2(\mathbf{L_2})_2$, **5**, to achieve a higher resolution of spectra. Figure 2.2.4, a proton NMR spectrum at low temperature (at 223K), displayed distinguishable peaks that were consistent with crystal structure (Figure 2.2.3). Although individual proton splitting could not be accounted for, peaks from 4.66 ppm to 3.98 ppm were seen to be attributed to $R^1CH_2OR^2$ (16 protons) and peaks from 3.61 ppm to 2.65 ppm corresponded to $R^3NH_2R^4$ (24 protons).

The reaction of $Zr(O^iPr)_4HO^iPr$ and $\mathbf{L_2}$ in a 2:1 stoichiometry afforded $Zr_3(\mathbf{L_2})(O^iPr)_8$, **7**, as the isolated product. The reaction was repeated under the correct stoichiometry of 3:1 and upon recrystallization gave colourless crystals. Although the structure can still be elucidated, the crystals diffracted weakly resulting in a disordered poor quality structure (Figure 2.2.5).

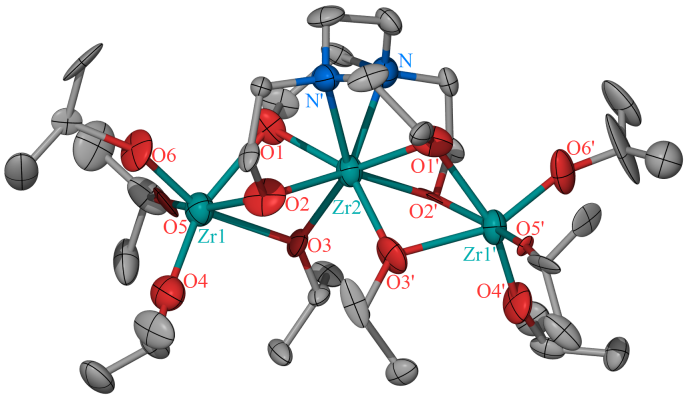

Figure 2.2.5: X-ray crystal structure of $Zr_3(\mathbf{L_2})(O^iPr)_8$, **7** (Thermal ellipsoids are drawn at 30% probability level. H atoms were omitted for clarity).

In the solid state, two metal centres (Zr(1) and Zr(3)) exhibit 6-coordinate geometry whilst Zr(2) displays an 8-coordinate geometry due to the chelating nature of the ligand. The proton spectrum, was consistent with the replacement of four isopropoxide groups with the ligand $\mathbf{L_2}$ (Figure 2.2.6).

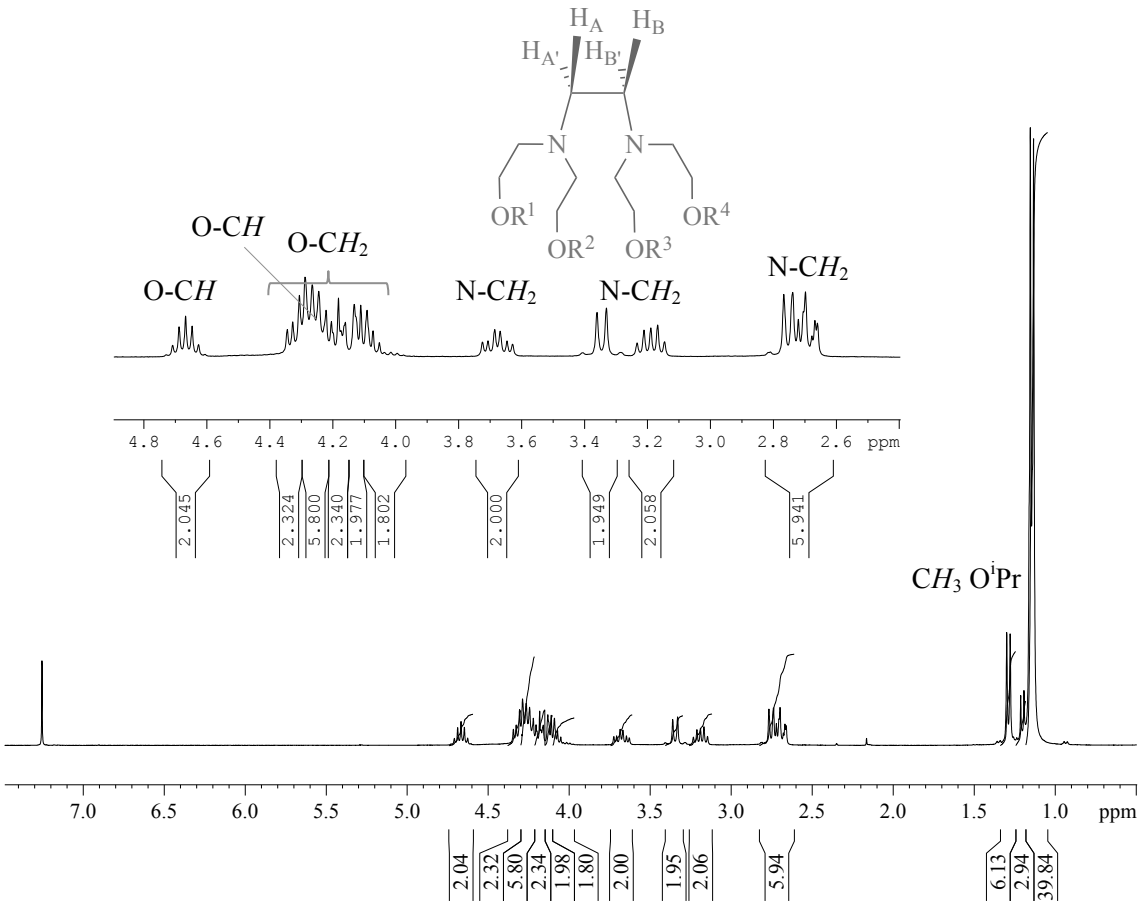

Figure 2.2.6: NMR spectrum of $Zr_3(\mathbf{L_2})(O^iPr)_8$, **7**, in $CDCl_3$ at 298K.

The complex proton spectrum of $Zr_3(\mathbf{L_2})(O^iPr)_8$, **7**, was assigned with the additional use of HMQC and COSY NMR spectroscopy techniques. The bridging isopropoxide C*H* moiety was displayed as a septet at 4.67 ppm. The remaining terminal isopropoxide C*H* moieties (4.32 ppm – 4.24 ppm) were hidden under various O-CH_2 multiplets at 4.36 – 4.03 ppm. A triplet of doublet (*td*) is observed at 3.68 ppm and a double doublet of doublets (*ddd*) at 3.26-3.13 ppm due to AA'BB' splitting. H_A is observed as *td* as H_A is first split by $H_{A'}$ forming a doublet ($^2J_{H\text{-}H}$ geminal coupling). Further splitting (2-fold) where H_A is split by H_B and $H_{B'}$ on the opposing carbon ($^3J_{HH}$ vicinal coupling). Multiplets are observed for the remaining CH_2 groups, while CH_3 isopropoxide groups are observed as doublets.

Under the same conditions, $Hf(O^iPr)_4HO^iPr$ was reacted with $\mathbf{L_2}$ in a 3:1 stoichiometry yielded analogous complex, $Hf_3(\mathbf{L_2})(O^iPr)_8$, **8**, (Figure 2.2.7).

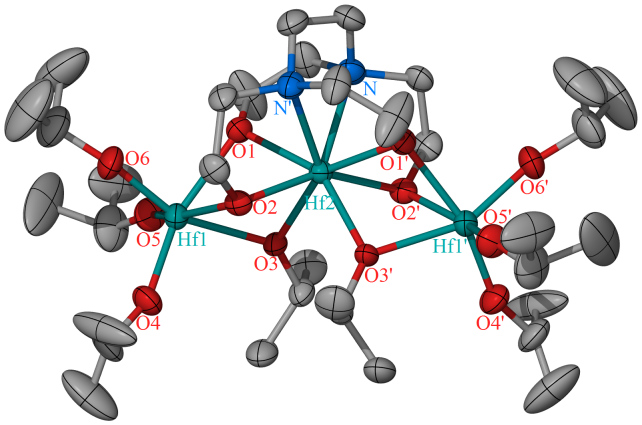

Figure 2.2.7: X-ray crystal structure of $Hf_3(\mathbf{L_2})(O^iPr)_8$, **8** (Thermal ellipsoids are drawn at 50% probability level. H atoms were omitted for clarity).

In the solid state, the adduct **8** consists of three metal centres bound to one ligand. Again, two metal centres lie in a 6 coordinate environment (Hf(1) and Hf(3)) adopting a *pseudo*-octahedral geometry, one central metal centre (Hf(2)) lies in an 8 coordinate environment. The M-O bond lengths are similar in both **7** and **8** however, there is a shortening of the M-N bond length on moving from zirconium to hafnium. This shortening is indicative of the lanthanide contraction whereby, hafnium has a slightly smaller atomic radii than zirconium. The lanthanide contraction describes the shielding effect of inner electrons (4*f*) on outer shell electrons (6*s*) from the nuclear charge (*Z*). Electrons in the 4*f* orbital exhibit poor shielding properties and do not compensate for the increase in *Z* leading to a lower atomic radius than expected.[4]

In summary, all Ti, Zr and Hf complexes originate from the Group 4 metal isopropoxide and as the amount of ligand in a complex increases so does the coordination number around the metal centre. $Ti_4(\mathbf{L_2})(O^iPr)_{12}$ **4**, and $Ti_4(\mathbf{L_2})_3(O^iPr)_4$ **3**, have an increased number of isopropoxide groups within their complex and can be thought of as isolated successive intermediates between the starting material $Ti(O^iPr)_4$ and the coordinately saturated $Ti_2(\mathbf{L_2})_2$. Again, $Zr_3(\mathbf{L_2})(O^iPr)_8$ **7**, and $Hf_3(\mathbf{L_2})(O^iPr)_8$ **8**, can be thought of as intermediates which were formerly $M(O^iPr)_4.HO^iPr$ and further addition of ligand leads to the loss of all remaining isopropoxide groups yielding the common structure $M_2(\mathbf{L_2})_2$ (Scheme 2.2.2).

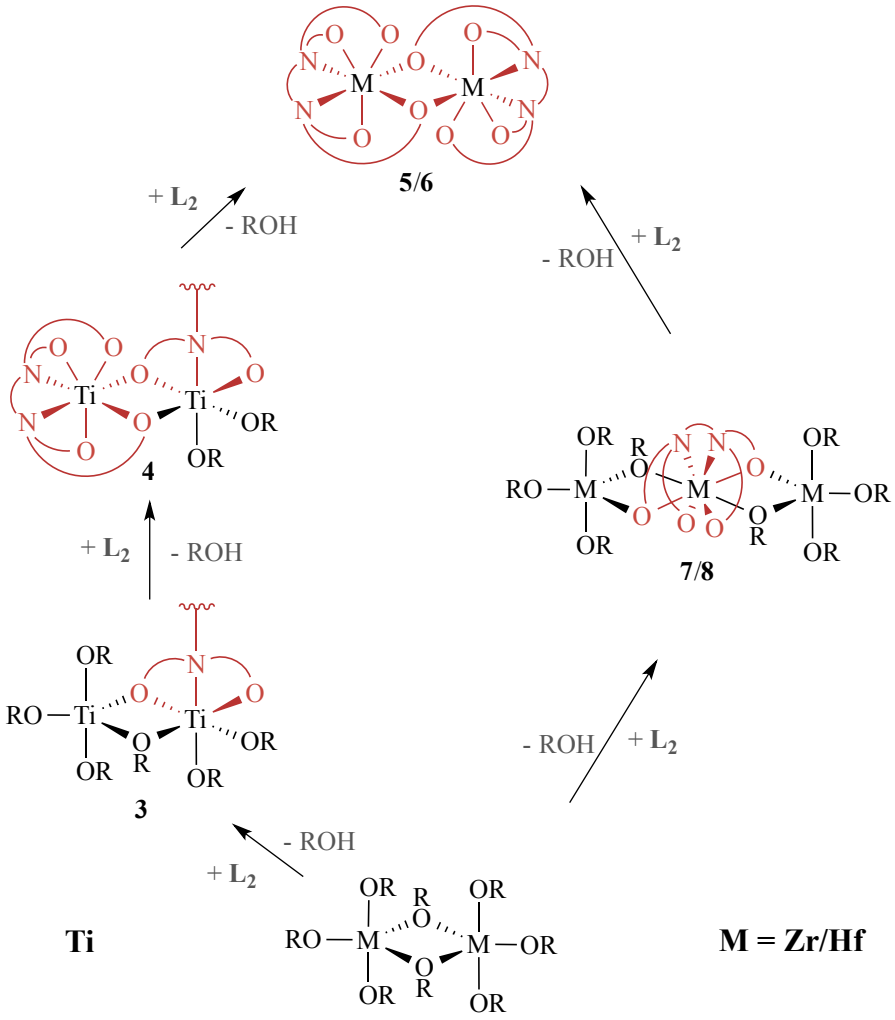

Scheme 2.2.2: Schematic diagram summarizing complexes synthesized illustrating ligand to dimer stoichiometry (R = ^{i}Pr).

2.3 Synthesis of L_3 Complexes

Gibson *et al.* demonstrated a general trend whereby increasing the steric bulk of phenoxy salen complexes in turn increased stereocontrol.[20] Attempts to enhance microstructural stereocontrol of Group 4 **L_2** complexes with the incorporation of bulky di-substituted phenol moieties onto the **L_2**-type backbone were undertaken. The ligands were synthesised *via* Mannich condensation as shown in Scheme 2.3.1.

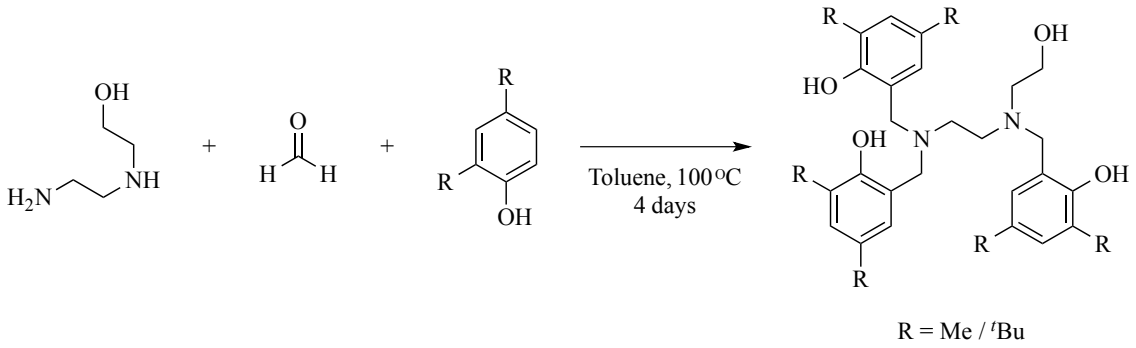

Scheme 2.3.1: Synthesis of ligand $\mathbf{L_3}$ (R = ^{t}Bu).

Initially, the synthesis of 2,4-dimethyldiaminetrisphenolate (a methyl substituted analogue ligand of $\mathbf{L_3}$, R=Me in Scheme 2.3.1) was attempted by the reaction of 2-[2-aminoethyl)amino] ethanol (1 eq.) in the presence of aqueous formaldehyde (3 eq.) followed by addition of 2,4-dimethylphenol (3 eq.) and stirred at 100°C in toluene for 3 days. The ^{1}H NMR spectrum illustrated the formation of numerous ill-defined products. Attempts to purify by recrystallization and column chromatography using various solvent systems failed to separate multiple observed products and the ligand was discarded.

2,4-di*tert*butyl diaminetrisphenolate ligand, $\mathbf{L_3}$, was synthesised in an analogous method as above using 2,4-di-*tert*-butylphenol instead of 2,4-dimethylphenol. The crude product was purified by column chromatography (eluent hexane:ethyl acetate 9:1) to afford $\mathbf{L_3}$. Mass spectrometry ([M+H]+: 781.58) and ^{1}H NMR spectrum were consistent with three di-*tert*-butyl phenol moieties (Figure 2.3.1).

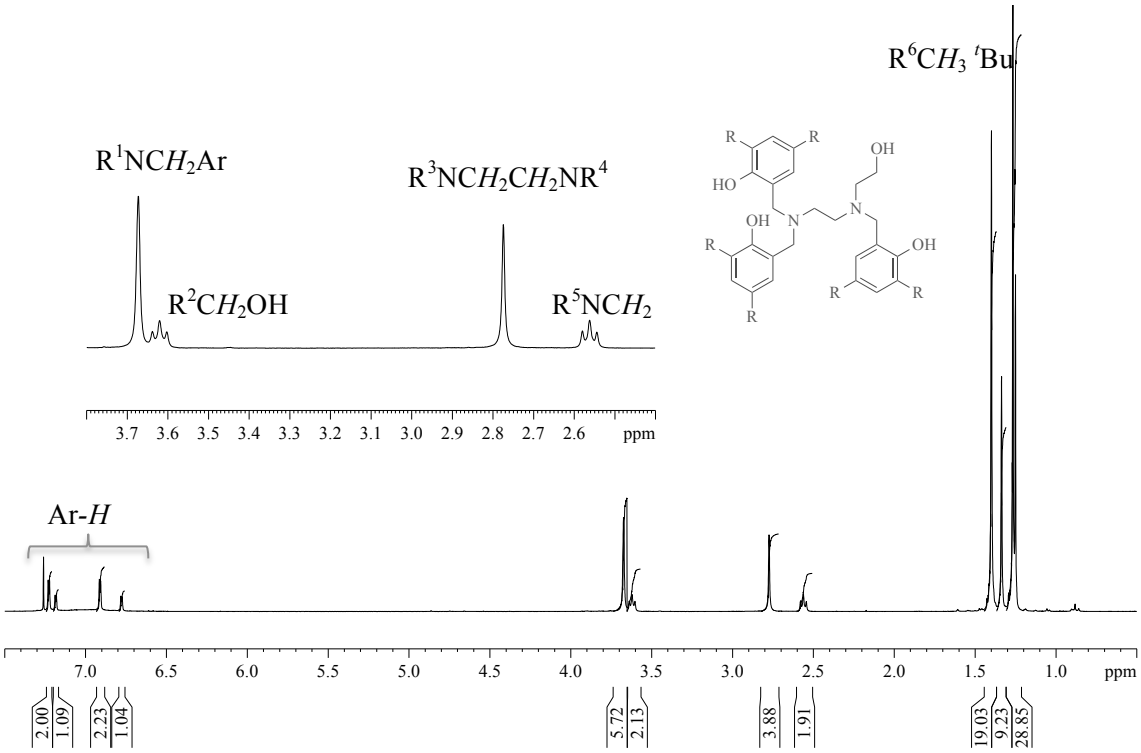

Figure 2.3.1: ^{1}H NMR spectrum of 2,4-di*tert*butyl diaminetrisphenolate ligand $\mathbf{L_3}$, in $CDCl_3$ at 298K.

In the ^{1}H NMR spectrum, singlets were observed for all R^1NCH_2-Ar protons in the NMR spectrum, as they were seen to be in the same environment (3.67 ppm, **Error! Reference source not found.**). The same is true for $R^3NCH_2CH_2NR^4$ protons where all four protons are in similar environments (2.78 ppm). The ethanol moiety however, shows two triplets for NCH_2CH_2OH protons (2.56 ppm and 3.61 ppm respectively) due $^{3}J_{HH}$ vicinal coupling. All aromatic protons appear as doublets with a $^{4}J_{HH}$-coupling of 2.4 Hz due to allylic 'w-coupling'.

$\mathbf{L_3}$ was reacted with $Ti(O^iPr)_4$ in a 1:1 stoichiometric reaction to yield the proposed structure of $Ti_2(\mathbf{L_3})_2$, **9** (Scheme 2.3.2).

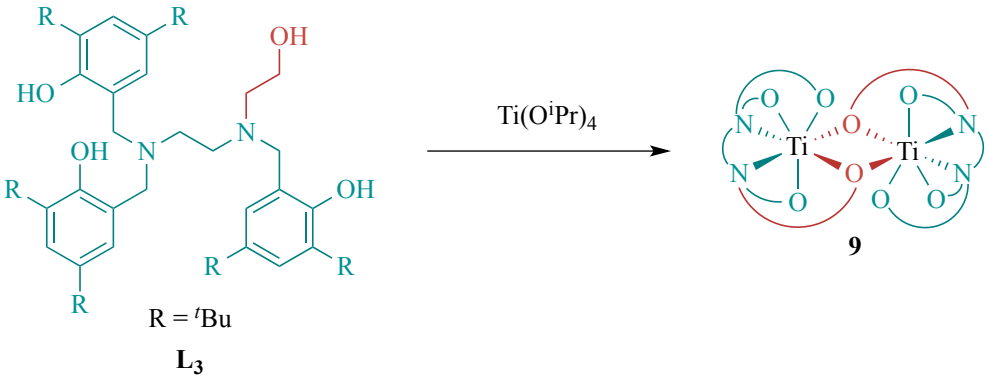

Scheme 2.3.2: Synthesis and schematically proposed structure of $Ti_2(\mathbf{L_3})_2$, **9** (chelating ligand moiety (green), bridging aliphatic alcohol (red)).

Although the complex was recrystallized, needle-type crystals formed which were unsuitable for single crystal X-ray crystallography. Elemental analysis was consistent with an empirical formula of $C_{49}H_{74}N_2O_4Ti$ (Anal: Calc. C: 73.29 %, H: 9.29 %, N: 3.49 %. Found C: 72.75 %, H: 9.22 %, N: 3.72 %). As the ligand $\mathbf{L_3}$ is an analogue of $\mathbf{L_2}$ with increased steric bulk, it is suggested that the most stable structure was formed consisting of two titanium metal centres with two ligands ($Ti_2(\mathbf{L_3})_2$, **9**) an analogue of $Ti_2(\mathbf{L_2})_2$. It is proposed that the aliphatic alcohol pendant arm of $\mathbf{L_3}$ may form a μ^2-bridge between the two titanium metal centres due to steric effects (Scheme 2.3.2). Characterisation by ^{1}H NMR and ^{13}C {H} NMR spectroscopy were consistent with a 1:1 Ti:ligand ratio (Figure 2.3.2).

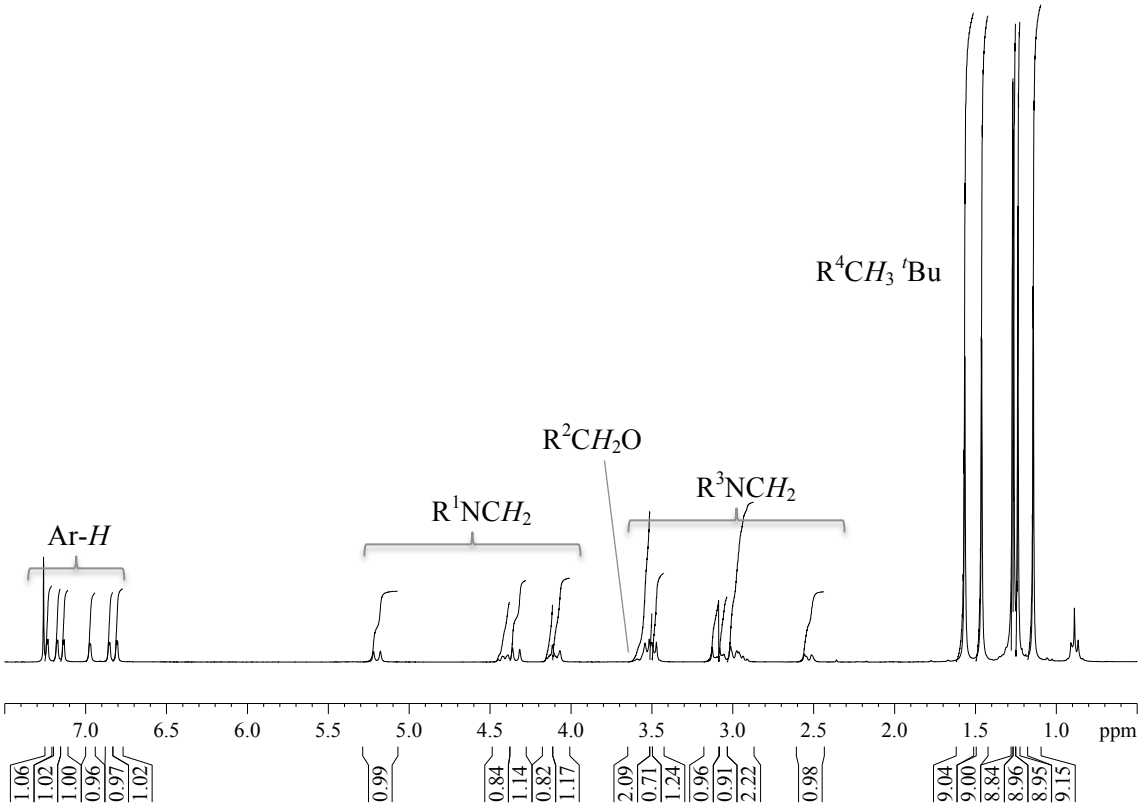

Figure 2.3.2: ^{1}H NMR spectrum of ligand Ti$\mathbf{L_3}$, **9**, in $CDCl_3$ at 298K.

In solution, all aromatic protons of Ti**L$_3$ 9**, are inequivalent and appear as doublets with $^4J_{HH}$ w-coupling of ~2.1 Hz. Although many of the R^{1}NCH_2 moieties displayed are overlapping, some doublets can be distinguished with $^2J_{HH}$ geminal coupling of ~13.0 Hz corresponding to inequivalent protons adjacent to the aromatic moiety. The remaining R^{3}NCH_2 multiplets experience both $^2J_{HH}$ geminal and $^3J_{HH}$ vicinal coupling. The overlapping R^{2}CH_2O multiplet at 3.64 – 3.54 ppm was deduced with the aid of COSY spectroscopy. The ^{t}Bu residues were observed as singlets due to the protons being equivalent.

The reaction was repeated using Zr(O^{i}Pr)$_4$.HO^{i}Pr and Hf(O^{i}Pr)$_4$.HO^{i}Pr instead of Ti(O^{i}Pr)$_4$ however, both reactions yielded products that were insoluble in all common solvents. An alternative method using tetrakis(dimethylamido)zirconium instead of zirconium isopropoxide with **L$_3$** was trialled under the same conditions. However, the reaction again yielded a product that was insoluble in all common solvents and the reactions were discarded.

Group 4 complexes as initiators in the solvent-free ROP of *rac*-LA

2.4 Solvent-free ROP of *rac*-LA at 135°C

The Group 4 initiators discussed in this chapter, were investigated for their ability as initiators in the ROP of sublimed *rac*-LA. As discussed in Chapter 1, monomer conversions were determined by NMR spectroscopy due to a distinct downfield shift in the methine region for the polymer methines being observed compared to the monomer methine protons. The tacticity of the polymers were established by homonuclear decoupling of the methine moiety from the methane region revealing distinct differing tetrads. Molecular weights were verified by GPC (calibrated with polystyrene standards, in THF, 35 °C, 1.0 ml/min).

Polymerisations of sublimed *rac*-LA, using initiators **1** to **9** were initially screened under solvent-free conditions at 135°C with a 300:1 monomer to monomeric initiator ratio. For initiators with no labile isopropoxide groups (Zr$_2$(**L$_2$**)$_2$ **5**, Hf$_2$(**L$_2$**)$_2$ **6**, and Ti$_2$(**L$_3$**)$_2$ **9**), one equivalent of benzyl alcohol was added as a co-initiator. Aliquots were take every hour for 4 h, again at 24 h and conversion determined by ^{1}H NMR spectroscopy (Figure 2.4.1).

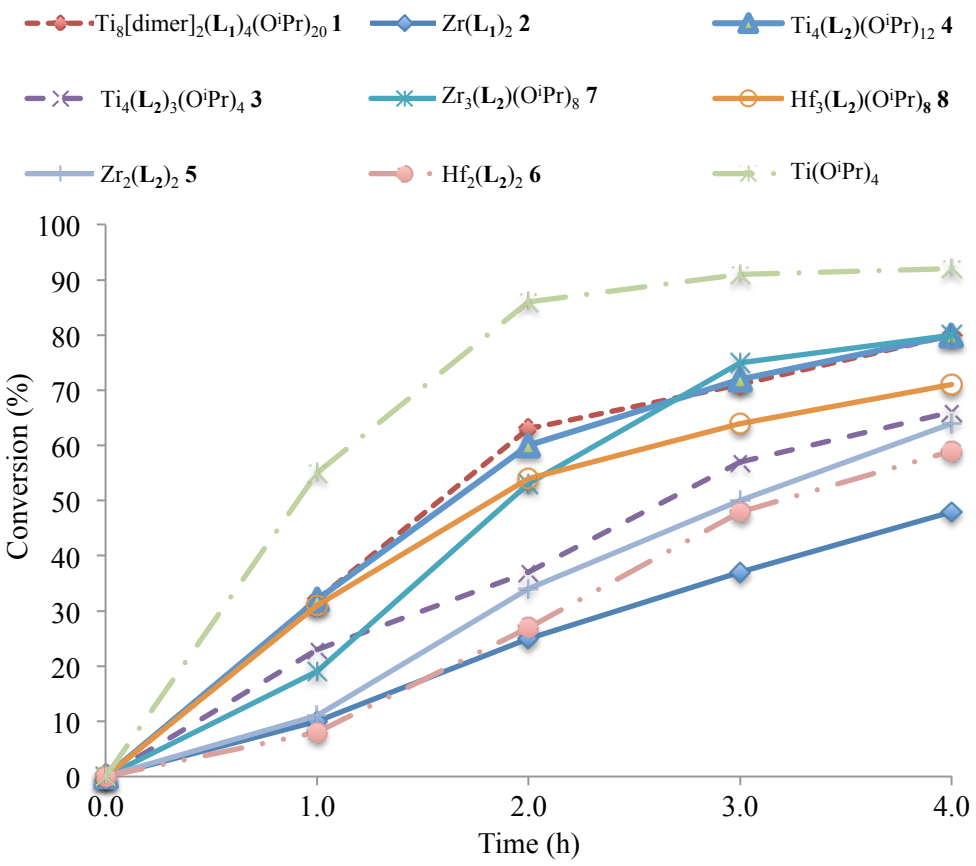

Figure 2.4.1: Reaction rate of lactide to PLA conversion in the solvent-free polymerisations of sublimed *rac*-LA at 135°C, 300:1 monomer to monomeric initiator ratio using initiators **1-8** and $Ti(O^iPr)_4$.

At 135°C, $Ti_8[dimer]_2(\mathbf{L_1})_4(O^iPr)_{20}$ **1** showed reasonable activity with 32 % conversion of monomer in 1 h whilst $Zr(\mathbf{L_1})_2$ **2** demonstrated moderate activity at 135°C with 48 % conversion of lactide in 4 h. The initiators with no isopropoxide groups ($Zr_2(\mathbf{L_2})_2$ **5**, and $Hf_2(\mathbf{L_2})_2$, **6**) were the least active converting less than 10% in 1 h whilst $Ti_2(\mathbf{L_3})_2$ **9** was completely inactive. **5** and **6**, the most stable initiators in the series, exhibit strong bonds to the chelating ligand reducing the accessibility of the metal centre to the approaching lactide monomer. This is also demonstrated by an increase in activity with increased isopropoxide groups ($Zr_3(\mathbf{L_2})(O^iPr)_8$ **7**, and $Hf_3(\mathbf{L_2})(O^iPr)_8$, **8**). A similar increase in activity is observed between $Ti_4(\mathbf{L_2})_3(O^iPr)_4$ **3**, and $Ti_4(\mathbf{L_2})(O^iPr)_{12}$ **4**. The most active initiators, **4** and **7** showed good activity yielding over 80% conversion to PLA in 4 h. At 135°C, kinetic data illustrates the metal is of less importance than the number of isopropoxide groups present in the initiator. Multiple initiation sites on the metal centre of the complex may have occurred, or the ligand may have initiated polymerisation potentially leading to branched or star-shaped polymers. Under the same conditions, commercially available $Ti(O^iPr)_4$ and $Zr(O^iPr)_4(HO^iPr)$ were trialled for the ROP of *rac*-LA.

Although $Ti(O^iPr)_4$ converted over 50% in 1 h, $Zr(O^iPr)_4(HO^iPr)$ was unreactive. The reactions were terminated by addition of methanol at 24 h, and the resulting polymers were analysed (Table 2.4.1).

Table 2.4.1: Solvent-free polymerisations of lactide at 135°C (300:1 monomer to monomeric initiator ratio).

Initiator	T (°C)	Time (h)	Conv. (%)	M_n (kg.mol^{-1})	$M_{n,\,theo}$ (kg.mol^{-1})	PDI	P_r
$Ti_8[dimer]_2(\mathbf{L_1})_4(O^iPr)_{20}$ **1**	135	24	88	5.2	38.1	1.47	0.54
$Zr(\mathbf{L_1})_2$ **2**	135	24	93	4.8	40.3	1.22	0.49
$Ti_4(\mathbf{L_2})_3(O^iPr)_4$ **3**	135	24	90	7.0	38.9	1.43	0.52
$Ti_4(\mathbf{L_2})(O^iPr)_{12}$ **4**	135	24	92	7.2	39.8	1.49	0.52
$Zr_2(\mathbf{L_2})_2$* **5**	135	24	78	2.6	33.8	1.53	0.52
$Hf_2(\mathbf{L_2})_2$* **6**	135	24	64	2.1	27.7	1.62	0.56
$Zr_3(\mathbf{L_2})(O^iPr)_8$ **7**	135	24	93	4.2	40.3	1.41	0.55
$Hf_3(\mathbf{L_2})(O^iPr)_8$ **8**	135	24	81	12.2	35.1	1.34	0.51
$Ti_2(\mathbf{L_3})_2$* **9**	135	34	0	-	-	-	-
$Ti(O^iPr)_4$	135	24	93	11.8	40.3	1.27	0.53
$Zr(O^iPr)_4(HO^iPr)$	135	24	0	-	-	-	-

* Addition of benzyl alcohol (1 equiv.) as co-initiator.

All polymerisations gave atactic PLA with P_r's of 0.49 to 0.54. $Ti_8[dimer]_2(\mathbf{L_2})_4(O^iPr)_{20}$ **1** showed moderate activity converting 88 % in 24 h with an observed M_n of 5.2 kg.mol^{-1}, a much lower M_n than theoretically calculated of 38.1 kg.mol^{-1} assuming that one initiator complex initiates one polymer chain. As previously discussed in this chapter, there are 20 isopropoxide groups within the structure of the initiator and the vast number of labile isopropoxide groups could account for the low M_n. Multiple polymer chains may have grown from each metal centre and formed many shorter chained polymers. $Zr(\mathbf{L_1})_2$ **2** converted 90 % in 24 h with a M_n of 4.8 kg.mol^{-1}. All Group 4 $\mathbf{L_2}$ complexes controlled polymerisations were observed for all initiators with PDI's ranging from 1.34 to 1.62. **4** and **7** were the most active converting over 90 % in 24 h with **8** affording the highest M_n (12.2 kg.mol^{-1}). Again, M_n values are much lower than expected (35.1 kg.mol^{-1}), this may be due to the vast number of isopropoxide initiator groups. Commercially available $Ti(O^iPr)_4$ showed high activity (93 % in 24 h), however, exhibited low molecular weight control (M_n 11.8 kg.mol^{-1}) whilst $Zr(O^iPr)_4(HO^iPr)$ was inactive.

In order to investigate the effect of co-initiator using $Hf_2(\mathbf{L_2})_2$ **6** on molecular weight control, ROP of sublimed *rac*-LA was trialled using **6** with varying equivalents of benzyl alcohol at 135°C, and the resulting polymers analysed (Table 2.4.2).

Table 2.4.2: Solvent-free polymerisations of *rac*-LA using $Hf_2(\mathbf{L_2})_2$, **6**, at 135°C.

Co-initiator (Benzyl alcohol)	T (°C)	Time (h)	Conv. (%)	M_n (kg.mol^{-1})	$M_{n,\,theo}$ (kg.mol^{-1})	PDI
2 eq.	135	24	53	5.9	11.5	1.35
4 eq.	135	24	49	4.8	5.4	1.40
10 eq.	135	24	48	1.3	2.1	1.35

Although the observed M_n is not comparable to previous experiments possibly due to monomer batch variation or inconsistencies of GPC traces at low molecular weights, the results in Table 2.4.2 are comparable to each other. As expected, as the quantity of co-initiator (benzyl alcohol) was increased from 2 eq. to 10 eq., a reduction in M_n of 5.9 to 1.3 kg.mol^{-1} respectively was observed. A higher amount of smaller chain-length polymers were generated. This confirms that the amount of co-initiator within the system influences the molecular weights of the resulting polymer.

Matrix assisted laser desorption and time of flight mass spectrometry (MALDI-ToF/MS) analysis of polymers can be used to determine end groups, repeat units within the polymer chain and examine molecular weight distributions, as discussed in Chapter 1. Polymers using $Ti_4(\mathbf{L_2})_3(O^iPr)_4$ **3**, $Ti_4(\mathbf{L_2})(O^iPr)_{12}$ **4**, and $Zr_3(\mathbf{L_2})(O^iPr)_8$ **7**, initiators at 135°C were characterised by MALDI-ToF as shown in Figure 2.4.2.

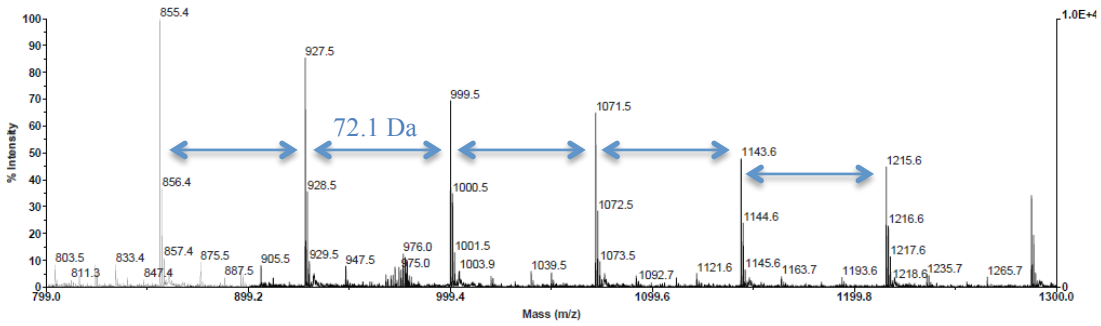

Figure 2.4.2: MALDI-ToF of PLA synthesised using $Zr_3(\mathbf{L_2})(O^iPr)_8$, **7**, at 135°C.

The major series for **3**, **4** and **7**, however, could not be identified and may be due to an alternative polymerisation route via ligand fragmentation. All possibilities of cyclic, fragmented and alternative end groups were investigated, none of which fitted the trend (Figure 2.4.2). The MS revealed a repeat unit of 72.1 Da in both series, which is indicative of the occurrence of transesterification.

In order to examine the active species within the reaction, VT-NMR spectroscopy was performed on $Ti_4(\mathbf{L_2})(O^iPr)_{12}$ **4,** at 135°C in d_{10} *o*-xylene (Figure 2.4.3).

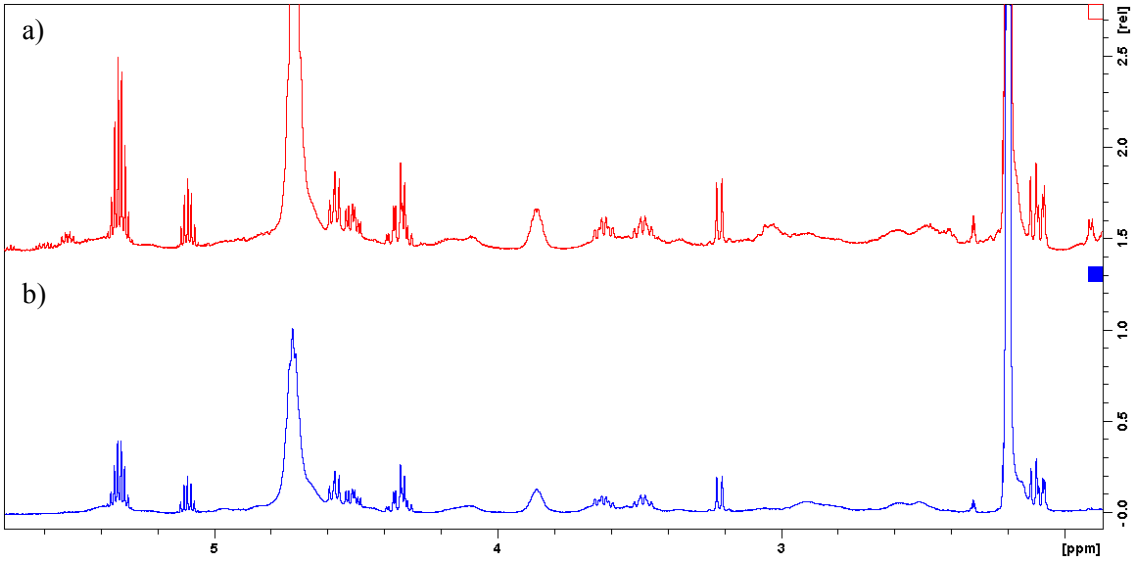

Figure 2.4.3: ^{1}H NMR spectra of $Ti_4(\mathbf{L_2})(O^iPr)_{12}$ **4**, at 25°C: **a)** after it was heated to 135 °C; **b)** without heating, in *o*-xylene d_{10}.

The initiator, **4**, was heated to 135°C and monitored by ^{1}H NMR spectroscopy at 10°C intervals. It was observed that there were no significant differences between spectra taken at 25°C before heating and the spectrum at 25°C after heating to 135°C. This indicates that the catalyst survives these high temperature reaction conditions.

2.5 Solvent-free ROP of *rac*-LA at 165°C

Polymerisations of sublimed *rac*-LA, using initiators **1** to **9** were screened under solvent-free conditions at an elevated temperature of 165 °C with a 300:1 monomer to initiator ratio. Again, for initiators with no labile isopropoxide groups ($Zr_2(\mathbf{L_2})_2$ **5**, $Hf_2(\mathbf{L_2})_2$ **6**, and $Ti_2(\mathbf{L_3})_2$ **9**), one equivalent of benzyl alcohol was added as a co-initiator. Aliquots were take every hour for 4 h, again at 24 h and conversion determined by ^{1}H NMR spectroscopy (Figure 2.5.1).

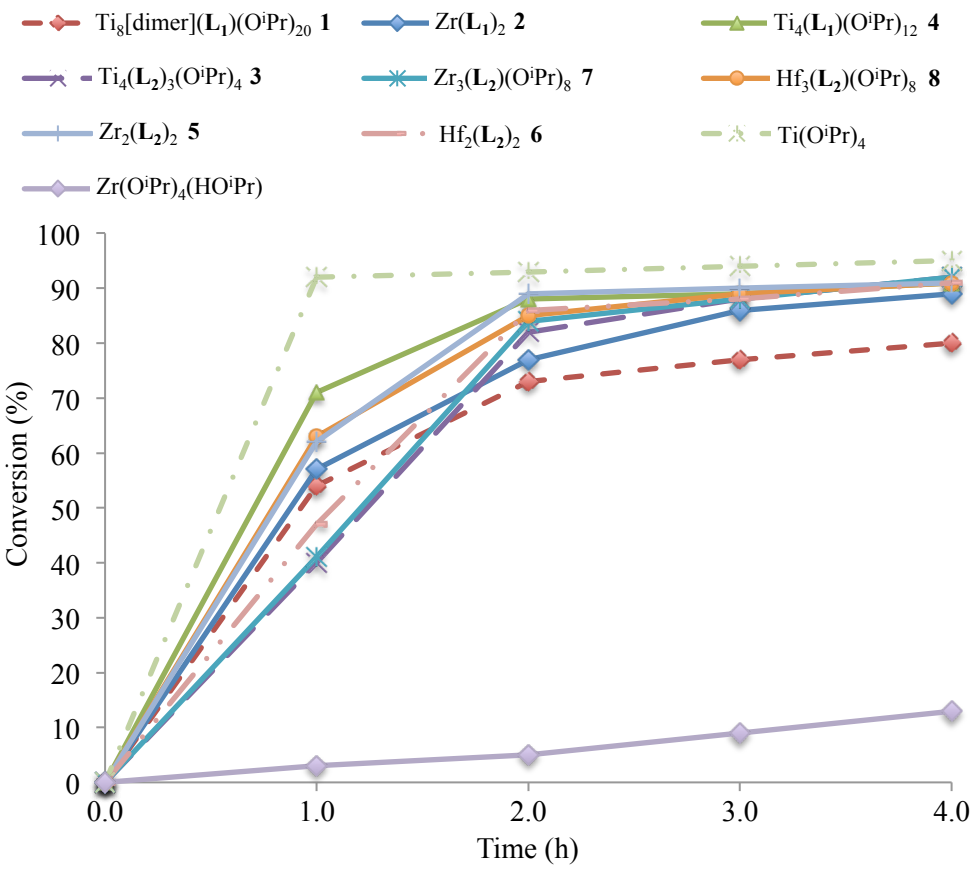

Figure 2.5.1: Conversion of lactide to PLA in the solvent-free polymerisations of sublimed *rac*-LA at 165°C, 300:1 monomer to initiator ratio.

At 165°C, $Ti_8[dimer]_2(\mathbf{L_1})_4(O^iPr)_{20}$ **1** and $Zr(\mathbf{L_1})_2$ **2** showed an increased activity with increased temperature with 55 % and 57 % conversion of monomer respectively in 1 h. All Group 4 $\mathbf{L_2}$ initiators displayed a significant increase in activity converting over 90 % in 4 h compared to polymerisations performed 135°C. The relative activity does not appear to be associated with either the identity of the metal centre or the number of isopropoxide groups. At this elevated temperature the initiators may be degrading forming an active species that is similar in each initiator. This is further supported later in this chapter whereby an induction period is observed for **4** using FT-IR spectroscopy to monitor the reaction. $Ti_2(\mathbf{L_3})_2$ **9**, was again inactive at 165°C. Commercially available $Ti(O^iPr)_4$ and $Zr(O^iPr)_4(HO^iPr)$ were also tested at 165°C. $Ti(O^iPr)_4$ was comparable to **4** converting 92% in 4 h, $Zr(O^iPr)_4(HO^iPr)$ however, showed poor activity only converting 12 % to polymer in 4 h. GPC measurements are shown below (Table 2.5.1).

Table 2.5.1: Solvent-free polymerisations of lactide at 165°C (300:1 monomer to monomeric initiator).

Initiator	T (°C)	Time (h)	Conv. (%)	M_n (kg.mol^{-1})	$M_{n,\,theo}$ (kg.mol^{-1})	PDI	P_r
Ti_8[dimer]$_2$(**L$_1$**)$_4$(O^{i}Pr)$_{20}$ **1**	165	24	91	1.1	39.4	1.34	0.52
Zr(**L$_1$**)$_2$ **2**	165	24	92	7.0	39.8	1.43	0.50
Ti_4(**L$_2$**)$_3$(O^{i}Pr)$_4$ **3**	165	24	96	6.0	41.5	1.60	0.55
Ti_4(**L$_2$**)(O^{i}Pr)$_{12}$ **4**	165	24	92	4.8	39.8	1.79	0.49
Zr_2(**L$_2$**)$_2$* **5**	165	24	97	5.4	41.9	1.65	0.54
Hf_2(**L$_2$**)$_2$* **6**	165	24	94	2.1	40.7	2.07	0.49
Zr_3(**L$_2$**)(O^{i}Pr)$_8$ **7**	165	24	96	5.9	41.5	1.49	0.59
Hf_3(**L$_2$**)(O^{i}Pr)$_8$ **8**	165	24	97	17.5	41.9	1.42	0.49
Ti_2(**L$_3$**)$_2$* **9**	165	24	0	-	-	-	-
Ti(O^{i}Pr)$_4$	165	24	95	13.2	41.1	1.41	0.49
Zr(O^{i}Pr)$_4$(HO^{i}Pr)	165	24	24	0.6	10.4	1.07	0.51

* Addition of benzyl alcohol (1 equiv.) as co-initiator.

At 165°C, all polymerisations yielded atactic PLA. The M_n of **1** was further lowered (1.1 kg.mol^{-1}) at this elevated temperature, this is indicative of an increased level of transesterification at a higher temperature. Zr(**L$_2$**)$_2$ gave over 90 % conversion of monomer after 24 h with M_n of 5.4 kg.mol^{-1}, a distinctly larger M_n, although still lower than expected. Group 4 **L$_2$** initiators gave atactic PLA with **7** exhibiting a slight heterotactic bias with a P_r of 0.59. Increased levels of transesterification were observed due to lower M_n than expected (43.0 kg.mol^{-1}) with further evidence of this phenomenon given by an increase in PDI with increase temperature. Markedly low M_n's could also be indicative of branched polymers possibly being produced. Further characterization was necessary in order to test this hypothesis and determine the structural architecture of the polymers. The Mark-Houwink plots of polymers prepared using **4** and **8** at 165°C, and **3** at 135°C (Table 2.5.2) were generated using an absolute GPC with light scattering, concentration and viscosity detectors.

Table 2.5.2: GPC viscometry measurements.

Sample	IV (dl/g)	MH a	MH log K	g'[1]	B_n[2]	λ[3]
$Ti_4(\mathbf{L_2})_3(O^iPr)_4$ **3** (135°C)	0.14	0.78	-3.82	0.66	2.49	18.2
$Hf_3(\mathbf{L_2})(O^iPr)_8$ **8** (165°C)	0.23	0.90	-4.33	0.79	1.54	11.1
$Ti_4(\mathbf{L_2})(O^iPr)_{12}$ **4** (165 °C)	0.13	0.33	-2.12	0.66	2.99	24.3

[1]g': $g' = IV_{branched} / IV_{linear}$. When g' equals 1 the sample is linear.[21]
[2]B_n: The absolute number of branches in a sample compared to a linear sample.
[3]λ : Lambda, the absolute number of branches compared to a linear sample per repeat unit.

Branched polymers are more compact than linear polymers at equal molecular weights and thus display a smaller hydrodynamic volume. A comparison of branched polymers relative to linear polymers (control) with similar molecular weights is given as g'.[21] The results are typical for branched polymers (g' < 1), tentatively suggesting branching to some extent is present in the resulting polymers (Table 2.5.2). This may be due to a degree of incorporation of the ligand into the polymer structure. Alternatively, transesterification may be promoted by another metal centre in the initiator. In this case, further investigations are required to prove branching of polymers occurred.

2.6 *In situ* Fourier Transform Infra-Red Spectroscopy (FT-IR)

To achieve a better understanding of ROP of lactide at 165°C, an initiator was trialled under more industrially relevant conditions. At 165°C, all initiators screened demonstrated similar activity and $Ti_4(\mathbf{L_2})(O^iPr)_{12}$ **4**, was selected for further investigation to deduce its viability as a replacement for $Sn(Oct)_2$. To mimic industrial conditions on a larger scale, non-sublimed *rac*-LA (35 g) was polymerized at 165°C with a much lower catalytic loading of 5000:1. The polymerisation kinetics were monitored by *in situ* FT-IR under a positive flow of argon in a jacketed vessel with a mechanical stirrer. The C-O-C asymmetric vibration of the monomer (1240 cm^{-1}) was integrated linearly from the baseline and monitored throughout the reaction to assess the depletion of monomer. Simultaneously, the C-O-C asymmetric vibration of the polymer (1185 cm^{-1}) was monitored to assess the relative concentration of the growing PLA polymer (Figure 2.6.1).

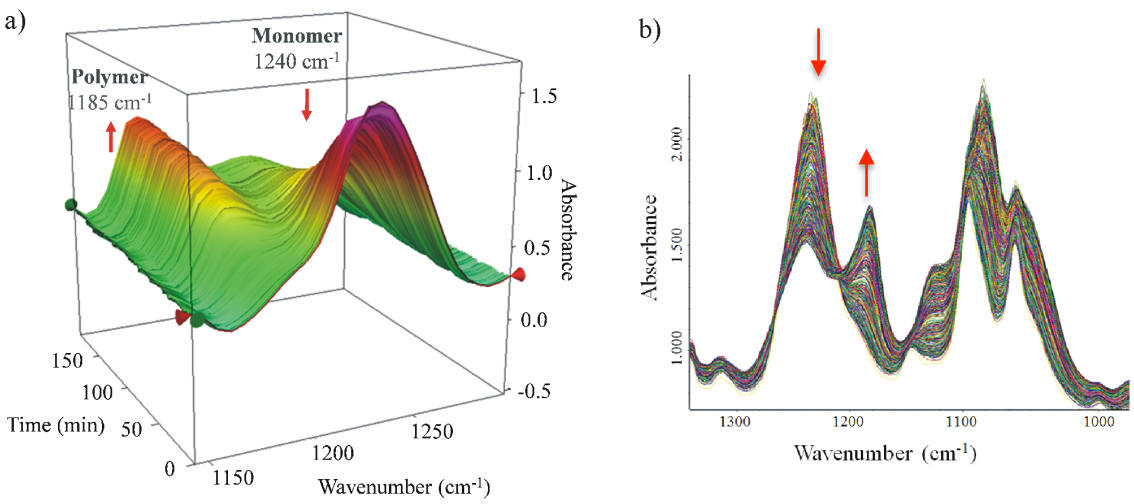

Figure 2.6.1: a) 3D time resolved FT-IR spectra, **b)** 2D time resolved FT-IR spectra of the polymerisation of *rac*-lactide with $Ti_4(\mathbf{L_2})(O^iPr)_{12}$ **4** at 165°C, 5000:1.

Rac-LA (35 g) was melted in the jacketed vessel at 165°C under a positive flow of argon. The initiator, **4**, was dissolved in a minimal amount of dry toluene, transferred to reaction vessel and stirred. An induction period was observed for the initial 5 minutes until the initiator dissolved fully. An identical method was applied for $Sn(Oct)_2$ with benzyl alcohol and the polymerisation was monitored by FT-IR. The same conditions were used for $Ti(O^iPr)_4$, however the polymerisation was monitored by ^1H NMR spectroscopy with an aliquot taken every 5 to 10 minutes due to lack of FT-IR availability (Figure 2.6.2a).

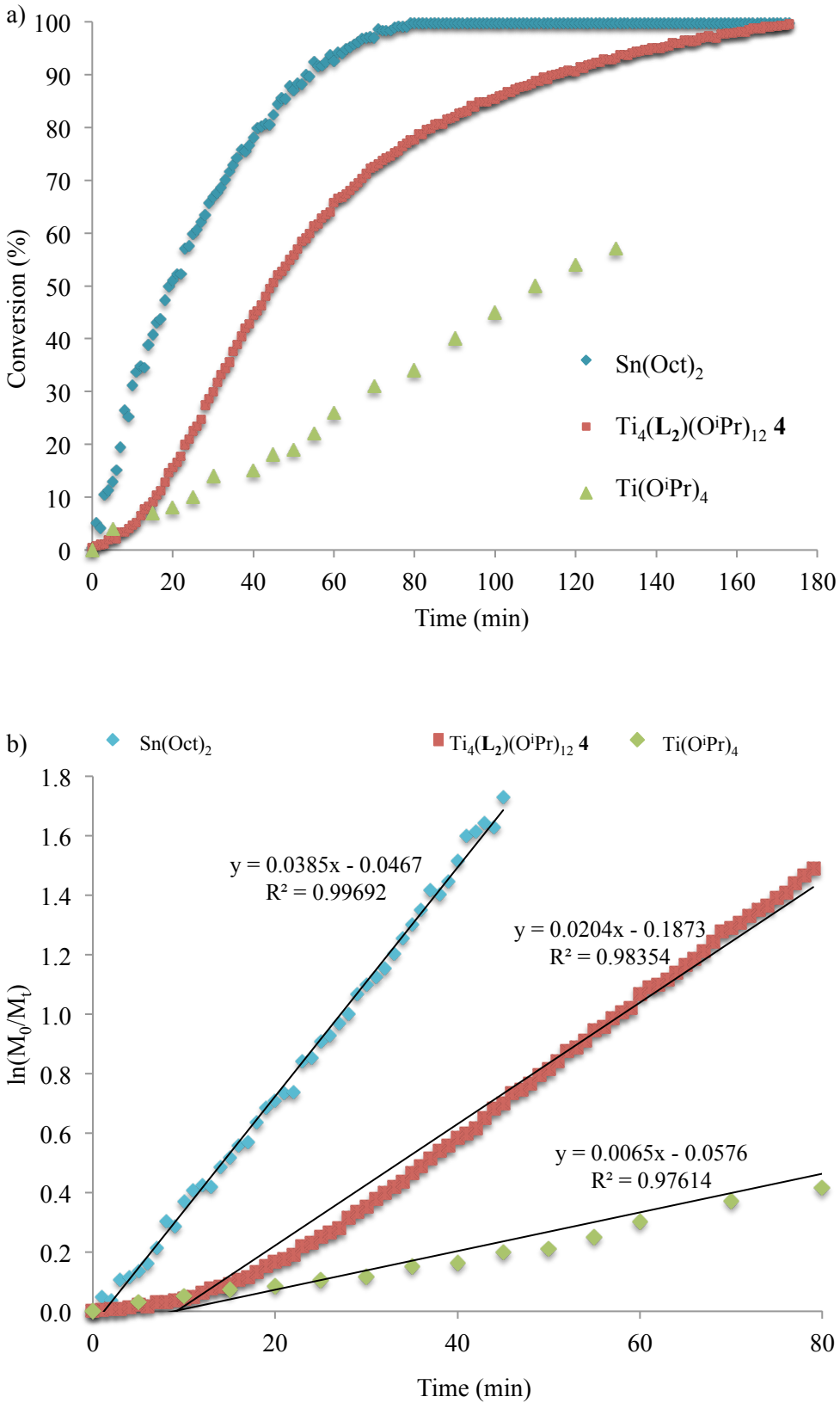

Figure 2.6.2: a) Solvent-free polymerisation rate of unsublimed *rac*-LA at 165°C, 5000:1 with $Sn(Oct)_2$ (blue), $Ti_4(\mathbf{L_2})(O^iPr)_{12}$ **4** (red) and $Ti(O^iPr)_4$ (green). **b)** Semi -log plot of $\ln[M_0/M_t]$ against time for ROP using $Sn(Oct)_2$ (blue), $Ti_4(\mathbf{L_2})(O^iPr)_{12}$ **4** (red) and $Ti(O^iPr)_4$ (green).

The polymerisation of recrystallized (non-sublimed) *rac*-LA with $Sn(Oct)_2$ was highly active and reached near completion within 1 h, as expected. The precursor to **4**, $Ti(O^iPr)_4$ was markedly less active under industrially relevant conditions converting only 57 % in over 2 h. This may be due the low stability of $Ti(O^iPr)_4$ to lactic acid and water impurities in the non-sublimed lactide, thus $Ti(O^iPr)_4$ is not a viable initiator for the ring-opening polymerisation under industrially relevant conditions. **4** was significantly more active than $Ti(O^iPr)_4$ under industrially relevant conditions and reached near completion in 3 h showing great potential as a viable initiator. The semi-logarithmic plot of **4** shows an apparent rate constant (k_{app}) of 0.0204 min^{-1} which is comparable to that of $Sn(Oct)_2$ (k_{app} = 0.0385 min^{-1}). $Ti(O^iPr)_4$ was considerably slower with k_{app} of 0.0065 min^{-1}. All showed *pseudo*-first order kinetics suggesting well-controlled polymerisation.

Table 2.6.1: Solvent-free polymerisations of lactide at 165°C, 5000:1

Initiator	T (°C)	Time (min)	Conv. (%)	M_n ($kg.mol^{-1}$)	$M_{n,\,theo}$ ($kg.mol^{-1}$)	PDI
$Sn(Oct)_2$	165	80	99	94.3	712.8	1.21
$Ti_4(\mathbf{L_2})(O^iPr)_{12}$ **4**	165	180	99	8.2	712.8	1.32
$Ti(O^iPr)_4$	165	130	99	37.4	712.8	1.56

For the amount of initiator used in the polymerisation (monomer: initiator 5000:1), $Ti_4(\mathbf{L_2})(O^iPr)_{12}$ **4** gave relatively low M_n of 8.2 $kg.mol^{-1}$. The PDI however, was smaller with reduced initiator loading. $Sn(Oct)_2$ generated a much higher M_n of 94.1 $kg.mol^{-1}$ with a relatively narrow PDI of 1.21. $Ti(O^iPr)_4$ displayed a moderate M_n of 37.4 $kg.mol^{-1}$ but with an increased PDI (PDI = 1.56).

2.7 Conclusion

Several new group 4 complexes have been prepared and characterized. The activity of these complexes was assessed for the ROP of sublimed *rac*-LA under solvent-free conditions at 135°C and 165°C. All initiators were active with the exception of $Ti_2(\mathbf{L_3})_2$. Group 4 complexes with lactic acid, $Ti_8[dimer]_2(\mathbf{L_1})_4(O^iPr)_{20}$ and $Zr(\mathbf{L_1})_2$, showed moderate activity. Whilst $Zr(\mathbf{L_1})_2$ was the least active at 135°C, it was shown to be one of the most active at 165°C (89% in 4 h) in this series. For Group 4 $\mathbf{L_2}$ complexes, at 135°C, activity was found to increase with an increase in the number of labile isopropoxide groups. Under these conditions, the identity of the metal was found to be of less importance than the number of labile initiator groups present, with

similar Zr, Hf and Ti complexes giving similar conversions. On increasing the temperature to 165°C, all the complexes demonstrated a higher activity irrespective of the identity of the metal or number of labile initiator groups. It is likely that the actual active species at elevated temperatures is a degradation product of the catalyst, rather than the original catalysts.

Unfortunately, complexes with increased steric bulk were inactive under these conditions. The most active titanium species, $Ti_4(\mathbf{L_2})(O^iPr)_{12}$, was further examined under conditions more closely replicating industrial polymerisations: at 165°C with a low initiator loading (5000:1) and using unsublimed lactide. Under these conditions, and in contrast to commercially available Group 4 metal alkoxides ($Ti(O^iPr)_4$ and $Zr(O^iPr)_4(HO^iPr)$), $Ti_4(\mathbf{L_2})(O^iPr)_{12}$, **4**, was found to be highly active, facilitating a >99 % polymerisation of the monomer to PLA within 3 hours thus highlighting the potential of Group 4 complexes as initiators for the commercial production of PLA.

2.8 Further work

The Group 4 metal complexes discussed in this chapter show promise and further work could be conducted into gradually varying the steric bulk of the ligand to extensively probe the potential of stereocontrol. In addition, large-scale polymerisations could be performed with the most promising initiator $Ti_4(\mathbf{L_2})(O^iPr)_{12}$ with unrecrystallised lactide. Investigations into the stability of $Ti_4(\mathbf{L_2})(O^iPr)_{12}$ in the presence of impurities (lactic acid and H_2O) in order to probe its potential as an initiator for L-LA or D-LA polymerisations with the intention of forming stereocomplexed PLA upon mixing of enantio-pure polymers.

2.9 References

(1) Dechy-Cabaret, O.; Martin-Vaca, B.; Bourissou, D. *Chem. Rev.* **2004**, *104*, 6147–6176.

(2) Platel, R. H.; Hodgson, L. M.; Williams, C. K. *Polym. Rev.* **2008**, *48*, 11–63.

(3) Jeffery, B. J.; Whitelaw, E. L.; Garcia-Vivo, D.; Stewart, J. A.; Mahon, M. F.; Davidson, M. G.; Jones, M. D. *Chem. Commun.* **2011**, *47*, 12328–12330.

(4) Chmura, A. J.; Davidson, M. G.; Jones, M. D.; Lunn, M. D.; Mahon, M. F.; Johnson, A. F.; Khunkamchoo, P.; Roberts, S. L.; Wong, S. S. F. *Macromolecules* **2006**, *39*, 7250–7257.

(5) Gendler, S.; Segal, S.; Goldberg, I.; Goldschmidt, Z.; Kol, M. *Inorg. Chem.* **2006**, *45*, 4783–4790.

(6) Sarazin, Y.; Howard, R. H.; Hughes, D. L.; Humphrey, S. M.; Bochmann, M. *Dalton Trans.* **2006**, 340–350.

(7) Whitelaw, E. L.; Jones, M. D.; Mahon, M. F. *Inorg. Chem.* **2010**, *49*, 7176–7181.

(8) Whitelaw, E. L.; Jones, M. D.; Mahon, M. F.; Kociok-Kohn, G. *Dalton Trans.* **2009**, 9020–9025.

(9) Hancock, S. L.; Mahon, M. F.; Kociok-Kőhn, G.; Jones, M. D. *Eur. J. Inorg. Chem.* **2011**, *2011*, 4596–4602.

(10) Hancock, S. L.; Mahon, M. F.; Jones, M. D. *Dalton Trans.* **2011**, *40*, 2033–2037.

(11) Kricheldorf, H. R.; Berl, M.; Scharnagl, N. *Macromolecules* **1988**, *21*, 286–293.

(12) Yeori, A.; Groysman, S.; Goldberg, I.; Kol, M. *Inorg. Chem.* **2005**, *44*, 4466–4468.

(13) Kakihana, M.; Tomita, K.; Petrykin, V.; Tada, M.; Sasaki, S.; Nakamura, Y. *Inorg. Chem.* **2004**, *43*, 4546–4548.

(14) Tulloch, A. A. D.; Cooper, A.; Duncan, R. H. Water-Stable Compounds, Catalysts and Catalysed Reactions. WO 2008/155568 A1, December 25, 2008.

(15) Gil, M. A.; Maringgele, W.; Dechert, S.; Meyer, F. *Zeitschrift für Anorg. und Allg. Chemie* **2007**, *633*, 2178–2186.

(16) Larsen, E. M.; Homeier, E. H. *Inorg. Chem.* **1972**, *11*, 2687–2692.

(17) Menge, W. M. P. B.; Verkade, J. G. *Inorg. Chem.* **1991**, *30*, 4628–4631.

(18) Kim, Y.; Jnaneshwara, G. K.; Verkade, J. G. *Inorg. Chem.* **2003**, *42*, 1437–1447.

(19) Chuck, C. J.; Davidson, M. G.; du Sart, G.; Ivanova-Mitseva, P. K.; Kociok-Köhn, G. I.; Manton, L. B. *Inorg. Chem.* **2013**, *52*, 10804–10811.

(20) Hormnirun, P.; Marshall, E. L.; Gibson, V. C.; White, A. J. P.; Williams, D. J. *J. Am. Chem. Soc.* **2004**, *126*, 2688–2689.

(21) Pitet, L. M.; Hait, S. B.; Lanyk, T. J.; Knauss, D. M. *Macromolecules* **2007**, *40*, 2327–2334.

Chapter 3

Co-polymerisation of lactide with commercially available co-monomers

3. Preamble

As discussed in Chapter 1, many different polymer architectures are possible from linear to branched co-polymers. The properties of these polymers are influenced by the sequence and proportion of monomers in the copolymer. The ability to exploit the change in thermal and mechanical properties of the polymer with the introduction of another monomer by copolymerization is of great interest both academically and industrially.[1] Industrially, the use of inexpensive commercially available monomers shows promise in both keeping costs down and also synthesising functional copolymers. In this chapter, we report incorporation of a range of commercially available monomers for copolymerisation with lactide. In order to prove the principle that such polymerisations can occur, reactions were performed under solution conditions (toluene, 80°C). The most promising monomers are discussed in this chapter and include ε-caprolactone, δ-valerolactone and ω-pentadecalactone (Figure 3.1). There are many methods to synthesise copolymers and an amalgamation of these methods (one-pot, sequential polymerisation, etc.) will be discussed in this chapter and subsequent physical and mechanical properties of polymers investigated. The ability to incorporate long flexible copolymer blocks with blocks of lactide will be probed, with the further intention of stereocomplexing the copolymers either with themselves or with the addition of another copolymer. Fusing the two principles of copolymerization and stereocomplexation to obtain a polymer with fine-tuned properties is a useful tool for the design of functional materials.

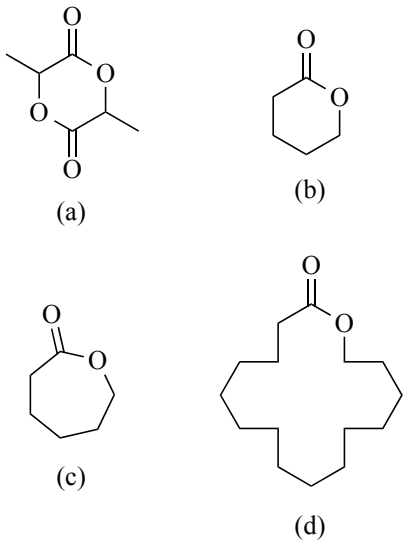

Figure 3.1: Commercially available monomers: (a) lactide; (b) δ-valerolactone; (c) ε-caprolactone; (d) ω-pentadecalactone.

The thermal properties of these copolymers such as melting temperature (T_m), glass transition temperature (T_g) and crystallisation temperatures (T_c) are investigated by differential scanning calorimetry (DSC). For comparison, previously reported data for the thermal properties of relevant homopolymers are given below in Table 3.1.

Table 3.1: Thermal Properties of various forms of PLA and other related polymers. [2–7]

	T_m (°C)	T_g (°C)	Ref.
Poly(L-lactide) (PLLA) or Poly(D-lactide) (PDLA)	170 - 190	50 - 65	Ref from [4]
Heterotactic PLA (P*het*LA)	-	< 45	Ref from [2]
Atactic PLA	-	45 - 55	Ref from [7]
Syndiotactic PLA	152	34	Ref from [6]
Stereocomplex-PLA (**sc**-PLA)	210 - 230	65 - 72	Ref from [2]
Poly-caprolactone (PCL)	57	-60	Ref from [3]
Poly-valerolactone (PVL)	60	-63	Ref from [7]
Poly-pentadecalactone (PPDL)	96	-25	Ref from [5]

3.1. Synthesis of tri-block co-polymers

For the synthesis of tri-block co-polymers, a Zr-based initiator ($L^{tBu}Zr(O^iPr)$) designed by Davidson and co-workers was utilized (Scheme 3.1.1) due to its high levels of stereocontrol coupled with high reactivity (k_{app} = 0.6 x 10^{-3} min^{-1}).[8]

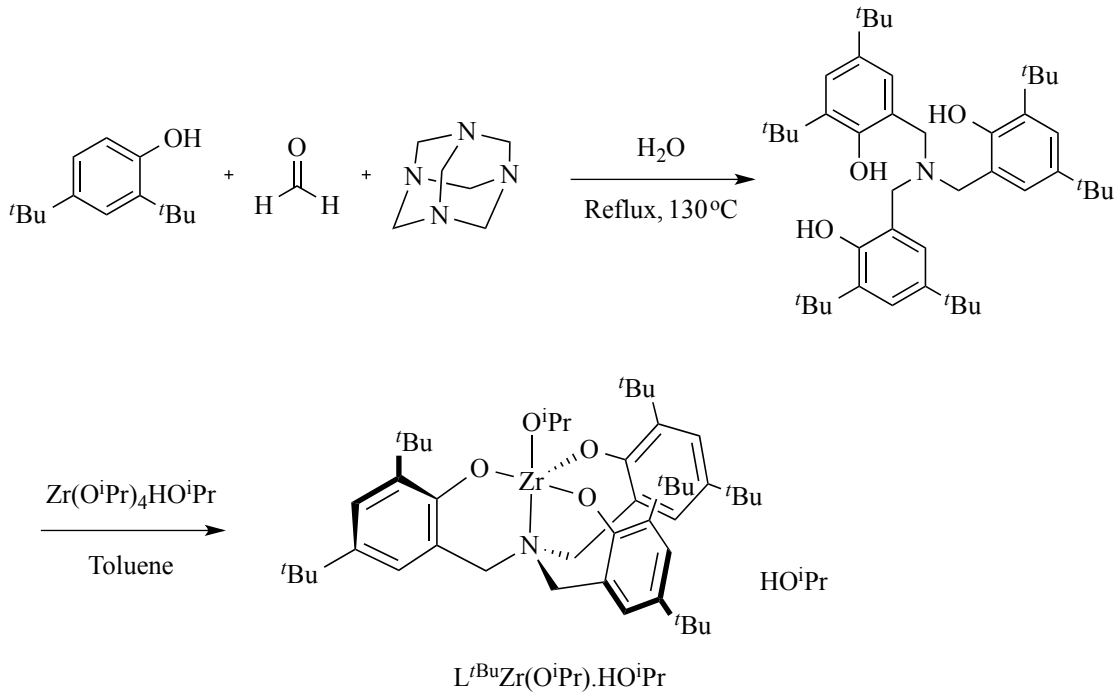

Scheme 3.1.1: Synthesis of $L^{tBu}Zr(O^iPr).HO^iPr$, an analogue of the previously reported $L^{tBu}Zr(O^iPr)$ by Davidson and co-workers.[8]

Initially, an ABC-type triblock polymer with a 'soft' B block was synthesised using L- and D-lactide (L-LA and D-LA) and ε-caprolactone (ε-CL). Although the properties of polymers of ε-CL and lactide are very different, they complement one another in such a way that PCL has good elasticity, drug permeability and thermal properties whereas PLA has good mechanical properties but poor elasticity.[9,10] Whilst such polymers have been previously reported in the literature, the use of $L^{tBu}Zr(O^iPr)$ has not been investigated, but would be advantageous as it has exhibited very good stereocontrol in the polymerisation of lactide whilst retaining high activity. Di-block polymers, (PLLA-PCL) and (PDLA-PCL), have been reportedly stereocomplexed in supercritical CO_2 to form polymers with 'soft' blocks along with enhanced thermal melt stability.[11] However, ABC type polymers have been little studied and are of great interest due to the potential for self-stereocomplexation of the individual PLLA and PDLA segments.

During the synthesis of $L^{tBu}Zr(O^iPr).HO^iPr$, various methods were used to remove the remaining isopropanol adduct (heat *in vacuo*, drying *via* azeotrope etc.), but were unsuccessful. Sequential polymerisation of the unsymmetrical ABC-type tri-stereoblock PLLA-PCL-PDLA polymer was trialled using L-LA, ε-CL and D-LA with $L^{tBu}Zr(O^iPr).HO^iPr$ (Figure 3.1.1).

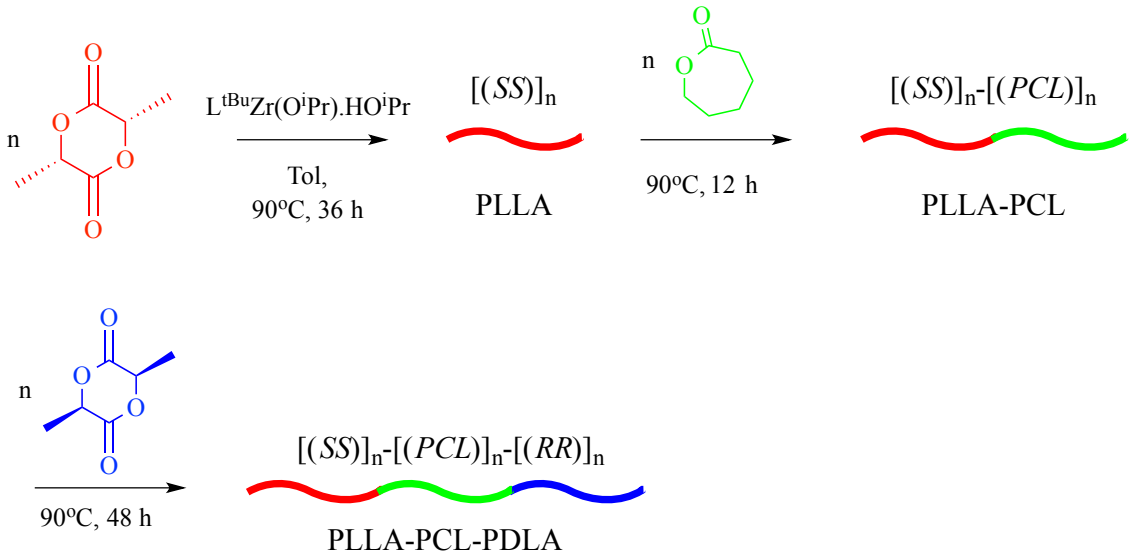

Figure 3.1.1: Sequential polymerization of ABC (PLLA-PCL-PDLA) type tri-stereoblock polymer.

The polymerization was performed using a monomer to initiator loading of 100:1 relative to all monomers (L-LA, ε-CL, D-LA). Initially, under inert conditions, sublimed L-LA and L$^{t\text{Bu}}$Zr(O^{i}Pr).HO^{i}Pr were dissolved in dry toluene and stirred at 90°C for 36 h. The reaction was monitored by ^{1}H NMR spectroscopy, and when near completion (93 % conversion), distilled ε-CL was added and the reaction was stirred for a further 12 h until near completion (>99 %). Upon further addition of sublimed D-LA, the reaction was stirred for 48 h and monitored until a completed (<99 %) tri-block co-polymer was formed.

In order to monitor the reaction, samples were taken for analysis after each polymer segment reached near completion. Upon completion of PLLA, an aliquot of the sample was dried under vacuum at 25°C and a ^{1}H NMR spectrum was taken (Figure 3.1.2a). The same was done for di-block PLLA-PCL and tri-block PLLA-PCL-PDLA co-polymers (Figure 3.1.2b and Figure 3.1.2c respectively).

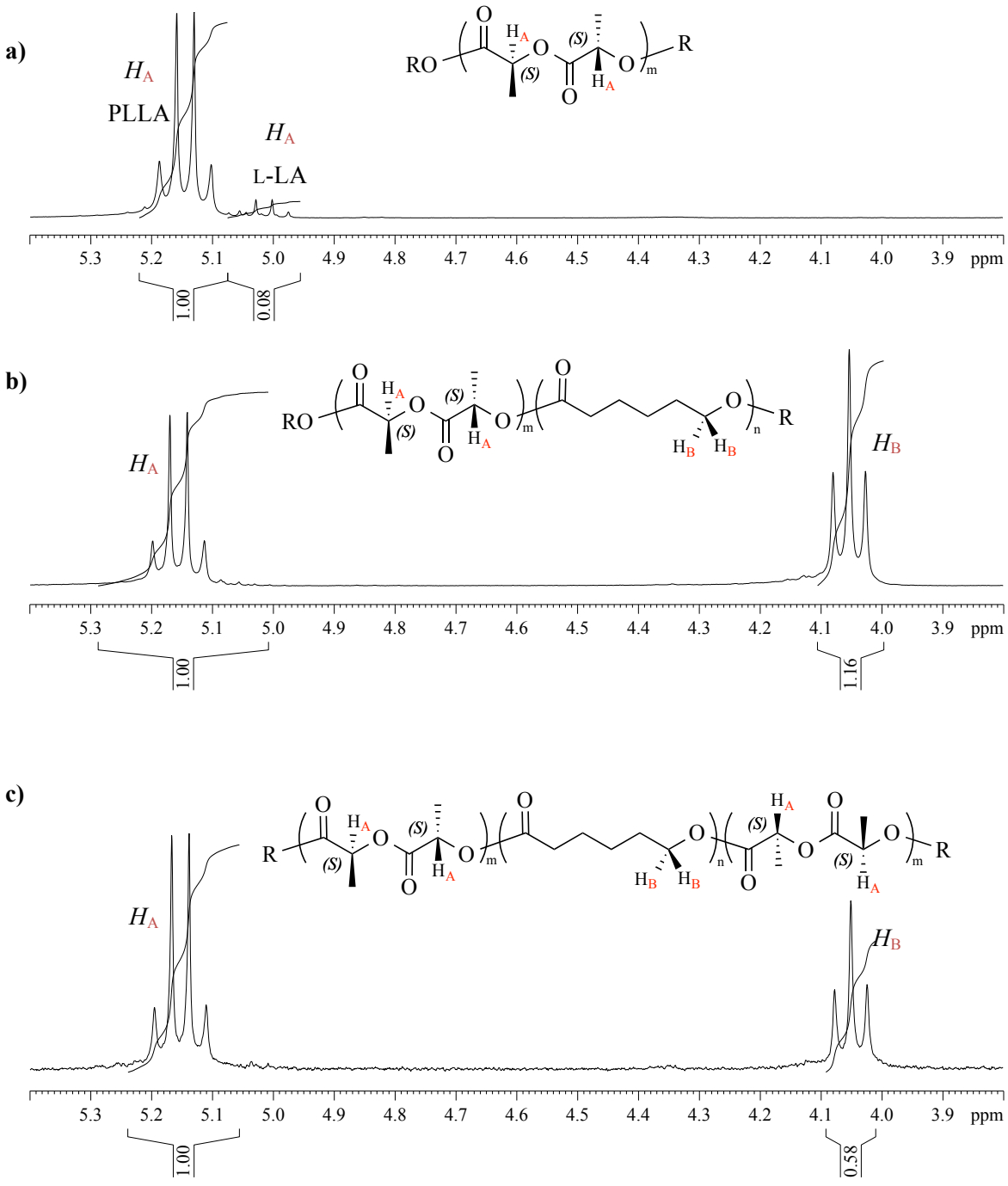

Figure 3.1.2: ^{1}H NMR spectrum in $CDCl_3$ at 298K of (a) PLLA; (b) PLLA-PCL; (c) PLLA-PCL-PDLA.

^{1}H NMR spectrum Figure 3.1.2a illustrates a quartet for the methine region of PLLA polymer (5.15 ppm), with a quartet for the unreacted monomer L-LA at 5.0 ppm. A conversion of 93% from L-LA monomer to PLLA polymer was calculated, which is explained in further detail in

Chapter 1. Figure 3.1.2b illustrates a ^{1}H NMR spectrum of the di-block copolymer, PLLA-PCL. It is shown that > 99% of ε -CL monomer was converted into polymer due to an up-field shift in the protons adjacent to the oxygen (RCH_2-O-R, PCL, 4.05 ppm). A quartet for the two methine (C*H*) protons of PLLA are observed at 5.15 ppm and a triplet for the methylene (CH_2) protons of PCL at 4.05 ppm. There is a ratio of 1:1.2, deduced by integration, suggesting that approximately equal equivalents of PLLA and PCL are present in the di-block co-polymer. This was expected as equal molar equivalents of monomers were added sequentially. Figure 3.1.2c, a ^{1}H NMR spectrum of tri-block co-polymer PLLA-PCL-PDLA, exhibits a ratio of 1:0.58 which accounts for four PLA methine protons (two for PLLA (H_A) and two for PDLA (H_A)) and two PCL methylene protons (H_B). This suggests that there is a 1:1.2:1 ratio of PLLA:PCL:PDLA in the tri-block co-polymer. **Figure 3.1.3** shows a ^{1}H NMR spectrum of the purified (by precipitation) tri-block co-polymer PLLA- PCL-PDLA.

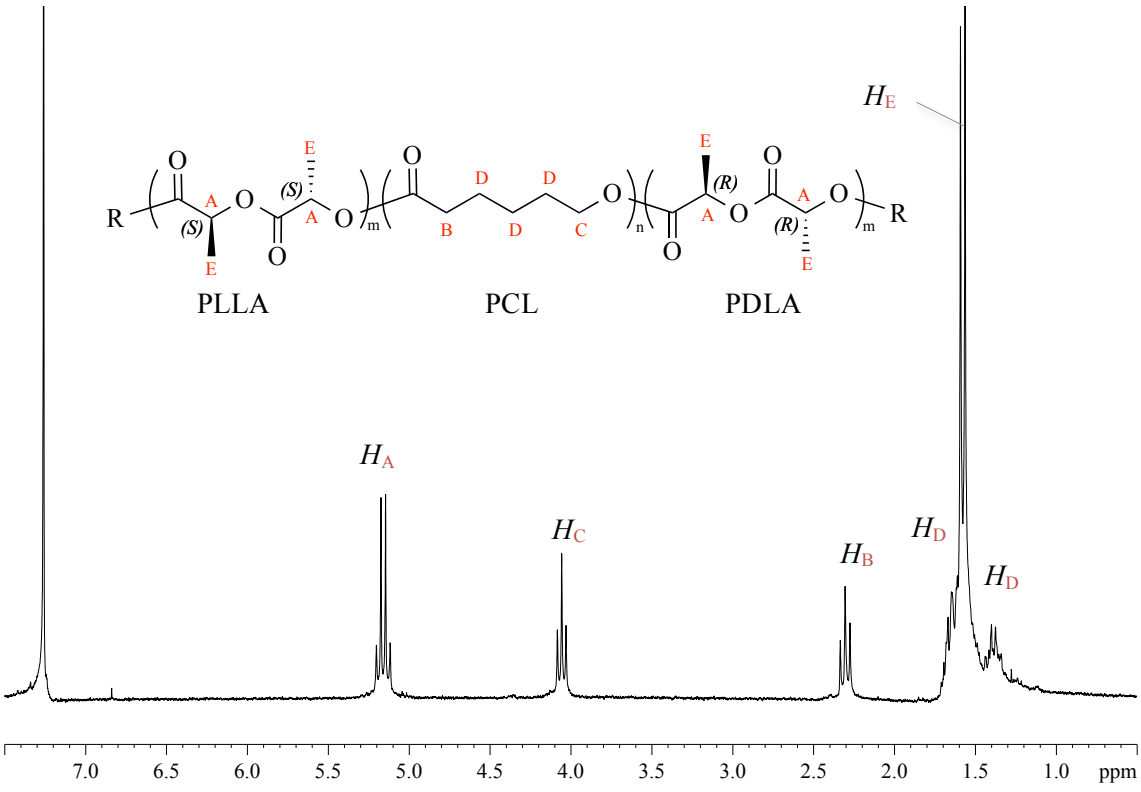

Figure 3.1.3: ^{1}H NMR spectrum of final tri-block co-polymer PLLA-PCL-PDLA in $CDCl_3$ at 298 K.

The ^{1}H NMR spectrum of final tri-block co-polymer (**Figure 3.1.3**) illustrates a quartet at 5.16 ppm for methine protons of PLA due to vicinal coupling ($^{3}J_{H\text{-}H}$ = 7.1 Hz) with the methyl moiety represented as a doublet at 1.58 ppm ($^{3}J_{H\text{-}H}$ = 7.1 Hz). Methylene protons of PCL

adjacent to oxygen (OCH_2), displayed as a triplet at 4.06 ppm (J = 6.7 Hz), was used in order to measure conversion (> 99 %). A triplet at 2.31 ppm is also observed for the methylene adjacent to the carbonyl moiety ($^3J_{H\text{-}H}$ = 7.6 Hz). Multiplets were observed between 1.73 – 1.28 ppm for the remaining methylene protons of PCL.

To confirm chain growth of the co-polymer after completion of each block, the remaining aliquots taken after completion of each polymer segment were dissolved in a small amount of dichloromethane and the polymers were precipitated with methanol. The polymeric material was filtered, washed with methanol and dried under vacuum. GPC analysis was used to determine growth in molecular weight (M_n). It is shown in Table 3.1.1 that upon addition of the next monomer, the polymer chains are in fact increased and form a hetero-polymer as opposed to individual homopolymers. Theoretically calculated M_n assumes one initiator complex initiates one polymer chain.

Table 3.1.1: GPC samples of PLLA-PCL-PDLA during sequential polymerization.

Polymer	M_n **kg.mol^{-1}**	$M_{n,\,theo}$ **kg.mol^{-1}**	**PDI**
PLLA	16.1	14.5	1.10
PLLA – PCL	37.3	25.6	1.46
PLLA-PCL-PDLA	Insoluble in THF		

Initially, PLLA was synthesised with a M_n of 16.0 kg.mol^{-1}. Upon addition of ε -CL, and with complete polymerisation, an increase in M_n was observed sugguesting a di-block co-polymer was synthesised. For both, the observed M_n was higher than the theoretically calculated. The final polymer (PLLA-PCL-PDLA) was insoluble in THF which is consistent with the possible synthesis of a stereocomplexed tri-block polymer, as the di-block readily dissolved in THF.

In order to determine the thermal properties of the resulting tri-block polymer, a sample was analysed by differential scanning calorimetry (DSC). For reference, literature values of homo-polymers are shown in Table 3.1. The thermal properties of the final triblock PLLA-PCL-PDLA polymer are shown below (Figure 3.1.4).

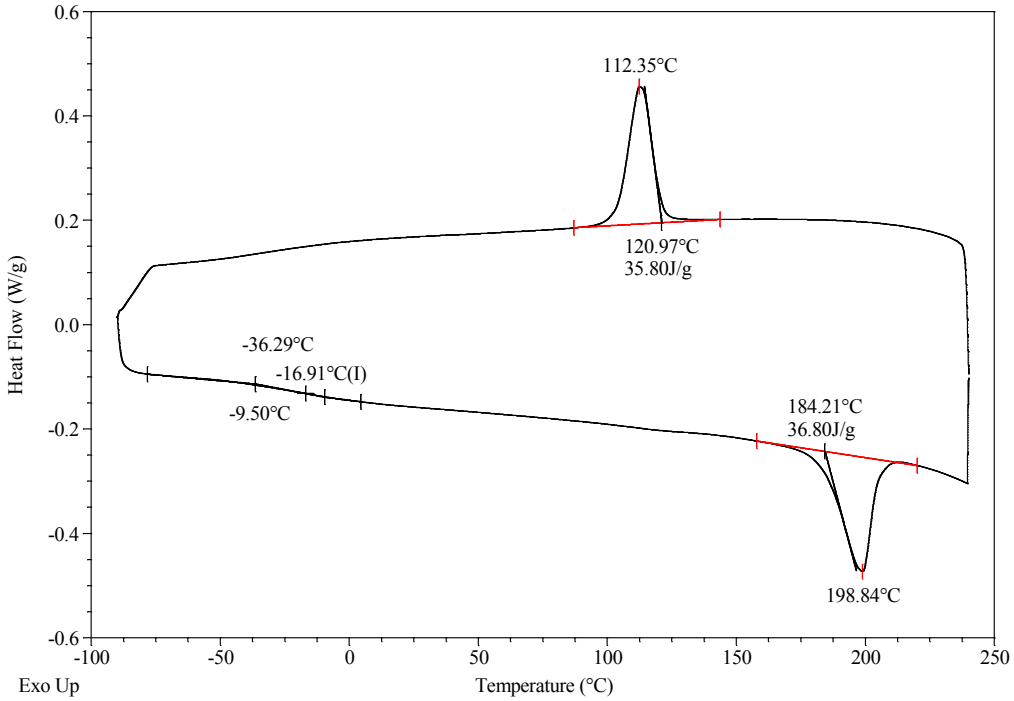

Figure 3.1.4: DSC trace of triblock PLLA-PCL-PDLA.

For **sc**-PLA, synthesised from homo-polymers of PLLA and PDLA, an expected melting temperature (T_m) would be between 210-230°C. However, in our case, a reduction in T_m (199°C) was observed and a T_c of 112°C. Furthermore, a possible increase in glass transition temperature of -17°C was observed for PCL (Lit. PCL T_g = -60°C). The observation of one T_g at -17°C may be due to short blocks (approximately 14.0 kg.mol^{-1} each). Additionally, conversion of L-LA to PLLA (93 %) followed by conversion of ε-CL to PCL may have yielded a co-polymer where the segments were missible, this may be due to unreacted L-LA monomer (7 %) interfering with the polymerisation of ε-CL, the thus allowing of a mixed T_g.

Stereocomplexation of this tri-block co-polymer can occur by two different pathways as shown below (Figure 3.1.5).

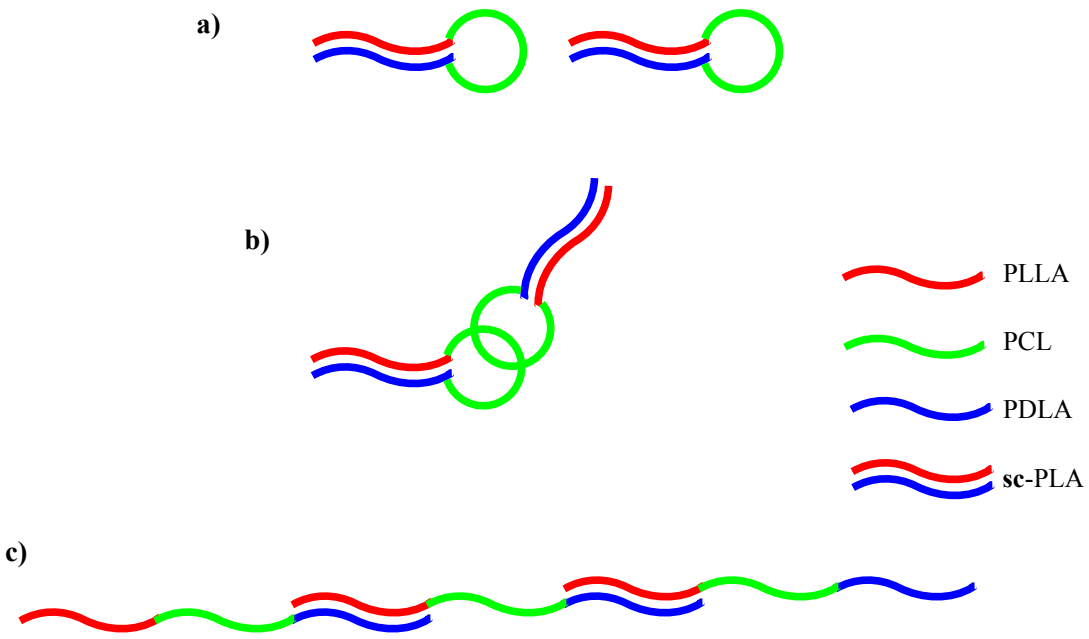

Figure 3.1.5: Sterecomplexation by **a)** intramolecular **b)** intra molecular with cross-linking and **c)** intermolecular pathways.

Firstly, intramolecular stereocomplexation, whereby the tri-block co-polymer stereocomplexed with itself. Furthermore, with intramolecular complexation loops and clusters may be formed. Secondly, intermolecular stereocomplexation can occur whereby separate tri-block polymer chains come together to form stereocomplexed PLA.

An analogous polymer was synthesised under the same conditions (100:100:100:1 LLA:VL:DLA:Initiator) using δ-valerolactone (δ-VL) instead of ε-CL as the co-monomer, as shown below (Figure 3.1.6).

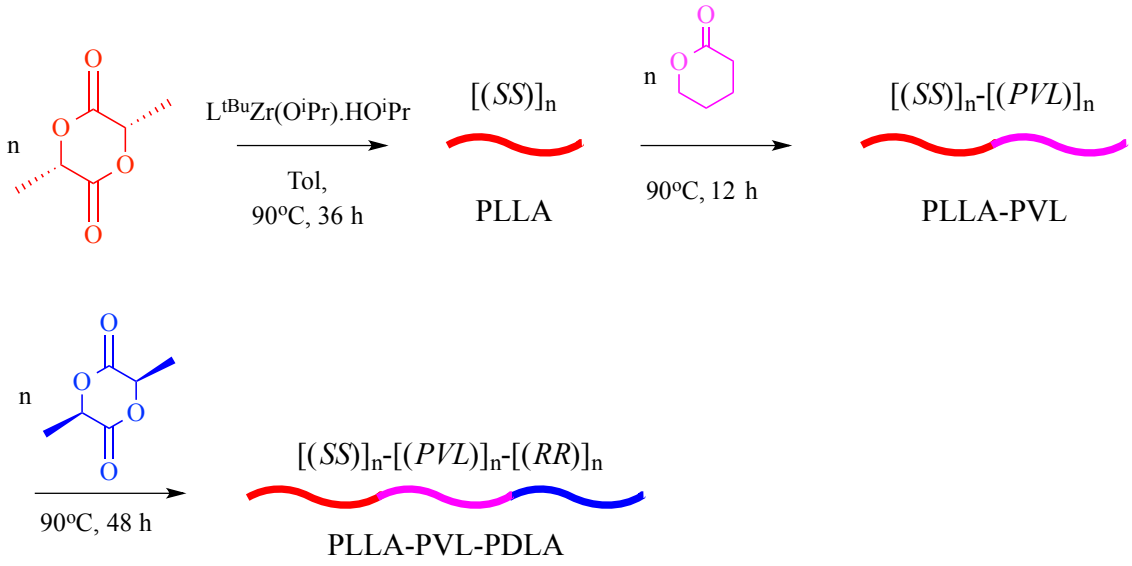

Figure 3.1.6: Sequential polymerization of tri-block co-polymer PLLA-PVL-PDLA.

A ^{1}H NMR spectrum of final polymer PLLA-PVL-PDLA displayed distinct peaks for PLA and PVL blocks (Figure 3.1.7).

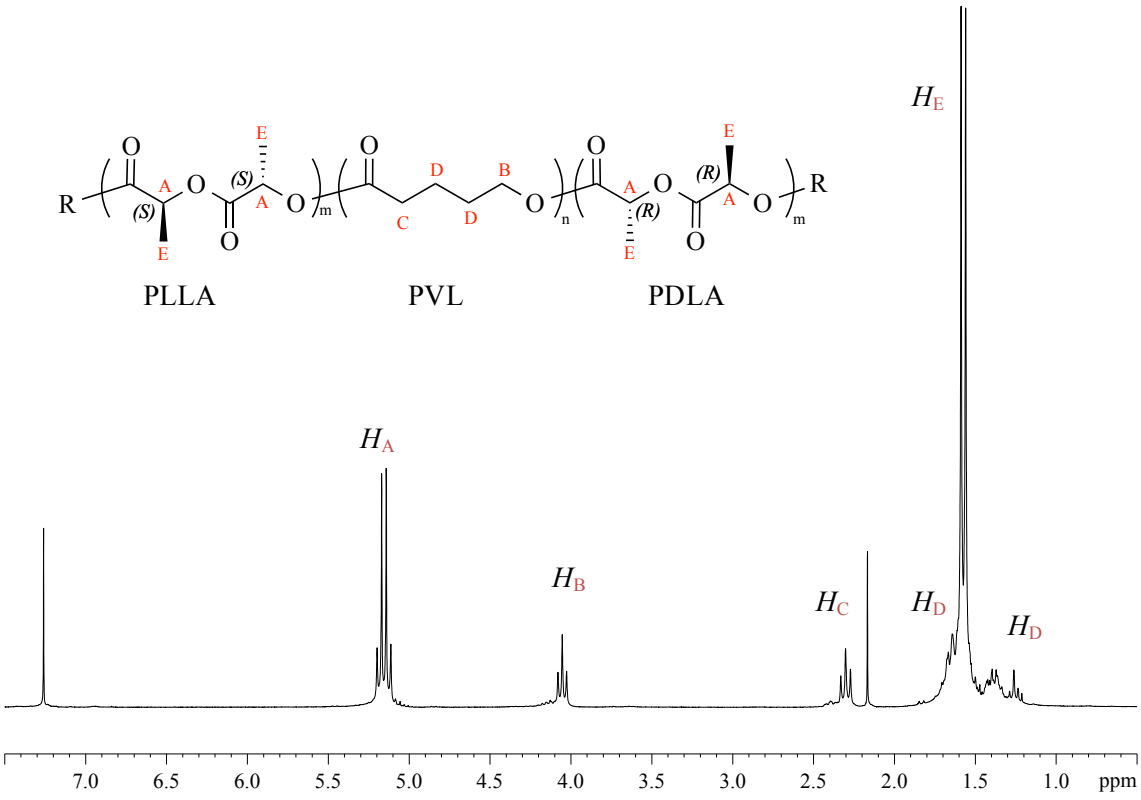

Figure 3.1.7: ^{1}H NMR spectrum of tri-block copolymer, PLLA-PVL-PDLA in $CDCl_3$ at 298K.

Tri-block co-polymer PLLA-PVL-PDLA, displayed a similar ^{1}H NMR spectrum to the analogous polymer PLLA-PCL-PDLA. A quartet is observed at 5.15 ppm ($^{3}J_{H\text{-}H}$ = 7.1 Hz) that attributes to four methine protons (H_A) of PLA which is coupled to a doublet at 1.58 ppm (J = 7.1 Hz) representing twelve methyl protons (H_E) of PLA. Methylene region (OCH_2) of PVL, displayed as a triplet (H_B, J = 6.6 Hz), was used in order to measure conversion (91 %), where the peak at 4.05 ppm denotes the polymer and a peak at 4.15 ppm denotes the unreacted valerolactone monomer. A triplet is also observed for the methylene protons (H_C) adjacent to the carbonyl moiety ($^{3}J_{HH}$ = 7.4 Hz). Multiplets between 1.73 and 1.20 ppm were observed for the remaining four methylene protons (H_D).

GPC was utilised in order to determine growth in molecular weight. It is shown in

Table 3.1.2 that an increase in M_n was observed with increased monomer feed suggesting and a hetero-polymer was synthesised as opposed to three distinct homopolymers.

Table 3.1.2: GPC data of PLLA-PVL-PDLA during sequential polymerization.

Polymer	**M_n kg.mol^{-1}**	**$M_{n,\,theo}$ kg.mol^{-1}**	**PDI**
PLLA	11.8	14.3	1.10
PLLA - PVL	26.4	24.2	1.41
PLLA-PVL-PDLA	Insoluble in THF		

Initially, a GPC trace of PLLA revealed a M_n (11.8 kg.mol^{-1}) relative to the theoretical value (M_n = 14.3 kg.mol^{-1}) with a narrow PDI of 1.10. The living characteristic of this system was supported by an increase in M_n (26.4 kg.mol^{-1}) upon sequential addition of δ-VL monomer. GPC analysis of triblock PLLA-PVL-PDLA was not possible due to the insolubility of the polymer in THF. Whilst a GPC trace could not be obtained, interestingly this could further support the synthesis of a stereocomplexed tri-block co-polymer as the di-block polymer was readily soluble. The thermal properties of the final tri-block co-polymer were investigated by DSC as shown below (Figure 3.1.8).

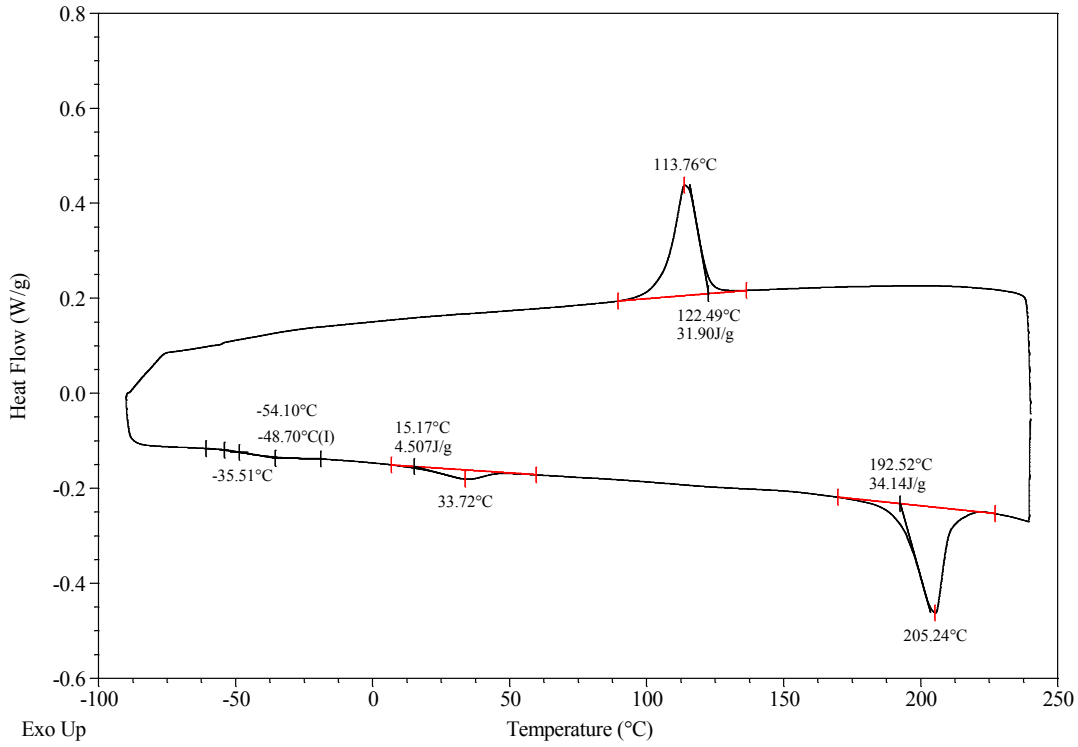

Figure 3.1.8: DSC trace of tri-block co-polymer PLLA-PVL-PDLA.

The T_m at 34°C attributes to PVL and is lower than the literature value (57 °C). Variations in T_m may be due to dependence on M_n, low isotactic lengths and heat/cooling rates of DSC analyses. T_m at 205 °C suggests a degree of stereocomplexation and is typical for stereoblock PLA as the PDLA is finally incorporated into the triblock. A T_g of -48°C was observed, higher than the literature value of -67°C for PVL homopolymer which could suggest slight phase mixing with the PLA segments and a T_c at 114°C further supports the formation of stereocomplexed PLA.

3.2. Synthesis of penta-block co-polymers

Interestingly, Davidson *et al.* reported the initiator, $L^{tBu}Zr(O^{i}Pr).HOiPr$, exhibits a heterotactic bias for the conversion of sublimed *rac*-LA. An inequivalent mixture of L- and D- lactide can be added to the initiator and will preferentially form heterotactic polymer (P*het*LA) with equal amounts of L and D alternating along the polymeric chain. When all of the minority stereoisomer has been consumed an isotactic PLA block is formed with the remaining lactide isomer originally in excess. The rate significantly decreases as the isotactic block starts to grow (Figure 3.2.1).

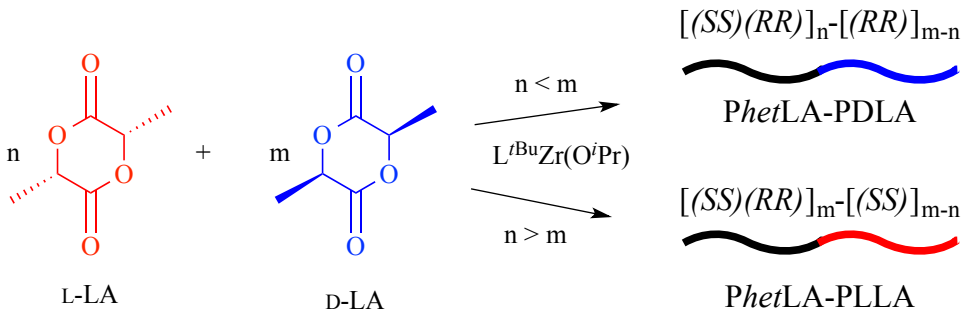

Figure 3.2.1: Synthesis of PLA di-stereoblock polymers.[12]

Exploitation of the heterotactic bias in the ring-opening polymerization of lactide with $L^{tBu}Zr(O^{i}Pr)$ was investigated. A penta-block co-polymer was synthesised with an aliphatic PCL linker (Figure 3.2.2).

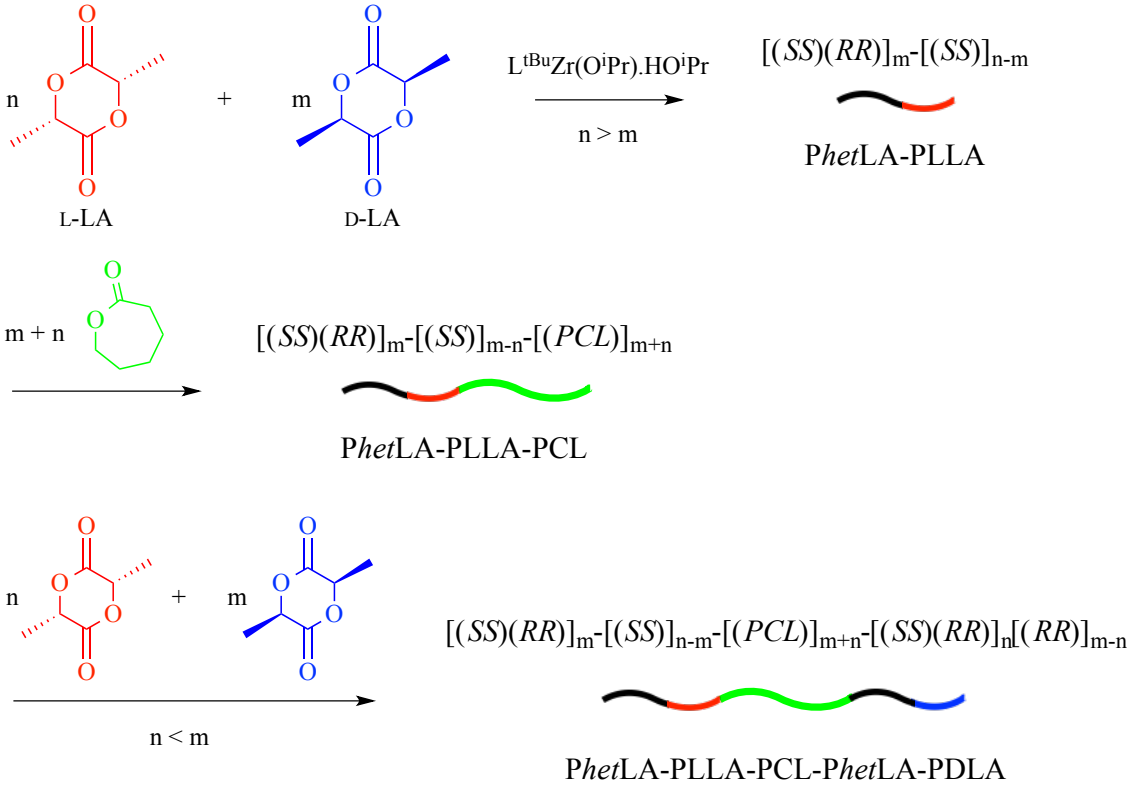

Figure 3.2.2: Synthesis of penta-block P*het*LA-PLLA-PCL-P*het*LA-PDLA in toluene at 90°C.

The polymerization was performed using an initiator loading of 100:100:100:1 (LA:CL:LA:Initiator). In solution, an inequivalent mixture of L- and D- LA (3:1 ratio

repectively, L-LA + D-LA = 100eq. overall LA) with the addition of $L^{tBu}Zr(O^{i}Pr).HO^{i}Pr$ preferentially formed heterotactic polylactide followed by a PLLA block (P*het*LA-PLLA with a 50:50 ratio). Once conversion reached near completion (96 %) sequential addition of ε-CL (100 eq.) was polymerised to afford P*het*LA-PLLA-PCL triblock (50:50:100 ratio). ^{1}H NMR spectrum of the tri-block co-polymer is shown below (Figure 3.2.3).

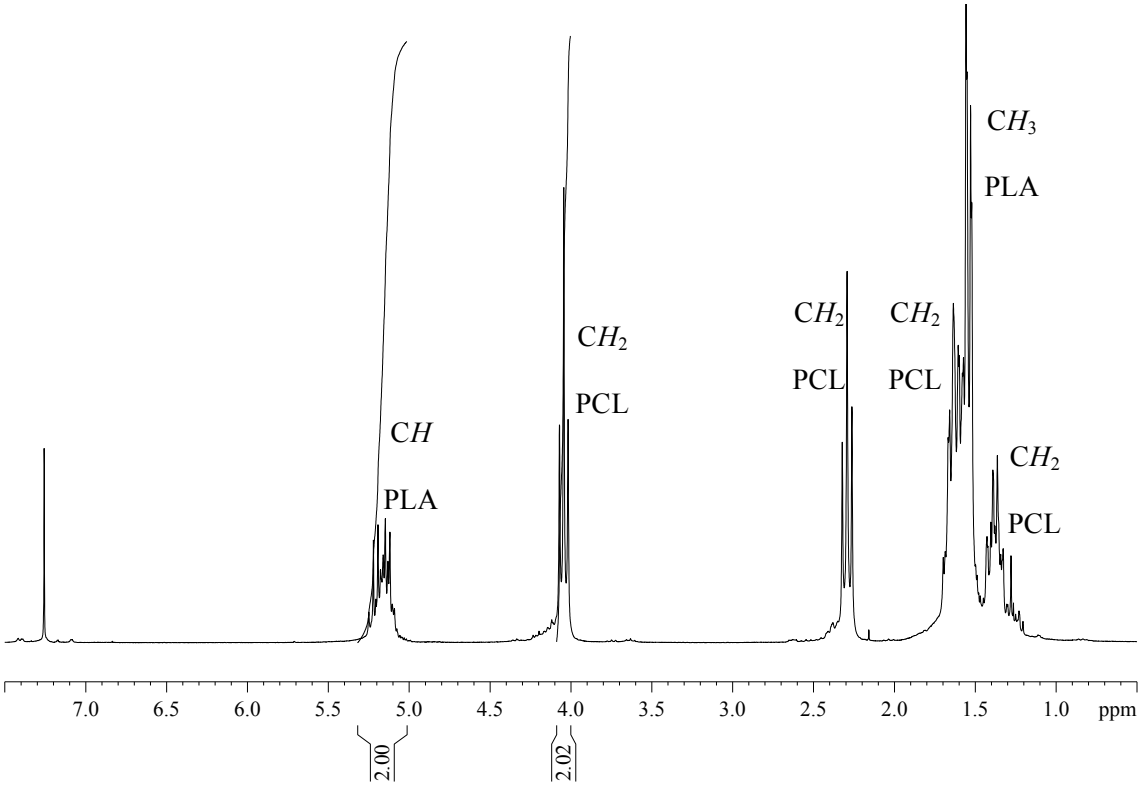

Figure 3.2.3: ^{1}H NMR spectrum of tri-block co-polymer P*het*LA-PLLA-PCL.

Figure 3.2.3 illustrates a ^{1}H NMR spectrum of the intermediate tri-block co-polymer P*het*LA-PLLA-PCL. A multiplet was observed at 5.05-5.45 ppm for the methine protons of PLA due to overlapping of quartets of both isotactic and heterotactic PLA being present. Additionally, two overlapping doublets are also observed for the methyl protons of PLA. Similar to PLLA-PCL-PDLA, triplets were observed for the methylene protons of PCL segment at 4.05 and 2.30 ppm. Again, a multiplet was observed for the remaining methylene protons of PCL. A 1:1 ratio of PLA:PCL was observed in the tri-block co-polymer due to equal equivalents of overall PLA and PCL were added sequentially.

Inequivalent amounts of L- and D- LA (1:3 respectively, L + D - LA = 100 eq. overall LA) were then added to the tri-block P*het*LA-PLLA-PCL and polymerised under the same conditions to

achieve the final pentablock polymer (P*het*LA-PLLA-PCL-P*het*LA-PDLA, 50:50:100:50:50 ratio). The monomer ratios within the polymer are shown below in Figure 3.2.4.

50 50 100 50 50

Figure 3.2.4: Equivalents of individual polymer segments within the co-polymer.

Figure 3.2.4 displays the theoretical equivalents of each segment within the final penta-block co-polymer. There are three main segments to the polymer: PLA (100 eq.), PCL (100 eq.) and another PLA (100 eq.) segment. Each PLA segment is then split in two, whereby the first half is heterotactic PLA (50 eq.) and the latter isotactic PLA (50 eq.) as shown above (Figure 3.2.4).

In order to elucidate polymer chain growth, GPC analysis was utilised and displayed formation of a penta-block co-polymer due to an increase in M_n after addition of each monomer (Table 3.2.1).

Table 3.2.1: GPC analysis of sequential polymerisation of penta-block co-polymer.

Polymer	**M_n kg.mol^{-1}**	**$M_{n,\,theo}$ kg.mol^{-1}**	**PDI**
P*het*LA-PLLA	7.2	13.9	1.12
P*het*LA-PLLA-PCL	10.4	25.6	1.08
P*het*LA-PLLA-PCL-P*het*LA-PDLA	15.8	39.9	1.15

A normalised GPC distribution curve illustrates the chain growth that occurred during the sequential steps (Figure 3.2.5).

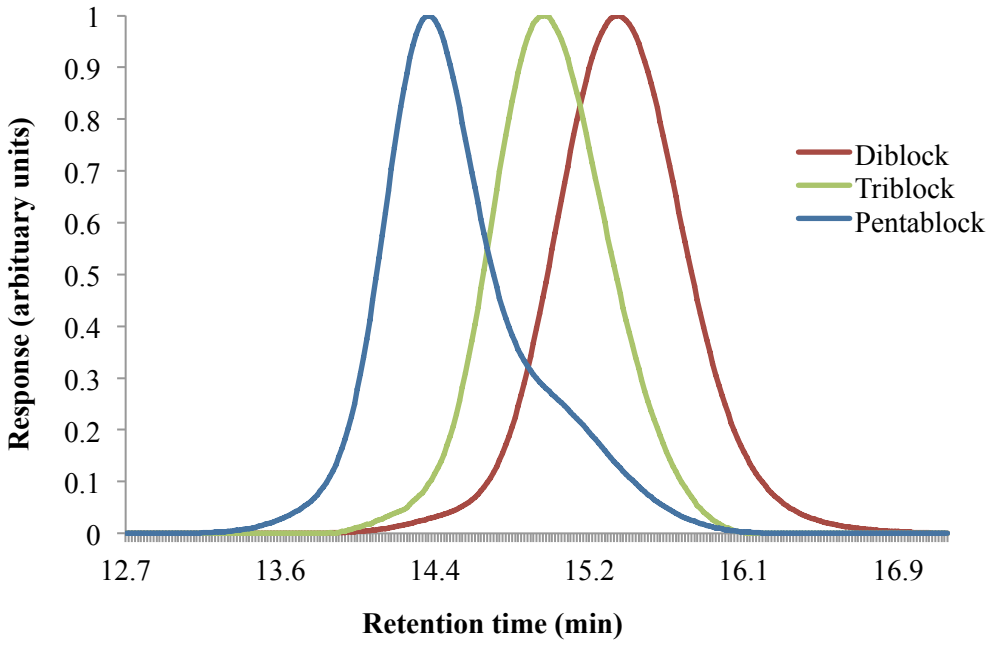

Figure 3.2.5: Normalised GPC distribution curve during synthesis of penta-block co-polymer.

The elution curve of the final penta-block co-polymer shows the presence of a shoulder peak on the the low molecular weight side which suggests that a number of triblock copolymers may not have partaken in the final polymerization step. This could have been caused by possible impurities in the new monomer batch or stirring issues as the polymeric material becomes more viscous. Analysis of the thermal properties of the final polymer by DSC interestingly gave no distinct peaks. This may be due to the majority of the polymeric domains being amorphous. Furthermore, an inability to obtain crystals may be due to the relatively small segments of isotactic enchainment within the final co-polymer.

Under the same conditions, the analogous polymer (P*het*LA-PLLA-PVL-P*het*LA-PDLA) was synthesised with a poly(δ-VL) linker (Figure 3.2.6).

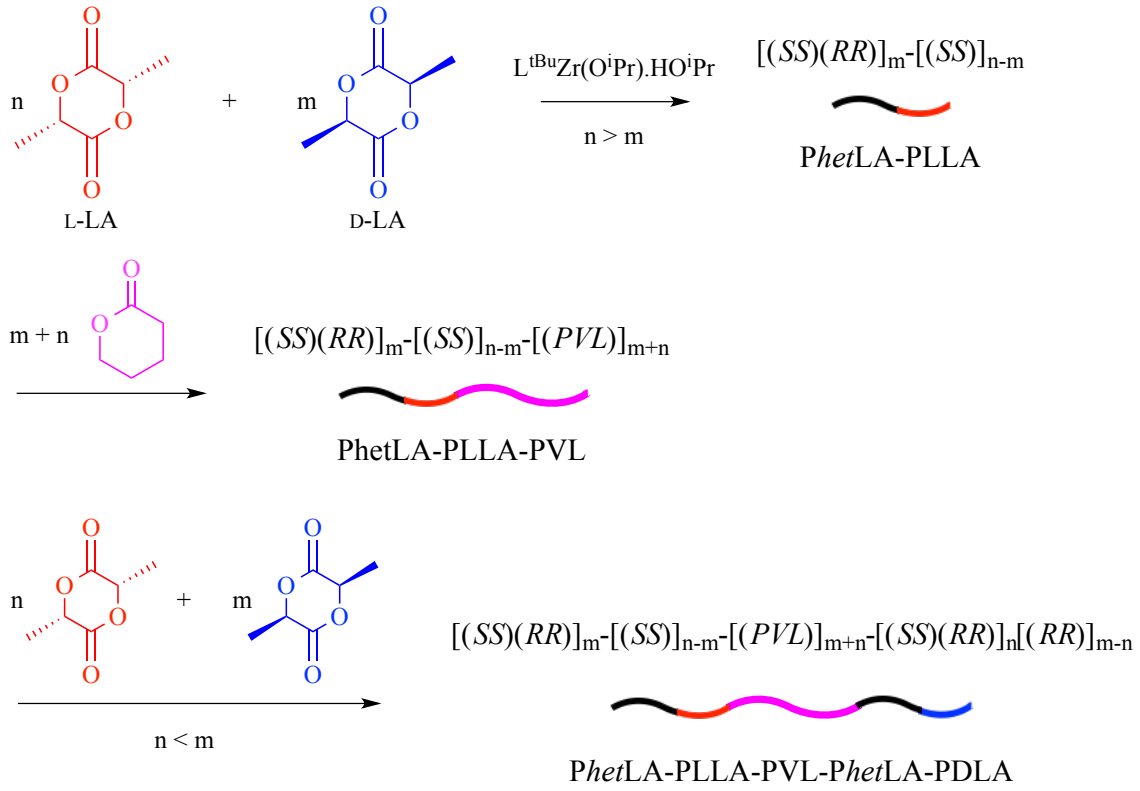

Figure 3.2.6: Synthesis of penta-block P*het*LA-PLLA-PVL-P*het*LA-PDLA in toluene at 90°C.

Firstly, di-block (P*het*LA-PLLA 1:1) was synthesised by one-pot polymerisation of inequivalent amounts of sublimed L- and D-LA (25% and 75% repectively) with initiator $L^{tBu}Zr(O^{i}Pr).HO^{i}Pr$. Sequential addition of monomer, distilled δ-VL, with reaction monitored by ^{1}H NMR spectroscopy (Figure 3.2.7).

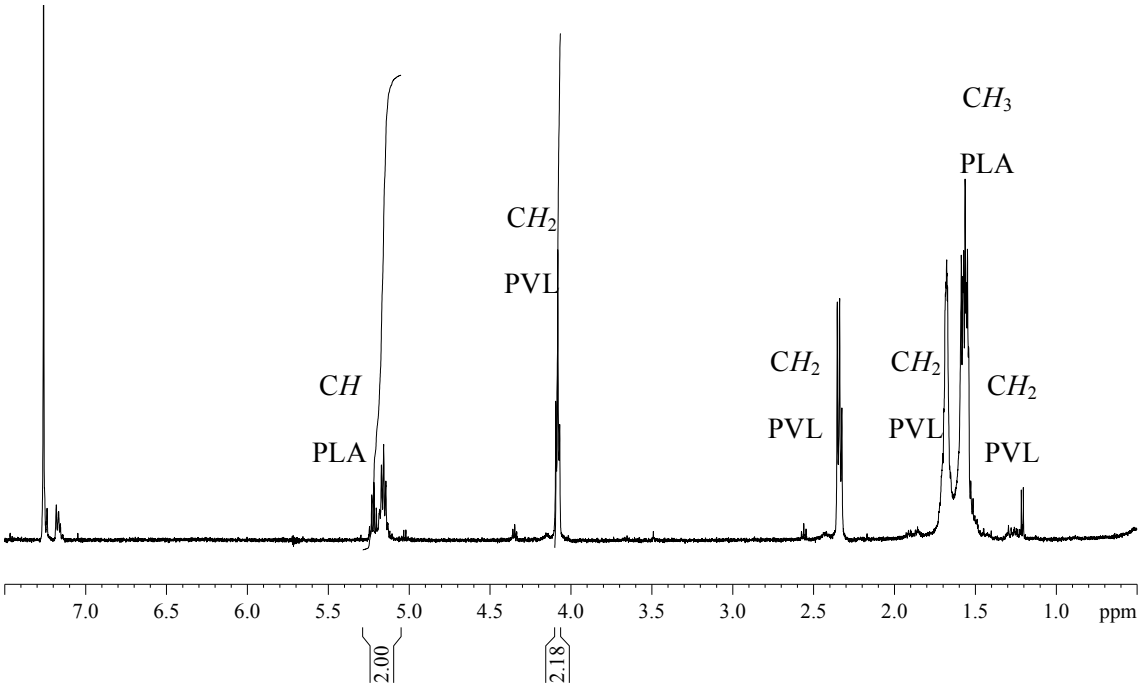

Figure 3.2.7: [1]H NMR spectrum of tri-block co-polymer P*het*LA-PLLA-PVL.

[1]H NMR spectrum displays an analogous spectrum to Figure 3.2.3 of P*het*LA-PLLA-PCL. Overlapping quartets are observed at 5.18 ppm for methine protons and a multiplet at 1.56 ppm for methyl protons of PLA. Two triplets at 4.08 and 2.34 ppm attribute the methylene protons of PVL. Multiplets are observed for the remaining methylene protons of PVL and the methyl protons of PLA (1.78 – 1.46 ppm). Inequivalent amounts of L- and D-LA (75% and 25% respectively) were added upon completion of the tri-block and a PLA: PVL ratio of 1:1.2 was observed. Physical polymer properties are investigated below using GPC (Table 3.2.2 and Figure 3.2.8). Theoretical M_n was calculated assuming assuming that one initiator complex initiates one polymer chain.

Table 3.2.2: GPC analysis of sequential polymerisation of penta-block co-polymer.

Polymer	M_n **kg.mol^{-1}**	$M_{n,\,theo}$ **kg.mol^{-1}**	**PDI**
P*het*LA-PLLA	6.6	14.3	1.11
P*het*LA-PLLA-PVL	16.6	24.2	1.25
P*het*LA-PLLA-PVL-P*het*LA-PDLA	24.9	38.50	1.15

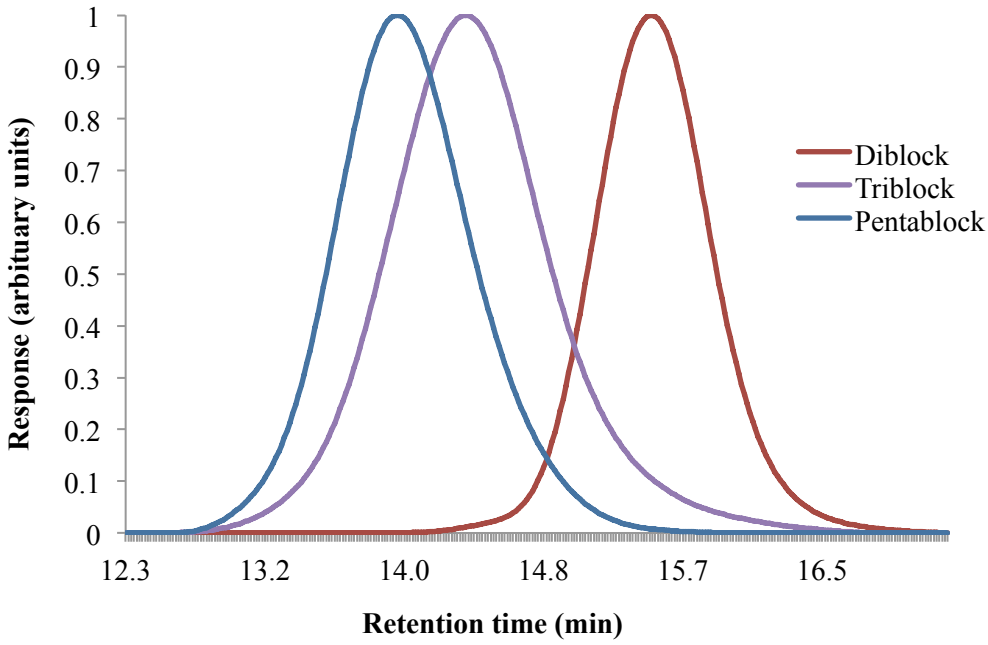

Figure 3.2.8: Normalised distribution curve by GPC during synthesis of penta-block co-polymer.

GPC traces of aliquots taken upon completion of each block illustrate with an increase in conversion, an increase in M_n was observed. PDI measurements remain relatively consistent indicating growing block co-polymer chains (Table 3.2.2). Furthermore, GPC traces appear monomodal, thus supporting the hypothesised synthesis of a penta-block co-polymer.

3.3. ω-Pentadecalactone (PDL) co-polymers

Polymerization of commercially available monomer ω-pentadecalactone (PDL) is of interest due to its long aliphatic chain. Hydrocarbon chains are increasingly flexible with increased length and PDL exhibits a long 15-carbon chain. Incorporating a longer aliphatic chain into the polymer could lead to more flexible amorphous domains within the polymers and when coupled with the potential of self-stereocomplexing lactide segments, could make for some interesting polymers. Literature reports show the enzymatic ring-opening polymerization of PDL to PPDL exhibits a T_g of -25°C and T_m at 96°C, which is similar to low density polyethylene (LDPE, T_m = 120°C).[15–18] Initially, the homo-polymerisation of PDL to poly-pentadecalactone (PPDL) was attempted under similar conditions as above (100:1 monomer to initiator ratio in toluene at 80°C). Unfortunately, no polymerisation was achieved with $L^{tBu}Zr(O^iPr).HO^iPr$, only monomer

remained. A range of different initiators were trialled including an initiator designed by Coates ((BDI-^{i}Pr)ZnN(SiMe$_3$)$_2$, Scheme 3.3.1), commercially available yttrium isopropoxide and organocatalyst 1,5,7-triazabicyclo[4.4.0]dec-5-ene (TBD) with benzyl alcohol, all yielding polymers.[19,20]

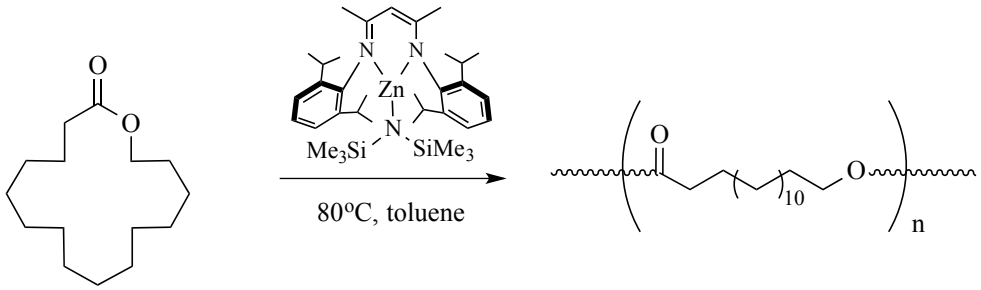

Scheme 3.3.1: Polymerisation of ω-pentadecalactone (PDL) to poly-pentadecalactone (PPDL).

The initiator designed by Coates and co-workers, ((BDI-^{i}Pr)ZnN(SiMe$_3$)$_2$), was reportedly active for the polymerisation of lactide, butyrolactone and valerolactone.[21,22] Interestingly, this initiator proved active for the polymerisation of PDL and was trialled for the synthesis of block co-polymers. Figure 3.3.1 displays an ^{1}H NMR spectra overlay of monomer PDL with polymer PPDL.

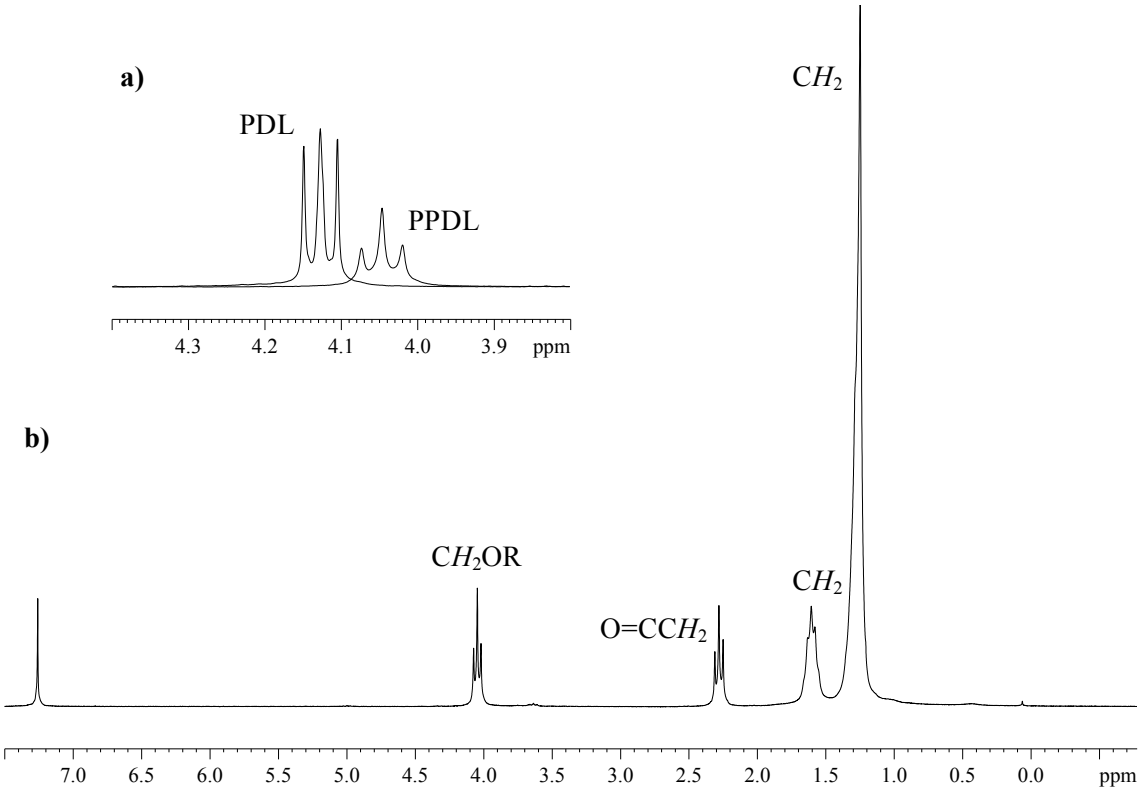

Figure 3.3.1: a) ^{1}H NMR spectrum to show conversion of PDL to PPDL. **b)** ^{1}H NMR spectrum of PPDL.

(BDI-^{i}Pr)ZnN(SiMe$_3$)$_2$ was selected as it displayed good activity for both lactide and PDL. It is illustrated that >99% of monomer was converted into polymer due to an upfield shift in the protons adjacent to the oxygen (RC*H*$_2$-OR) as shown below (Figure 3.3.1). ^{1}H NMR spectrum of PPDL displays a triplet at 4.05 ppm which can be attributed to methylene protons adjacent to oxygen, with a triplet at 2.30 ppm that corresponds to methylene protons adjacent to a carbonyl moiety. A further triplet is displayed at 1.60 ppm along with a multiplet between 1.41 and 1.16 ppm for the remaining C*H*$_2$ protons.

3.3.1. Synthesis of di-block co-polymer

Synthesis of a di-block copolymer of PLLA-PPDL was attempted in a one-pot one-step method. Equal amounts of L-LA and PDL were reacted with (BDI-^{i}Pr)ZnN(SiMe$_3$)$_2$ in a ratio of 100:100:1 in toluene at 80°C. The reaction was monitored by ^{1}H NMR spectroscopy, it was observed that whilst PLLA was synthesised (96% in 24hrs), no PPDL formed and thus not yielding a di-block copolymer. The same is true for the reaction of PDL and D-LA with the same initiator, thus suggesting the initiator preferentially polymerises lactide. Sequential

polymerisation was trialled firstly with the polymerisation of PDL, which reached 84% conversion in 24 h. Addition of L-LA converted to PLLA (93% in 24 h) suggesting formation of either the desired di-block polymer, or a mixture of the two homo-polymers (Figure 3.3.2). The same was true for the analogous polymer containing D-LA.

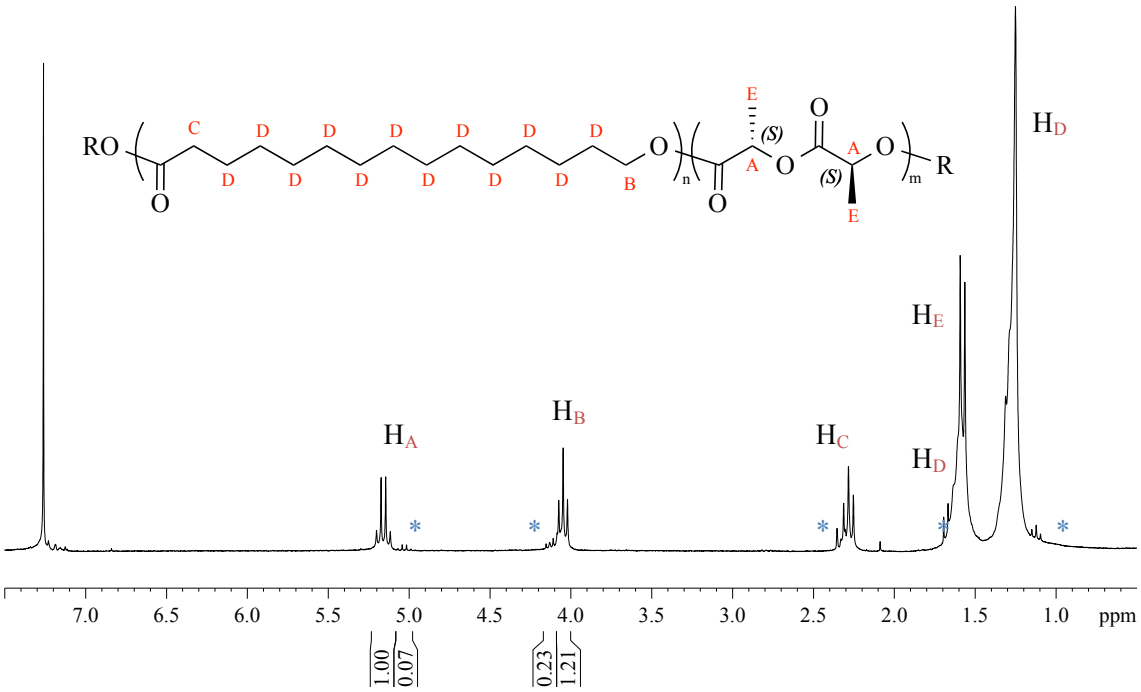

Figure 3.3.2: ^{1}H NMR spectrum of PPDL-PLLA in $CDCl_3$ at 298K. * (blue) denotes presence of unreacted monomer.

Figure 3.3.2 displays a ^{1}H NMR spectrum of di-block co-polymer PPDL-PLLA, before the final work-up and wash with methanol, thus unreacted monomers (*) were still present to enable calculation of final conversion. Methine protons of PLLA are displayed as a quartet (H_A) at 5.16 ppm ($^{3}J_{H\text{-}H}$ = 7.1 Hz), with another quartet visible for the monomer L-LA at 5.04 ppm. Again, triplets at 4.05 ppm and 2.28 ppm were observed for methylene protons (H_B and H_C respectively) of PPDL along with multiplets between 1.70 - 1.17 ppm (H_D). A doublet at 1.58 ppm ($^{3}J_{H\text{-}H}$ = 7.1 Hz), coupled to the methine protons (H_A), attributes to methyl protons (H_E) of PLLA.

Under standard GPC techniques (eluent: THF, flow rate: 1.0 ml.min^{-1}, polystyrene standards), no rational peaks for the homopolymer of PPDL were observed. Duchateau *et al*. successfully reported GPC traces of PPDL using the eluent 1,2,4-trichlorobenzene at 160°C with M_n calculated with respect to polyethylene standards.[19,20,23] Unfortunately, GPC techniques under these conditions were unavailable for use. ^{1}H NMR spectroscopy analyses of the di-block co-

polymers was used instead to determine conversion and potential ratios of polymer segments within the co-polymer. Whilst it is unclear if homo-polymers or a co-polymer were synthesised, a 1:1.2 ratio of PLLA:PPDL was observed *via* ^{1}H NMR spectroscopy (Figure 3.3.2) suggesting similar equivalents of monomers are present in the final polymers.

Equal amounts of PPDL-PLLA and PPDL-PDLA (final worked-up polymers) were firstly dissolved in CH_2Cl_2 with the solvent allowed to evaporate slowly over 7 days to form a stereocomplexed co-polymer. Any remaining solvent was removed *in vacuo* and the subsequent polymer was analysed by DSC (Figure 3.3.3).

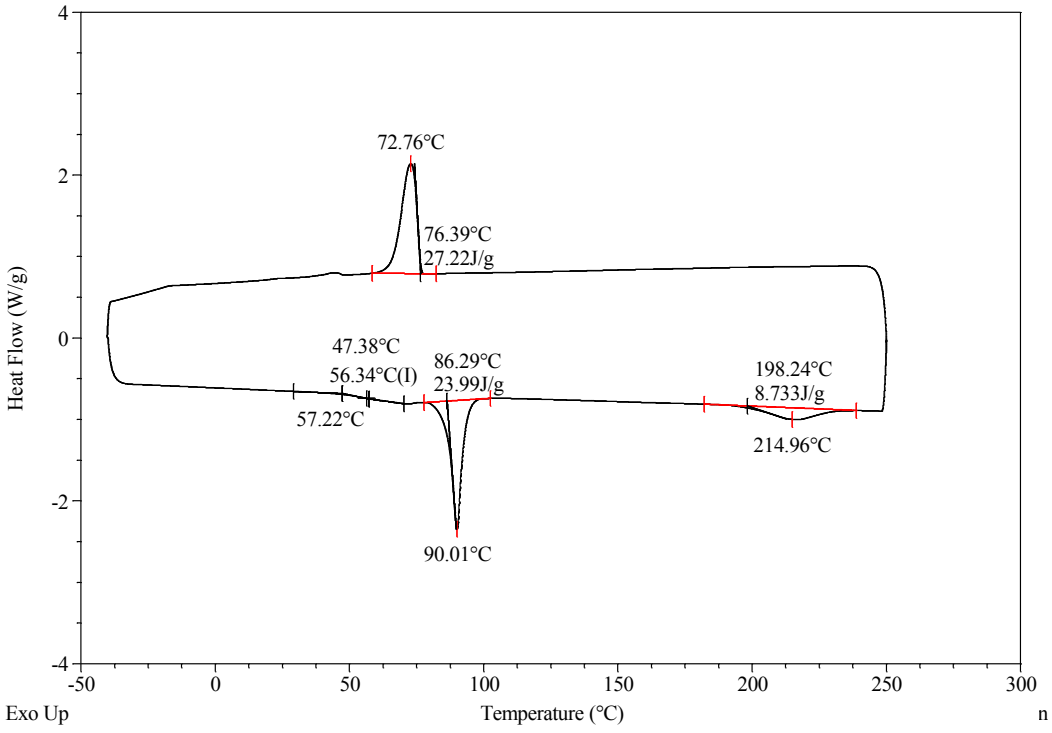

Figure 3.3.3: DSC of stereocomplexation (PPDL-PLLA with PPDL-PDLA).

DSC analysis was undertaken in order to determine domains of stereocomplexed PLA within the copolymer. Figure 3.3.3 shows a T_c was observed on the first cycle at 73°C whilst the second cycle displayed a T_g of 57°C corresponding to the PPDL segment of the polymer, and two T_m's at 90°C and 214°C attributing to PPDL and **sc**-PLA respectively. The T_m at 214°C further supports formation of stereocomplexed domains within the co-polymer.

The reaction whereby the polymerisation of LA was reacted first, followed by the sequential addition of PDL upon completion. Here, PLA was synthesised but no polymerisation of PDL occurred. This indicates that the relatively large PDL ring is unable to insert into the metal-LA bond possibly due to steric hinderance. On the other hand, the relatively small lactide ring can insert into the metal-PDL bond forming PPDL-PLA di-blocks.

3.3.2. Synthesis of tri-block co-polymer

Duchateau and co-workers, have synthesised di-block copolymers of PPDL and PCL using an organo-catalyst (TBD) with benzyl alcohol as a co-initiator.[19,24] To our knowledge, it has not been reported with the addition of a PLA block. This could lend itself to the possibility of stereocomplexed PLA with interesting properties. Initially, the synthesis of co-polymers with PCL was trialled in order to allow PLLA-PCL-PPDL block co-polymers to by synthesised. However, sequential polymerisation to yield PCL-PPDL was unsuccessful. Sequential polymerisation of PDL, CL and L-LA was then trialled to afford tri-block PPDL-PCL-PLLA using initiator (BDI-^{i}Pr)ZnN(SiMe$_3$)$_2$ (100:100:100:1 catalytic loading). The reaction was monitored by ^{1}H NMR spectroscopy, with the analogous co-polymer PPDL-PCL-PDLA synthesised in the same manner. Thermal analyses of these polymers are shown below (Figure 3.3.4).

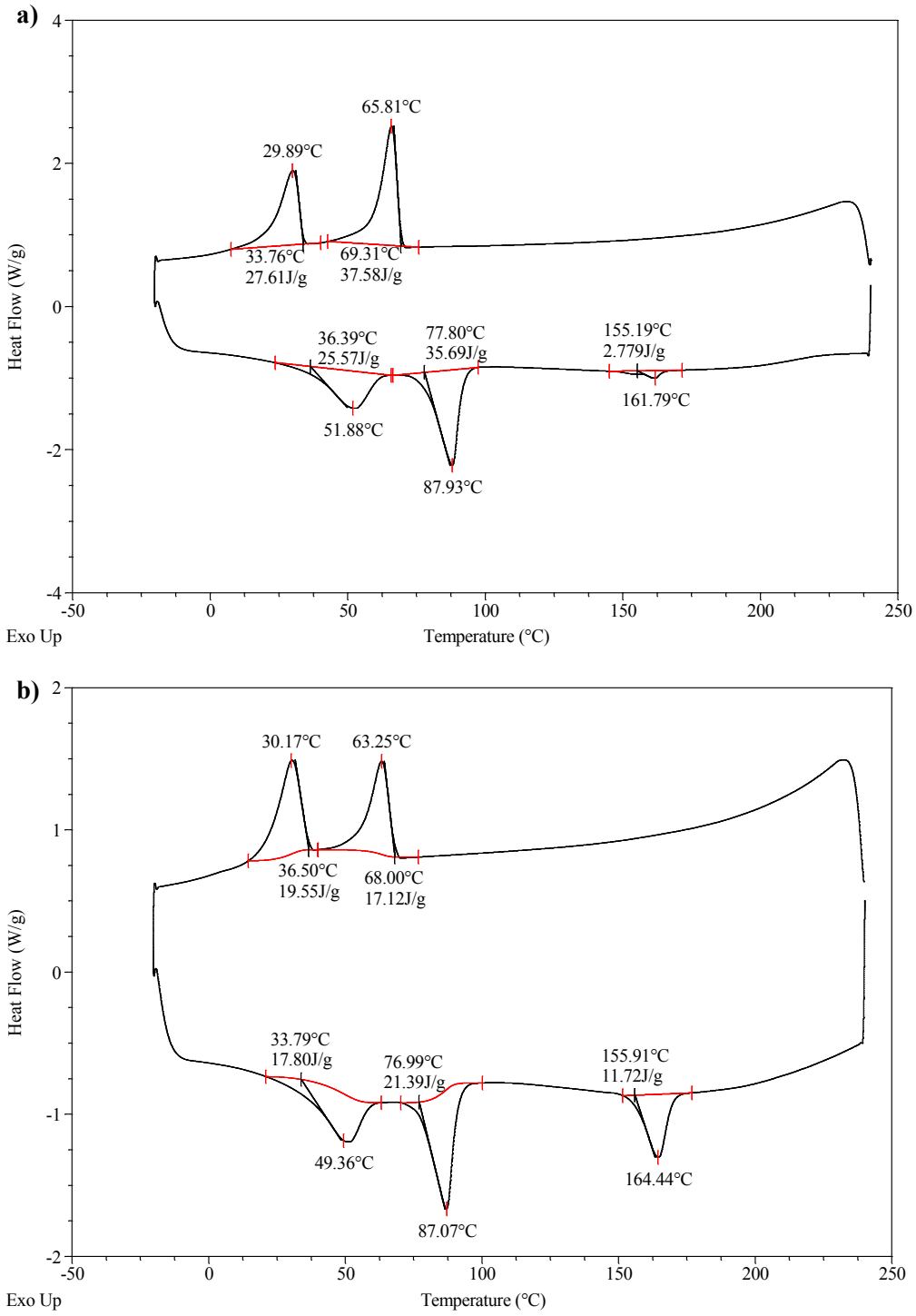

Figure 3.3.4: DSC trace of **a)** PDL-PCL-PLLA and **b)** PDL-PCL-PDLA.

DSC trace of PDL-PCL-PLLA (Figure 3.3.4a) has three T_m peaks at 52°C, 88°C and 161.79°C attributing to PCL, PDL and PLLA respectively. The temperatures are lower than expected for homopolymers due to their incorporation into the copolymer. Two peaks are observed for T_c,

one at 63°C for PLLA and the other at 30°C corresponding to PDL. PDL-PCL-PLLA and PDL-PCL-PDLA co-polymers were then stereocomplexed together and analysed by ^{1}H NMR spectroscopy (Figure 3.3.5).

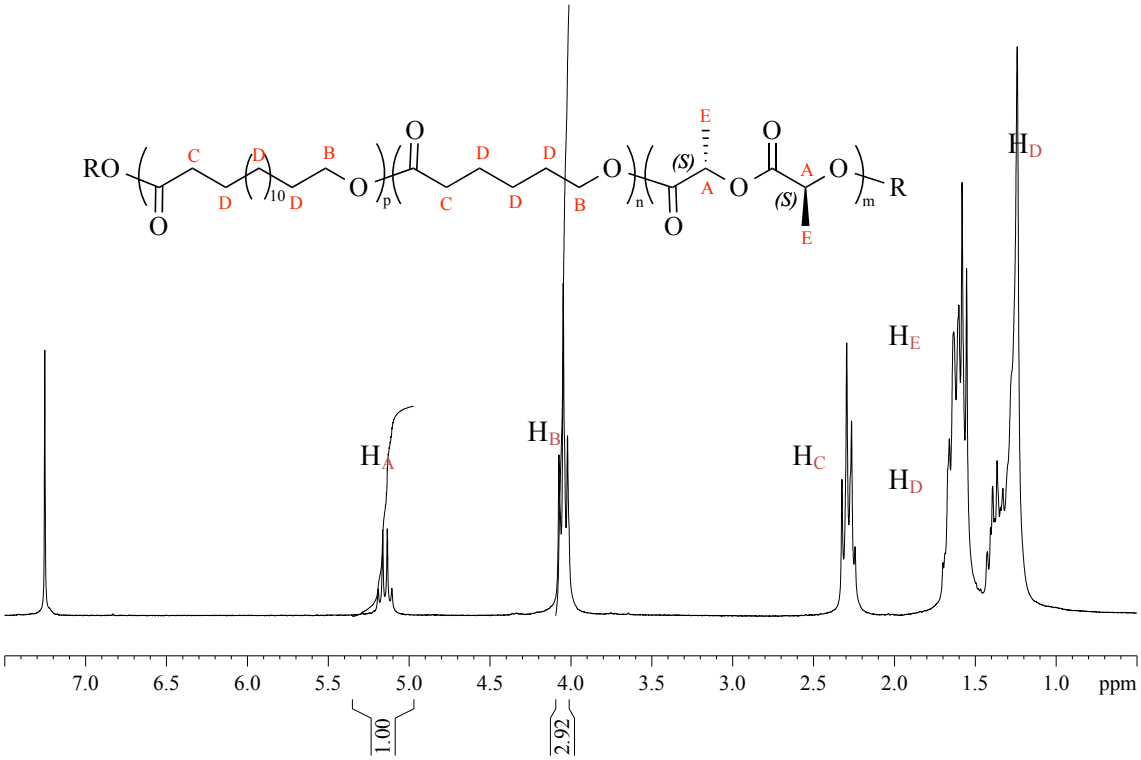

Figure 3.3.5: ^{1}H NMR spectrum in $CDCl_3$ at 298 K of PPDL-PCL-PLLA with PPDL-PCL-PDLA.

Figure 3.3.5 shows a ^{1}H NMR spectrum of the stereocomplexation of co-polymers PPDL-PCL-PLLA with PPDL-PCL-PDLA. A quartet at 5.17 ppm attributes to methine protons (H_A) of PLA. Overlapping triplets at 4.05 ppm correspond to methylene protons adjacent to oxygen (H_B) in both PPDL and PCL. Here, a 1:2.9 ratio of PLA: (PPDL+PCL) was observed. Ideally, an expected ratio of 1:2 was expected due to two methine PLA protons (H_A) and four methylene protons (H_B, two from PPDL and two from PCL). Thermal analysis by DSC was performed on PPDL-PCL-PLLA and PPDL-PCL-PDLA tri-block co-polymers (Figure 3.3.6).

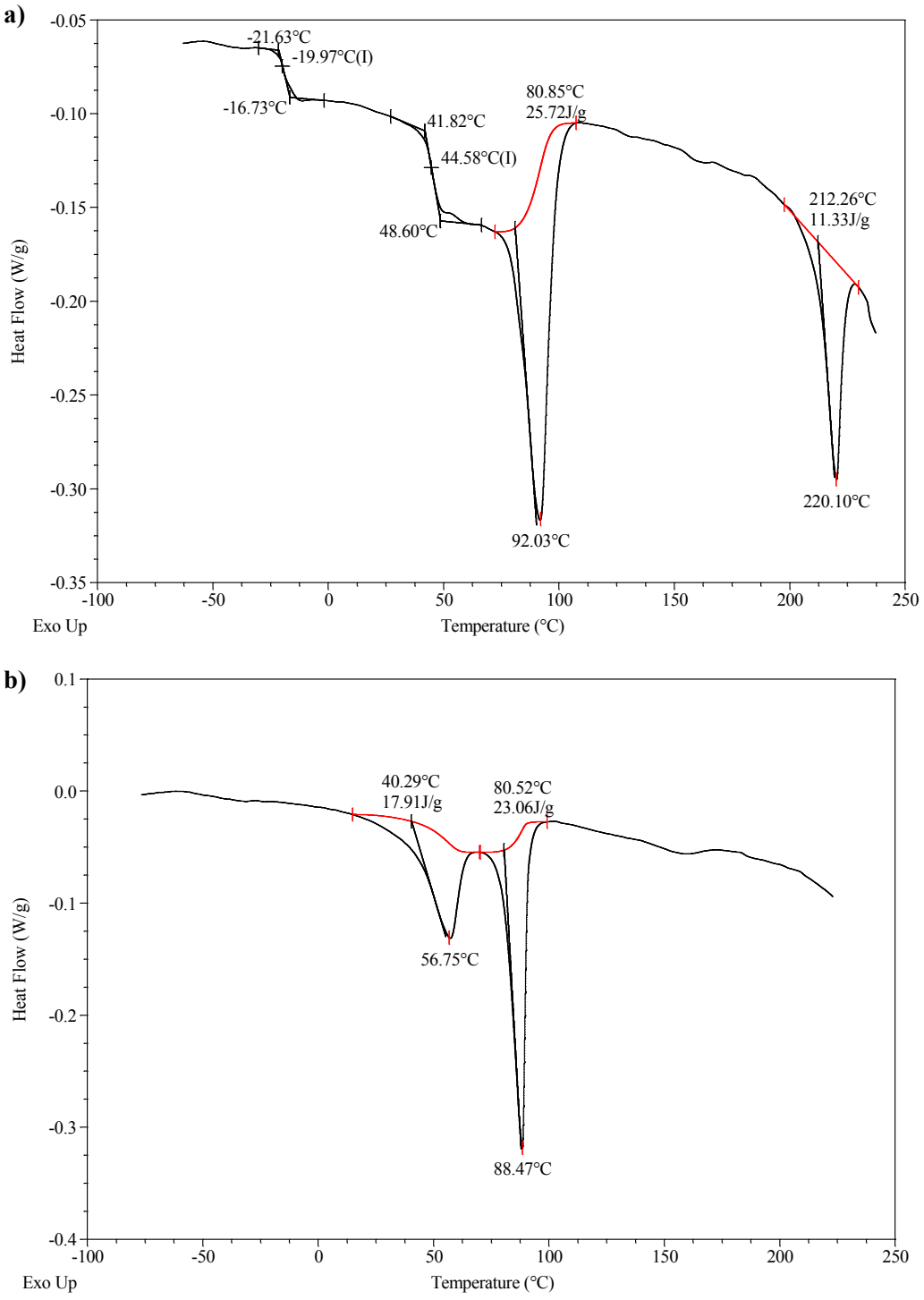

Figure 3.3.6: DSC traces of **a)** first heat and **b)** second heat of stereocomplex triblock PPDL-PCL-PLA.

The first heat generated many thermal events for the stereocomplexed tri-block PPDL-PCL-PLA. Glass transition temperatures of the first heat (T_{g1}) of -20°C and 45°C are attributed to

PPDL and PLA respectively. A T_{m1} of 92°C for PPDL was observed along with a T_{m2} at 220°C, corresponding to **sc**-PLA (Figure 3.3.6a). Although it is still unknown whether co-polymers of homo-polymers were synthesised, the presence of stereocomplexed PLA is still clear (T_m 220°C). As previously reported in this chapter, when PLA is incorporated into a co-polymer and stereocomplexed, a reduction in T_m was usually observed. Here, **sc**-PLA T_m of 220°C may suggest either lactide homo-polymers were stereocomplexed, high molecular weight or more isotactic enrichment. Upon cooling, two cold crystallisation temperatures (T_c) were observed. Figure 3.3.6b illustrates the second heating of the sample, interestingly, no T_{g2}'s are observed whilst two T_{m2}'s at 56.75°C and 88.47°C are attributed to PCL and PDL respectively. No T_{m2} for **sc**-PLA was observed possibly due to rapid cooling which may lead to insufficient crystallisation and thus no stereocomplex reformation.

3.4. Conclusion

Various copolymers were synthesised using commercially available, inexpensive monomers (LA, CL, VL, PDL) were synthesised. Initially, unsymmetrical ABC tri-block copolymers containing L-LA, CL and D-LA were produced using $\mathbf{L^{tBu}}$Zr(O^{i}Pr).HO^{i}Pr as initiator and partially characterised. Whilst GPC analysis of the final polymer was inconclusive, the tri-block copolymers insolubility in THF suggested a stereocomplex tri-block was formed. DSC traces further supported stereocomplexation with a T_m of 199°C. The analogous polymer utilizing δ-VL instead of ε-CL was also synthesised and characterised. The ability to exploit the initiator $\mathbf{L^{tBu}}$Zr(O^{i}Pr).HO^{i}Pr bias towards the formation of heterotactic PLA from *rac*-LA lends itself to the synthesis of unsymmetrical penta-block co-polymers. Whilst DSC traces were inconclusive, GPC analyses supported the living polymerisation of the system, showing growing polymer chains (Figure 3.2.5). Co-polymers incorporating PDL were synthesised using initiator (BDI-^{i}Pr)ZnN(SiMe$_3$)$_2$ (Scheme 3.3.1). Here, addition of smaller monomer (LA or CL) to the PDL propagating chain was possible. However, the addition of macrocycle PDL to a chain of PCL or PLLA was not due to size. Although it is unclear if homo-polymers or co-polymers were synthesised, distinct thermal traces suggest the presence of **sc**-PLA domains.

3.5. Further work

Further investigations into morphology and rheology of block co-polymers could be performed to gain more information about these polymeric materials. A study of varying the block lengths in order to optimise polymeric properties could lead to co-polymers with tailor made properties. Synthesis of isopropoxide derivative of (BDI-^{i}Pr)ZnN(SiMe$_3$)$_2$ developed by Coates *et al.* to increase activity of initiator in the lactide copolymerisation with PDL. Furthermore, characterisation of lactide co-polymers of PDL using GPC techniques described by Duchateau *et al.* could be utilised.

3.6. References

(1) Hiljanen-Vainio, M.; Karjalainen, T.; Seplala, J. *J. Appl. Polym. Sci.* **1996**, *59*, 1281–1288.

(2) Tsuji, H. *Macromol. Biosci.* **2005**, *5*, 569–97.

(3) Chun, Y. S.; Kyung, Y. J.; Jung, H. C.; Kim, W. N. *Polymer* **2000**, *41*, 8729–8733.

(4) Albertsson, A. C.; Varma, I. K. *Degrad. Aliphatic Polyesters* **2002**, *157*, 1–40.

(5) De Geus, M.; van der Meulen, I.; Goderis, B.; van Hecke, K.; Dorschu, M.; van der Werff, H.; Koning, C. E.; Heise, A. *Polym. Chem.* **2010**, *1*, 525–533.

(6) Ovitt, T. M.; Coates, G. W. *J. Am. Chem. Soc.* **1999**, *121*, 4072–4073.

(7) Dove, A. P. *Chem. Commun.* **2008**, 6446–6470.

(8) Chmura, A. J.; Davidson, M. G.; Frankis, C. J.; Jones, M. D.; Lunn, M. D. *Chem. Commun.* **2008**, 1293–1295.

(9) Li, G.; Lamberti, M.; Pappalardo, D.; Pellecchia, C. *Macromolecules* **2012**, *45*, 8614–8620.

(10) Purnama, P.; Jung, Y.; Kim, S. H. *Macromolecules* **2012**, *45*, 4012–4014.

(11) Kang, M. K.; Jung, Y.; Kim, S. H. *Macromol. Res.* **2013**, *21*, 1036–1041.

(12) Frankis, C. Thesis 2012.

(13) Wunderlich, B. *J. Therm. Anal. Calorim.* **2011**, *106*, 85–91.

(14) Ikada, Y.; Jamshidi, K.; Tsuji, H.; Hyon, S. H. *Macromolecules* **1987**, *20*, 904–906.

(15) Lebedev, B.; Yevstropov, A. *Makromol. Chemie-Macromolecular Chem. Phys.* **1984**, *185*, 1235–1253.

(16) Focarete, M. L.; Scandola, M.; Kumar, A.; Gross, R. A. *J. Polym. Sci. Part B-Polymer Phys.* **2001**, *39*, 1721–1729.

(17) Gazzano, M.; Malta, V.; Focarete, M. L.; Scandola, M.; Gross, R. A. *J. Polym. Sci. Part B Polym. Phys.* **2003**, *41*, 1009–1013.

(18) Van der Meulen, I.; Gubbels, E.; Huijser, S.; Sablong, R.; Koning, C. E.; Heise, A.; Duchateau, R. *Macromolecules* **2011**, *44*, 4301–4305.

(19) Bouyahyi, M.; Pepels, M. P. F.; Heise, A.; Duchateau, R. *Macromolecules* **2012**, *45*, 3356-3366.

(20) Zhong, Z.; Dijkstra, P. J.; Feijen, J. *Macromol. Chem. Phys.* **2000**, *201*, 1329–1333.

(21) Rieth, L. R.; Moore, D. R.; Lobkovsky, E. B.; Coates, G. W. *J. Am. Chem. Soc.* **2002**, *124*, 15239–48.

(22) Yin, Q.; Tong, R.; Xu, Y.; Baek, K.; Dobrucki, L. W.; Fan, T. M.; Cheng, J. *Biomacromolecules* **2013**, *14*, 920–9.

(23) Lendlein, A.; Schmidt, A.; Kratz, K.; Schultz, J. *Eur. Pat. Appl.* **2003**.

(24) Pepels, M. P. F.; Bouyahyi, M.; Heise, a.; Duchateau, R. *Macromolecules* **2013**, *46*, 4324–4334.

Chapter 4

Synthesis of co-monomers and kinetics of lactide co-polymerisations

4. Preamble

There are many different pathways to synthesise new lactone monomers, some of which are discussed in this chapter. Polymerisation of monomers with differing properties under a controlled fashion into a co-polymer is of great interest as discussed in the previous chapters. Lactide is a symmetrical monomer for which nucleophillic attack of the co-initiator can occur on either side of the ring. When using an unsymmetrical analogue of lactide with a bulky substituent on one side of the ring, in combination with an initiator which is active for the polymerisation of lactide (such as $\mathbf{L}^{t\mathrm{Bu}}\mathrm{ZrO}^{i}\mathrm{Pr}.\mathrm{HO}^{i}\mathrm{Pr}$), ring-opening polymerisation should occur at the methyl site with the possibility of forming either an alternating homo-polymer (Me R Me R Me R) or co-polymer. The co-polymerisation of lactide with different monomers at various stoichiometric amounts and their differing properties will be investigated. Furthermore, the exploitation of the heterotactic bias of initiator $\mathbf{L}^{t\mathrm{Bu}}\mathrm{ZrO}^{i}\mathrm{Pr}.\mathrm{HO}^{i}\mathrm{Pr}$ (see chapter 3) towards *rac*-LA will be probed in order to synthesise either alternating or random co-polymers.

4.1. Synthesis of Monomers

There are various methods to synthesise unsymmetrical monomers, as discussed in chapter 1. The simplest method is to react under inert conditions a commercially available α-hydroxy acid with 2-bromopropionyl bromide in the presence of triethyl amine to yield the desired cyclic monomer (Scheme 4.1.1).

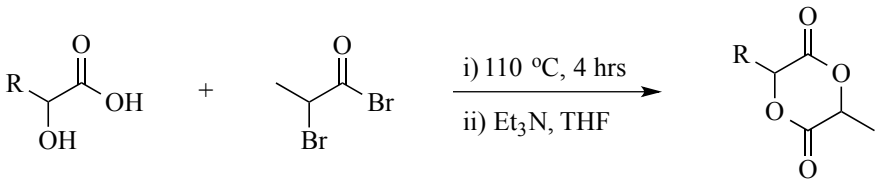

Scheme 4.1.1: Synthesis of unsymmetrical mono-substituted lactide.

Few α-hydroxy acids are commercially available and they appear to be relatively expensive. The ability to synthesise α-hydroxy acids widens the range of monomers that can be obtained. There are two pathways of synthesising α-hydroxy acids, firstly, Möller *et al.* developed a synthetic pathway that involved treating an aldehyde with sodium cyanide to afford an α-hydroxyl acid (Method A, Scheme 4.1.2a).[1] Secondly, an alternative route to the synthesis of α-hydroxy acids is to reflux the relevant bromo-hydroxy acid in the presence of potassium hydroxide in water (Method B, Scheme 4.1.2b).

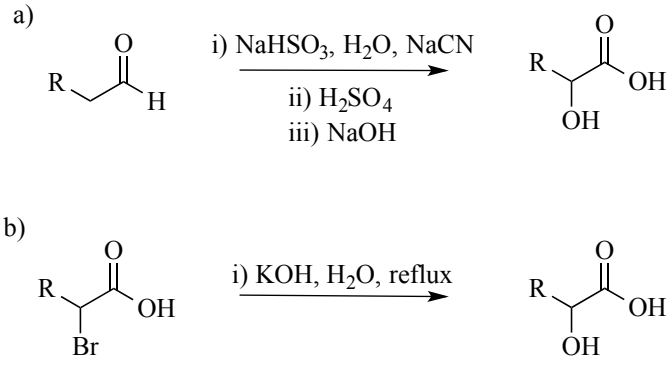

Scheme 4.1.2: Synthesis of α-hydroxy acids *via* a) Method A (aldehyde) and b) Method B **(**bromo-hydroxy acid).

The relevant α-hydroxy acid was then reacted with inexpensive, commercially available 2-bromopropionyl bromide, in the presence of triethyl amine to afford the cyclic monomer. The monomers that were successfully synthesised are shown below (Figure 4.1.1).

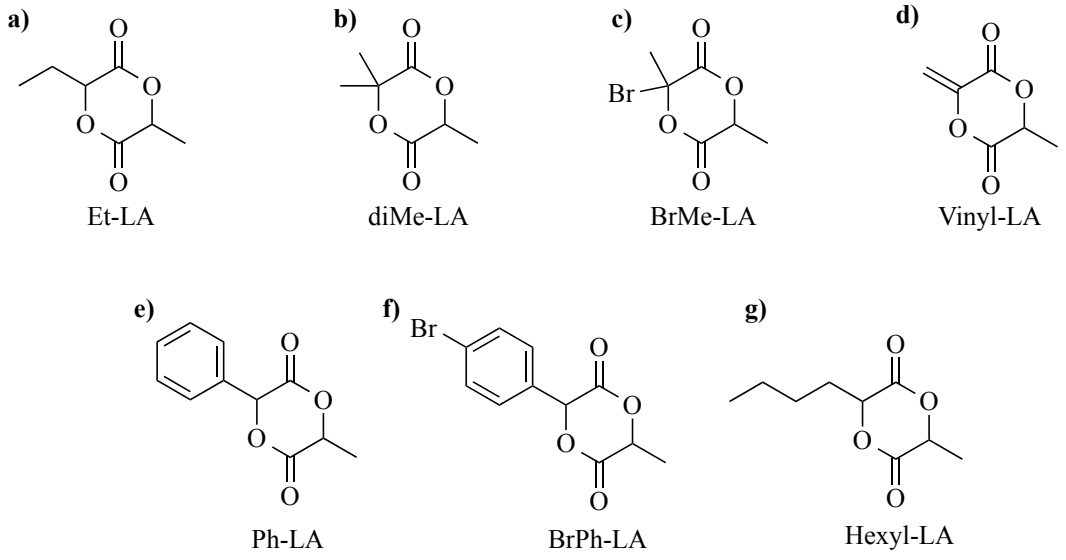

Figure 4.1.1: Summary of monomers synthesised in this chapter; **a)** Et-LA; **b)** diMe-LA; **c)** BrMe-LA; **d)** vinyl-LA; **e)** Ph-LA and **f)** BrPh-LA **g)** Hexyl-LA.

Methylethylglycolide (Et-LA) was synthesised directly from 2-hydroxybutyric acid to form the cyclic monomer by a modified synthesis developed by Baker and co-workers.[2] Similar methods were used to synthesise methyldimethylglycolide (diMe-LA), methylphenylglycolide (Ph-LA) and methylbromophenylglycolide (BrPh-LA) from hydroxyisobutyric acid, DL-mandelic acid and 4-bromo-DL-mandelic acid respectively.[3,4]

3-methyl-6-hexyl-1,4-dioxane-2,5-dione (Hexyl-LA) was synthesised *via* Method A (Scheme 4.1.2a), initially treating heptaldehyde with sodium cyanide to afford 2-hydroxyoctanoic acid (Figure 4.1.2). All monomers were purified further, as described in chapter 5.

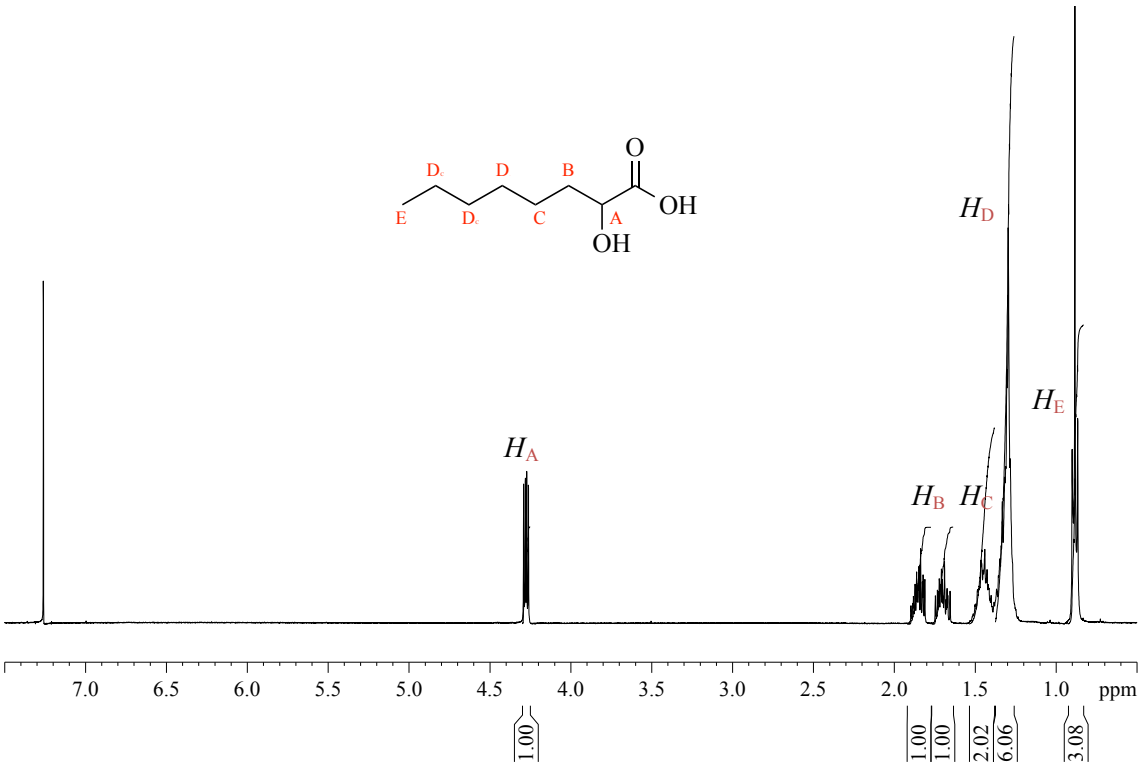

Figure 4.1.2: ^{1}H NMR spectrum of 2-hydroxyoctanoic acid.

Figure 4.1.2 illustrates the ^{1}H NMR spectrum of 2-hydroxyoctanoic acid. Two overlapping doublets at 4.28 ppm and 4.27 ppm (both ^{3}J = 7.5 Hz) are observed for the methine proton (H_A) as the methylene protons (H_B) are inequivalent. Multiplets at 1.91 ppm to 1.64 ppm are observed for the methylene protons H_B. Additionally two multiplets are observed at 1.54 ppm to 1.39 ppm and 1.39 ppm to 1.22 ppm, attributed to methylene protons H_C and H_D respectively. A triplet is observed for the methyl protons (H_E) at 0.88 ppm (^{3}J = 6.8 Hz). The α-hydroxyacid was added to 2-bromopropionyl bromide in the presence of triethyl amine to give 3-methyl-6-hexyl-1,4-dioxane-2,5-dione (hexyl-LA) as shown below in the ^{1}H NMR spectrum (Figure 4.1.3).

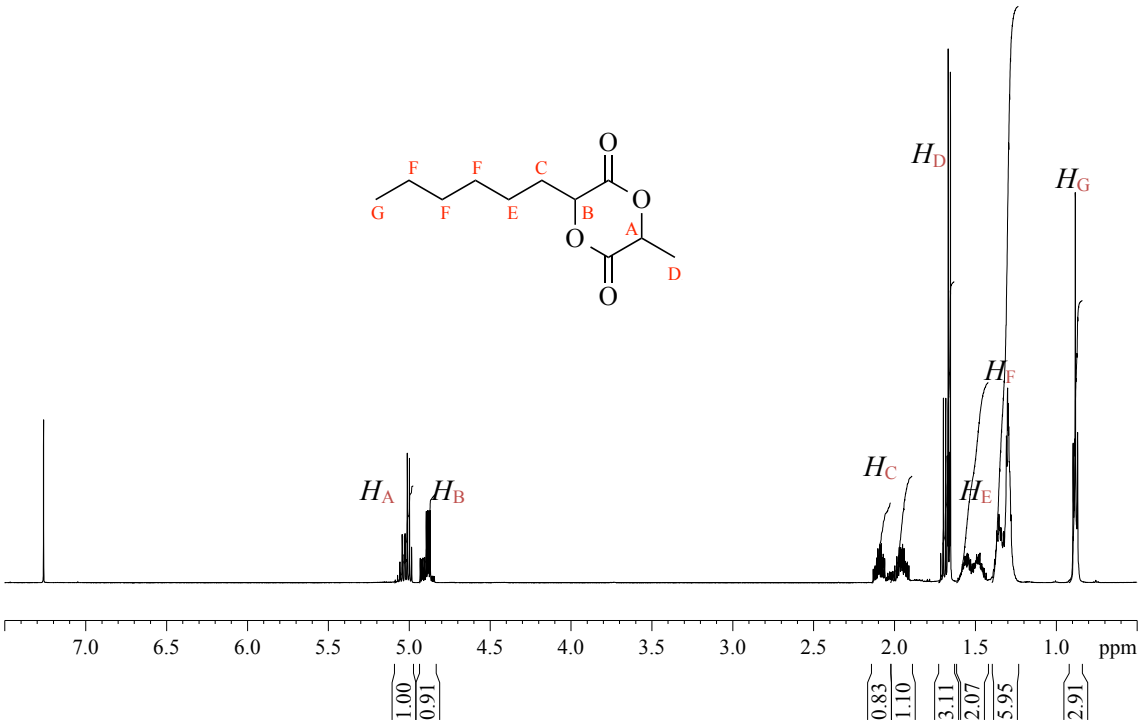

Figure 4.1.3: ^{1}H NMR spectrum of 3-methyl-6-hexyl-1,4-dioxane-2,5-dione (hexyl-LA).

As shown above (Figure 4.1.3), methine protons (H_A and H_B) are displayed as multiplets (5.09-4.97 ppm and 4.94-4.83 ppm) with the remaining multiplets attributed to methylene protons (H_C, H_E and H_F). The tertiary methyl moiety corresponds to an overlapping of doublets at 1.68 ppm (H_D, ^{3}J = 6.7 Hz) due to vicinal coupling with H_A and geminal coupling with the other H_D protons. The remaining methyl protons are displayed as a triplet at 0.88 ppm (^{3}J = 7.1 Hz).

Hillmyer and co-workers developed a synthesis for the vinyl monomer (vinyl-LA) as shown below (Figure 4.1.4).

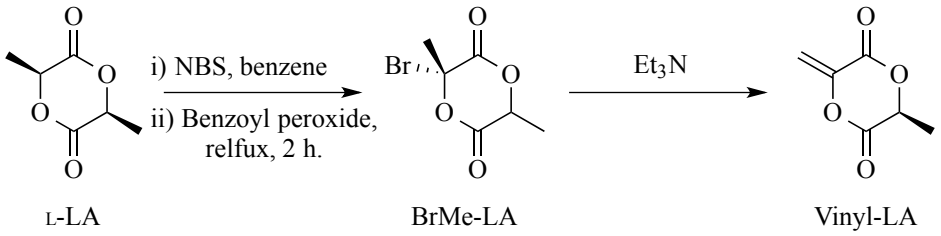

Figure 4.1.4: Synthesis of vinyl-LA.[5]

L-LA was reacted with *N*-bromosuccinamide with benzene as solvent. The reaction was heated under reflux followed by dropwise addition of benzyol peroxide and stirred for 2 hours. The intermediate (3*R*, 6*S*)-3-bromo-3,6-dimethyl-1,4-dioxane-2,5-dione (BrMe-LA) was isolated and characterised . The reaction then proceeded in CH_2Cl_2 with the presence of triethyl amine to

afford vinyl-LA. All of the above monomers were trialled for the ROP of using various initiators.

4.2. Co-polymerisations with lactide

Initially the monomers synthesised in Section 4.1 were trialled for co-polymerisations with lactide. All co-polymerisations discussed in this section were performed on NMR-scale (combined monomers moles: 3.46 x 10^{-4} mol), 100:1 combined monomers: initiator ratio with $\mathbf{L}^{t\mathrm{Bu}}\mathrm{ZrO}^{i}\mathrm{Pr}.\mathrm{HO}^{i}\mathrm{Pr}$ initiator in d_8 toluene (0.6 ml) at 353 K are shown below (Table 4.2.1).

Table 4.2.1: Initial screening of co-monomers for lactide polymerisation

Monomer	**Ratio Mon:*rac*-LA**	M_n **kg.mol^{-1}**	$M_{n,\,theo}$ **kg.mol^{-1}**	**PDI**
BrMe-LA	1:1	-	-	-
Vinyl-LA	1:1	-	-	-
Et-LA	1:1	4.3	15.0	1.22
DiMe-LA	1:1	-	-	-
Ph-LA	1:1	9.9	17.4	1.08
BrPh-LA	1:1	5.9	21.2	1.18
Hexyl-LA	1:1	-	-	-

Et-LA, Ph-LA and BrPh-LA were all active in the co-polymerisation with lactide. Conversely, BrMe-LA, vinyl-LA, diMe-LA and hexyl-LA failed to co-polymerise, and no conversion of the monomer was observed. Various other initiators were trialled for the polymerisation of vinyl-LA (Section 4.2.1) and a full kinetic study was performed for co-monomers; Et-LA, Ph-LA and BrPh-LA.

4.2.1. Vinyl-LA co-polymerisations

Hillmyer and co-workers reported the synthesis of vinyl-LA as an intermediate in the synthesis of other monomers via a Diels-Alder reaction.[5] To our knowledge, the homo-polymerisation of this monomer has not been reported and could yield polymers with ample post-polymerisation derivation options. Initially, the solvent-free polymerisation of recrystallized vinyl-LA was trialled using the initiator developed by Davidson and co-workers, $\mathbf{L}^{t\mathrm{Bu}}\mathrm{ZrO}^{i}\mathrm{Pr}.\mathrm{HO}^{i}\mathrm{Pr}$, with a monomer loading of 300:1 (monomer: initiator) at 135°C however, no reaction occurred and only monomer remained. Secondly, the commercially available initiator tin octanoate $\mathrm{Sn(Oct)_2}$

(tin(II) 2-ethylhexanoate) (300:1 monomer to initiator loading) with benzyl alcohol as a co-initiator (1.0 equivalent) was trialled at 135°C, with success, and the ^{1}H NMR spectra of vinyl-LA monomer and polymer obtained are shown below (Figure 4.2.1).

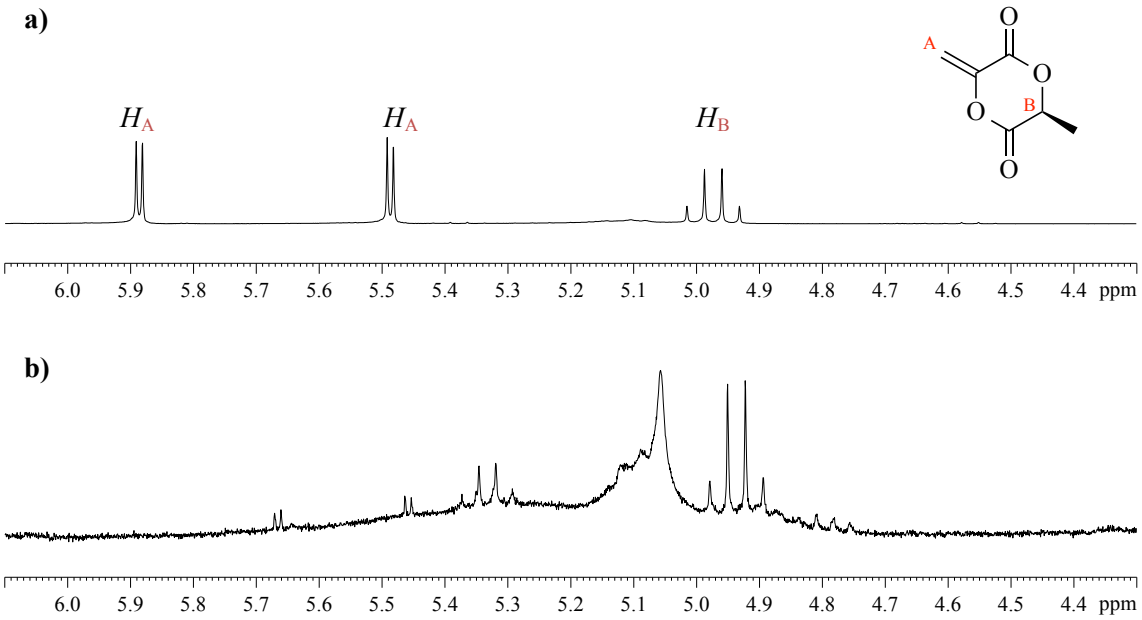

Figure 4.2.1: ^{1}H NMR spectra of vinyl-LA **a)** monomer and **b)** polymer.

The vinyl-LA polymeric material was insoluble in all common solvents, however an ^{1}H NMR spectrum was achieved upon prolonged heating in DMSO. For the monomer, there are two distinct doublets at 5.88 and 5.48 ppm that are split due to geminal coupling (^{2}J = 3.0 Hz) of the protons on unsaturated double bond. A quartet at 4.96 ppm corresponds to the methine proton with a coupling constant of ^{3}J = 6.0 Hz. Figure 4.2.1 b) illustrates that polymeric material was synthesised however, unreacted monomer remained. DSC analyses displayed no thermal events, thus suggesting the polymer is amorphous. Unfortunately, as the polymeric material was insoluble in THF, no GPC analyses were obtained. Cross-linking may have occurred during polymerisation.

Alternatively, Duchateau and co-workers reported the commercially available organic initiator TBD was active for the polymerisation of LA, and was thus trialled for the polymerisation of vinyl-LA.[6] The reaction was performed in solution (CH_2Cl_2) at 25°C with a much lower catalytic loading. Initially L-LA was polymerised using 100:0.1:1 monomer: initiator: co-initiator loadings and converted >99% monomer in 5 minutes. Co-polymerisation was then carried out with the addition of 5% and 10% vinyl monomer. The reaction was performed under the same conditions however, no conversion occurred suggesting vinyl-LA may inhibit catalytic

activity. This may be due to impurities in the monomers, inhibiting the initiator's behaviour. Various monomer: initiator ratios were tested with successful polymerisations of L-LA with 5% vinyl monomer under the optimal conditions of 100:2.5:1 L-LA+5%vinyl-LA: TBD: benzyl alcohol and for 10% vinyl monomer 100:5.0:1 (Table 4.2.2).

Table 4.2.2: GPC analyses for co-polymers of L-LA with vinyl-LA.

Monomer	**Initiator eq.**	**Conv.**	M_n **kg.mol^{-1}**	$M_{n,\,theo}$ **kg.mol^{-1}**	**PDI**
L-LA	0.1	99 %	33.2	142.7	1.68
L-LA + 5% vinyl-LA	2.5	57 %	37.9	82.1	1.42
L-LA + 10% vinyl-LA	5.0	99 %	36.2	142.7	1.62

A trend was observed of increased molecular weight with increased amounts of vinyl-LA. No thermal events occur by DSC which is indicative of extensive cross-linking.

4.3. Kinetic investigations of co-polymerisation

Et-LA, Ph-LA and BrPh-LA monomers were all active in the co-polymerisation with lactide using **L**$^{t\text{Bu}}$ZrO^{i}Pr.HO^{i}Pr. This section investigates lactide co-polymerisations using **L**$^{t\text{Bu}}$ZrO^{i}Pr.HO^{i}Pr and various monomer ratios in a one-pot synthesis.

4.3.1. Et-LA Polymerisations

In order to synthesise a random co-polymer, the rates of reaction should be similar. As Et-LA is very similar in structure to lactide, the possibility of synthesising a co-polymer is plausible. The syntheses of both homo-polymers and co-polymers of lactide with Et-LA were done using initiator **L**$^{t\text{Bu}}$ZrO^{i}Pr.HO^{i}Pr. All co-polymerisations discussed in this section were performed on NMR-scale (combined monomer moles; 3.46 x 10^{-4} mol), 100:1 combined monomer: initiator ratio with **L**$^{t\text{Bu}}$ZrO^{i}Pr.HO^{i}Pr initiator in d_8 toluene (0.6 ml) at 353 K. The reactions were monitored in situ by ^{1}H NMR spectroscopy. Inconveniently, the different polymer peaks overlapped (Figure 4.3.1), so that a series of equations were derived in order to calculate conversion accurately (Equation 4.1).

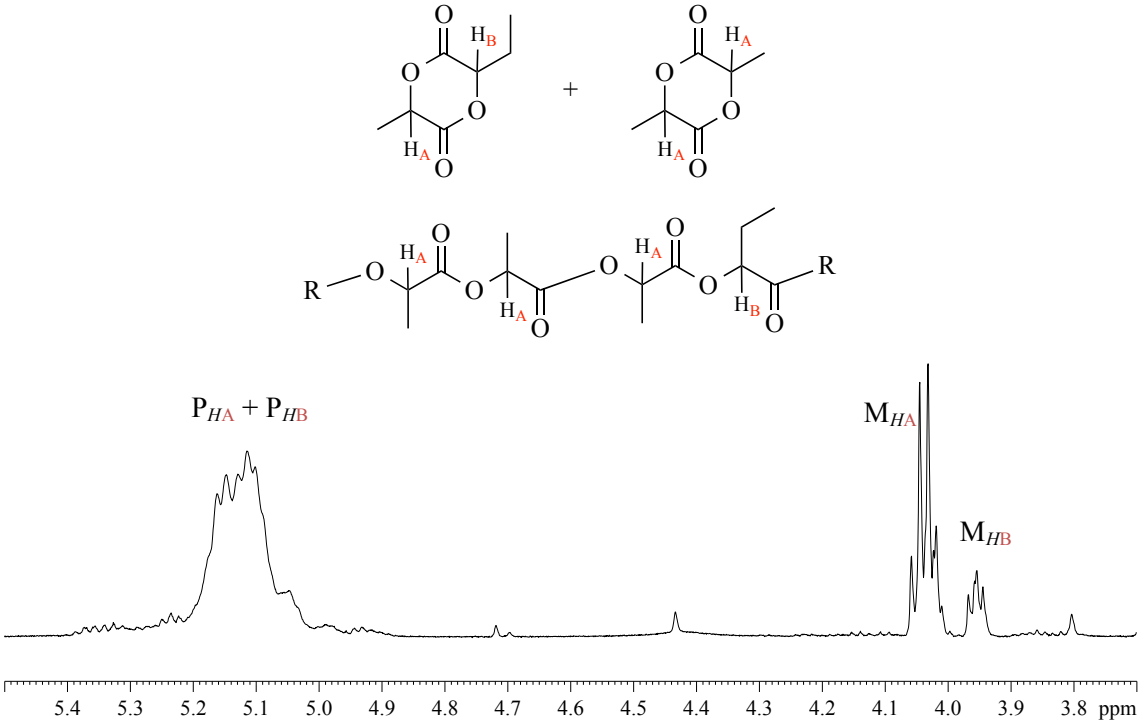

Figure 4.3.1: *In situ* ^{1}H NMR spectrum during co-polymerisation of Et-LA and *rac*-LA (50:50:1 monomer: monomer: initiator ratio) using **L**$^{t\text{Bu}}$ZrO^{i}Pr.HO^{i}Pr.

In order to calculate conversion during reaction, *in situ* ^{1}H NMR spectroscopy was used. Here, both the monomer peaks and the polymer peaks are overlapping (Figure 4.3.1). The triplet at 3.95 ppm corresponds to the methine proton of Et-LA adjacent to the ethyl moiety. The overlapping quartet at 4.03 ppm attributes to the methine protons of both Et-LA and *rac*-LA adjacent to the methyl moiety (three protons; two from *rac*-LA and one from Et-LA). The polymer peaks for the conversion of both monomers was observed as a multiplet at 4.87 – 5.39 ppm. In order to calculate conversion of each monomer to the desired co-polymer, an equation was devised as shown below (Equation 4.1).

Equation 4.1: Devised equation to calculate conversion during co-polymerisation of Et-LA and *rac*-LA.

(i)

$$\frac{[M_A]_0}{[M_B]_0} = \alpha = \frac{M_A + P_A}{M_B + P_B}$$

$$\alpha(M_B + P_B) = M_A + P_A \quad \text{(ii)}$$

Simultaneous equations:

$$\alpha P_B - P_A = M_A - \alpha M_B \quad \text{(iii)}$$

$$P_A + P_B = \beta \quad \text{(iv)}$$

$$(1 + \alpha)P_B = \beta + M_A - \alpha M_B \quad \text{(v)}$$

Rearrange:

$$P_B = \frac{\beta + M_A - \alpha M_B}{1 + \alpha} \quad \text{(vi)}$$

$$P_B = \beta - P_A \quad \text{(vii)}$$

$$P_A = \frac{\beta(1 + \alpha) - \beta - M_A + \alpha M_B}{1 + \alpha} \quad \text{(viii)}$$

$$P_A = \frac{\alpha\beta - M_A + \alpha M_B}{1 + \alpha} \quad \text{(ix)}$$

It was known that the monomer concentration of *rac*-LA to Et-LA was 1:1, thus M_{HA} corresponds to three protons and M_{HB} corresponds to one proton. From this, along with the integral for the combined co-polymer, conversion can be calculated as described above (Equation 4.1). Using these equations, conversion of the monomers to polymer was determined. ^{1}H NMR spectrum was taken every 15 minutes for 8 hours as shown below (Figure 4.3.2).

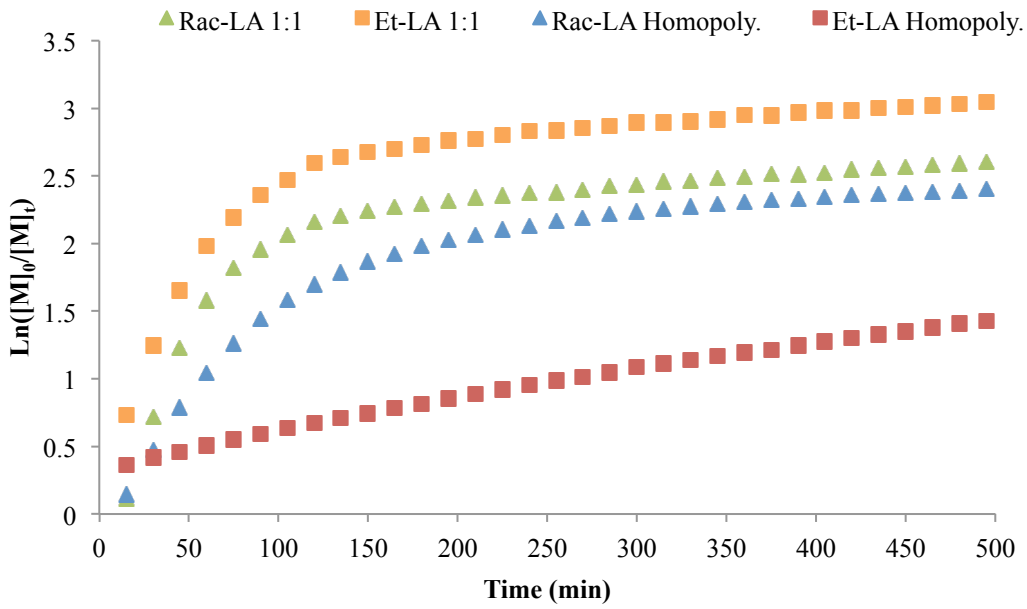

Figure 4.3.2: Semi-log plot of homo-polymerisation of *rac*-LA (blue), Et-LA (red) and the 1:1 co-polymerisation of *rac*-LA (green) and Et-LA (orange) using $\mathbf{L}^{t\mathrm{Bu}}\mathrm{ZrO}^{i}\mathrm{Pr.HO}^{i}\mathrm{Pr}$ (100:1 combined monomer: initiator loading) in toluene- d_8.

Figure 4.3.2 illustrates the semi-log plot for homo-polymerisations of *rac*-LA and Et-LA. It was observed that *rac*-LA has a much faster reaction rate than Et-LA. However, when the two monomers are co-polymerised together at a 1:1 monomer: monomer ratio the reaction rates appear to be enhanced and to converge. The apparent rate constants (k_{app}) for these reactions are shown below with calculated linear regression displayed in brackets (Table 4.3.1).

Table 4.3.1: Apparent rate constants for homo-polymerisation of *rac*-LA (blue), Et-LA (red) and the co-polymerisation with a *rac*-LA (green) to Et-LA (orange) monomer ratio of 1:1 using $\mathrm{L}^{t\mathrm{Bu}}\mathrm{ZrO}^{i}\mathrm{Pr.HO}^{i}\mathrm{Pr}$ (100:1 combined monomer: initiator loading) in d_8 tol.

$[\mathrm{LA}]_0$	:	$[\mathrm{Et\text{-}LA}]_0$	k_{app} LA (min^{-1})	k_{app} EtLA (min^{-1})
1	:	1	0.0285 (±0.004)	0.0326 (±0.0001)
1	:	0	0.0173 (±0.003)	-
0	:	1	-	0.0030 (±0.0001)

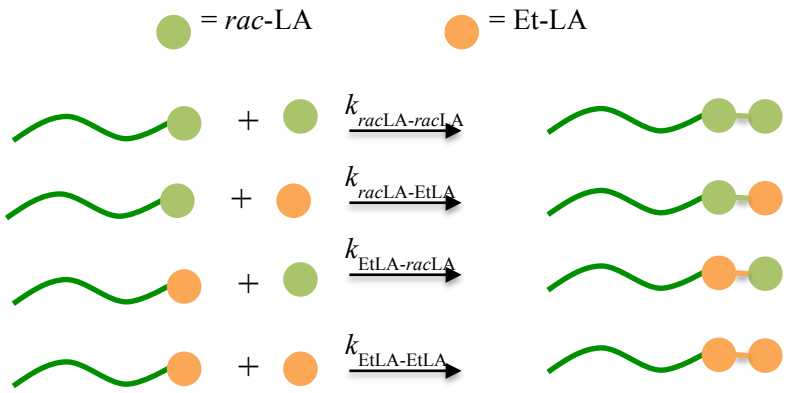

Figure 4.3.3: Reaction rates of co-polymerisation of *rac*-LA (green) and Et-LA (orange).

For the homo-polymerisation of *rac*-LA a k_{app} of 0.0173 min^{-1} was observed, which was significantly faster than that of Et-LA (k_{app} = 0.0030 min^{-1}). As described in Figure 4.3.3 this suggests that the addition of *rac*-LA monomer to a polymer chain propagating from a poly(*rac*-LA) moiety ($k_{racLA\text{-}racLA}$) is a lot faster than the addition of a Et-LA monomer to a polymer chain propagating from a polyEt-LA moiety ($k_{EtLA\text{-}EtLA}$), therefore $k_{racLA\text{-}racLA}$ >> $k_{EtLA\text{-}Et\text{-}LA}$. Conversely, during the co-polymerisation (1:1 *rac*-LA:Et-LA), the k_{app} values for both monomers were similar. Here, both *rac*-LA and Et-LA experienced an increase reaction rates (k_{app} = 0.0285 min^{-1} and 0.0326 min^{-1} respectively). Interestingly, at this monomer ratio (1:1), the apparent rate constants are similar. Statistically, using linear regression, both rates (k_{app} = 0.0285 min^{-1} (±0.004) and 0.0326 min^{-1} (±0.0001) for *rac*-LA and Et-LA respectively) are within the same range. An alternative co-polymer is likely to have occurred, with EtLA homo-polymer block tendencies. This behavioural phenomenon is well documented with co-polymerisations behaving very differently to their homo-polymerisation counterparts. As the reaction rates are closer at 1:1 monomer ratio, this suggests the formation of a true co-polymer may be possible. Investigations into the co-polymerisation of *rac*-LA and Et-LA were undertaken. Similar calculations were performed using different ratios, of which the kinetic plots are displayed below (Figure 4.3.4).

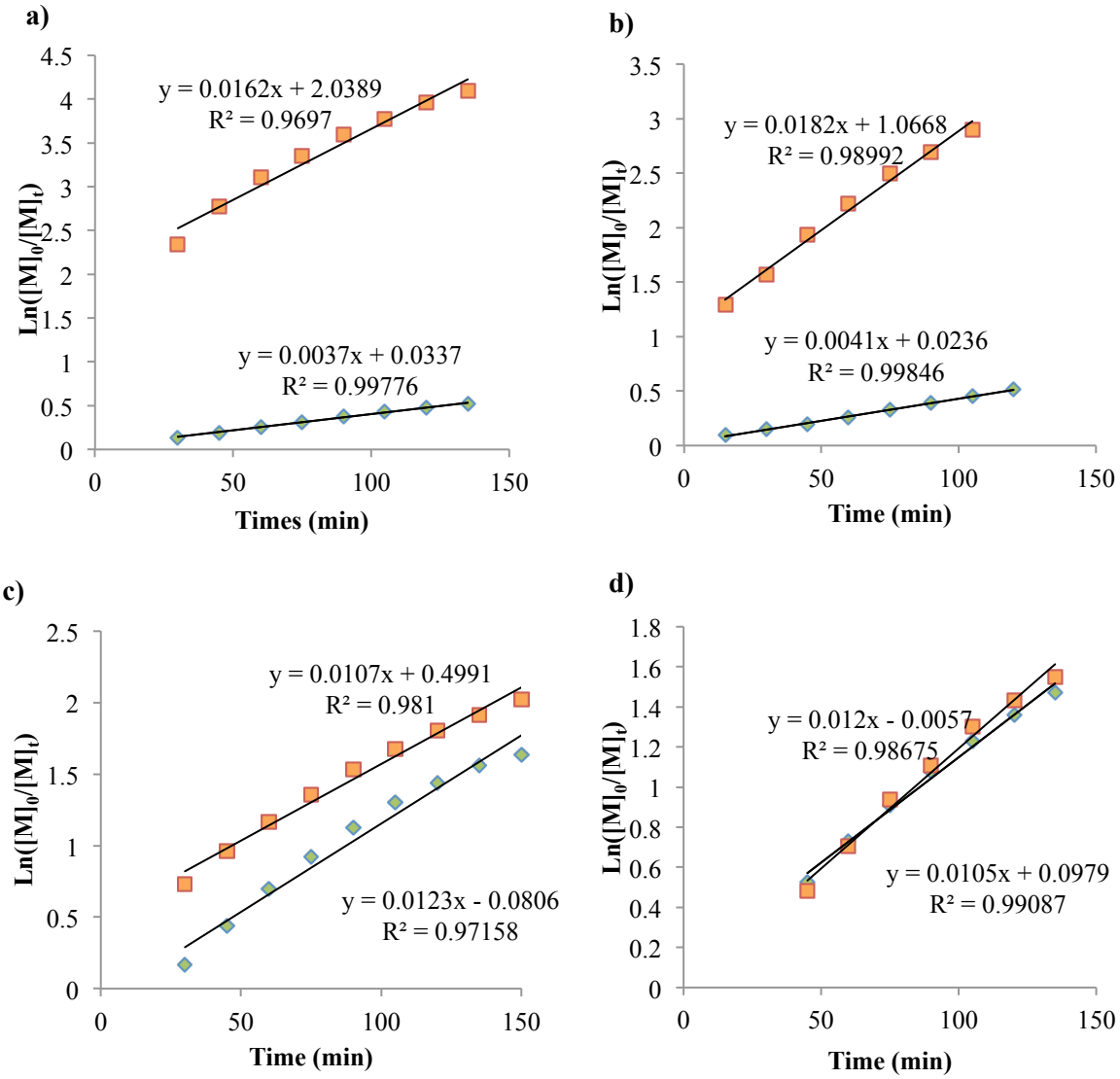

Figure 4.3.4: Semi-log plot of co-polymerisation using $\mathbf{L}^{t\mathrm{Bu}}\mathrm{ZrO}^{i}\mathrm{Pr}.\mathrm{HO}^{i}\mathrm{Pr}$ (100:1 combined monomer: initiator loading) with a *rac*-LA (green) to Et-LA (orange) monomer ratio of **a)** 9:1, **b)** 4:1, **c)** 3:1, **d)** 1:3.

At 9:1 *rac*-LA: Et-LA, the reaction rates observed (*rac*-LA k_{app} = 0.004 min^{-1} and Et-LA k_{app} = 0.016 min^{-1}) suggest that the initial co-polymerisation occurred at a fast rate, followed by the slow rate of the remaining homo-polymer segment ($k_{12} \sim k_{21} > k_{11}$). As the amount of co-monomer is increased the reaction rates increase whereby at 1:3 *rac*-LA: Et-LA monomer ratio the apparent rate constants appear to be very similar. This suggests formation of a true random co-polymer where the addition of either monomer to either polymer end are similar or the reactivity ratios r_1 and r_2 both approximately 1 ($k_{rac\text{LA-}rac\text{LA}} \sim k_{rac\text{LA-EtLA}} \sim k_{\text{EtLA-}rac\text{LA}} \sim k_{\text{EtLA-EtLA}}$). Unfortunately, reactivity ratios could not be calculated due to high initial conversion illustrated was over 15 % (must be >20%).

Coates *et al*. reported the ROP of lactide using a chiral salen aluminium complex for which the chirality of the metal complex and the chirality of the alkoxide moiety played a crucial role in the influence of stereoselectivity in the initial ring-opening event.[7] In our case, similar activity may be observed as in the initial ring-opening event, the initiator could preferentially ring-open an Et-LA monomer instead of a *rac*-LA monomer. Thus high initial conversion of Et-LA was displayed.

A full semi-log plot of copolymerisation at 1:3 *rac*-LA: Et-LA is shown below.

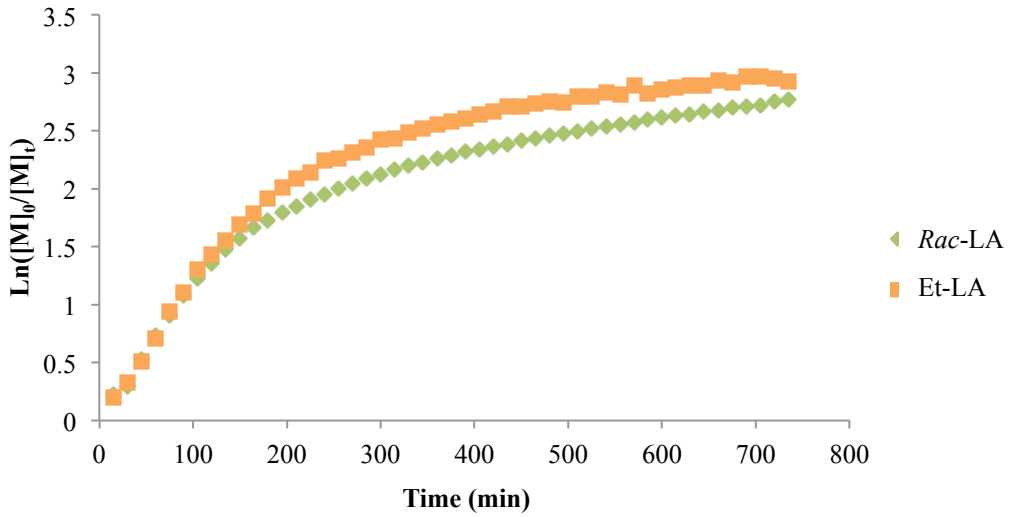

Figure 4.3.5: Semi-log plot of co-polymerisation using **L**$^{t\text{Bu}}$ZrO^{i}Pr.HO^{i}Pr (100:1 combined monomer: initiator loading) with a *rac*-LA (green) to Et-LA (orange) monomer ratio of 1:3.

Figure 4.3.5 displays a full semi-log plot of co-polymerisation using L$^{t\text{Bu}}$ZrO^{i}Pr.HO^{i}Pr (100:1 combined monomer: initiator loading) with a *rac*-LA (green) to Et-LA (orange) monomer ratio of 1:3. Initially, the rates appear similar, corresponding to a co-polymerisation where $k_{12} \sim k_{21}$. However, when all the minor monomer (*rac*-LA) was consumed the reaction rate decreases significantly similar to that of the homo-polymer due to $k_{\text{EtLA-EtLA}} << k_{\text{EtLA-}rac\text{LA}} \sim k_{rac\text{LA-EtLA}}$.

All polymerisations were terminated after 8 hours with addition of methanol (0.2 ml). The solvent was removed and the resulting polymer was washed with methanol to remove any unreacted monomers. The polymers were dried *in vacuo* and GPC was used to determine molecular weights (Table 4.3.2).

Table 4.3.2: GPC analyses of co-polymers of *rac*-LA with Et-LA.

$[LA]_0$	:	$[Et\text{-}LA]_0$	M_n kg.mol^{-1}	$M_{n,\,theo}$ kg.mol^{-1}	PDI	T_g (°C)
9	:	1	54.0	14.5	1.18	38
			10.8		1.17	
4	:	1	10.7	14.6	1.33	37
3	:	1	32.0	14.7	1.22	38
			6.6		1.14	
1	:	1	3.5	15.0	1.22	16
1	:	3	2.7	15.4	1.24	0
0	:	1	2.4	15.7	1.15	3

Initially, at 9:1 *rac*-LA:Et-LA, a bimodal GPC trace was observed with a high-molecular weight GPC trace (M_n = 54.0 kg.mol^{-1}), along with a much smaller polymer (M_n = 10.8 kg.mol^{-1}). This bimodal trace suggests two different polymers were synthesised, possibly a *rac*-LA homo-polymer (M_n = 54.0 kg.mol^{-1}) and a *rac*-LA and Et-LA co-polymer (M_n = 10.8 kg.mol^{-1}). Interestingly, at 1:1 *rac*-LA:Et-LA, a mono-modal trace was observed suggesting a co-polymer may have been synthesised. A trend of decreasing M_n coupled with a decrease in T_g was observed with increasing quantities of Et-LA further suggesting co-polymerisation.

4.3.2. Ph-LA Polymerisations

Poly(Ph-LA) has increased T_g (85°C) compared to polylactide (60°C) which is of great significance in the industrial market. Interestingly, the properties of polymandelide (T_g 100°C)[8] coupled with the degradability of lactide could lend themselves to a promising degradable co-polymer. All co-polymerisations discussed for now on in this chapter were performed on NMR-scale (combined monomer moles; 3.46 x 10^{-4} mol), 100:1 combined monomer: initiator ratio in d_8 toluene (0.6 ml) at 353 K.

An initial screening of $\mathbf{L}^{t\mathrm{Bu}}\mathrm{ZrO}^{i}\mathrm{Pr}.\mathrm{HO}^{i}\mathrm{Pr}$ as an initiator in the ring-opening homo-polymerisations of *rac*-LA, L-LA and Ph-LA was completed at 80°C with a 100:1 monomer to initiator ratio in toluene-d_8. The reactions were monitored *in situ* by ^{1}H NMR spectroscopy (Figure 4.3.6).

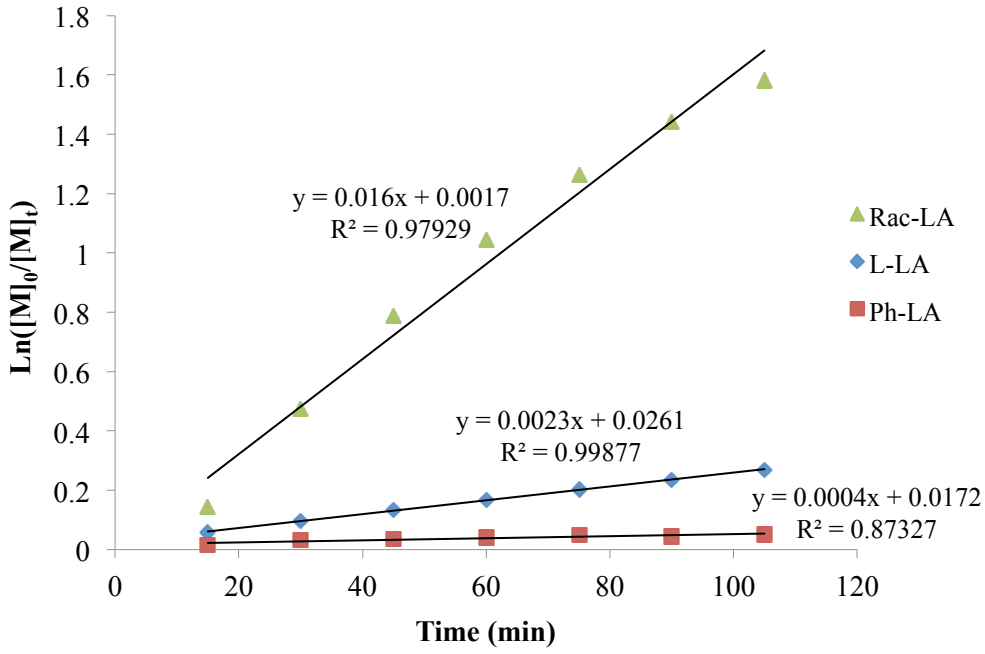

Figure 4.3.6: Semi-log plot of the homo-polymerisation of *rac*-LA (green), L-LA (blue) and Ph-LA (red) with $\mathbf{L}^{t\mathrm{Bu}}\mathrm{ZrO}^{i}\mathrm{Pr}.\mathrm{HO}^{i}\mathrm{Pr}$, 100:1 monomer:initiator loading, 80°C in d_8 tol.

Previously, Davidson *et al.* reported the homo-polymerisation of *rac*-LA and L-LA in $CDCl_3$ at 25°C with a 100:1 monomer to initiator to have a *pseudo*-first order rate constant (k_{app}) of 4.2 x 10^{-3} min^{-1} and 0.6 x 10^{-3} min^{-1} resepctively.[9] Under our conditions (100:1 monomer to initiator loading in toluene-d_8, 80°C), kinetic analyses suggest *pseudo*-first order for *rac*-LA and L-LA with an apparent rate constant (k_{app}) of 16.0 x 10^{-3} min^{-1} and 2.3 x 10^{-3} min^{-1} respectively. This is consistent with the previously reported data and is due to the initiator preferentially forming heterotactic PLA over isotactic PLA. Baker and co-workers reported the synthesis and polymerisation of Ph-LA using *rac*-(Salbinap)-AlO^{i}Pr initiators affording low M_w polymers.[3] In our case, the homo-polymerisation of *rac*-Ph-LA (100:1 monomer to initiator loading in d_8 tol, 80°C) suggests pseudo-first order kinetics with an observed k_{app} of 0.4 x 10^{-3} min^{-1}, considerably slower than the *rac*-LA and L-LA counterparts. The reduction in k_{app} may be due to the steric hindrance of the phenyl ring prohibiting the coordination of the initiator activating the carbonyl group *alpha* to the aromatic moiety. Nevertheless, during polymerisation *in situ* NMR spectra were used to determine conversion (Figure 4.3.7).

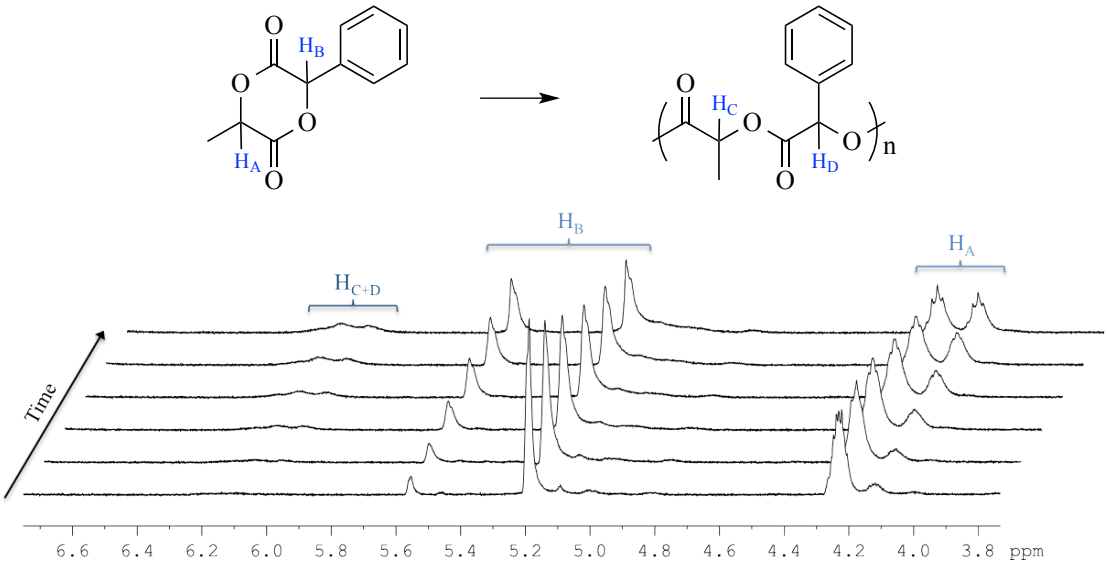

Figure 4.3.7: ^{1}H NMR spectra (stacked) for the homo-polymerisation of Ph-LA with **L**$^{t\text{Bu}}$ZrO^{i}Pr.HO^{i}Pr, 100:1 monomer:initiator loading, 80°C in d_8 tol.

Upon closer inspection of the ^{1}H NMR spectra during polymerisation, it can be seen that whilst polymerisation does occur, epimerisation of the monomer is observed simultaneously. Baker and co-workers reported the preferred monomers configuration during synthesis was the enantiomers with stereocentres of *SS* or *RR*.[3] During polymerisation, and in the presence of the initiator, the delocalised electrons within the aromatic ring pull electron density away from the lactide backbone forcing the adjacent H_B to be more acidic. This in turn leads to epimerisation, which is displayed in the ^{1}H NMR (Figure 4.3.7). Epimerisation is the process of forming an epimer *via* a change of one stereocentre in a molecule that has more than one stereocentre. This leads to the formation of diastereoisomers with the configuration *SR* or *RS*, from *SS* and *RR* respectively, where H_B is displayed as a downfield shift from δ 5.21 ppm to 5.58 ppm. This in turn has an effect on H_A, demonstrated by an upfield shift from δ 4.25 ppm to 4.18 ppm, whilst the growing polymer chain is observed as a broad multiplet at δ 6.23-5.85 ppm. It was observed that the epimerisation lead to a statistical mixture of enantiomers and diastereoisomers (1:1).

A range of copolymers were synthesised with five different monomer ratios. Initially, 1:1 ratio of *rac*-LA and Ph-LA was synthesised under the same conditions as above (Figure 4.3.6). Kinetic analyses were carried out using *in situ* by NMR and conversions determined by integrating both monomer and polymer peaks.

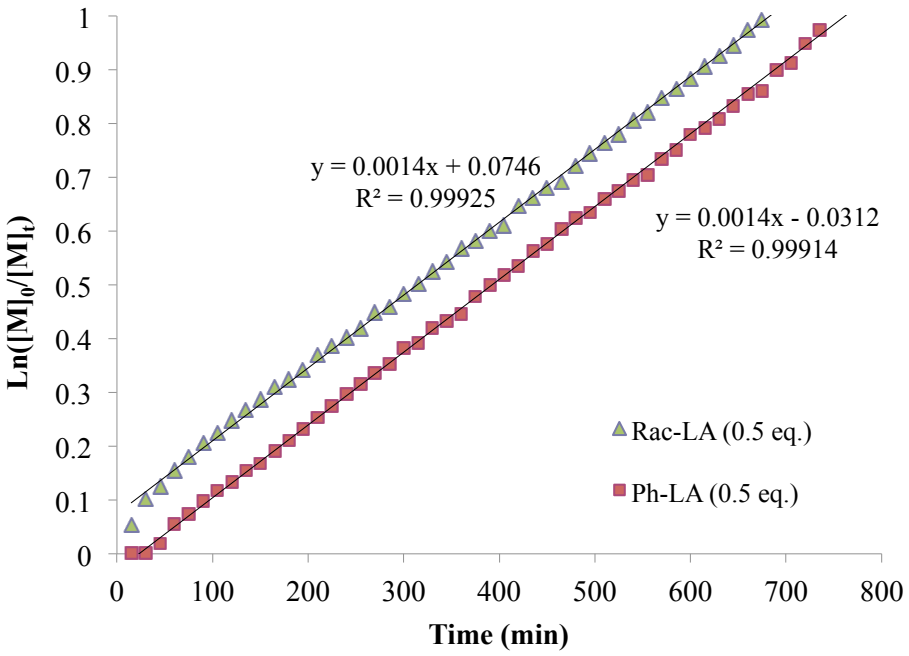

Figure 4.3.8: Semi-log plot of polymerisation of *rac*-LA (green) and Ph-LA (red) with $\mathbf{L}^{t\mathrm{Bu}}\mathrm{ZrO}^{i}\mathrm{Pr}.\mathrm{HO}^{i}\mathrm{Pr}$, 50:50:1 *rac*-LA:Ph-LA:initiator loading, 80°C in d_8 tol.

Whilst the homopolymerisation rates of reaction were very different, during a 1:1 copolymerisation of *rac*-LA and Ph-LA the rates appear to be similar (k_{app} *rac*-LA and Ph-LA are both 1.4 x10^{-3} min^{-1}). However, this does not prove the formation of a perfectly alternating or a truly random copolymer as it is unknown whether the active site chain ends in a Ph-LA or a LA monomer and thus what sequence the initiator would preferentially polymerise the monomers.

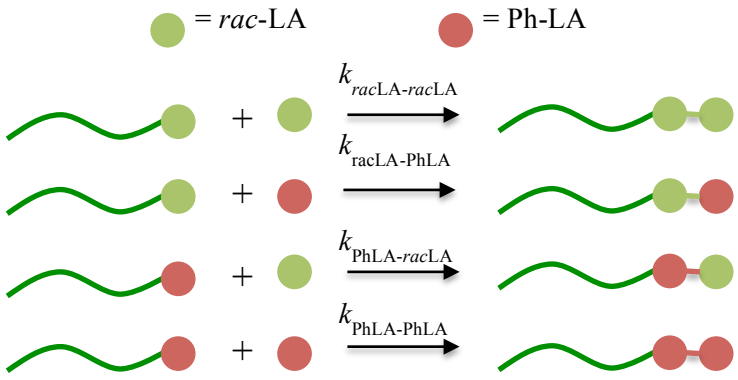

Figure 4.3.9: Reaction rates of co-polymerisation of *rac*-LA (green) and Ph-LA (red).

The possible microstructures include block, random, and alternating polymers. Further investigation of the microstructure by MALDI-ToF analyses and determination of reactivity ratios was required. MALDI-ToF analysis can be used in order to determine both the end groups and the microstructural sequence of the polymer. A proposed (not measured) schematic is shown below illustrating a perfectly alternating co-polymer (Scheme 4.3.1).

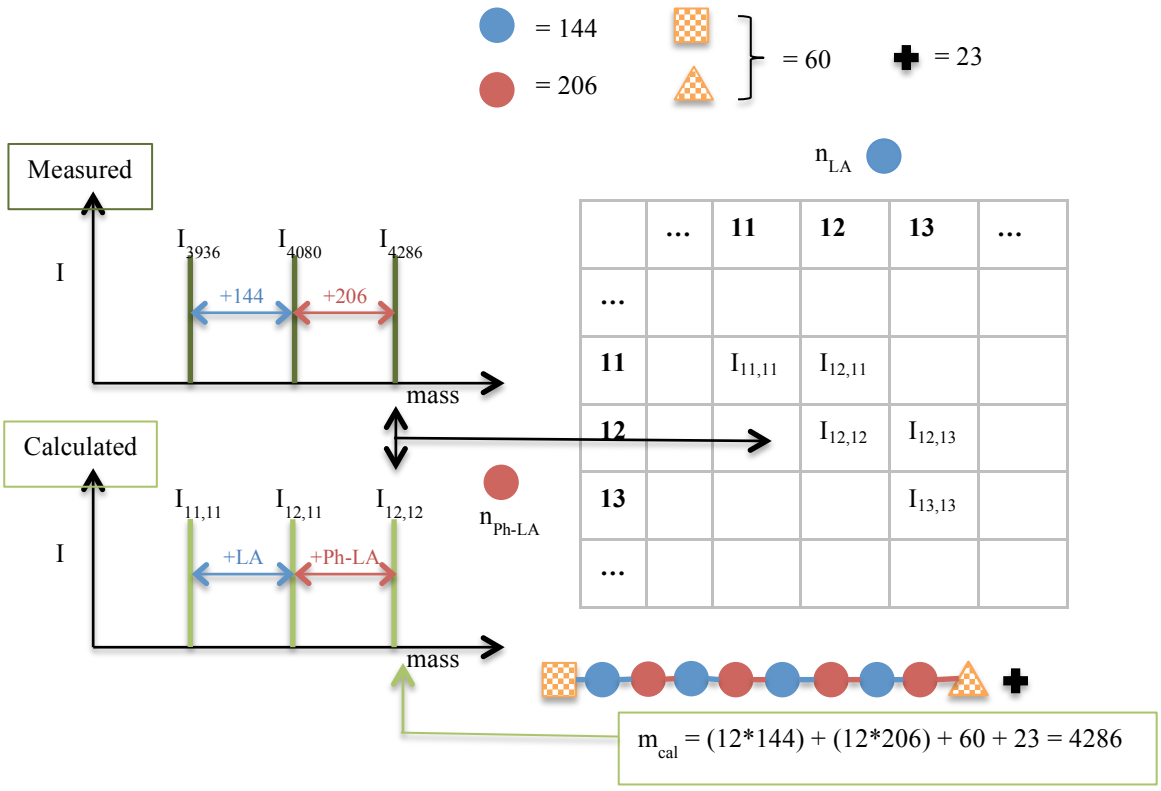

Scheme 4.3.1: Proposed (not measured) schematic representation using MALDI-ToF analysis of perfectly alternating copolymer with monomers *rac*-LA (blue) and Ph-LA (red), end groups (yellow patterned) and sodium cation (+).

A modified schematic by Duchateau *et al.* (Scheme 4.3.1),[10] illustrates the possible interpretation of MALDI-ToF analysis in order to depict the microstructure of the copolymer. For a perfectly alternating co-polymer, a peak at 3936 m/z would correspond to a calculated intensity of eleven LA monomers with eleven Ph-LA monomers, with a sodium cation and an isopropoxide initiating group. Interestingly, if the next peak was to be 4080 m/z, this would indicate the addition of a LA monomer, if this was then followed by an addition of a Ph-LA monomer a peak at 4286 m/z would be detected.

In 1944, Mayo and Lewis investigated the behaviour of the monomers methylmethacrylate and styrene in free radical co-polymerisation.[11] They developed a theoretical equation to determine the reactivity ratios of the co-polymerisation and thus establish the final microstructure of the polymer. Polymerisations consisting of five different monomer ratios, ranging from 9:1 to 1:9, were used to calculate reactivity ratios of the reaction. There are various methods to determine reactivity ratios as discussed in chapter 1. Mayo and Lewis devised an equation (Equation 4.2) using the kinetic data of co-polymerisations at low conversions (below 15 %). Firstly, kinetic analyses of polymerisations with varying monomer:monomer ratios were investigated. Under the same conditions as for the homo-polymerisations, the reaction of $\mathbf{L}^{t\mathrm{Bu}}\mathrm{ZrO}^{i}\mathrm{Pr}.\mathrm{HO}^{i}\mathrm{Pr}$ with monomers *rac*-LA and Ph-LA was performed with a combined monomer to initiator ratio of 100:1. Whilst the overall concentration remained constant for all co-polymerisations, the *rac*-LA to Ph-LA monomer to monomer ratio differed. Initially, polymerisations with *rac*-LA: Ph-LA monomer ratios of 9:1 and 3:1 were adopted as shown below (Figure 4.3.10).

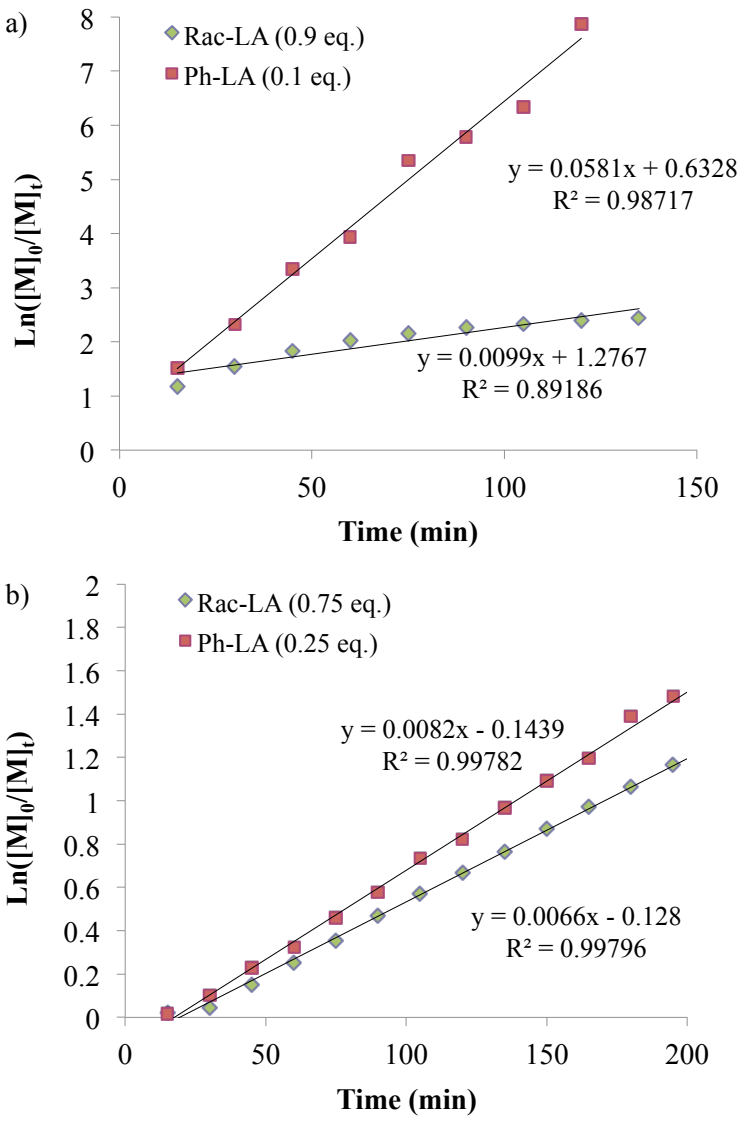

Figure 4.3.10: Copolymerisation using ZrL$^{t\text{Bu}}$O^{i}Pr with a *rac*-LA (green) to Ph-LA (red) monomer ratio of a) 9:1 and b) 3:1.

Firstly, a 9:1 monomer to monomer ratio was employed and kinetic analyses were undertaken as shown in Figure 4.3.10a. Surprisingly, it is observed that polymerisation of *rac*-LA demonstrates a much slower k_{app} (9.9 x 10^{-3} min^{-1}) than that of its homopolymerisation (k_{app} = 14.0 x 10^{-3} min^{-1}). Conversely, the polymerisation of Ph-LA demonstrates a much faster k_{app} (5.8 x 10^{-2} min^{-1}) than that of its homopolymerisation (k_{app} = 0.4 x 10^{-3} min^{-1}). Although there are examples of this phenomenon in the literature with the copolymerisation of ε-CL and LA, there is still no explanation.[12–14] The reverse *rac*-LA to Ph-LA monomer ratios were polymerised (1:9 and 1:3 equivalents) as shown in Figure 4.3.11.

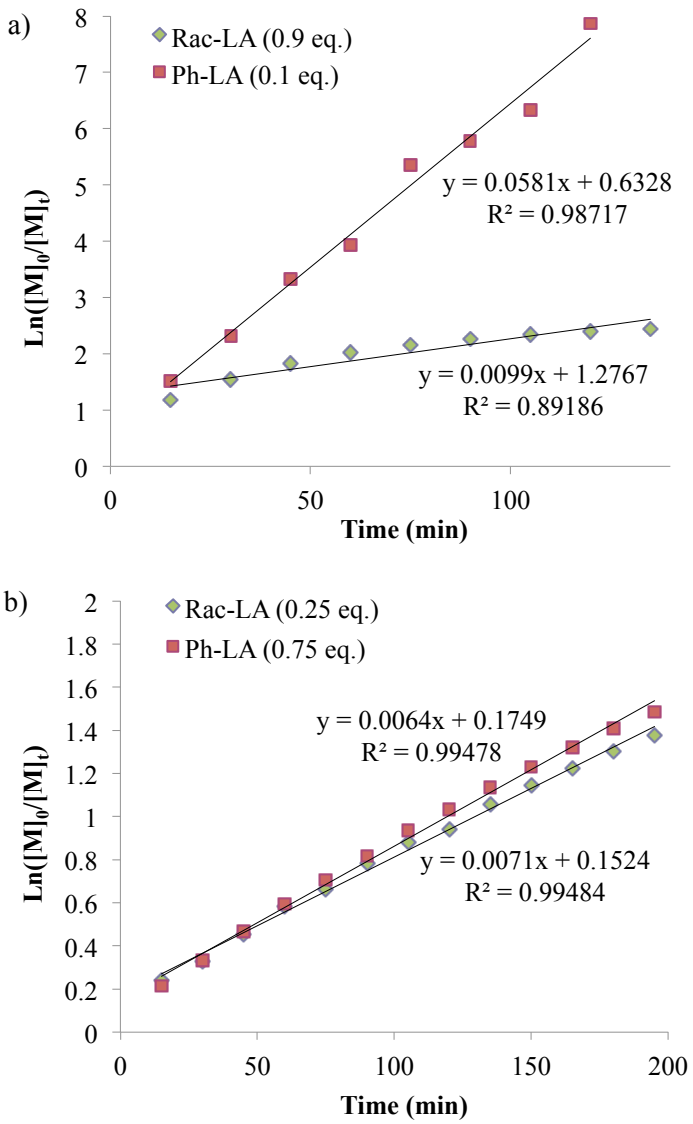

Figure 4.3.11: Copolymerisation using $\mathbf{L}^{t\mathrm{Bu}}\mathrm{ZrO}^{i}\mathrm{Pr}.\mathrm{HO}^{i}\mathrm{Pr}$ (100:1 combined monomer: initiator loading) with a *rac*-LA (green) to Ph-LA (red) monomer ratio of **a**) 1:9 and **b**) 1:3.

A *rac*-LA to Ph-LA monomer ratio of 1:9 was employed and the kinetic analyses examined (Figure 4.3.11a). Whilst the polymerisation rate of *rac*-LA was faster (k_{app} = 1.0 x 10^{-2} min^{-1}) than *rac*-LA homo-polymerisation (k_{app} = 16.0 x 10^{-3} min^{-1}), the behaviour mimics the homo-polymerisation, as it is faster than the Ph-LA co-polymerisation (7.4 x 10^{-3} min^{-1}). Kinetic analyses of polymerisation with *rac*-LA to Ph-LA monomer ratio of 1:3 (Figure 4.3.11b) displays similar co-polymerisation rates for *rac*-LA (k_{app} = 7.1 x 10^{-3} min^{-1}) and Ph-LA (k_{app} = 6.4 x 10^{-3} min^{-1}). This observation suggests that as the ratio's get closer to 1:1 the k_{app}'s also converge to a similar rate.

Equation 4.2: Mayo-Lewis equation for the co-polymerisation of *rac*-LA with Ph-LA.

$$F_1 = 1 - F_2 = \frac{r_1 {f_1}^2 + f_1 f_2}{r_1 {f_1}^2 + 2 f_1 f_2 + r_2 {f_2}^2}$$

$$r_1 = \frac{k_{1,1}}{k_{1,2}} \qquad r_2 = \frac{k_{2,2}}{k_{2,1}}$$

As discussed in Chapter 1, the Mayo Lewis equation was used to determine the reactivity ratios of the co-polymerisation of *rac*-LA with Ph-LA where f_1 and f_2 are the mole fraction of LA and Ph-LA in the feed. F_1 and F_2 are the mole fraction of LA and Ph-LA in co-polymer. r_1 and r_2 are the reactivity ratios of LA and Ph-LA respectively in the co-polymer.

Table 4.3.3: Reactivity ratios for the co-polymerisation of *rac*-LA with Ph-LA.

$[LA]_0$ (f_1)	$[Ph\text{-}LA]_0$ (f_2)	LA conv. (%)	Ph-LA conv. (%)	LA copolymer (F_1)	Ph-LA copolymer (F_2)
0.9	0.1	13. 12	13.11	0.89	0.10
0.75	0.25	2.04	0.01	0.83	0.18
0.5	0.5	11.32	11.21	0.49	0.50
0.25	0.75	7.12	8.19	0.25	0.75
0.1	0.9	9.03	6.41	0.15	0.85
$r_{1(calc)} = 0.74$					
$r_{2(calc)} = 0.69$					

The reactivity ratios (r_1 and r_2) derived from the Mayo-Lewis equation are similar in values and are below 1. Florczak and Duda investigated chiral Schiff base enantiomers and their effect on the co-polymerisation of ε-caprolactone and L,L-lactide which also exhibited similar reactivity ratios to one another.[14] This trend indicates the microstructure of the copolymer is a statistical distribution of *rac*-LA and Ph-LA monomer units along the polymeric chain. A random co-polymerisation displays $r_1 = r_2 = 1$ and for a true alternating polymer $r_1 = r_2 = 0$. Conversely, in our case, r_1 and r_2 are less that 1 but higher than 0 indicating the synthesis of a random co-polymer. A plot of co-polymer composition (F_1) versus monomer feed ratio (f_1) was used to further investigate the microstructural sequence of the co-polymers (Figure 4.3.12).

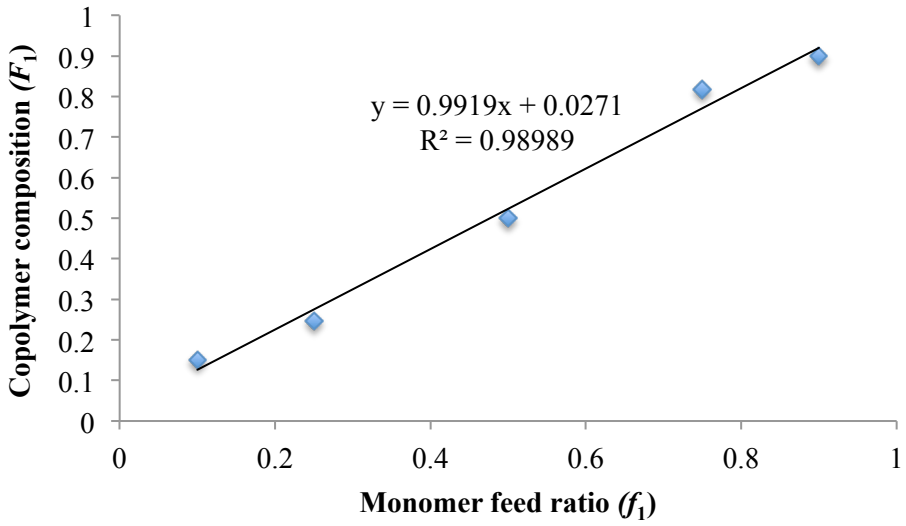

Figure 4.3.12: Graph of co-polymer composition (F_1) versus monomer feed ratio (f_1).

For a truly random co-polymer a plot of copolymer composition (F_1) versus monomer feed ratio (f_1) would display a straight line with the intercept at 0, gradient of 1 and an R^2 value close to 1. Here, in our case, the monomer feed ratio (f_1) directly relates to the copolymer composition (F_1) as illustrated by the gradient of the curve having a value close to 1 (0.9919, Figure 4.3.12). This is further supported by the trend-line both fitting the data well (R^2 = 0.98989) and having an intercept close to 0 (0.0271), corroborating the previous conclusion that a random copolymer was synthesised. Selected physical and thermal properties of the synthesised co-polymers are shown below (Table 4.3.4).

Table 4.3.4: GPC and DSC analyses of co polymers of *rac*-LA and Ph-LA at various monomers ratios.

$[LA]_0$	:	$[Ph\text{-}LA]_0$	M_n kg.mol^{-1}	$M_{n,\,theo}$ kg.mol^{-1}	PDI	T_g (°C)
9	:	1	10.0	15.0	1.79	44
3	:	1	12.2	15.9	1.13	43
1	:	1	9.1	17.4	1.08	55
1	:	3	33.8	18.9	1.24	66
			5.6		1.17	
1	:	9	21.9	19.8	1.06	67
			6.6		1.17	

As the amount of Ph-LA increased within the lactide co-polymer, the molecular weight generally increased. For lactide: PhLA monomer ratios of 1:3 and 1:9, bimodal GPC traces were observed suggesting two different polymers may have been synthesised. Interestingly, polyPh-LA is similar to polymandelide, and expresses a high T_g value due to possible π-π stacking of the aromatics in the polymer chain. This is observed in Table 4.3.4 whereby with increased portion of Ph-LA present in the lactide co-polymer, an increase in T_g was observed. Molecular weight may also influence the T_g as an increase in molecular displays an increase in T_g

4.3.3. BrPh-LA Polymerisations

Whilst polyPh-LA mimics similar functionality to polystyrene, the analogous monomer BrPh-LA should exhibit similar characteristics with the advantage of possible functionalization after polymerisation with nucleophilic substitution at the bromo-substituent. Initially, an NMR-scale homo-polymerisation of BrPh-LA (monomer moles; 3.46 x 10^{-4} mol), was performed with $\mathbf{L}^{t\mathrm{Bu}}\mathrm{ZrO}^{i}\mathrm{Pr}.\mathrm{HO}^{i}\mathrm{Pr}$ (100:1 monomer: initiator ratio) in d_8 toluene (0.6 ml) at 353 K. Then, a co-polymerisation of BrPh-LA with *rac*-LA was screened with a combined monomer: initiator ratio of 100:1. The reactions were monitored by NMR spectroscopy and a comparison of homo-polymerisations versus co-polymerisations are shown below and the reaction rates determined by semi-log plots (Figure 4.3.13).

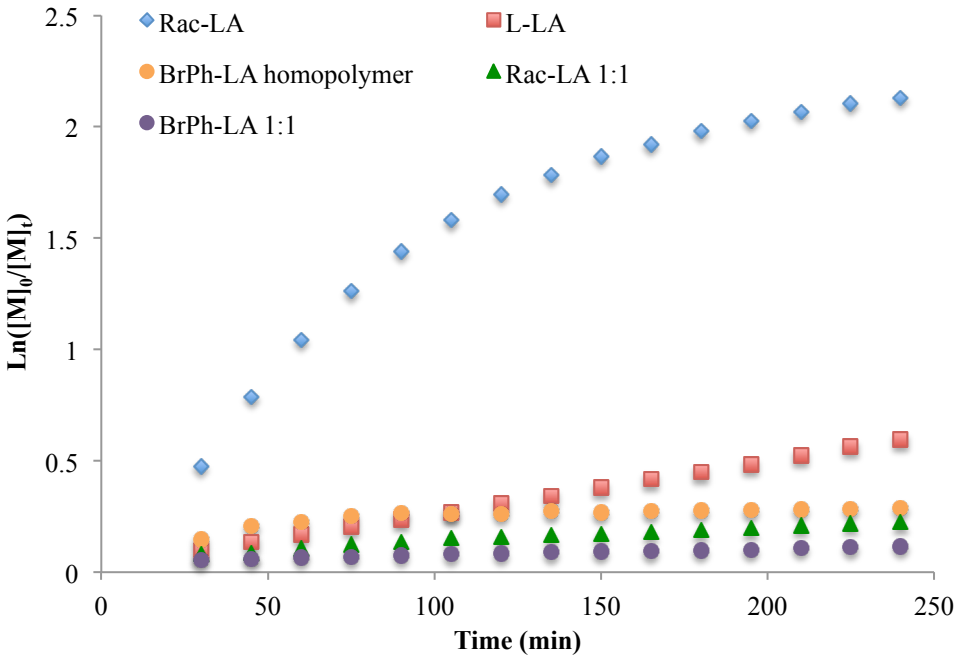

Figure 4.3.13: Semi-log plot of the homo-polymerisation of *rac*-LA (blue), L-LA (red), BrPh-LA (orange) and 1:1 co-polymerisation *rac*-LA (green) and BrPh-LA (purple) with $\mathbf{L}^{t\mathrm{Bu}}$ZrO^{i}Pr.HO^{i}Pr, 100:1 monomer:initiator loading, 80°C in d_8 tol.

Again, as seen for Ph-LA, the homo-polymerisation rates of *rac*-LA and BrPh-LA were very different (k_{app} = 0.016 and 0.0004 min^{-1} respectively) suggesting $k_{rac\mathrm{LA}}$-$k_{rac\mathrm{LA}}$ >> k_{BrPhLA}-k_{BrPhLA} During 1:1 co-polymerisation, the rates of reaction decrease for both monomers and appear to have similar k_{app} values of 0.0008 and 0.0005 min^{-1} for *rac*-LA and BrPh-LA respectively. This suggests that at 1:1 co-polymerisation ratio k_{BrPhLA}-$k_{rac\mathrm{LA}}$ ~ k_{BrPhLA}-k_{BrPhLA}, suggesting a true co-polymer may have been synthesised. A simplified graphic of the co-polymerisation is shown below (Figure 4.3.14).

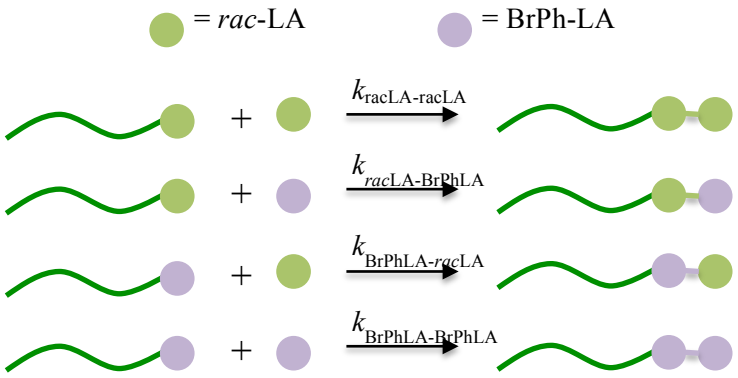

Figure 4.3.14: Reaction rates of co-polymerisation of *rac*-LA (green) and BrPh-LA (purple).

Further investigations into the co-polymerisation of *rac*-LA and BrPh-LA were undertaken using different ratios ranging from 9:1 to 1:9 *rac*-LA to BrPh-LA. For each of them, kinetic plots are displayed below (Figure 4.3.15).

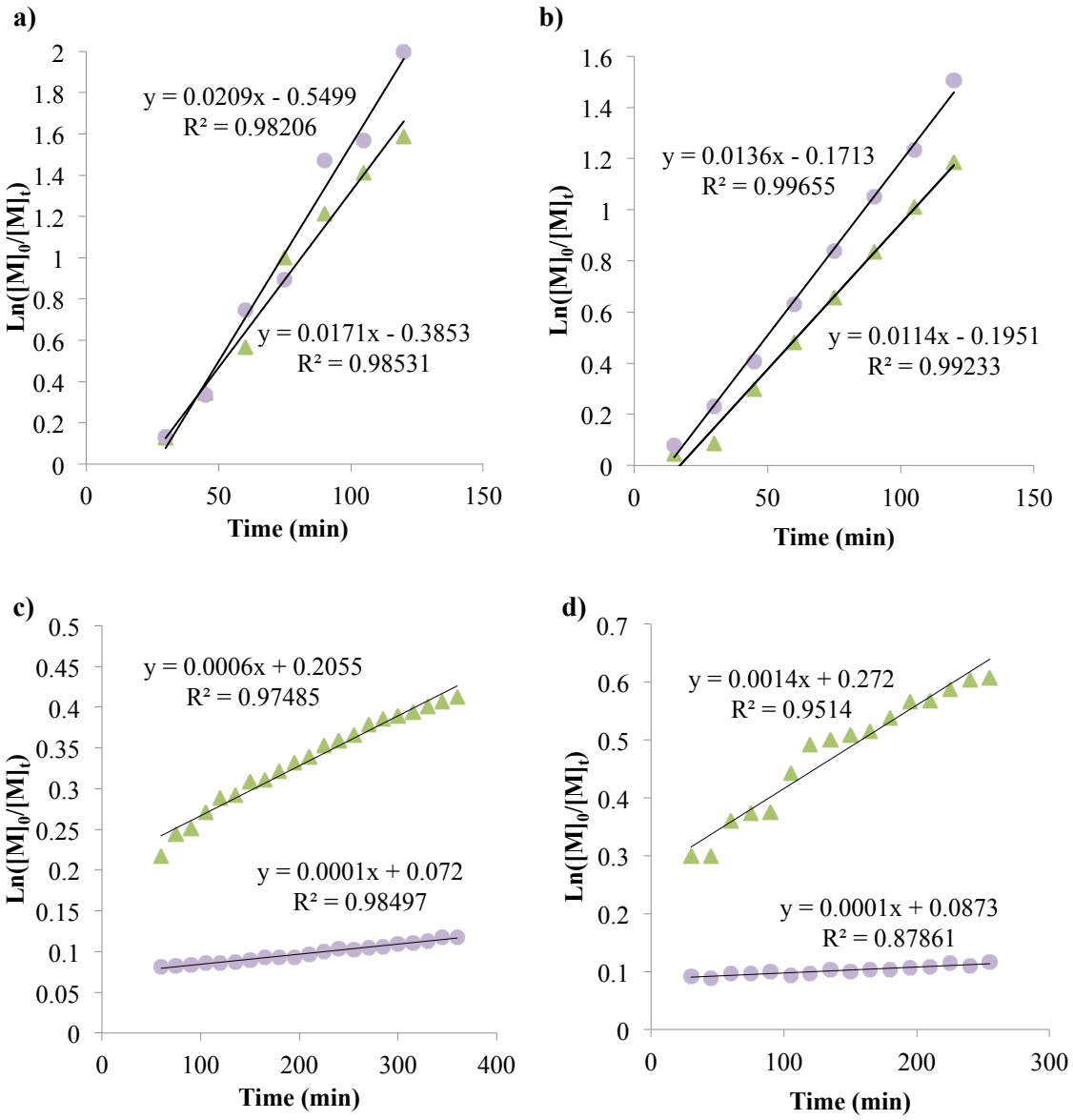

Figure 4.3.15: Semi-log plot of co-polymerisation using $^{t\text{Bu}}$ZrO^{i}Pr.HO^{i}Pr (100:1 combined monomer: initiator loading) with a *rac*-LA (green) to BrPh-LA (purple) monomer ratio of **a)** 9:1, **b)** 3:1, **c)** 1:3, **d)** 1:9.

For the co-polymerisation of *rac*-LA and BrPh-LA when *rac*-LA was in excess (9:1 and 3:1), BrPh-LA reaction rate was faster than that of *rac*-LA. This is the opposite of what was observed for the homo-polymerisations where *rac*-LA had a much faster reaction rate. This could be due to $k_{rac\text{LA-BrPhLA}} > k_{rac\text{LA-}rac\text{LA}}$. Due to the low concentration of BrPh-LA in the reaction,

conversion to near completion occurs fairly rapidly. The opposite was observed with increased concentration of BrPh-LA (1:3 and 1:9 *rac*-LA: BrPh-LA). Here, a much faster reaction rate was observed for *rac*-LA. This could be due to $k_{\text{BrPhLA-BrPhLA}} << k_{rac\text{LA-kBrPhLA}} < k_{rac\text{LA-}rac\text{LA}}$. As the co-polymerisation rate of *rac*-LA is so much faster, this suggests that a co-polymer is synthesised initially until most of the *rac*-LA monomer has been consumed, followed by a block segment of polyBrPh-LA homopolymer. Reactivity ratios were calculated for the copolymerisaiton of *rac*-LA with BrPh-LA (Table 4.3.5) in the same fashion as for Ph-LA.

Table 4.3.5: Reactivity ratios for the co-polymerisation of *rac*-LA with Ph-LA.

$[LA]_0$ (f_1)	$[BrPh\text{-}LA]_0$ (f_2)	LA conv. (%)	BrPh-LA conv. (%)	LA copolymer (F_1)	BrPh-LA copolymer (F_2)
0.9	0.1	6.94	7.02	0.91	0.09
0.75	0.25	4.88	6.08	0.70	0.30
0.5	0.5	5.99	5.41	0.53	0.47
0.25	0.75	13.39	8.95	0.36	0.64
0.1	0.9	22.03	9.79	0.22	0.78
$r_{1(\text{calc})} = 0.55$					
$r_{2(\text{calc})} = 0.32$					

The reactivity ratios (r_1 and r_2) derived from the Mayo-Lewis equation are less than 1 (r_1 = 0.5429 and r_2 = 0.3226). This trend indicates the microstructure of the copolymer is a statistical distribution of *rac*-LA and BrPh-LA monomer units along the polymeric chain. As expected, these results are similar to that discussed previously in this chapter for the co-polymerisation of rac-LA and Ph-LA. As r_1 and r_2 are again less that 1 but higher than 0, this indicates the synthesis of a random co-polymer with alternating tendencies. A plot of co-polymer composition (F_1) versus monomer feed ratio (f_1) was used to further investigate the microstructural sequence of the co-polymers (Figure 4.3.16).

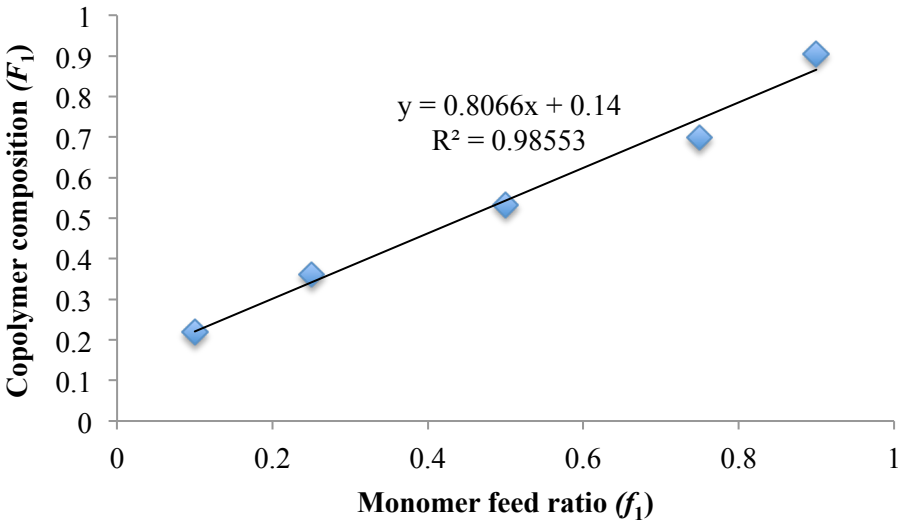

Figure 4.3.16: Plot of co-polymer composition (F_1) versus monomer feed ratio (f_1).

For a truly random co-polymer a plot of copolymer composition (F_1) versus monomer feed ratio (f_1) would display a straight line with the intercept at 0, gradient of 1 and an R^2 value close to 1. Here, in our case, the monomer feed ratio (f_1) directly relates to the copolymer composition (F_1) as illustrated by the gradient of the curve having a value close to 1 (0.8066, Figure 4.3.16), although not as close to 1 as that observed for the lactide co-polymerisation with Ph-LA. This is further supported by the trend-line both fitting the data well (R^2 = 0.98553) and having an intercept close to 0 (0.14). Again, although this suggests a random copolymer was synthesised, coupling this information with the reactivity ratios reported previously in this chapter, the overall microstructural sequence of the co-polymer is thought to be a random co-polymer with alternating tendencies (similar to copolymerisation of *rac*-LA and Ph-LA).

Table 4.3.6: GPC and DSC analyses of co polymers of *rac*-LA and BrPh-LA at various monomer: monomer ratios.

$[LA]_0$	:	$[BrPh\text{-}LA]_0$	M_n kg.mol^{-1}	$M_{n,\,theo}$ kg.mol^{-1}	PDI	T_g (°C)
9	:	1	8.9	15.7	1.37	41
3	:	1	4.7	17.8	1.26	52
1	:	1	5.0	21.3	1.18	66
1	:	3	3.4	24.8	1.17	67
1	:	9	2.1	26.9	1.18	69

With increased ratio of BrPh-LA, a decrease in molecular weights was observed. As expected, as the quantity of BrPh-LA in the co-polymerisation is increased there is a general trend of increased T_g. Increase amount of aromatic substituents should increase thermal properties coupled with the possible further stability due to π-π stacking afford some very interesting co-polymers.

4.4. Conclusions

A series of monomers were synthesised and co-polymerised with lactide. Lactide co-polymerisations with 5% and 10% vinyl-LA was achieved using TBD and benzyl alcohol. Due to Et-LA exhibiting similar properties to lactide, co-polymerisation with varying monomer stoichiometries with $\mathbf{L}^{t\mathrm{Bu}}\mathrm{ZrO}^{i}\mathrm{Pr}.\mathrm{HO}^{i}\mathrm{Pr}$ was trialled. A trend of decreasing M_n was observed with increasing quantities of Et-LA which could contribute to a lowering of T_g, suggesting co-polymerisation. Ph-LA and BrPh-LA were also tested in co-polymerisation under the same conditions with varying monomer amounts. Kinetic studies illustrated random co-polymers were synthesised with lactide where increased amounts of Ph-LA or BrPh-LA afforded co-polymers with increased thermal properties. The ability to synthesise a polymer that can mimic characteristics of polystyrene and yet exhibit degradability has huge industrial potential.

4.5. Further work

In this chapter, a series of promising co-polymers have been synthesised. In order to probe the morphology further, ^{13}C NMR spectroscopy could be utilised to investigate the microstructural linking of the repeat units. Large scale reactions yielding grams of polymer would enable rheology experiments. Further investigations into the polymerisations using enantiopure monomers to try and exploit the heterotactic bias of the initiator would potentially yield very interesting alternating co-polymers.

4.6. References

(1) Trimaille, T.; Gurny, R.; Möller, M. *J. Biomed. Mater. Res. A* **2007**, *80*, 55–65.

(2) Jing, F.; Smith, M. R.; Baker, G. L. *Macromolecules* **2007**, *40*, 9304–9312.

(3) BAKER L., 9600 Deer Trail, Haslett, MI 48840 (US), G.; SMITH R., III, 238 Oxford Road, East Lansing, MI 48823 (US), M. PROCESS FOR THE PREPARATION OF POLYMERS OF DIMERIC CYCLIC ESTERS, June 14, 2001.

(4) Trimaille, T.; M□ller, M.; Gurny, R. *J. Polym. Sci. Part A Polym. Chem.* **2004**, *42*, 4379–4391.

(5) Jing, F.; Hillmyer, M. A. *J. Am. Chem. Soc.* **2008**, *130*, 13826–13827.

(6) Bouyahyi, M.; Pepels, M. P. F.; Heise, A.; Duchateau, R. **2012**.

(7) Chisholm, M. H.; Gallucci, J. C.; Quisenberry, K. T.; Zhou, Z. *Inorg. Chem.* **2008**, *47*, 2613–2624.

(8) Liu, T.; Simmons, T. L.; Bohnsack, D. A.; Mackay, M. E.; Smith, M. R.; Baker, G. L. *Macromolecules* **2007**, *40*, 6040–6047.

(9) Chmura, A. J.; Davidson, M. G.; Frankis, C. J.; Jones, M. D.; Lunn, M. D. *Chem. Commun.* **2008**, 1293–1295.

(10) Huijser, S.; Mooiweer, G. D.; van der Hofstad, R.; Staal, B. B. P.; Feenstra, J.; van Herk, A. M.; Koning, C. E.; Duchateau, R. *Macromolecules* **2012**, *45*, 4500–4510.

(11) Mayo, F. R.; Lewis, F. M. *J. Am. Chem. Soc.* **1944**, *66*, 1594–1601.

(12) Vion, J. M.; Jerome, R.; Teyssie, P.; Aubin, M.; Prudhomme, R. E. *Macromolecules* **1986**, *19*, 1828–1838.

(13) Vanhoorne, P.; Dubois, P.; Jerome, R.; Teyssie, P. *Macromolecules* **1992**, *25*, 37–44.

(14) Florczak, M.; Duda, A. *Angew. Chemie Int. Ed.* **2008**, *47*, 9088–9091.

Chapter 5

Conclusion

Overall, a series of active initiators were synthesised and characterised for the ROP of *rac*-lactide under solvent-free conditions. These initiators were based on Group 4 metals complexed to ligands $\mathbf{L_1}$, $\mathbf{L_2}$ and $\mathbf{L_3}$. The resulting polymers were characterised using GPC, DSC, and NMR, and $Ti_4(\mathbf{L_2})(O^iPr)_{12}$, **4**, was found to be the most active initiator showing comparable activity to the commercially used tin(II) hexanoate. Commercially available monomers were also trialled for ROP using $\mathbf{L^{tBu}}Zr(O^iPr).HO^iPr$, whereby block co-polymers were synthesised and the heterotactic bias of the initiator was exploited to form penta-block co-polymers. A series of unsymmetrical monomers were synthesised and polymerised to synthesise co-polymers using different stoichiometric amounts of monomers. Kinetic studies were performed to probe the activity of the initiator and deduce the microsctructure of the resulting co-polymers.

Chapter 2 describes the synthesis of several new group 4 complexes that were trialled in the ROP of sublimed *rac*-LA under solvent-free conditions at 135°C and 165°C. All initiators were active with the exception of $Ti_2(\mathbf{L_3})_2$. Titanium and zirconium were successfully complexed to lactic acid ligand to form $Ti_8[dimer]_2(\mathbf{L_1})_4(O^iPr)_{20}$ and $Zr(\mathbf{L_1})_2$ and gave an insight into possible binding mode lactide derivatives to group 4 metals during polymerisation. Both initiators exhibited moderate activity in the ROP of *rac*-lactide. While $Zr(\mathbf{L_1})_2$ was the least active at 135°C, it was shown to be one of the most active at 165°C (89% in 4 h) in this series. For Group 4 $\mathbf{L_2}$ complexes, activity was found to increase with an increase in the number of labile isopropoxide groups at 135°C, indicating the identity of the metal was found to be of less importance than the number of labile initiator groups present, with similar Zr, Hf and Ti complexes giving similar conversions. When an elevated temperature of 165°C was trialled, all the complexes demonstrated a higher activity irrespective of the identity of the metal or number of labile initiator groups. It is likely that the actual active species at elevated temperatures is a degradation product of the catalyst, rather than the original catalyst. In order to enhance stereocontrol, complexes with increased steric bulk were trialled but remained inactive under these conditions. The most active titanium species of the series, $Ti_4(\mathbf{L_2})(O^iPr)_{12}$, was further examined under conditions more closely replicating industrial polymerizations: at 165°C with a low initiator loading (5000:1) and using unsublimed (recrystallized) lactide. Under these conditions, and in contrast to commercially available Group 4 metal alkoxides ($Ti(O^iPr)_4$ and $Zr(O^iPr)_4(HO^iPr)$), $Ti_4(\mathbf{L_2})(O^iPr)_{12}$, **4**, was found to be highly active, facilitating a >99 % polymerization of the monomer to PLA within 3 hours thus highlighting the potential of Group 4 complexes as initiators for the commercial production of PLA. Although $Ti(O^iPr)_4$ exhibited a far higher activity and molecular weight control at 135°C and 165°C with sublimed *rac*-lactide than **4**, under more industrially relevant conditions (5000:1 initiator loading at 165°C) a far lower activity was observed. This loss in activity and control indicates that $Ti(O^iPr)_4$ would not

be suitable for scale up to industrial conditions. In contrast, the synthesised initiator $Ti_4(\mathbf{L_2})(O^iPr)_{12}$, **4**, does not work as well under the conditions of 135°C and 165°C with sublimed *rac*-lactide, however, when recrystallized (unsublimed) lactide is used under more industrial conditions the activity and control during polymerisation was much higher. In the future, further large-scale polymerisations could be performed with the most promising initiator $Ti_4(\mathbf{L_2})(O^iPr)_{12}$ with unrecrystallised lactide. Investigations into the stability of $Ti_4(\mathbf{L_2})(O^iPr)_{12}$ in the presence of impurities (lactic acid and H_2O) in order to probe its potential as an initiator for L-LA or D-LA polymerisations with the intention of forming stereocomplexed PLA upon mixing of enantio-pure polymers. The initiators synthesised in this chapter could also be trialled for the ROP of other lactones and the activity probed.

Chapter 3 describes the synthesis of various copolymers using commercially available, inexpensive monomers (LA, ε-CL, VL, PDL). Initially, unsymmetrical ABC tri-block copolymers containing L-LA, ε-CL and D-LA were produced using $\mathbf{L^{tBu}}Zr(O^iPr).HO^iPr$ as initiator and characterised using GPC, NMR and DSC. While GPC analysis of the final polymer was inconclusive, the tri-block copolymers insolubility in THF suggested a stereocomplex tri-block was formed. In chapter 3, DSC traces of the tri-block copolymers further supported stereocomplexation with a T_m of 199°C. The analogous polymer utilizing δ-VL instead of ε-CL was also synthesised and characterised. The ability to exploit the initiator $\mathbf{L^{tBu}}Zr(O^iPr).HO^iPr$ bias towards the formation of heterotactic PLA from *rac*-LA lends itself to the synthesis of unsymmetrical penta-block co-polymers. While the DSC traces were inconclusive and showed no thermal analysis results, this further indicates cross-linking within the polymer. GPC analyses supported the living polymerisation of the system, showing growing polymer chains with sequentially added monomer. Co-polymers incorporating PDL were synthesised using initiator $(BDI\text{-}^iPr)ZnN(SiMe_3)_2$ where addition of a relatively small monomer (LA or CL) to the PDL propagating chain resulted in a co-polymer. However, the addition of macrocyclic monomer PDL to a chain of PCL or PLLA was not possible, potentially due to steric hinderance whereby a large monomer cannot coordinate and insert onto a block of smaller monomer chains. Although it is unclear if homo-polymers or co-polymers were synthesised, distinct thermal traces suggest the presence of **sc**-PLA domains. Further investigations into morphology and rheology of block co-polymers could be performed to gain more information about these polymeric materials. In addition, repeating the polymerisations under more industrially relevant conditions would indicate if such co-polymers were viable commercially. Further investigations into the polymer architecture could be performed using GPC analysis with different solvent systems to attempt to dissolve the polymers and gain accurate molecular weights. In addition SAXS and WAXS analysis may be utilized to determine the morphology and phase separation

of blocks within the co-polymer. A study of varying the block lengths in order to optimise polymeric properties could lead to co-polymers with tailor made properties. Synthesis of isopropoxide derivative of (BDI-^{i}Pr)ZnN(SiMe$_3$)$_2$ developed by Coates *et al.* to increase activity of initiator in the lactide copolymerisation with PDL both in solution and under melt conditions would be interesting. Furthermore, characterisation of lactide co-polymers of PDL using GPC techniques described by Duchateau *et al.* could be utilised to probe the morphology and microsctructure of the polymers synthesised.

Chapter 4 describes the synthesis of a series of monomers were synthesised and co-polymerised with lactide. Lactide co-polymerisations with 5% and 10% vinyl-LA was achieved using TBD and benzyl alcohol. Due to Et-LA exhibiting similar properties to lactide, co-polymerisation with varying monomer stoichiometries with **L**$^{t\text{Bu}}$ZrO^{i}Pr.HO^{i}Pr was trialled. A trend of decreasing M_n was observed with increasing quantities of Et-LA which could contribute to a lowering of T_g, suggesting co-polymerisation. Ph-LA and BrPh-LA were also tested in co-polymerisation under the same conditions with varying monomer amounts. Kinetic studies illustrated random co-polymers were synthesised with lactide where increased amounts of Ph-LA or BrPh-LA afforded co-polymers with increased thermal properties. The ability to synthesise a polymer that can mimic characteristics of polystyrene and yet exhibit degradability has huge industrial potential. In order to probe the morphology further, ^{13}C NMR spectroscopy could be utilised to investigate the microstructural linking of the repeat units. Large scale reactions yielding grams of polymer would enable rheology experiments. Further investigations into the polymerisations using enantio-pure monomers to try and exploit the heterotactic bias of the initiator would potentially yield very interesting alternating co-polymers. Sequential polymerisation to afford block co-polymers incorporating isotactic PLA segments could lead to stereocomplexed domains within the co-polymer. The polymerisations (both block and random co-polymers) could be performed under more industrially relevant solvent-free conditions in order to test the viability of these systems in the commercial market. There is a lot of scope to investigate these interesting co-polymers in the future.

Chapter 6

Experimental

6 Experimental

6.1 Methods

In this section, important methods utilized throughout this work will be discussed.

6.1.1 Kinetics of polymerisation

A majority of lactide polymerisations can be described using the second-order rate law (see below).

$$-d[LA]/dt = k_p[LA]_t[I]_0^n$$

Where k_p is propagation rate constant, $[LA]_0$ is initial lactide concentration, $[I]_0$ is initial initiator concentration and n is order of initiator concentration (aggregation number).[1]

However, this can be simplified to a *pseudo*-first order rate law, given below, as only a catalytic amount of the initiator ([I]) was used and the monomer is in such excess the monomer concentration ([LA]) more or less stays the same. It also takes into account any impurities within the reaction such as lactic acid and water which may kill the catalyst.

$$-d[LA]/dt = k_{app}[LA]_t$$

Here, k_{app} is the first order rate constant. Integration, then simplification gives the following equation;

$$\ln\left(\frac{[LA]_0}{[LA]_t}\right) = kt$$

A plot of $\ln([LA]_0/[LA]_t)$ against time allows the *pseudo*-first order rate constant to be calculated from the gradient.

6.1.2 Gel-permeation chromatography (GPC)

Gel-permeation chromatography is used to determine the weight average molecular weight (M_w), number average molecular weight (M_n) and polydispersity index (PDI) of the polymer synthesised, *via* size exclusion.[2] A sample of the polymeric material is injected into a column containing porous beads. The beads allow small weight materials to enter the pores and elute from the column slower, while larger molecular weight materials cannot enter the pores of the beads and elute quicker. The eluting solvent (THF) can be analysed continuously using a detector calculating the concentration by weight of the polymer, as shown below (Figure 6.1.1).

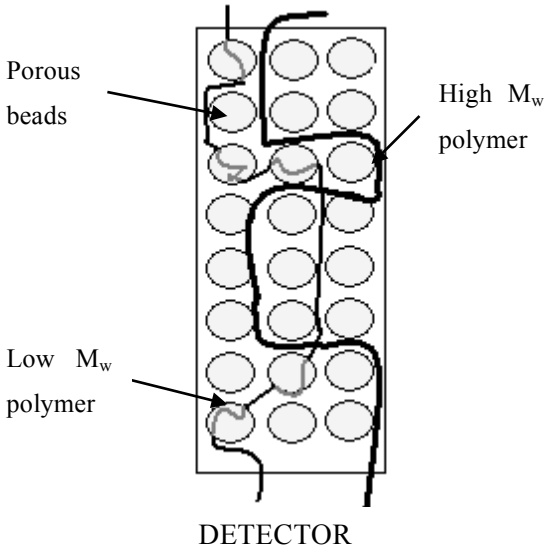

Figure 6.1.1: Diagram of GPC column.

Polystyrene of a known molecular weight is used to calibrate the system. The retention time of the sample can be compared to the calibration graph (response against retention time of standard), thus determining the molecular weights with respect to the standard. There are two main types of detectors available; concentration sensitive detectors and molecular weight sensitive detectors. Concentration sensitive detectors such as UV absorption, differential refractometer (DRI) or refractive index (RI) detectors, infrared (IR) absorption and density detectors. Molecular weight sensitive detectors such as low angle light scattering detectors (LALLS) and multi angle light scattering (MALLS).[3]

PLA material contains a variety of polymer chains with different chain lengths and molecular weights. The number average molecular weight (M_n) is dependent on the number of chains with each molecular weight.

$$M_n = \frac{\sum_i n_i M_i}{\sum_i n_i}$$

Where the Σn_i is the total number of molecules in the sample. $\Sigma n_i M_i$ is the sum of the weight of each molecule.

The weight average molecular weight (M_w) can be calculated from the relative weight of each fraction (w_i), which is expressed as $n_i M_i$.

$$M_w = \frac{\sum_i w_i M_i}{\sum_i w_i} = \frac{\sum_i n_i M_i^2}{\sum_i n_i}$$

The M_w is influenced by the larger fractions of the polymer. Thus, M_w tends to have a larger value than M_n. The polydispersity index (PDI) can be calculated from the M_w and M_n. It describes the distribution of polymer chains with differing lengths.

$$\text{PDI} = M_w/M_n$$

For lactide polymerisations whereby $k_{initiation} > k_{propagation}$ the chain length can be predicted using the following equation:

$$Mn = \frac{Monomer\ ratio \times Conversion \times monomer\ (M_n)}{Initiator\ ratio} + \text{End group } (M_n)$$

Intrinsic viscosity (IV) is a measure of how branched a polymer sample is, providing Mark Houwink-Sakurada parameters are readily available. In solution, branched polymers exhibit a smaller hydrodynamic volume compared to linear polymers are they are more compact. Experimentally, the degree of branching can be calculated by comparison to a known polymer of similar molecular weight, where g' is a contraction factor (Equation 6.1.1). When g' equals 1 the sample is linear.[4]

Equation 6.1.1: Mark Houwink-Sakurada equation.

$$g' = [IV]_{branched} / [IV]_{linear}$$

6.1.3 Differential scanning calorimetry (DSC)

Differential scanning calorimetry (DSC) is a thermo-analytical technique. In our case a heat-flux system was used that requires two aluminium tzero pans; one containing the polymeric sample and an empty pan for reference. Inside a single cell, both pans are heated or cooled at the same rate and the relevant heat capacities are recorded. As thermal transitions occur in the sample, the difference between the sample pan and reference pan will result in a depiction of the heat flux into or out of the sample, thus revealing both exo- and endothermal events.

As a polymeric sample is heated, the amorphous regions may change from the glassy to the rubbery state, a phenomenon which is observed as a jump in the heat capacity of the material. This point is called the glass transition (T_g) temperature. The amorphous material may become crystalline exhibiting an exothermic rearrangement which results in a peak from the base-line, known as the crystallisation temperature (T_c). As the temperature is increased further an endothermic trace is observed which correlates to the melting temperature (T_m) of the polymeric material.

6.1.4 FT-IR

For IR measurements a Bruker Matrix-MF FT-IR spectrometer equipped with a diamond ATR probe (IN350 T) suitable for Mid-IR *in situ* reaction monitoring was used. Reactions were performed under inert conditions in a specifically designed jacketed vessel fitted with a mechanical stirrer and connected to a Huber PETITE FLEUR-NR circulation thermostat (Figure 6.1.2).

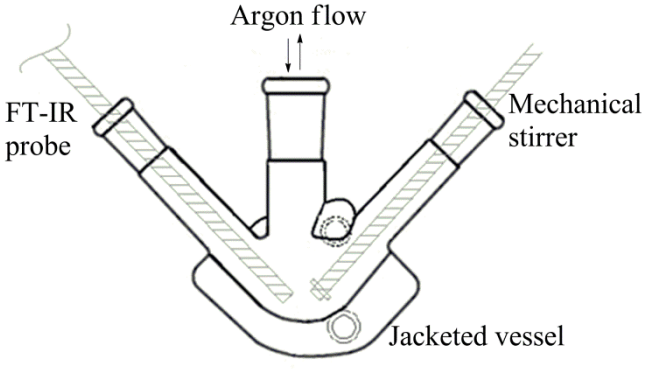

Figure 6.1.2: Drawing of FT-IR reaction vessel.

The jacketed vessel was placed under a positive pressure of argon and heated to the reaction temperature of 165 °C. The lactide (recrystallized) was added (35 g) and allowed to melt with stirring from the overhead mechanical stirrer. A background spectrum was recorded at this point before the probe was placed in the reaction solution. The initiator (5000:1 monomer:initiator loading) was dissolved in a minimal amount of toluene and transferred using a cannula into the reaction under argon. Spectra were collected over a set period of time and the decrease in the C-O-C lactide peak was calibrated against ^{1}H NMR spectrum measurements. To assess the applicability of selected catalysts for the industrial polymerisation of lactide solvent-free conditions at 165 °C and a 5000:1 monomer:initiator ratio were assessed. The asymmetric C-O-C vibration gives a characteristic peak at 1240 cm^{-1} and as such can be used to determine the monomer concentration (Figure 6.1.3).

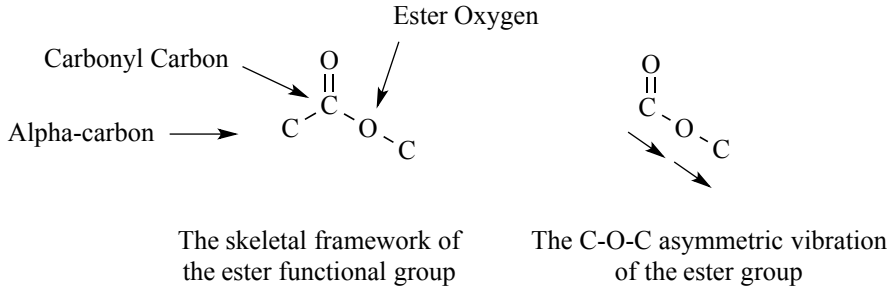

Figure 6.1.3: Skeletal framework and C-O-C asymmetric stretching of the ester functional group.[5]

For the polymer, this peak is shifted to 1185 cm^{-1} and the integral of these peaks are related to the concentration and used to accurately assess the kinetics.[5–7]

6.2 General considerations

For the preparation and characterization of metal complexes, all reactions and manipulations were performed under an inert atmosphere of argon using standard Schlenk or glovebox techniques. All solvents were dried using a solvent purification system. The ligand, *N,N,N',N'*-tetrakis(2-hydroxyethyl)ethylenediamine ($TOEEDH_4$) (technical grade Sigma-Aldrich), was dried under vacuum, dissolved in dry THF to afford a 1M solution and stored under an inert atmosphere. $Ti(O^{i}Pr)_4$ (97%, Aldrich) was purified by vacuum distillation prior to use, $Zr(O^{i}Pr)_4{}^{i}PrOH$ (99.9%, Aldrich) and $Hf(O^{i}Pr)_4{}^{i}PrOH$ (99%, Aldrich) were used without further purification. Yields were obtained from recrystallized products. Solution NMR experiments were performed $CDCl_3$ at ambient temperature unless otherwise stated using a Bruker Advance-250, Bruker Advance-300, Bruker DRX400 or Bruker DRX500 MHz FT-NMR spectrometer. Norell 5mm NMR tubes were used for ligand characterisation, while Young's tapped NMR

tubes were used for metal complex characterisation. All chemical shifts were quoted as δ values in ppm relative to residual protio solvent resonances; all J-coupling constants are given in Hertz. Elemental analyses of ligands, metal complexes and monomers was carried out at London Metropolitan University, London.

Suitable crystals were selected for single crystal X-ray diffraction using the oil drop technique, in perfluoropolyether oil and mounted at 150(2) K. Intensity data were collected on an Nonius Kappa CCD single crystal diffractometer using graphite monochromated Mo-Kα radiation (λ = 0.71073 Å). Data were processed using the Nonius Software.[8] A symmetry-related (multi-scan) absorption correction was applied. Crystal parameters and details on data collection, solution and refinement for the complexes are provided. The structures were solved by direct methods using the program SIR97[9] followed by full-matrix least squares refinement on F^2 using SHELXL-97 implemented in the WINGX-1.80 suite of programs throughout.[10] Hydrogen atoms were placed in calculated positions and isotropically refined using a riding model. Additional programs used for analysing data and graphically manipulating them included: SHELXL,[11] PLATON,[12,13] and ORTEP 3 for Windows.[14]

6.3 Synthetic Procedures

6.3.1 Synthesis of complexes

Preparation of $Ti_8[dimer]_2(L_1)_4(O^iPr)_{20}$, 1: Lactic acid ($L_1$, 0.45 g, 10.0 mmol) was dried in *vacuo* and dissolved in dry isopropanol (10 ml) with stirring. $Ti(O^iPr)_4$ (1.42 g, 5.00 mmol) was then added dropwise *via* syringe to the solution of lactic acid and stirred at 0 °C for 1 hour. The reaction was warmed to room temperature and stirred for a further 1 hour. The solvent was removed *in vacuo* and the dry residue was recrystallized from dichloromethane to yield an off white solid. Yield = 36 %. El. Anal: Calc for $C_{96}H_{20}O_{42}Ti_8$ C: 47.86 %, H: 8.37 %. Found C: 41.37 %; H: 8.31 %. ^{1}H NMR (300.22 MHz, $CDCl_3$, 298 K) δ 5.27-4.70 (m, 20H, C*H*-O^{i}Pr), 4.51 (q, J = 6.0 Hz, 4H, C*H*), 4.21-3.90 (m, 4H, C*H*) 1.41-1.10 (m, 144H, CH_3).

Preparation of $Zr(L_1)_2$, 2: To a solution of tetrakis(ethylmethylamino) zirconium (0.025 g, 0.093 mmol) in toluene (2 ml) was added ligand lactic acid (0.069 g, 0.093 mmol) and stirred at 25 °C for 12 hours. The solvent was removed *in vacuo* and the product was washed with hot toluene. Yield = 56 %. El. Anal: Calc for $C_6H_8O_6Zr$ C: 26.96 %, H: 3.02 %. Found C: 26.87 %; H: 3.15 %.

Preparation of $Ti_4(L_2)_3(O^iPr)_4$, 3: $Ti(O^iPr)_4$ (1.5 ml, 5.06 mmol) was added to 1M solution of $TOEEDH_4$ (**L_2**) in THF (3.81 ml, 3.81 mmol) dropwise with a syringe and stirred for 16 hours at 50 °C. The solvent was removed *in vacuo* and the dry residue was recrystallized from dichloromethane. Isolated crystalline yield = 24 %. El. Anal: Calc for $C_{42}H_{88}N_6O_{16}Ti_4$ C: 44.85 %; H: 7.89 %, N: 7.47 %. Found C: 44.68 %, H: 7.81 %, N: 7.39 %. ^{1}H NMR (300.22 MHz, $CDCl_3$, 298 K): δ 4.92-4.74 (m, 4H, OC*H*), 4.73-4.18 (m, 20H, ROCH_2), 4.17-3.93 (m, 4H, ROCH_2), 3.69-3.53 (m, 4H, RNCH_2), 3.51-3.15 (m, 14H, RNCH_2), 3.14-3.00 (m, 4H, RNCH_2), 3.00-2.70 (m, 14H, RNCH_2), 1.31-1.15 (m, 24H, RCH_3). ^{13}C{^{1}H} NMR (75.0 MHz, $CDCl_3$, 298 K): δ 74.16 (O(*C*H)), 71.39 (O(*C*H_2)), 69.44 (O(*C*H_2)), 69.09 (O(*C*H_2)), 64.78 (N(*C*H_2)), 61.61 (N(*C*H_2)), 61.04(N(*C*H_2)), 60.98 (N(*C*H_2)), 60.52 (N(*C*H_2)), 60.06 (N(*C*H_2)), 26.64 (R*C*H_3), 25.43 (R*C*H_3).

Preparation of $Ti_4(L_2)(O^iPr)_{12}$, 4: $Ti(O^iPr)_4$ (1.48 ml, 5.00 mmol) was added to 1M solution of $TOEEDH_4$ (**L_2**) in THF (1.25 ml, 1.25 mmol) dropwise with a syringe and stirred for 16 hours at 50 °C. The solvent was removed *in vacuo* and the dry residue was recrystallized from dichloromethane. Isolated crystalline yield = 28 %. El. Anal: Calc for $C_{46}H_{104}N_2O_{16}Ti_4$ C: 48.77 %, H: 9.25 %, N: 2.47 %. Found C: 48.65 %, H: 9.15 %, N: 2.39 %. ^{1}H NMR (300.22 MHz, $CDCl_3$, 298 K): δ 4.85 (sept, J = 6.0 Hz, 2H, O-C*H*), 4.79-4.53 (m, 4H, O-CH_2), 4.48 (sept, J = 6.0 Hz, 10H, O-C*H*), 4.42-3.96 (m, 4H, O-CH_2), 3.73-3.32 (m, 4H, N-CH_2), 3.32-3.03 (m, 4H, N-CH_2), 3.02-2.69 (m, 4H, N-CH_2), 1.23 (d, J = 6.0 Hz, 60H, RCH_3), 1.19 (d, J = 6.0 Hz, 12H, RCH_3)**.** ^{13}C{^{1}H} NMR (75.0 MHz, $CDCl_3$, 298 K): δ 72.0 (O(*C*H)), 68.5 (O(*C*H_2)), 64.1 (O(*C*H_2)), 61.3 (N(*C*H_2)), 55.5 (N(*C*H_2)), 51.0 (N(*C*H_2)), 26.5 (R*C*H_3), 25.3 (R*C*H_3).

Preparation of $Zr_2(L_2)_2$, 5: $Zr(O^iPr)_4(HO^iPr)$ (0.55 g, 2.32 mmol) in THF (5 ml) was added to 1M solution of $TOEEDH_4$ (**L_2**) in THF (2.32 ml, 2.32 mmol) with a syringe. The reaction was stirred overnight at 50 °C. The solvent was removed *in vacuo* and the dry residue was recrystallized from THF. Isolated crystalline yield = 28 %. El. Anal: Calc for $C_{20}H_{40}N_4O_8Zr_2$ C: 37.13 %, H: 6.23 %, N: 8.66 %. Found C: 37.01 %; H: 6.23 %, N: 8.47 %. ^{1}H NMR (300.22 MHz, $CDCl_3$, 298 K): δ 4.71-3.90 (m, 16H, O-CH_2), 3.80-2.38 (m, 24H, N-CH_2). ^{13}C{^{1}H} NMR (75.0 MHz, $CDCl_3$, 298 K): δ 67.0 (O(*C*H_2)), 60.8 (N(*C*H_2)).

Preparation of $Hf_2(L_2)_2$, 6: $Hf(O^iPr)_4(HO^iPr)$ (0.42 g, 1.01 mmol) in THF (10 ml) was added to 1M solution of $TOEEDH_4$ (**L_2**) in THF (1.0 ml, 1.0 mmol) dropwise with a syringe and stirred for 16 hours. The solvent was removed *in vacuo* and the dry residue was recrystallized from dichloromethane. Isolated crystalline yield: 14 %. El. Anal: Calc for $C_{20}H_{40}N_4O_8Hf_2$ C: 29.24 %, H: 4.91 %, N: 6.82 %. Found C: 29.13 %; H: 5.00 %, N: 6.72 %. ^{1}H NMR (300.22 MHz, $CDCl_3$, 298 K): δ 4.75-4.01 (m, 16H, O-CH_2), 3.79-3.49 (m, 2H, N-CH_2), 3.49-3.18 (m, 8H, N-

CH_2), 3.18-2.50 (m, 14H, N-CH_2). $^{13}C\{^1H\}$ NMR (75.0 MHz, $CDCl_3$, 298 K): δ 66.5 (O(*C*H_2)), 60.9 (N(*C*H_2)).

Preparation of $Zr_3(L_2)(O^iPr)_8$, 7: $Zr(O^iPr)_4(HO^iPr)$ (0.97 g, 2.50 mmol) in THF (10 ml) was added to 1M solution of $TOEEDH_4$ (**L_2**) in THF (0.83 ml, 0.834mmol) dropwise with a syringe and stirred for 16 hours at room temperature. The solvent was removed *in vacuo* and the dry residue was recrystallized from toluene. Isolated crystalline yield = 34 %. El. Anal: Calc for $C_{34}H_{76}N_2O_{12}Zr_3$ C: 41.72 %, H: 7.82 %, N: 2.86 %. Found C: 42.27 %, H: 7.86 %, N: 2.74 %. ^1H NMR (300.22 MHz, $CDCl_3$, 298 K): δ 4.67 (sept, J = 6.0 Hz, 2H, O-C*H*), 4.36-4.32 (m, 2H, O-CH_2), 4.32-4.24 (m, 6H, O-C*H*), 4.24-4.19 (m, 2H, O-CH_2), 4.18-4.11 (m, 2H, O-CH_2), 4.10-4.03 (m, 2H, O-CH_2), 3.68 (td, J = 6.0 Hz + 12.0 Hz, 2H, N-CH_2), 3.43-3.27 (m, 2H, N-CH_2), 3.26-3.13 (ddd, 2H, N-CH_2), 2.80-2.64 (m, 6H, N-CH_2), 1.28 (d, J = 6.0 Hz, 6H, RCH_3), 1.20 (d, J = 6.0 Hz, 6H, R-CH_3), 1.14 (d, J = 6.0 Hz, 36H, R-CH_3). $^{13}C\{^1H\}$ NMR (75.0 MHz, $CDCl_3$, 298 K): δ 69.6 (O(*C*H)), 69.1 (O(*C*H)), 67.7 (O(*C*H_2)), 64.6 (N(*C*H_2)), 64.1 (O(*C*H_2)), 62.1 (N(*C*H_2)), 59.8 (N(*C*H_2)), 27.5 (R*C*H_3), 26.6 (R*C*H_3), 26.3 (R*C*H_3).

Preparation of $Hf_3(L_2)(O^iPr)_8$, 8: $Hf(O^iPr)_4(HO^iPr)$ (0.42 g, 1.01 mmol) in THF (10 ml) was added to 1M solution of $TOEEDH_4$ (**L_2**) in THF (0.33 ml, 0.33 mmol) dropwise with a syringe and stirred for 16 hours at room temperature. The solvent was removed *in vacuo* and the dry residue was recrystallised from dichloromethane. Isolated crystalline yield = 14 %. El. Anal: Calc for $C_{34}H_{76}N_2O_{12}Hf_3$ C: 32.92 %, H: 6.18 %, N: 2.26 %. Found C: 32.78 %, H: 6.06 %, N: 2.33 %. ^1H NMR (300.22 MHz, $CDCl_3$, 298 K): δ 4.79 (sept, J = 6.0 Hz, 2H, O-C*H*), 4.50-4.41 (m, 2H, O-CH_2), 4.41-4.28 (m, 6H, O-C*H*), 4.28-4.19 (m, 2H, O-CH_2), 4.19-4.08 (m, 2H, O-CH_2), 4.08-3.94 (m, 2H, O-CH_2), 3.67 (td, J = 6.0 Hz + 12.0 Hz, 2H, N-CH_2), 3.38-3.29 (m, 2H, N-CH_2), 3.29-3.16 (m, 2H, N-CH_2), 2.89-2.83 (m, 2H, N-CH_2), 2.77-2.65 (m, 4H, N-CH_2), 1.28 (d, J = 6.0 Hz, 6H, R-CH_3), 1.20 (d, J = 6.0 Hz, 6H, R-CH_3), 1.18-1.09 (m, 36H, R-CH_3). $^{13}C\{^1H\}$ NMR (75.0 MHz, $CDCl_3$, 298 K): δ 68.5 (O(*C*H)), 66.9 (O(*C*H_2)), 64.8 (N(*C*H_2)), 63.6 (O(*C*H_2)), 62.4 (N(*C*H_2)), 60.0 (N(*C*H_2)), 26.6 (R*C*H_3), 26.1 (R*C*H_3), 25.5 (R*C*H_3).

Preparation of Ligand L_3: 2-[(2-aminoethyl)amino]ethanol (0.82 ml, 8.0 mmol) and 37 % formaldehyde aqueous solution (1.95 ml, 24 mmol) were stirred neat at for 110 °C for 15 minutes. 2,4-ditertbutyl phenol (5.0 g, 24mmol) in 5 ml toluene was then added and stirred at 100°C for 4 days. Purification by column chromatography (eluent hexane: ethyl acetate 9:1). Yield = 62 %. Anal: Calc for $C_{49}H_{77}N_2O_4$ C: 77.52 %, H: 10.36 %, N: 3.69 %. Found C: 77.47 %, H: 10.35 %, N 3.68 %. Mass spec: Calc for [M+H]+: 781.58. Found: 781.58. ^1H NMR (300.22 MHz, $CDCl_3$, 298 K) δ 7.22 (d, J = 2.4 Hz, 2H, Ar-*H*), 7.18 (d, J = 2.4 Hz, 1H, Ar-*H*), 6.91 (d, J = 2.4 Hz, 2H, Ar-*H*), 6.77 (d, J = 2.4 Hz, 1H, Ar-*H*), 3.67 (s, 6H, RNCH_2), 3.61 (t, J =

5.3, 2H, RCH_2OH), 2.78 (s, 4H, RNCH_2), 2.56 (t, J = 5.3, 2H, RNCH_2), 1.40 (s, 18H, CH_3 ^{t}Bu), 1.34 (s, 9H, CH_3 ^{t}Bu), 1.27 (s, 18H, CH_3 ^{t}Bu), 1.25 (s, 9H, CH_3 ^{t}Bu). ^{13}C{^{1}H} NMR (75.0 MHz, $CDCl_3$, 298 K) δ 153.7, 152.4, 141.9, 141.0, 136.2, 136.1, 125.3, 123.8, 123.8, 123.3, 121.6, 121.2 (Ar-*C*), 60.1, 59.6, 57.5, 55.9, 52.0, 50.9 (RN*C*H_2), 35.0, 34.9, 34.3, 34.3 (*C* ^{t}Bu), 31.8, 31.8, 29.9, 29.7 (*C*H_3 ^{t}Bu).

Preparation of $Ti_2(L_3)_2$, 9. **L_3** (0.1 g, 0.132 mmol) was dissolved in toluene (3 ml) to which Ti(O^iPr)$_4$ (40 µl, 132 mmol) was added and stirred at 25 °C for 14 hours. The solvent was removed *in vacuo* and product was recrystallized from hexane, filtered, washed and dried. Isolated yield = 43 %. Anal: Calc for $C_{49}H_{74}N_2O_4Ti$ C: 73.29 %, H: 9.29 %, N: 3.49 %. Found C: 72.75 %, H: 9.22 %, N: 3.72 %. ^{1}H NMR (300.22 MHz, $CDCl_3$, 298 K) δ 7.23 (d, J = 2.3 Hz, 1H, Ar-*H*), 7.17 (d, J = 2.1 Hz, Ar-*H*), 7.14 (d, J = 2.3 Hz, 1H, Ar-*H*), 6.97 (d, J = 2.1 Hz, 1H, Ar-*H*), 6.85 (d, J = 2.2 Hz, 1H, Ar-*H*), 6.80 (d, J = 2.2 Hz, 1H, Ar-*H*), 5.19 (d, J = 12.8 Hz, 1H, RNCH_2), 4.48-4.35 (m, 1H, RNCH_2), 4.33 (d, J = 13.4 Hz, 1H, RNCH_2), 4.17-4.11 (m, 1H, RNCH_2), 4.08 (d, J = 13.8 Hz, 1H, RNCH_2), 3.64-3.54 (m, 2H, RCH_2O), 3.52 (d, J = 12.8 Hz, 1H, RNCH_2), 3.49 (d, J = 13.4 Hz, 1H, RNCH_2), 3.10 (d, J = 13.8 Hz, 1H, RNCH_2), 3.06 (d, J = 12.8 Hz, 1H, RNCH_2), 3.04-2.87 (m, 2H, RNCH_2), 2.53 (d, J = 13.5 Hz, 1H, RNCH_2), 1.57 (s, 9H, CH_3 ^{t}Bu), 1.46 (s, 9H, CH_3 ^{t}Bu), 1.27 (s, 9H, CH_3 ^{t}Bu), 1.26 (s, 9H, CH_3 ^{t}Bu), 1.24 (s, 9H, CH_3 ^{t}Bu), 1.14 (s, 9H, CH_3 ^{t}Bu). ^{13}C{^{1}H} NMR (75.0 MHz, $CDCl_3$, 298 K) δ 141.7, 141.0, 139.5, 136.1, 135.8, 135.5, 126.0, 125.9, 124.2 (Ar-*C*), 124.1, 123.9, 123.9, 123.4, 123.4, 122.8 (Ar-*C*H), 70.4, 67.4, 65.4, 62.6, 61.7, 61.1, 59.2 (RN*C*H_2), 35.5, 35.4, 35.1, 34.4, 34.4, 34.3 (*C* ^{t}Bu), 31.9, 31.9, 31.8, 30.3, 30.1, 29.8 (*C*H_3 ^{t}Bu).

6.3.2 Synthesis of monomers

Preparation of methylethylglycolide (Et-LA): Prepared via a modified synthesis as previously described in the literature by Baker and co-workers (Chapter 4).[15] Under inert conditions, 2-hydroxybutyric acid (4.16 g, 0.04 mol) and 2-bromopropionyl bromide (5.03 ml, 0.048 mol) were stirred in dry THF (10 ml) and cooled in an ice bath. A mixture of Et_3N (7.25 ml, 0.052 mol) in THF (25 ml) was added dropwise with stirring. The solution was cooled and stirred overnight. The solution was filtered to remove a white solid and the filtrate was evaporated to dryness. The resulting oil was dissolved in ethyl acetate, washed with 2M HCl (3 x 50 ml), sat. aq. NaCl, dried over MgSO4, then concentrated to yield a crude linear acid ester. The viscous liquid was mixed with acetone (800 ml) and $NaHCO_3$ (13.5 g), and refluxed for two days. The solids were removed by filtration and the acetone was evaporated to dryness. The crude product was dissolved in ethyl acetate, dried over $MgSO_4$, filtered and the solvent removed by rotary

evaporator. The crude product was twice purified by vacuum distillation (50°C). ^{1}H NMR (300 MHz, $CDCl_3$, 298 K) δ 5.00 (q, 1H, J = 6.3 Hz, C*H*), 4.88 - 4.08 (m, 1H, C*H*), 2.23 – 1.93 (m, 2H, CH_2), 1.67 (d, 3H, J = 6.7 Hz, CH_3), 1.12 (t, 3H, J = 7.3 Hz, CH_3). ^{13}C{^{1}H} NMR (75 MHz, $CDCl_3$, 298 K) δ 167.5 (R*C*=O), 72.3 (R*C*H), 23.5 (R*C*H_2), 15.9 (R*C*H_3), 8.8 (R*C*H_3). Yield = 45 %. Anal: Calc for $C_{11}H_{10}O_4$ C: 53.16 %; H: 6.37 %. Found C: 52.96 %, H: 6.35%.

Preparation of methylphenylglycolide (Ph-LA): Prepared as previously described in the literature (Chapter 4).[16] Under inert conditions, *rac*-mandelic acid (2.0 g, 0.013mol) and 2-bromopropionyl bromide (1.38 ml, 0.013 mol) were heated at 80°C until HBr evolution ceased (1 hr). The solution was cooled and 400 ml of acetone was added followed by Et_3N (3.66 ml, 0.026 mol) and refluxed for 6 hrs. After removal of solvents, ethyl acetate was added (200 ml) and the suspension was washed with 2N HCl solution, saturated aqueous $NaHCO_3$, water and the organic layer was dried over $MgSO_4$. The monomer was recrystallized from toluene. Yield = 46 %. Anal: Calc for $C_7H_{10}O_4$ C: 64.07 %; H: 4.89 %. Found C: 64.02 %, H: 5.00 %. ^{1}H NMR (400 MHz, $CDCl_3$, 298 K) δ 7.45 – 7.31 (m, 5H, Ar-*H*), 5.22 (s, 1H, C*H*), 4.21 (q, J = 6.7 Hz, 1H, C*H*), 1.45 (d, J = 6.7 Hz, 3H, CH_3). ^{13}C{^{1}H} NMR (100 MHz, $CDCl_3$, 298 K) δ 167.1, 165.8 (R*C*=O), 131.5, 130.1, 129.1, 127.6 (Ar-*C*H), 77.9, 72.9 (R*C*H), 16.5 (R*C*H_3).

Preparation of methylbromophenylglycolide (BrPh-LA): Procedure used was modified from literature as described in Chapter 4.[16] Under inert conditions, 4-bromo-DL-mandelic acid (5.0 g, 0.022 mol) and 2-bromopropionyl bromide (2.27 ml, 0.022 mol) were heated at 80°C until HBr evolution ceased (1 hr). The solution was cooled and 400 ml of acetone was added followed by Et_3N (6.03 ml, 0.043 mol) and refluxed for 6 hrs. After removal of solvents, ethyl acetate was added (200 ml) and the suspension was washed with 2N HCl solution, saturated aqueous $NaHCO_3$, water and the organic layer was dried over $MgSO_4$. The monomer was recrystallized from toluene. Yield = 52 %. Anal: Calc for $C_{11}H_9BrO_4$ C: 46.34 %; H: 3.18 %. Found C: 46.18 %, H: 2.99 %. ^{1}H NMR (500 MHz, $CDCl_3$, 298 K) δ 7.59 (d, J = 8.4 Hz, 2H, Ar-*H*), 5.89 (s, 1H, C*H*), 5.18 (q, J = 6.8 Hz, 1H, C*H*), 1.68 (d, J = 6.8 Hz, 3H, CH_3).

Preparation of methyldimethylglycolide (DiMe-LA): Procedure used was modified from literature as described in Chapter 4.[17] Under inert conditions, hydroxyisobutyric acid (2.5 g, 24 mmol) and 2-bromopropionyl bromide (1.26 ml, 0.013 mol) were heated at 80°C until HBr evolution ceased (3 hrs). The solution was cooled and 150 ml acetone was added followed by Et_3N (50 mmol) and refluxed for 3 hrs. The suspension was cooled and triethylammonium salts were removed by filtration. The solvents were removed and the resulting mixture was dissolved in solvent system ethyl acetate:hexane 1:1 (200 ml). After filtration over silica gel, the solvents

were removed in vacuo and the crude product was recrystallized from ethyl acetate:hexane mixture (1:10). Yield = 42 %. Anal: Calc for $C_7H_{10}O_4$ C: 53.16 %, H: 6.37 %. Found C: 53.27 %, H: 6.27 %. ^{1}H NMR (300 MHz, $CDCl_3$, 298 K) δ 5.09 (q, J = 6.8 Hz, 1H, C*H*), 1.71 (m, 6H, CH_3), 1.69 (s, 3H, CH_3). $^{13}C\{^1H\}$ NMR (75 MHz, $CDCl_3$, 298 K) δ 168.8, 166.9 (R*C*=O), 80.8 (R*C*), 73.1 (R*C*H), 26.4, 25.5, 17.6 (R*C*H_3).

Preparation of vinyl-LA monomer;

a) Preparation of (3*S*, 6*S*)-3-bromo-3,6-dimethyl-1,4-dioxane-2,5-dione (BrMe-LA): Prepared as previously described in the literature (Chapter 4).[18] Under inert conditions, L-lactide (20 g, 0.138 mol) and *N*-bromosuccimide (27.2g, 0.153 mol) were dissolved in benzene (100 ml) and brought to reflux. Dropwise addition of benzoyl peroxide (0.672 g, 2.77 mmol) in benzene (10 ml) over 20 minutes. The reaction was monitored by TLC. After monomer was consumed, the reaction was cooled and solid removed by filtration. The filtrate was evaporated to dryness and dissolved in dichloromethane, washed with saturated sodium bisulfite (3 times) and saturated aqueous NaCl. The organic layer was dried over $MgSO_4$ and recrystallized from ethyl acetate to give yellow crystals. Yield = 51 %. Anal: Calc for $C_6H_7BrO_4$ C: 32.31 %, H: 3.16 %. Found C: 32.15 %, H: 3.27 %. ^{1}H NMR (300 MHz, $CDCl_3$, 298 K) δ 5.55 (q, J = 6.0 Hz, 1H, C*H*), 2.70 (s, 3H, CH_3), 1.75 (s, J = 6.0 Hz, 3H, CH_3). $^{13}C\{^1H\}$ NMR (75 MHz, $CDCl_3$, 298 K) δ 164.2, 160.1 (R*C*=O), 80.1 (R*C*), 72.6 (R*C*H), 29.7, 18.2 (R*C*H_3).

b) Preparation of (6*S*)-3-methylene-6-methyl-1,4-dioxane-2,5-dione (vinyl-LA): Prepared as previously described in the literature (Chapter 4).[18] Under inert conditions, (3*R*, 6*S*)-3-bromo-3,6-dimethyl-1,4-dioxane-2,5-dione (BrMe-LA, 9.36 g, 0.04 mol) was dissolved in dichloromethane (100 ml), cooled to 0 °C and stirred under argon. Triethylamine (6.45 g, 0.046 mol) were added dropwise *via* a dropping funnel over 1 hour. The reaction was stirred at 0 °C for 1 hour, warmed to room temperature and stirred for a further 1 hour. The reaction mixture was washed thrice with 1 M hydrochloric acid and once with sodium chloride solution. The organic layer was dried over $MgSO_4$ and evaporated to dryness. The pale yellow solid was recrystallized from ethyl acetate. Yield = 28 %. Anal: Calc for $C_6H_6O_4$ C: 50.71 %, H: 4.26 %. Found C: 50.68 %, H: 4.25 %. ^{1}H NMR (300.22 MHz, $CDCl_3$, 298 K) δ 5.94 (d, J = 3.0 Hz, 1H, CH_2), 5.54 (d, J = 3.0 Hz, 1H, CH_2), 5.05 (q, J = 6.0 Hz, 1H, C*H*), 1.70 (d, J = 6.0 Hz, 3H, CH_3). $^{13}C\{^1H\}$ NMR (75 MHz, $CDCl_3$, 298 K) δ 163.0, 157.8 (R*C*=O), 143.0 (R*C*), 110.6 (R*C*H_2), 72.5 (R*C*H), 17.5 (R*C*H_3). Mp = 100 – 102°C.

Preparation of hexyl-LA monomer;

a) Preparation of 2-hydroxyoctanoic acid: Prepared as previously described in the literature (Chapter 4).[19] Heptaldehyde (11.40 g, 0.1 mol) was added to a solution of $NaHSO_3$ (15.6 g, 0.15 mol) in 200 ml water and stirred for 30 minutes. Addition of a solution of NaCN (6.4 g, 0,13 mol) in 50 ml water and stirred for a further 15 minutes. The upper layer upon separation of phases was poured directly into 40 v% sulphuric acid (30 ml) and heated to 130°C for 3 hrs, then poured into 100 ml 6N NaOH and stirred for 12 hrs. The alkaline solution was washed twice with Et_2O (30 ml), then acidified with 2M HCl, and extracted thrice with Et_2O (30 ml). The combined latter Et_2O phases were washed with brine, dried over $MgSO_4$ and solvents removed. Crude product was recrystallized from toluene. Yield = 42 %. ^{1}H NMR (400 MHz, $CDCl_3$, 298 K) δ 4.27 (dd, J = 7.5 Hz, 1H, RC*H*), 1.91-1.79 (m, 1H, RCH_2), 1.76-1.64 (m, 1H, RCH_2), 1.55-1.39 (m, 2H, RCH_2), 1.39-1.20 (m, 6H, RCH_2), 0.88 (t, J = 7.0 Hz, 3H, RCH_3).

b) Preparation of 3-methyl-6-hexyl-1,4-dioxane-2,5-dione (hexyl-LA). Prepared as previously described in the literature (Chapter 4).[19] Under inert conditions, 2-bromopropionyl bromide (1.36 ml, 13.0 mmol) was added dropwise to 2-hydroxyoctanoic acid (2.0 g, 12.4 mmol) and stirred at 85° for 12 hrs. The reaction was cooled, addition of acetone (300 ml) and Et_3N (3.5 ml, 2.5 mmol) and stirred at 60°C for 3 hrs. The reaction was cooled and triethylammonium bromide salts were removed by filtration and solvents were removed *in vacuo*. The resulting mixture was dissolved in 100 ml ethyl acetate:hexane (1:2) and filtered over silica gel. The solvents were removed and the crude product was recrystallized from hexane (-20°C). Yield = 14 %. ^{1}H NMR (500 MHz, $CDCl_3$, 298 K) δ 5.09-4.97 (m, 1H, RC*H*), 4.94-4.83 (m, 1H, RC*H*), 2.14-2.03 (m, 1H, RCH_2), 2.03-1.89 (m, 1H, RCH_2), 1.72-1.63 (m, 3H, RCH_3), 1.61-1.42 (m, 2H, RCH_2), 1.39-1.23 (m, 6H, RCH_2), 0.88 (t, J = 7.0 Hz, 3H, RCH_3).

6.4 Polymerisations

6.4.1 General considerations

L-lactide (Puralact L Polymer Grade, 99+ %, Purac) and D-lactide (Puralact D Polymer Grade, 99+ %, Purac) were recrystallized from toluene and sublimed twice before use unless stated otherwise. *Rac*-lactide was obtained by dissolving equal amounts of L- and D-lactide, recrystallized from toluene and sublimed twice. All metal complexes were synthesised as described previously in this chapter. Monomer conversion was derived from ^{1}H NMR

spectroscopy and polymer microstructure determined by homonuclear decoupled ^{1}H NMR as discussed in Chapter 1.

Gel Permeation Chromatography (GPC) analyses of polymers were performed on a Polymer Laboratories PL-GPC 50 integrated system using a PLgel 5 *ί*m MIXED-D 300 x 7.5 mm column at 35 °C, THF eluent with a flow rate of 1.0 mL/min. The polydispersity index (PDI) was determined from M_w/M_n, where M_n is the number-average molecular weight and *M*w the weight-average molecular weight. The polymers were referenced to 11 narrow molecular weight polystyrene standards with a range of M_w 615-5680000 Da.

Thermal analyses of polymers were performed using Differential Scanning Calorimetry (DSC, TA instruments, Q2000) with nitrogen as the purge gas and calibrated using Indium standards (T_m 156.6). Crystallisation temperatures (T_c) were obtained from the first cool, whilst glass transition temperatures (T_g) and melting temperatures (T_m) were obtained by linear extrapolation from the second heat. Polymers were heated at a rate of 10°C/min from -50°C to 220°C, whereas stereocomplexed polymers were heated at a rate of 10°C/min from -50°C to 250°C. MALDI-ToF analyses was carried out by the EPSRC National Mass Spectrometry Service Centre (NMSSC) at the University of Wales, Swansea.

For IR measurements a Bruker Matrix-MF FT-IR spectrometer equipped with a diamond ATR probe (IN350 T) suitable for Mid-IR *in situ* reaction monitoring was used. Reactions were performed under inert conditions in a specifically designed jacketed vessel fitted with a mechanical stirrer and connected to a Huber PETITE FLEUR-NR circulation thermostat (Figure 6.1.2).

6.4.2 Polymerisations – Typical Syntheses

Polymerisations –Typical syntheses from Chapter 2

Bulk polymerisation (300:1 monomer:initiator loading, 135°C or 165°C): Typically, under inert conditions *rac*-LA (1.0 g, 6.93 mMol) and the initiator (0.0231 mMol) were stirred together at either 135°C or 165°C in a thick walled Young's vessel. If no isopropoxide groups were present in the initiator, 1 equivalent of benzyl alcohol was added (for initiators **5** and **6**). The reaction was monitored by ^{1}H NMR every hour for 4 h and at 24 h. At 24 h, the reaction was cooled and quenched with MeOH (0.5 ml). The resulting solid was dissolved in CH_2Cl_2 (5 ml) and the polymer was precipitated with MeOH to remove any unreacted monomer. The polymer was then dried in *vacuo*.

Polymerisations –Typical syntheses from Chapter 3

Sequential synthesis of unsymmetrical tri-block polymer (solution, 90°C) (PLLA-PCL-PDLA 1:1:1): Under inert conditions, sublimed L-LA (0.72 g, 5.0 mMol) was dissolved in toluene (5 ml) to which the initator $L^{tBu}Zr(O^iPr).HO^iPr$ (44 mg, 0.05 mMol) was added and stirred in a Young's ampuole at 90 °C for 36 h. An aliquot of 0.2 ml was removed from the reaction mixture with monomer conversion and M_w calculated using ^{1}H NMR spectroscopy and GPC respectively. When the reaction reached near completion, addition of ε-caprolatone (0.55 ml, 5.0 mMol) via syringe and the reaction was stirred at 90°C for 5 h. After polymerisation of ε-CL was near completion, addition of D-LA (0.72 g, 5.0 mMol) and the reaction was stirred at 90°C for a further 36 h. An aliquot was taken from the reaction medium to determine monomer conversion. The reaction was quenched with 0.2 ml MeOH and solvent removed *in vacuo*. The resulting polymer was dissolved in CH_2Cl_2 and any unreacted monomer removed by precipitated with MeOH. ^{1}H NMR (250 MHz, $CDCl_3$, 298 K) δ 5.16 (q, 4H, J = 7.1 Hz, C*H*, PLA), 4.06 (t, 2H, J = 6.7 Hz, R-O-CH_2R, PCL), 2.31 (t, 2H, J = 7.6 Hz, RCH_2=O, PCL), 1.73 – 1.26 (m, 6H, CH_2, PCL), 1.58 (d, 12H, J = 7.1 Hz, CH_3, PLA).

Sequential synthesis of unsymmetrical tri-block polymer (solution, 90°C) (PLLA-PVL-PDLA 1:1:1): Under inert conditions, sublimed L-LA (0.72 g, 5.0 mMol) was dissolved in toluene (5 ml) to which the initator $L^{tBu}Zr(O^iPr).HO^iPr$ (44 mg, 0.05 mMol) was added and stirred in a Young's ampoule at 90°C for 36 h. An aliquot of 0.2 ml was removed from the reaction mixture with monomer conversion and M_w calculated using ^{1}H NMR spectroscopy and GPC respectively. When the reaction reached near completion, addition of δ-valerolatone (0.46 ml, 5.0 mMol) via syringe and reaction was stirred at 90°C for 5 h. After polymerisation of δ-VL was near completion, addition of D-LA (0.72 g, 5.0 mMol) and the reaction was stirred at 90°C for a further 36 h. An aliquot was taken from the reaction medium to determine monomer conversion. The reaction was quenched with 0.2 ml MeOH and solvent removed *in vacuo*. The resulting polymer was dissolved in CH_2Cl_2 and any unreacted monomer removed by precipitated with MeOH. ^{1}H NMR (250 MHz, $CDCl_3$, 298 K) δ 5.15 (q, 4H, J = 7.1 Hz, C*H*, PLA), 4.05 (t, 2H, J = 6.6 Hz, R-O-CH_2R, PCL), 2.30 (t, 2H, J = 7.4 Hz, RCH_2=O, PCL), 1.73 – 1.20 (m, 8H, CH_2, PCL), 1.58 (d, 12H, J = 7.1 Hz, CH_3, PLA).

Stereocomplex of unsymmetrical tri-block copolymers: A tri-block copolymer (100 mg) was dissolved in CH_2Cl_2 and stirred for 30 minutes. The solvent was allowed to evaporate slowly through a needle punctured through a suba-seal over 1 week. The polymer was dried in *vacuo* to remove residual solvent.

Synthesis of unsymmetrical penta-block polymer (solution, 90°C) (P*het*LA-PLLA- PεCap - P*het*LA-PDLA 1:1:1): Under inert conditions, in a Young's ampoule sublimed L-LA (0.432 g, 3.0 mMol) and D-LA (0.288 g, 2.0 mMol) were dissolved in toluene (5 ml) to which the initator $L^{tBu}Zr(O^{i}Pr).HO^{i}Pr$ (44 mg, 0.05 mMol) was added and stirred at 90°C for 36 h. An aliquot of 0.2 ml was removed from the reaction mixture with monomer conversion and M_w calculated using ^{1}H NMR spectroscopy and GPC respectively. When the reaction reached near completion, addition of ε-caprolatone (0.55 ml, 5.0 mMol) *via* syringe and reaction was stirred at 90°C for 4 h. After polymerisation of ε-CL was near completion, addition of L-LA (0.288 g, 2.0 mMol) and D-LA (0.432 g, 3.0 mMol) and the reaction was stirred at 90°C for a further 36 h. An aliquot was taken from the reaction medium to determine monomer conversion. The reaction was quenched with 0.2 ml MeOH and solvent removed *in vacuo*. The resulting polymer was dissolved in CH_2Cl_2 and any unreacted monomer removed by precipitated with MeOH.

Synthesis of unsymmetrical penta-block polymer (solution, 90°C) (P*het*LA-PLLA-PδVL-P*het*LA-PDLA 1:1:1): Under inert conditions, in a Young's ampoule sublimed L-LA (0.432 g, 3.0 mMol) and D-LA (0.288 g, 2.0 mMol) were dissolved in toluene (5 ml) to which the initator $L^{tBu}Zr(O^{i}Pr).HO^{i}Pr$ (44 mg, 0.05 mMol) was added and stirred at 90°C for 36 h. An aliquot of 0.2 ml was removed from the reaction mixture with monomer conversion and M_w calculated using ^{1}H NMR spectroscopy and GPC respectively. When the reaction reached near completion, addition of δ-valerolatone (0.46 ml, 5.0 mMol) via syringe and reaction was stirred at 90°C for 5 h. After polymerisation of δ-VL was near completion, addition of L-LA (0.288 g, 2.0 mMol) and D-LA (0.0.432 g, 5.0 mMol) and the reaction was stirred at 90°C for a further 36 h. An aliquot was taken from the reaction medium to determine monomer conversion. The reaction was quenched with 0.2 ml MeOH and solvent removed *in vacuo*. The resulting polymer was dissolved in CH_2Cl_2 and any unreacted monomer removed by precipitated with MeOH. ^{1}H NMR (250 MHz, $CDCl_3$, 298 K) δ 5.28-5.08 (m, 4H, J = 7.1 Hz, C*H*, PLA), 4.08 (t, 2H, J = 6.1 Hz, R-O-CH_2R, PVL), 2.33 (t, 2H, J = 7.2 Hz, RCH_2=O, PCL), 1.73 – 1.50 (m, 4H, CH_2, PVL), 1.58-1.55 (m, 12H, CH_3, PLA).

Synthesis of stereocomplexed unsymmetrical penta-block copolymers: A penta-block copolymer (100 mg) was dissolved in CH_2Cl_2 and stirred at 25°C for 30 minutes. The solvent was allowed to evaporate slowly over 1 week through a suba-seal punctured with a needle. The polymer was dried under high vacuum to remove residual solvent.

Synthesis of PPDL (tol, 90°C): Under inert conditions, in a Young's ampoule, recrystallised ω-PDL (0.25 g, 1.04 mMol) was dissolved in toluene (5 ml) to which (BDI-^{i}Pr)ZnN(SiMe$_3$)$_2$ (7 mg, 0.01 mMol) was added and stirred at 90°C for 24 h. An aliquot of 0.2 ml was removed from

the reaction mixture with monomer conversion and M_w calculated using ^{1}H NMR spectroscopy and GPC respectively. The reaction was quenched with 0.2 ml MeOH and solvent removed *in vacuo*. The resulting polymer was dissolved in CH_2Cl_2 and any unreacted monomer removed by precipitated with MeOH. ^{1}H NMR (250 MHz, $CDCl_3$, 298 K) δ 4.05 (t, 2H, J = 6.7 Hz, R-O-C*H*$_2$R), 4.05 (t, 2H, J = 6.6 Hz, R-O-C*H*$_2$R, PCL), 2.30 (t, 2H, J = 7.4 Hz, RC*H*$_2$=O), 1.60 (t, 4H, J = 6.7 Hz, C*H*$_2$), 1.41-1.16 (m, C*H*$_2$).

Synthesis of di-block polymer PPDL-PLLA (tol, 90°C): Under inert conditions, in a Young's ampoule, recrystallised ω-PDL (0.25 g, 1.04 mMol) was dissolved in toluene (5 ml) to which (BDI-^{i}Pr)ZnN(SiMe$_3$)$_2$ (7 mg, 0.01 mMol) was added and stirred at 90°C for 24 h. When the reaction reached near completion, L-LA (0.15 g, 1.04 mMol) was added and the reaction stirred at 90°C for a further 18 h. An aliquot was taken from the reaction medium to determine monomer conversion. The reaction was quenched with 0.2 ml MeOH and solvent removed *in vacuo*. The resulting polymer was dissolved in CH_2Cl_2 and any unreacted monomer removed by precipitated with MeOH.

Synthesis of di-block polymer PPDL-PDLA (tol, 90°C): Under inert conditions, in a Young's ampoule, recrystallised ω-PDL (0.25 g, 1.04 mMol) was dissolved in toluene (5 ml) to which (BDI-^{i}Pr)ZnN(SiMe$_3$)$_2$ (7 mg, 0.01 mMol) was added and stirred at 90°C for 24 h. An aliquot of 0.2 ml was removed from the reaction mixture with monomer conversion and M_w calculated using ^{1}H NMR spectroscopy and GPC respectively. When the reaction reached near completion, D-LA (0.15 g, 1.04 mMol) was added and the reaction stirred at 90°C for a further 18 h. An aliquot was taken from the reaction medium to determine monomer conversion. The reaction was quenched with 0.2 ml MeOH and solvent removed *in vacuo*. The resulting polymer was dissolved in CH_2Cl_2 and any unreacted monomer removed by precipitated with MeOH.

Synthesis of stereocomplexed di-block copolymer (PPDL-PLLA + PPDL-PDLA): Di-block copolymers PPDL-PLLA (50 mg) and PPDL-PDLA (50 mg) were dissolved in CH_2Cl_2 and stirred at 25°C for 30 minutes. The solvent was allowed to evaporate slowly through a needle punctured through a suba-seal over 7 days. The polymer was dried under high vacuum to remove residual solvent.

Synthesis of unsymmetrical tri-block polymer PPDL-PCL-PLLA (tol, 90°C): Under inert conditions, in a Young's ampoule, recrystallised ω-PDL (0.25 g, 1.04 mMol) was dissolved in toluene (5 ml) to which (BDI-^{i}Pr)ZnN(SiMe$_3$)$_2$ (7 mg, 0.01 mMol) was added and stirred at 90°C for 24 h. An aliquot of 0.2 ml was removed from the reaction mixture with monomer conversion and M_w calculated using ^{1}H NMR spectroscopy and GPC respectively. When the

reaction reached near completion (78 %), addition of ε-CL (0.12 ml, 1.04 mMol) *via* syringe and reaction was stirred at 90°C for 6 h. After polymerisation of ε-CL was near completion (84 %), L-LA (0.149 g, 1.04 mMol) was added and the reaction stirred at 90°C for a further 24 h. An aliquot was taken from the reaction medium to determine monomer conversion (55 %). The reaction was quenched with 0.2 ml MeOH and solvent removed *in vacuo*. The resulting polymer was dissolved in CH_2Cl_2 and any unreacted monomer removed by precipitated with MeOH.

Synthesis of unsymmetrical tri-block polymer PPDL-PCL-PDLA (tol, 90°C): Under inert conditions, in a Young's ampoule, recrystallised ω-PDL (0.25 g, 1.04 mMol) was dissolved in toluene (5 ml) to which (BDI-^{i}Pr)ZnN(SiMe$_3$)$_2$ (7 mg, 0.01 mMol) was added and stirred at 90°C for 24 h. An aliquot of 0.2 ml was removed from the reaction mixture with monomer conversion and M_w calculated using ^{1}H NMR spectroscopy and GPC respectively. When the reaction reached near completion (75 %), addition of ε-CL (0.12 ml, 1.04 mMol) *via* syringe and reaction was stirred at 90°C for 6 h. After polymerisation of ε-CL was near completion (85 %), D-LA (0.149 g, 1.04 mMol) was added and the reaction stirred at 90°C for a further 24 h. An aliquot was taken from the reaction medium to determine monomer conversion (88 %). The reaction was quenched with 0.2 ml MeOH and solvent removed *in vacuo*. The resulting polymer was dissolved in CH_2Cl_2 and any unreacted monomer removed by precipitated with MeOH.

Synthesis of stereocomplexed unsymmetrical tri-block copolymer (PPDL-PCL-PLLA + PPDL-PCL PDLA): Tri-block copolymers PPDL-PCL-PLLA (50 mg) and PPDL-PCL-PDLA (50 mg) were dissolved in CH_2Cl_2 and stirred at 25°C for 30 minutes. The solvent was allowed to evaporate slowly through a needle punctured through a suba-seal over 7 days. The polymer was dried under high vacuum to remove residual solvent.

6.4.3 Kinetic Investigations

Polymerisations –Typical syntheses from Chapter 4

Synthesis of lactide co-polymer with 5% vinyl-LA: Under inert conditions, in a Young's ampoule L-LA (1.0 g, 6.94 mMol) and vinyl-LA (49 mg, 0.347 mMol) were dissolved in CH_2Cl_2 with benzyl alcohol (7.2 μl). Addition of 1,5,7-triazabicyclo[4.4.0]dec-5-ene (TBD, 0.9 mg) in CH_2Cl_2. The reaction was stirred for 5 minutes at 25°C. Benzoic acid was added to quench the reaction and solvent removed *in vacuo*.

Synthesis of lactide co-polymer with 10% vinyl-LA: Under inert conditions, in a Young's ampoule L-LA (1.0 g, 6.94 mMol) and vinyl-LA (99 mg, 0.347 mMol) were dissolved in

CH_2Cl_2 with benzyl alcohol (7.2 µl). Addition of 1,5,7-triazabicyclo[4.4.0]dec-5-ene (TBD, 0.9 mg) in CH_2Cl_2. The reaction was stirred for 5 minutes at 25°C. Benzoic acid was added to quench the reaction and solvent removed *in vacuo*.

Solution co-polymerisation (NMR scale, tol, 90°C): Typically, combined monomer (3.46 mMol) and the initiator $L^{tBu}Zr(O^iPr).HO^iPr$ (3 mg, 0.03 mMol) were dissolved in d8 toluene (0.6 ml) in a Young's NMR tube, which was immediately placed on an NMR spectrometer programmed to run the sample every 15 minutes. Once the reaction had reacted near completion (>95%) the reaction was quenched with 0.2 ml MeOH, dissolved in CH_2Cl_2 and precipitated with MeOH to remove any unreacted monomer and dried *in vacuo*.

6.5 References

(1) Platel, R. H.; Hodgson, L. M.; Williams, C. K. *Polym. Rev.* **2008**, *48*, 11–63.

(2) Trathnigg, B.; Kollroser, M. *J. Chromatogr. A* **1997**, *768*, 223–238.

(3) Trathnigg, B. *Prog. Polym. Sci.* **1995**, *20*, 615–650.

(4) Pitet, L. M.; Hait, S. B.; Lanyk, T. J.; Knauss, D. M. *Macromolecules* **2007**, *40*, 2327–2334.

(5) Messman, J. M.; Storey, R. F. *J. Polym. Sci. Part A Polym. Chem.* **2004**, *42*, 6238–6247.

(6) Braun, B.; Dorgan, J. R.; Dec, S. F. *Macromolecules* **2006**, *39*, 9302–9310.

(7) Yu, Y.; Storti, G.; Morbidelli, M. *Ind. Eng. Chem. Res.* **2011**, *50*, 7927–7940.

(8) Otwinowski, Z.; Minor, W. *Macromol. Crystallogr. Pt A* **1997**, *276*, 307–326.

(9) Altomare, A.; Burla, M. C.; Camalli, M.; Cascarano, G. L.; Giacovazzo, C.; Guagliardi, A.; Moliterni, A. G. G.; Polidori, G.; Spagna, R. *J. Appl. Crystallogr.* **1999**, *32*, 115–119.

(10) Farrugia, L. *J. Appl. Crystallogr.* **1999**, *32*, 837–838.

(11) Hubschle, C. B.; Sheldrick, G. M.; Dittrich, B. *J. Appl. Crystallogr.* **2011**, *44*, 1281–1284.

(12) Platon, A. *Utr. Univ. Utrecht, Netherlands, AL Spek* **1998**.

(13) Spek, A. *Acta Crystallogr. Sect. A* **1990**, *46*, c34.

(14) Farrugia, L. *J. Appl. Crystallogr.* **1997**, *30*, 565.

(15) Jing, F.; Smith, M. R.; Baker, G. L. *Macromolecules* **2007**, *40*, 9304–9312.

(16) BAKER L., 9600 Deer Trail, Haslett, MI 48840 (US), G.; SMITH R., III, 238 Oxford Road, East Lansing, MI 48823 (US), M. PROCESS FOR THE

PREPARATION OF POLYMERS OF DIMERIC CYCLIC ESTERS, June 14, 2001.

(17) Trimaille, T.; Moller, M.; Gurny, R. *J. Polym. Sci. Part A Polym. Chem.* **2004**, *42*, 4379–4391.

(18) Jing, F.; Hillmyer, M. A. *J. Am. Chem. Soc.* **2008**, *130*, 13826–13827.

(19) Trimaille, T.; Gurny, R.; Möller, M. *J. Biomed. Mater. Res. A* **2007**, *80*, 55–65.

APPENDIX – Single crystal X-ray data

Ti_8[dimer]$_2$(L_1)$_4$(O^iPr)$_{20}$, 1.

Identification code	**Ti_8[dimer]$_2$(L_1)$_4$(O^iPr)$_{20}$, 1**
Empirical formula	C96 H200 O42 Ti8
Formula weight	2409.76
Temperature	150(2) K
Wavelength	0.71073 A
Crystal system, space group	Monoclinic, P 2
Unit cell dimensions	a = 12.3075(4) A alpha = 90 deg. b = 18.1587(7) A beta = 90.077(2) deg. c = 30.3631(9) A gamma = 90 deg.
Volume	6785.8(4) A^3
Z, Calculated density	2, 1.179 Mg/m^3
Absorption coefficient	0.515 mm^-1
F(000)	2576
Crystal size	0.35 x 0.35 x 0.18 mm
Theta range for data collection	3.01 to 25.35 deg.
Limiting indices	-14<=h<=14, -21<=k<=21, -36<=l<=36
Reflections collected / unique	50710 / 20075 [R(int) = 0.0846]
Completeness to theta = 25.35	91.3 %
Absorption correction	Semi-empirical from equivalents
Max. and min. transmission	0.9130 and 0.8403
Refinement method	Full-matrix least-squares on F^2
Data / restraints / parameters	20075 / 31 / 1334
Goodness-of-fit on F^2	1.123
Final R indices [I>2sigma(I)]	R1 = 0.0950, wR2 = 0.1736
R indices (all data)	R1 = 0.1646, wR2 = 0.1999
Absolute structure parameter	0.04(4)
Largest diff. peak and hole	0.482 and -0.372 e.A^-3

$Ti_4(L_2)_3(O^iPr)_4$, 3

Identification code	**$Ti_4(L_2)_3(O^iPr)_4$, 3**
Empirical formula	C44 H92 Cl4 N6 O16 Ti4
Formula weight	1294.64
Temperature	150(2) K
Wavelength	0.71073 A
Crystal system, space group	Triclinic, P $\bar{1}$
Unit cell dimensions	a = 9.5477(4) A alpha = 86.886(2) deg. b = 12.3817(5) A beta = 85.008(2) deg. c = 12.9853(7) A gamma = 78.112(3) deg.
Volume	1495.42(12) A^3
Z, Calculated density	1, 1.438 Mg/m^3
Absorption coefficient	0.759 mm^-1
F(000)	682
Crystal size	0.38 x 0.25 x 0.10 mm
Theta range for data collection	3.83 to 27.64 deg.
Limiting indices	-12<=h<=12, -16<=k<=16, -16<=l<=16
Reflections collected / unique	17013 / 17013 [R(int) = 0.0000]
Completeness to theta = 27.64	96.7 %
Absorption correction	Semi-empirical from equivalents
Max. and min. transmission	0.9279 and 0.7613
Refinement method	Full-matrix least-squares on F^2
Data / restraints / parameters	17013 / 0 / 340
Goodness-of-fit on F^2	1.112
Final R indices [I>2sigma(I)]	R1 = 0.1104, wR2 = 0.2394
R indices (all data)	R1 = 0.1270, wR2 = 0.2495
Extinction coefficient	0.042(3)
Largest diff. peak and hole	1.434 and -2.150 e.A^-3

$Ti_4(L_2)(O^iPr)_{12}$, 4

Identification code	**$Ti_4(L_2)(O^iPr)_{12}$, 4**
Empirical formula	C46 H104 N2 O16 Ti4
Formula weight	1132.91
Temperature	150(2) K
Wavelength	0.71073 A
Crystal system, space group	Triclinic, P -1
Unit cell dimensions	a = 9.7827(3) A alpha = 87.910(2) deg. b = 10.9231(3) A beta = 75.866(2) deg. c = 15.2538(5) A gamma = 79.555(2) deg.
Volume	1554.39(8) A^3
Z, Calculated density	1, 1.210 Mg/m^3
Absorption coefficient	0.553 mm^-1
F(000)	610
Crystal size	0.38 x 0.25 x 0.10 mm
Theta range for data collection	4.03 to 27.50 deg.
Limiting indices	-12<=h<=12, -14<=k<=14, -19<=l<=19
Reflections collected / unique	20206 / 6993 [R(int) = 0.0564]
Completeness to theta = 27.50	98.1 %
Absorption correction	Semi-empirical from equivalents
Max. and min. transmission	0.9468 and 0.8174
Refinement method	Full-matrix least-squares on F^2
Data / restraints / parameters	6993 / 0 / 339
Goodness-of-fit on F^2	1.045
Final R indices [I>2sigma(I)]	R1 = 0.0446, wR2 = 0.1044
R indices (all data)	R1 = 0.0656, wR2 = 0.1161
Largest diff. peak and hole	0.355 and -0.411 e.A^-3

$Zr_2(L_2)_2$, 5

Identification code	**$Zr_2(L_2)_2$, 5**
Empirical formula	C40 H80 N8 O16 Zr4
Formula weight	1294.00
Temperature	150(2) K
Wavelength	0.71073 A
Crystal system, space group	monoclinic, C 2/c
Unit cell dimensions	a = 14.7560(4) A alpha = 90 deg. b = 9.6140(4) A beta = 101.494(2) deg. c = 19.3510(5) A gamma = 90 deg.
Volume	2690.16(15) A^3
Z, Calculated density	2, 1.597 Mg/m^3
Absorption coefficient	0.823 mm^-1
F(000)	1328
Crystal size	0.20 x 0.10 x 0.05 mm
Theta range for data collection	5.54 to 27.40 deg.
Limiting indices	-18<=h<=18, -12<=k<=12, -24<=l<=23
Reflections collected / unique	19738 / 3017 [R(int) = 0.1084]
Completeness to theta = 27.40	98.5 %
Max. and min. transmission	0.9600 and 0.8527
Refinement method	Full-matrix least-squares on F^2
Data / restraints / parameters	3017 / 0 / 154
Goodness-of-fit on F^2	1.195
Final R indices [I>2sigma(I)]	R1 = 0.2542, wR2 = 0.5774
R indices (all data)	R1 = 0.2607, wR2 = 0.5798
Largest diff. peak and hole	9.150 and -7.911 e.A^-3

$Zr_3(L_2)(O^iPr)_8$, 7

Identification code	**$Zr_3(L_2)(O^iPr)_8$, 7**
Empirical formula	C35 H78 N2 O12 Zr3
Formula weight	992.65
Temperature	150(2) K
Wavelength	0.71073 A
Crystal system, space group	triclinic, P-1
Unit cell dimensions	a = 15.2050(7) A alpha = 87.456(3) deg. b = 16.8120(8) A beta = 84.855(3) deg. c = 18.0700(10) A gamma = 87.529(3) deg.
Volume	4592.5(4) A^3
Z, Calculated density	4, 1.436 Mg/m^3
Absorption coefficient	0.722 mm^-1
F(000)	2072
Crystal size	0.50 x 0.40 x 0.13 mm
Theta range for data collection	2.98 to 25.10 deg.
Limiting indices	-17<=h<=17, -19<=k<=19, -21<=l<=21
Reflections collected / unique	51740 / 15043 [R(int) = 0.1058]
Completeness to theta = 25.10	91.9 %
Max. and min. transmission	0.9120 and 0.7141
Refinement method	Full-matrix least-squares on F^2
Data / restraints / parameters	15043 / 0 / 946
Goodness-of-fit on F^2	1.091
Final R indices [I>2sigma(I)]	R1 = 0.2378, wR2 = 0.5442
R indices (all data)	R1 = 0.2734, wR2 = 0.5651
Largest diff. peak and hole	3.766 and -2.672 e.A^-3

$Hf_3(L_2)(O^iPr)_8$, 8

Identification code	**$Hf_3(L_2)(O^iPr)_8$, 8**
Empirical formula	C34 H76 Hf3 N2 O12
Formula weight	1240.44
Temperature	200(2) K
Wavelength	0.71073 A
Crystal system, space group	Monoclinic, C 2/c
Unit cell dimensions	a = 23.6691(6) A alpha = 90 deg. b = 10.3738(2) A beta = 97.2430(10) deg. c = 19.0472(5) A gamma = 90 deg.
Volume	4639.50(19) A^3
Z, Calculated density	4, 1.776 Mg/m^3
Absorption coefficient	6.748 mm^-1
F(000)	2424
Crystal size	0.50 x 0.50 x 0.15 mm
Theta range for data collection	4.09 to 27.56 deg.
Limiting indices	-30<=h<=30, -13<=k<=13, -24<=l<=24
Reflections collected / unique	34294 / 5326 [R(int) = 0.1251]
Completeness to theta = 27.56	99.1 %
Absorption correction	Semi-empirical from equivalents
Max. and min. transmission	0.4309 and 0.1334
Refinement method	Full-matrix least-squares on F^2
Data / restraints / parameters	5326 / 1 / 282
Goodness-of-fit on F^2	1.034
Final R indices [I>2sigma(I)]	R1 = 0.0413, wR2 = 0.1026
R indices (all data)	R1 = 0.0539, wR2 = 0.1099
Largest diff. peak and hole	2.259 and -1.774 e.A^-3